Mathematical modelling of population and disease control in patchy environments

Rachel Anne Lintott

Thesis submitted for the degree of

Doctor of Philosophy

Computing Science and Mathematics

University of Stirling

May 2014

Abstract

Natural populations may be managed by humans for a number of reasons, with mathematical modelling playing an increasing role in the planning of such management and control strategies. In an increasingly heterogeneous, or 'patchy' landscape, the interactions between distinct groups of individuals must be taken into account to predict meaningful management strategies. Invasive control strategies, involving reduction of populations, such as harvesting or culling have been shown to cause a level of disturbance, or spatial perturbation, to these groups, a factor which is largely ignored in the modelling literature.

In this thesis, we present a series of deterministic, differential equation models which are used to investigate the impact of this disturbance in response to control. We address this impact in two scenarios. Firstly, in terms of a harvested population, where extinction must be prevented whilst maximising the yield obtained. Secondly, we address the impact of disturbance in an epidemic model, where the aim of the control strategy is to eradicate an endemic pathogen, or to prevent the invasion of a pathogen into a susceptible population. The movement of individuals between patches is modelled as both a constant rate, and a function which is increasing with population density. Finally, we discuss the 'optimal' control strategy in this context.

We find that, whilst a population harvested from a coupled system is able to produce an inflated yield, this coupling can also cause the population to be more resistant to higher harvesting efforts, increasing the effort required to drive the population to extinction. Spatial perturbation raises this extinction threshold further still, providing a survival mechanism not only for the individuals that avoid being killed, but for the population as a whole.

With regards to the eradication of disease, we show that disturbance may either raise or lower the pathogen exclusion threshold depending on the particular characteristics of the pathogen. In certain cases, we have shown that spatial perturbation may force a population to be susceptible to an infectious invasion where its natural carrying capacity would prevent this.

Acknowledgements

This work has been funded by the University of Stirling Horizon Studentship, and I must begin by thanking the University for this award, without which this thesis would not have been possible.

The work presented here would not have been possible without the support, encouragement and patience of my two supervisors Andy Hoyle and Rachel Norman. You have made the last few years possible, and I can't thank you enough for everything you've done for me.

I would like to acknowledge the fantastic CS and Maths division as a whole for being a great place to work, chat, eat cake and drink coffee. Thanks to all the support staff, Grace, Linda, Gemma, Lynn, Sam and Graham for brightening up the day, solving problems and generally looking after me. In particular I must thank my office mates Nicky McPherson and Scott Denholm, who paved the way for me and made this roller-coaster feel do-able. To Jen McKeown and Gill Ogg for going through it all with me, and to Iona Paterson for providing an injection of enthusiasm and optimism over the past few months. I know you'll all succeed in whatever you choose to do, and it's been a privilege to work alongside such a wonderful group of people.

My thanks must also go to Niamh Johnstone and Sophie Barrack for my weekly reminder that I love maths. Thanks to the wonderful Laura Kubasiewicz and Jenny Wallace for providing ecological insight, the occasional glass of wine, and lots of laughs. Finally, my sincerest thanks go to my family for their enduring love and support. To Marion and John for welcoming me into your family, for your words of encouragement and genuine interest in what I do. To Mum, Dad and Chris for being my safe haven in the storm of academia, I wouldn't be here if it weren't for the lifetime of love and support that you've all given me. Finally, to Paul, you have provided me with inspiration and encouragement throughout this whole process, along with a shoulder to cry on and I wouldn't have reached this point without you. This thesis is dedicated to you.

Contents

Chapter 1

Introduction and literature review

1.1 Introduction

Humans have been controlling wildlife populations for thousands of years. Modern motivations for population control are wide ranging and include, amongst others, hunting or harvesting for food, culling populations for conservation purposes or disease control, and trophy hunting of so called 'big game'. This thesis will use mathematical modelling to assess how the movement of wild or free ranging animals affects the impact of these control strategies. This chapter begins with a review of the motivations for the control of animal species, before detailing the importance of mathematical modelling in devising control strategies. The spatial considerations when controlling populations are then discussed, and the mathematical literature is reviewed for approaches to this problem. Finally, context is given to the problem of spatial perturbation and its implications for population control.

1.2 Control of natural populations

In an increasingly overpopulated world, the interactions between humans and wildlife are becoming more frequent. Either directly or indirectly, human populations are having an increasing effect on wildlife across the world. Direct interactions between humans and wildlife occur in a variety of ways, from habitat management to the culling or harvesting of species. It is the latter of these that we shall discuss throughout this thesis. Wildlife control through

the killing of individuals may be referred to as either harvesting or culling depending on the motivation for control. There are three main drivers for culling or harvesting wildlife, the term 'culling' is usually used when populations are reduced for conservation reasons [140],[22] or in an attempt to control the spread of disease [31],[72],[127]. 'Harvesting' is usually only used when we are interested in the yield achieved, that is, the number of individuals we are able to remove [119],[53]. Wild populations are therefore 'harvested' purely for their value to humans, and 'culled' if their death has a wider ecological impact.

Management of wild populations is a key aspect of conservation science. Invasive alien species such as signal crayfish (*Pacifastacus leniusculus*) [45], or the grey squirrels (*Scirius carolinensis*) [136] are a major cause of population decline of native species through competition for resources, the introduction of infection or through a combination of these factors. Culling of invasive species is often the most efficient way to reduce their numbers rapidly, and has been used widely in the UK for the control of grey squirrels [100]. However culling methods such as shooting of individuals can be costly and time consuming, particularly if the invasive species has already been allowed to establish itself in the habitat [137]. Culling practices are not limited to invasive species, and native populations may also be controlled for conservation purposes. For example, Red deer (*Cervus elaphus)*) numbers in Scotland have been increasing for decades, with such high densities having long term impact on native woodlands and other conservation sites due to grazing. Culling is one option for control of this wild population [95].

Disease control is possibly the most well reported, and controversial reason for wild animal culling. Many commentators have made the distinction between the control of wildlife for the eradication of a pathogen, and the control of wildlife to prevent the transmission of infection to humans or domestic animals [11], [149]. Wobeser suggests that 'one could argue that any intervention to alter the course of infectious disease in wild animals is an undesirable intrusion' [149] and it is because of this danger that the majority of culls occur to prevent the spread of infection to human or domestic hosts. For example, raccoon and skunk populations in North America can carry rabies and are often found at high densities in urban areas. This increases the risk of transmission of infection to the human population, and both

vaccination and culling strategies have been used to control these populations [28]. Red fox (*Vulpes vulpes*) populations are regularly subject to culling in Europe due to their ability to spread rabies to livestock and domestic animals [127]. In August 2013 the UK government announced the start of a badger cull in the counties of Gloucestershire and Somerset for the control of bovine tuberculosis (bTB) [109]. Transmission of bTB between domestic cattle and wild badgers (*Meles meles*) is well documented [80]. Cattle are regularly culled to prevent the spread of infection within the domestic population, but it is widely believed that eradication will be impossible without the control of the infection in the wildlife reservoir. Badger culls have been used in the past to control bTB and the randomised badger culling trial (RBCT) was an extensive trial to assess the effectiveness of a badger cull on the prevalence of bTB in cattle [152] [82].

The third major driver for the removal of animals from their natural environment is the harvesting of populations for food. The hunting of wild meat for human consumption is a major cause of extinction of species and loss of biodiversity, as well as providing a key source of both food and income to many rural communities [104]. The problems associated with hunting are not limited to terrestrial species, and centuries of overfishing of aquatic stocks has also been a major contributing factor to the decline of many marine species [81].

The change over time of a population and their response to culling or harvesting practice is a dynamic process which lends itself to mathematical modelling. The models detailed throughout this thesis are given mathematically by systems of ordinary differential equations, the analysis of which is well understood, featuring in most undergraduate texts. Mathematically, the properties of these models can be determined either through analysis, or in most cases through numerical approximation using ODE solvers available in programmes such as MATLAB. The application of deterministic systems of ODEs to the fields of biology and ecology has a long and rich history, and has lead to advances within both of these fields as well as to the field of mathematics [105], [25]. Biological systems are however inherently stochastic and there will inevitably be elements of the environment which cannot be captured by the

model. This stochasticity leads to chance happenings and the collection of noisy data. The purpose of deterministic modelling is therefore not to produce perfect predictions of biological dynamics, but to inform of the underlying mechanisms which cause the general trends observed in the field, and to determine key relationships.

1.3 Mathematical modelling of population and disease control

1.3.1 Models of harvested populations

Continuous time mathematical modelling of biological populations is traditionally traced back to Malthus' 'An essay on the Principle of Population' (1798) [96]. This discussion of the growth of populations via the processes of reproduction and death lead to the formulation of the well known, so called 'Malthus model' for population growth. Malthus hypothesised that, if provided with sufficient resources, each individual in the population would reproduce at a constant rate b, and would die at a constant rate d. The change in population, N, over time can then be given by

$$\frac{dN}{dt} = bN - dN. \tag{1.1}$$

The solution of this differential equation can be found explicitly to be

$$N(t) = N_0 e^{(b-d)t} \tag{1.2}$$

hence this model predicts that the population grows exponentially over time if $b > d$ or decays exponentially if $b < d$. Natural populations are not, however, provided with sufficient resources, but are bounded by constraints such as food, space, number of mates, or competition from other species. These factors all impose a limit to the naturally obtainable population size. This limit is often referred to as the carrying capacity of the environment, and can be defined as 'the maximum population size that can be supported indefinitely by a given environment, at which intraspecific competition has reduced the per capita net rate of increase to zero' [17]. The term 'intraspecific competition' in this definition refers to competition for resources between members of the same species, and is often modelled by a reduction in the growth rate as the size of the population reaches this limit. The logistic model for

population growth was first presented by Verhulst in 1838 [143] and has become a central tenet of mathematical biology. In this model, the change over time of the population size is given by

$$\frac{dN}{dt} = rN(1 - N/K). \tag{1.3}$$

The intrinsic growth rate is hence $r(1 - N/K)$ and is clearly population dependent. For a small population, $N \approx 0$, the population grows exponentially at rate r. As N increases, the growth rate slows, and approaches 0 as $N \to K$. The parameter K is therefore the carrying capacity of the population. Whilst the logistic model is used extensively throughout the population dynamics literature, it is not the only model allowing for a limited population. In many models of infectious disease spread (for example [6], and those found in [84]), the growth rate of the population is given by

$$\frac{dN}{dt} = a - bN. \tag{1.4}$$

In this case, new individuals are recruited into the population at a constant rate, a which is independent of the population size. The death rate however increases as the population size increases and the population reaches an equilibrium ($dN/dt = 0$) at its carrying capacity given by $N = a/b$. The constant per capita death rate b has units of 1/time, and $1/b$ is the average lifespan of an individual from this population. Since this formulation of population growth is linear, it is mathematically simpler and enables a deeper level of analysis than the non-linear logistic model.

It is a natural extension of these basic models to determine the effects that a culling or harvesting strategy will have on a population. Harvesting models have been in existence since the early 20th century, with the first models being developed in the contexts of fisheries [19],[118]. Early models detailed the dynamic effect of a constant harvesting effort on a single population, often taking into account the age or size structure of the harvested population [117], [44]. Brauer and Sanchez [26] analysed a range of mathematical models with constant-yield harvesting for single species systems as well as systems of two hosts in competition with each other. Constant yield harvesting assumes that a constant number of individuals is

removed per unit time regardless of the size of the population, an example of which is

$$\frac{dN}{dt} = rN\left(1 - \frac{N}{K}\right) - H.$$

This formulation of harvesting effort has a practical interpretation, and the parameter H can simply defined as the number of individuals harvested per unit time. This is based on the assumption that the target yield is reached whatever the population size. This model is in equilibrium, with $dN/dt = 0$ when

$$N = K \pm \sqrt{K^2 - \frac{4KH}{r}}/2$$

and hence has no real equilibrium for yields above $H_c = Kr/4$. This harvesting rate of H_c therefore represents the critical value above which no positive equilibrium can be achieved and this model has no biological relevance [26].

An alternative formulation of the harvesting problem is that found in Beddington and May [14] [99]. In this case, the harvesting effort is given by a constant rate multiplied by the population size hN. The harvested, logistic growth model is therefore given by

$$\frac{dN}{dt} = rN\left(1 - \frac{N}{K}\right) - hN.$$

The harvesting rate here is thought of as the product of the effort applied, in terms of, for example, number of ships, length of time spent fishing, and the 'catchability' of the population. This formulation captures the notion of 'catch per unit effort', which is a measure commonly used in the harvesting of natural populations. It is for this reason that this model will be used as the basis of the work presented in chapter 2.

1.3.2 Modelling disease control

Mathematics has been used in the study of epidemiology for many years, with initial work by Bernoulli [18] in the mid 18th century. The early 20th century saw a boom in mathematical epidemiology and the development of the first structured compartmental models by Ross and

Hudson [120] and Kermack and McKendrick [86]. These models detail the transition of individuals within a population through three infectious compartments or classes. Individuals can be classed as either susceptible, those who have not encountered the disease but are able to become infected, infected, those individuals who currently have the disease and are able to transmit it to the susceptible population, and recovered individuals who are assumed to have gained lifelong immunity to the disease. This SIR model has been the basis for many modern studies. Specific properties of particular diseases are easily incorporated into this type of model through the addition or removal of compartments. Latency in infection, i.e an incubation period between becoming infected, and being infectious, can be included by creating an exposed class where individuals are infected with the disease but unable to infect others, whilst removal of the recovered class allows us to model the effect of reinfection.

Transmission of infection can be modelled in a number of ways depending on the biology of the system. In the compartmental models considered throughout this thesis, we consider only direct transmission of a pathogen between susceptible and infected individuals, rather than considering indirect transmission of the pathogen via a vector or environmental transmission. When considering direct transmission of infection the two most commonly used expressions are frequency-dependent or density-dependent transmission. Frequency-dependent transmission of infection, given by the term $\beta SI/N$ suggests that the contact rate between individuals, and therefore transmission of infection is independent of the total population size N [101]. In this case, individuals are assumed to make a fixed number of contacts per unit time, and this contact rate does not increase with the population size. Density-dependent transmission βSI makes the assumption that the higher the concentration of individuals, the more contacts there are between susceptible and infected, and transmission increases with population density. As a crude approximation, it has been claimed that density dependent transmission is more appropriate for the spread of infection through wildlife species, where the social structure present in human populations is not as distinct [84]. Whilst it is clear from the literature that there is an element of debate over what form, if any, disease transmission should be reduced down to [101], [15], [94], in order to build on previously well understood models throughout this thesis transmission is assumed to be density dependent.

In subsequent models we will introduce the idea of a population within a patch. The definition of a patch, in this context, is a group of individuals which are within close contact with each other, a very small scale example of which would be the individuals within a badger sett. A larger population within each patch, therefore results in an increased contact rate between individuals and hence an increased chance of disease transmission.

The study of epidemics through mathematical modelling has lead to an understanding of the necessary conditions required for a disease to 'take off' and to cause an epidemic to persist within a population. As an example, the model given by equation (1.5) is a simple SI model. In this case, it is assumed that the host does not recover from the disease, the disease is fatal and the infectious period is $1/\gamma$, the parameterγ is therefore the rate at which infected individuals die from their infection. All other parameters in this model are as described above,

$$\begin{aligned} \frac{dS}{dt} &= a - \beta SI - bS \\ \frac{dI}{dt} &= \beta SI - bI - \gamma I. \end{aligned} \tag{1.5}$$

Bovine tuberculosis in the badger population is one example of this type of infection where hosts can live with the disease, but rarely recover from it once infected.

This model has two equilibria, given by (S^*, I^*), the disease free, E_0 and the endemic E_1 where

$$E_0 = \left(\frac{a}{b}, 0\right), \qquad E_1 = \left(\frac{b+\gamma}{\beta}, \frac{b}{\beta}\left(\frac{\beta a}{b(b+\gamma)} - 1\right)\right). \tag{1.6}$$

Equilibrium E_1 is only biologically realistic when it is positive, since a negative population of individuals does not make sense. This is achieved when $\frac{a\beta}{b(b+\gamma)} > 1$. If this inequality is reversed, then the infectious population in this equilibrium becomes negative. We are able to analyse the local stability of these equilibria by considering the Jacobian matrix of this system. The Jacobian matrix is the matrix of partial derivatives of the dynamical system.

Rewriting the system given in (1.5) as

$$\frac{dS}{dt} = f(S, I) \tag{1.7}$$

$$\frac{dI}{dt} = g(S, I), \tag{1.8}$$

the Jacobian of this system is given by

$$J(S, I) = \begin{pmatrix} \frac{\partial f}{\partial S} & \frac{\partial f}{\partial I} \\ \frac{\partial g}{\partial S} & \frac{\partial g}{\partial I} \end{pmatrix}. \tag{1.9}$$

For the system (1.5) the Jacobian is therefore given by

$$J(S, I) = \begin{pmatrix} -b - \beta I & -\beta S \\ \beta I & \beta S - b - \gamma \end{pmatrix}. \tag{1.10}$$

This matrix, evaluated at the equilibrium gives the linearisation of the system at that point. Local stability of the equilibria can be ascertained by looking at the eigenvalues of the Jacobian at that point. Eigenvalues with positive real part mean that any small perturbations from the equilibria will diverge from this point over time. If both eigenvalues are positive, the equilibrium is hence unstable. If both eigenvalues have negative real part, then small perturbations from the equilibrium will decrease over time, and hence their trajectories will return to the equilibrium. In this case, the point is said to be stable. If there is a mixture of eigenvalues with positive and negative real parts, then the equilibrium is said to be a saddle point. In this case, trajectories near to the equilibrium will move away from the point in the positive direction, and towards it in the negative direction. The aim of this thesis is to find the necessary conditions for disease eradication from the systems concerned. This is equivalent to finding the conditions where the disease free equilibrium is stable, and hence where the eigenvalues of the Jacobian, evaluated at the disease free equilibrium, have negative real part.

In the above model, the disease free equilibrium E_0 has eigenvalues $\lambda_1 = -b$, and $\lambda_2 =$

$\beta(a/b) - b - \gamma$. This equilibrium is therefore locally asymptotically stable when

$$\begin{aligned} \frac{\beta a}{b} - b - \gamma &< 0 \\ \frac{\beta a}{b(b+\gamma)} &< 1. \end{aligned} \tag{1.11}$$

Hence, the disease free equilibrium is locally stable precisely when the endemic equilibrium is not biologically relevant. By the same analysis, the endemic equilibrium is found to be stable if this inequality is reversed and

$$\frac{\beta a}{b(b+\gamma)} > 1.$$

This threshold of disease persistence/extinction is also known as the basic reproduction ratio of the infection, denoted R_0, which is defined as 'the expected number of secondary cases produced, in a completely susceptible population, by a typical infected individual during its entire period of infectiousness' [38]. The condition $R_0 > 1$ must therefore be satisfied for an infectious disease to take off in a naive population. The basic reproductive ratio is at the heart of epidemiology, and has been used for many years in the evaluation of control strategies. Since the early 1980s, this quantity has been calculated for, and used in the treatment of many infectious diseases, particularly of humans [7]. Diekmann and Heesterbeek [38] presented a generalisation of the calculation of R_0 to structured populations, whilst Van den Driessche and Watmough [141] presented a general framework for the calculation of R_0 in compartmental ODE models. It has been argued that R_0 is *'the most important quantity in the study of epidemics'* [74]. In equation (1.11), it is clear that for this simple model, the two equations are equivalent, and any control strategy which successfully reduces $R_0 < 1$, also forces the expression $\beta S - \gamma - b < 0$. This expression is thought of as the rare invader approximation [64],[60], and it is this condition which is calculated throughout this thesis. The rare invader approximation gives the dynamics of infection under the assumption that the population is entirely susceptible. The introduction of a very small number of infected individuals in this case will either lead to the spread of infection $\beta S - \gamma - b > 0$, or to the infection to die out before it becomes established $\beta S - \gamma - b < 0$. The majority of mathematical models of disease spread have assumed a single host population where all the individuals interact equivalently with all

others. These traditional homogeneous mixing models [86],[6] have been developed to include elements such as age structure, or multiple species interactions, as reviewed by Hethcote [76] however it is only in recent times that spatial dynamics have been more thoroughly considered. In the following sections, we shall discuss the importance of considering the movement of populations on a spatial scale, the implications of this movement for the spread of infectious disease, along with a review of recent modelling techniques.

1.4 The importance of spatial interactions in population control

1.4.1 Ecological Factors Affecting Dispersal

Dispersal of individuals is an essential trait for living species. The resources available within an area of habitat will only support a given number of adults, and it is often necessary or at least beneficial for a proportion of the population, or the juvenile offspring to disperse to establish their own territories [88]. From a genetic point of view, dispersal is obviously advantageous in terms of genetic diversity. Movement away from the family nest will reduce the inbreeding in a population. Obstacles to natural dispersal have been shown to be deleterious to the genetic variation within a species [49].

Factors which affect dispersal will depend on the species being considered and the landscape inhabited. Wiens [148] suggests that there are two decisions which influence when and how an individual disperses. An individual must decide to begin dispersal, to leave its maternal, home patch in search of new habitat. This may be prompted by factors such as local population density, genetic predisposition, age or reproductive status. The second decision to be considered is the choice to stop dispersing, to settle at an appropriate new patch. The choice of patch may be decided by properties of the habitat which make it particularly suitable, or by the individual's physiological factors such as exhaustion.

It is impossible in a mathematical model to capture the methods of, and motivations for

dispersal generally for all situations. Species may move between patches for different reasons, which may affect how this movement should be modelled. Hansson [71] highlights three categories of factors affecting dispersal. These are firstly migration due to lack of resources. A low supply of food, or nest sites or other resources will lead to movement to other habitats. The second category is the conflict between individuals for resources. This is clearly linked to the first reason, as limited resources will often lead to more conflict. The second category makes explicit the fact that, in this case it is the inferior competitors which will be forced out of the patch. The final category is the interior motivation for migration to avoid inbreeding. This is described as a genetic predisposition to move away from the home patch, and is seen in many species with dispersal varying between sexes depending on the species. In most mammal species it is the male offspring which will usually leave to establish territories, with several females inhabiting an area with only one or relatively few males. Conversely, in many bird species it is the female which will leave the maternal nest in search of mates and territory [65].

In terms of mathematical modelling, the form that migration will take will depend entirely on the biological motivations for the movement. For example, migration could be assumed to occur at a constant rate with a constant proportion of individuals leaving the home patch regardless of the within patch dynamics. This approach is commonly taken in metapopulation models [69], [9]. Alternatively, migration may be dependent on the local conditions, for example the density of the resident population [5]. Hansson suggests [71], intuitively, that if the motivation for movement is a genetic predisposition, then migration is likely to be a constant rate, where migration removes a constant proportion of all juveniles. If migration is influenced by external factors, as in the first and second categories above, then the number of individuals leaving a patch will depend on the resources available to them in their home patch. It seems intuitive to assume that as the density of individuals within a patch increases, the migration out of the patch will also increase, although in some communities of small rodents an inverse relationship has been found with offspring staying in the home patch at high population densities [71]. Many species exhibit the allee effect; there is a minimum population size, below which the population cannot survive [33]. In this case, migration at low population levels would have a detrimental effect, suggesting that there would be a minimum population

size below which migration simply does not occur.

The benefits a species gains in choosing to migrate must be weighed against the costs of dispersal. There is no guarantee, when leaving an area of habitat, that the individual will find other suitable habitat in which to nest or forage etc. In some species then there may be an evolutionary trade-off between the ability to migrate, and cope with the possibility of less favourable habitats and the effects of inbreeding depression.

1.4.2 Mathematical modelling of spatial dynamics

All of the models previously discussed are based on the assumption that the interactions between individuals are homogeneous, i.e. all individuals mix randomly with all others in the population. However, in a world where many species naturally live in closely connected social groups such as familial clans (e.g badgers [8]) or high density nests (e.g social insects such as bumblebee species [59]), and many more populations are forced into fragmented groups due to habitat fragmentation [50], it is important to realise the impact of spatial structure in population dynamics and the transmission of disease. Kareiva [83] detailed three common approaches to mathematical modelling of spatial population dynamics. Firstly continuum modelling views space as a constant variable and models the movement of individuals as through reaction-diffusion type equations [112], [78]. These models take the form of partial differential equations, and are often given by

$$\frac{\partial u(x,t)}{\partial t} = f(u(x,t)) + D\frac{\partial^2 u(x,t)}{\partial x^2}. \tag{1.12}$$

This form assumes that all individuals within a population move randomly, and at the same rate regardless of space or time [78]. Here D is the diffusion coefficient, giving the rate of dispersal of individuals across the spatial environment. Reaction diffusion modelling of spatially explicit populations has been an important facet of spatial modelling, being used for a wide range of applications for example, biological invasions [125] or pathogen dispersal [146]. The second category of spatial models are stepping stone models, where the population is subdivided into patches, which have a specific location [87]. In these models, the spatial distribution

of patches is explicitly defined, with individuals only permitted to move to their immediate neighbours. In this way, the distance between patches can be defined as the number of 'steps', and the difference between long and short range movement can be analysed. Stepping stone models are commonly used in terms of genetic drift, and in the field of population dynamics this type of model may fall under the umbrella of 'metapopulation model'. This is the third and final type of spatial model as specified by Kareiva [83]. These models do not necessarily, explicitly define the spatial location of the patches that the population is divided into, rather distinct populations are coupled through dispersal. It is common in these models to assume that the patches are fully connected, and individuals leaving each patch have an equal probability of entering any of the other patches in the metapopulation. Of these broad categories, the work presented in this thesis falls most comfortably into the metapopulation domain.

Metapopulation modelling began in earnest in the 1960s with the Levins model [91], [92]

$$\frac{dp}{dt} = mp(1-p) - ep. \tag{1.13}$$

This ODE model follows the change over time of $p(t)$, which is the fraction of habitat patches in a system which are occupied at time t. This fraction is determined by the local extinction rate e, and the local colonisation rate of empty patches m. In this original model, the within patch population dynamics were not considered, rather patches were characterised by the presence or absence of a species. Levins' model has been widely used in the ecological literature [142], [70], [89] and developed to incorporate the local population dynamics within a patch [68], [10]. This approach, coupled with a rich literature in network theory and analysis [34], has lead to metapopulation models being used in many applications such as the spread of cholera after the Haitian earthquake in 2010 [138], and in the control of foot and mouth disease in the UK [85], [52]. The work presented in this thesis aims to evaluate the impact the culling or harvesting strategies has on the local populations within a patchy metapopulation. It is therefore essential for this purpose, that local population dynamics are modelled explicitly. This work evaluates the importance of combined harvesting or culling strategies where neighbouring patches of habitat are controlled independently, and hence the space considered is divided into discrete

areas, rather than being modelled as a continuous landscape.

1.5 Disturbance and spatial perturbation in response to control

As well as considering the effects of spatial structure on local population and disease control, this thesis takes a novel approach to modelling the impact of spatial perturbation or disturbance of individuals in response to human intervention. Throughout this thesis, the terms 'spatial perturbation' and 'disturbance' are used interchangeably, to mean a change in behaviour of individuals in response to the culling or harvesting activities. This effect has most commonly been discussed in reference to badger populations culled for the control of bovine TB [102],[139]. The perturbation effect, defines the increase in disease incidence in response to culling strategies, and was observed during the randomised badger culling trial, which aimed to evaluate the effectiveness of badger culling as a method of TB control in cattle [150],[42],[43]. As well as the implications of human disturbance with respect to disease control, there is a rich literature of the impact of disturbance in terms of conservation strategies for many species [55]. In particular studies have detailed the impact of human disturbance on the breeding success of sea birds such as kittiwakes *Rissa tridactyla* and guillemots *Uria aalge* [12]. A study by Thomas also found that human visits disturbed hibernating little brown (*Myotis lucifugus*), and northern long eared (*Myotis septentrionalis*) bat species, causing a marked increase in flight activity [132].

Despite the implications of spatial perturbation, this effect is a factor which is largely overlooked, with models assessing the impact of control strategies in isolation whilst neglecting the explicit effects of disturbance. Swinton *et. al.* (1997) investigated this perturbation effect for a badger population by assuming that transmission of bovine tuberculosis increased with removal of individuals [129], and a recent PhD thesis by Prentice [114], addresses the problem more generally in a stochastic, spatial framework, however to date there has been no thorough investigation of the general effects of perturbation on simple deterministic population or disease models. We incorporate this phenomenon into the simple patch models as an increase

in movement rate directly dependent on the rate of control applied.

1.6 Thesis plan and outline

The models presented throughout this thesis have been developed to assess the importance of the effects of spatial coupling, and disturbance on both population and disease control strategies. In terms of population control, we will investigate two main issues. Firstly the impact of coupling and spatial perturbation on the conditions necessary to cause population extinction, addressing the question of whether disturbance makes it easier or harder to drive a population extinct. Secondly, we address the impact of perturbation on the yield obtained from simple harvesting models. In terms of disease control, we will investigate the impact of coupling and disturbance on the necessary conditions for disease eradication. This takes the form of threshold analysis and involves approximating the disease thresholds through numerical simulations. The effect of the form of movement or coupling of patches is also discussed, with a comparison between a constant per capita rate of movement, and a density dependent rate. This thesis is broken into the following chapters

1. **Chapter 2: Harvesting populations with constant movement**

   Here we present two basic population models, a constant recruitment and a logistic growth model over two distinct patches. We assume that the populations in each patch are coupled through the movement of individuals, which occurs at a constant per capita rate in the absence of harvesting. Spatial perturbation is then included into these models in two ways. Firstly we assume that movement out of the patch increases linearly with the harvesting effort applied, and secondly we assume this increase saturates at high levels of harvesting.

2. **Chapter 3: Disease control in coupled patches with constant movement (published in Journal of Theoretical Biology (2013))**

   This chapter presents an SI model over two patches coupled by constant movement. We evaluate the effect of two forms of spatial perturbation (linear and saturating) on the pathogen exclusion thresholds. In this case, the perturbation effect increases with the total number removed, rather than simply the effort applied. This model is then ex-

tended to a two host model where one species is free ranging and the other is restricted. This model is loosely based on the transmission of bovine tuberculosis between cattle and badgers.

3. **Chapter 4: Harvesting populations with density dependent movement**

   In this chapter we relax the assumption of constant dispersal or movement between the patches. We investigate the behaviour of both the constant recruitment and the logistic model for a density dependent dispersal function. It is assumed that individuals are more likely to leave a patch if the population density is high, and more likely to remain in a sparsely populated patch. We then investigate the addition of linear spatial perturbation on both these cases.

4. **Chapter 5: Disease control in populations with density dependent movement**

   Here we investigate the spread of disease throughout a two patch system governed by the form of density dependent dispersal detailed in chapter 4. We present both the necessary conditions for disease eradication, as well as the effect of density dependent movement on the transient dynamics of the populations both with and without spatial perturbation.

5. **Chapter 6: Optimal control of disease in 2 and 3 patches**

   This chapter presents a discussion of the optimal disease control strategy in the coupled system. Using Lagrangian optimisation techniques we aim to determine the control strategy which minimises the effort applied, and maximises the population size remaining. This is done in the two patch model before being extended to a three patch system, where we consider a fully connected configuration, and a linearly connected configuration.

Chapter 2

Harvesting populations in patchy environments with constant dispersal

2.1 Introduction: Why dynamics of harvesting is important

Resources may be harvested for a number of reasons. The definition of the term 'resource' is used in its widest sense here, referring to a supply of a substance (living or not) which has some benefit to humans. Types of benefit may include financial (for example precious metals), nutritional (crops, livestock etc), environmental (conservation of endangered species, rainforests, etc), or to provide energy (e.g. fossil fuels). It is inevitable that non-renewable resources will decline monotonically as a result of harvesting, hence the need to invest in alternatives in the event of supplies running out. However, harvesting of renewable resources requires a more subtle approach. Renewable resources will regenerate, and continue to be produced given appropriate conditions. Harvesting of these resources can therefore be done sustainably in order to maintain the resource at appropriate levels.

Addressing what the appropriate levels of harvesting may be is not trivial, particularly when harvesting refers to the removal of a proportion of a living population. Shea [124] discusses

the management of animal populations with respect to the sometimes conflicting areas of conservation, harvesting and control. The driving concerns when removing individuals from a population will differ depending on the reasons for removal. Conservation will be concerned with preventing species extinction, harvesting will be concerned with financial benefit, and obtaining the maximal, sustainable yield, and control will be constrained by reducing the population beyond some threshold. Population control may be carried out for a number of reasons, including pest control [131], the reduction of species densities to protect prey species or vegetation [126], or in order to control the spread of infectious diseases. Consideration of population control requirements alongside conservation efforts is required in order to achieve the desired result without forcing the controlled population to extinction.

Throughout this chapter we aim to evaluate the effect of harvesting or culling on a living population, initially we consider a single population distributed homogeneously throughout an environment, and offer a review of the maximal sustainable yield in this system. This is then extended to a single species inhabiting a patchy environment consisting of two patches, with dispersal between the patches occurring. Finally, this chapter addresses the impact that the response to disturbance caused by harvesting activity has on the yield obtained by that activity.

2.2 Basic Modelling: Single harvested population

Modelling the interaction of natural regeneration and harvesting effort is done in a basic way by a single ordinary differential equation of the form

$$\frac{dN}{dt} = f(N) - c(N), \tag{2.1}$$

as seen in Britton [27] and Murray [105]. If, on average, individuals survive in the population for a time of $1/c$ prior to harvesting, then the harvesting rate can be given by a constant term c and is a measure of the effort put into harvesting per unit time. The number removed per unit time, or the yield, is then given by cN. The growth function $f(N)$ may take any relevant form. Here we consider two density dependent growth functions, firstly a constant

recruitment model with a per capita death rate, and secondly a logistic growth model with density dependent births.

2.2.1 Constant Recruitment

In the constant recruitment model, it is assumed that the population size is limited by the available resources. This formulation entails the assumption that births or recruitment into the population occur at a constant rate, which is density independent. Death, and therefore removal from the population occurs at a constant per capita rate, and the number removed per unit time therefore increases with population density. In this case equation (2.1) is given by

$$\frac{dN}{dt} = a - bN - cN \tag{2.2}$$

This type of model is particularly relevant in open populations such as marine systems where local production of offspring can have little effect on the overall growth rate, with new recruits mainly coming from outside the population [30]. Constant recruitment models may also be relevant for farmed stocks such as fisheries where the recruitment or stocking is managed [103].

In this model, in the absence of harvesting, the population reaches a natural equilibrium at $N = a/b$. Due to the constant recruitment into the population, this model has no zero equilibrium, and the population can never go extinct. The effect of harvesting therefore causes a reduction in population to a lower equilibrium of $N = a/(b + c)$ which tends to 0 as $c \to \infty$ and causes a reduction in equilibrium by half when $c = b$. This model however encounters the problem that it requires an infinite amount of removal to harvest or cull the population to extinction. Once harvesting is stopped the population will regenerate. This is perhaps not as unrealistic as it initially seems. Areas which have a low, or non-existent population due to over culling may regenerate in the absence of control due to the influx of individuals from surrounding areas making use of the low population density, and hence low competition levels and the resulting abundance of available resources.

2.2.2 Logistic Growth

The second growth function considered is the well documented logistic growth

$$f(N) = rN\left(1 - \frac{N}{K}\right)$$

where K is the carrying capacity of the environment. Here the population grows rapidly for small populations, but growth slows as the population gets larger eventually reaching an equilibrium when $N = K$. This growth rate incorporates the idea that the rate of reproduction of a population within an area, and therefore the population size is dependent on the amount of resource within that area. The resource can only support a finite number or density of individuals, hence the growth of the population slows as this maximum carrying capacity is reached. In this case, equation (2.1) is given by

$$\frac{dN}{dt} = rN\left(1 - \frac{N}{K}\right) - cN \tag{2.3}$$

This model has been discussed in detail by Murray [105], and Beddington *et al.* [14] and has equilibria at $N = 0$ (extinction) and $r(1 - N/K) = c$, when harvesting balances the natural growth rate. In this case, the harvested equilibrium is achieved at $N^* = K(1-c/r)$. It is clear that when $c > r$, then this equilibrium is negative, and stability analysis confirms that there is a transcritical bifurcation at $c = r$, as shown in figure 2.1. The yield, given at equilibrium by $Y = cN^*$ is found to be $Y = Kc - Kc^2/r$ which attains its maximum value when $c = r/2$ as shown in figure 2.2. Harvesting this population at the maximum sustainable rate gives a maximum sustainable yield of $Y_{max} = rK/4$ and leads to a reduction in population size from $N = K$ to $N = K/2$. This result suggests the counter-intuitive idea that, if the growth rate is large enough, $r > 2$, then it is possible to reduce the population to $K/2$, whilst attaining a yield $Y_{max} > K/2$. This is a consequence of the strength of density dependence acting on the growth rate. At low densities, the population regenerates at a high enough rate, that over half of the population can be removed to maintain the equilibrium at $K/2$.

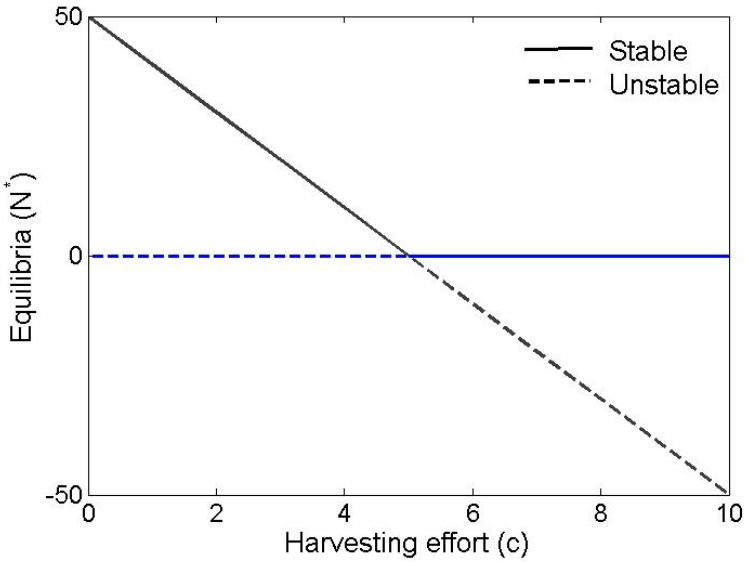

Figure 2.1: Bifurcation diagram showing change in stability at $x = r = 5$. when $c < r$ harvested population is stable, when $c > r$, zero equilibrium is stable and population is extinct.

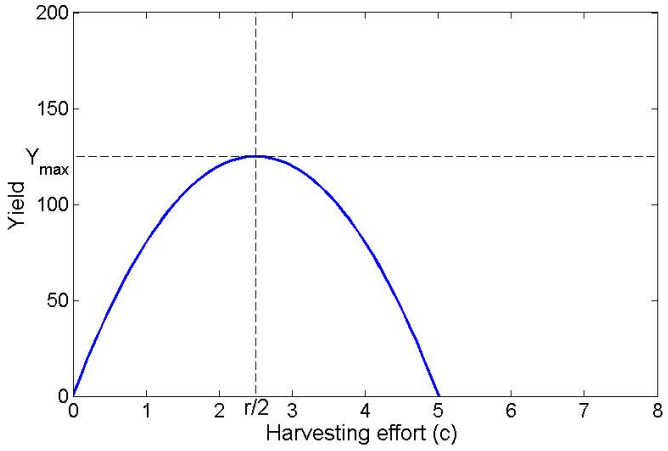

Figure 2.2: Yield obtained from logistic model with $r = 5$.

2.3 Harvesting and yield in two coupled patches

2.3.1 Dynamics of coupled patches

The simplest way to model spatial heterogeneity of populations is to simply split the single population over two patches. Within each patch, the population will grow according to a given growth function $f_i(N_i)$, where $f_i'(N_i) < 0$ such that the intrinsic growth rate slows as the population increases. The general two patch model without harvesting is thus given by

$$\frac{dN_1}{dt} = f_1(N_1) - m_1 N_1 + m_2 N_2 \tag{2.4}$$

$$\frac{dN_2}{dt} = f_2(N_2) - m_2 N_2 + m_1 N_1 \tag{2.5}$$

where m_i is the constant per capita rate of movement out of patch i and into patch j. The carrying capacity of each patch, K_i, is thought of as the stable population size of the patch in isolation. Transition of individuals between patches is likely to change this equilibrium such that a patch with a large number of immigrants will swell to higher numbers than a patch with low immigration rates. Holt [79] detailed the behaviour of this model if movement between patches occurs at equal rates, finding that as $m_1 = m_2 = m \to \infty$, both patches tend to a common size. That is, increasing the rate of movement between patches has a homogenising effect. A summary of Holt's analysis is given below. We then show that the equal dispersal case can be extended to give limiting properties if movement is asymmetric where $m_1/m_2 = \phi$.

Taking the general model given in (2.4-2.5) with $m_1 = m_2 = m$, Holt [79] found conditions on the equilibrium values of the populations by taking the sum and the difference of these equations at equilibrium, giving

$$f_1(N_1) = -f_2(N_2) \tag{2.6}$$

$$2m = \frac{f_1(N_1) - f_2(N_2)}{N_1 - N_2} \tag{2.7}$$

These conditions are represented graphically, for logistic growth, in Figure 2.3. In this fig-

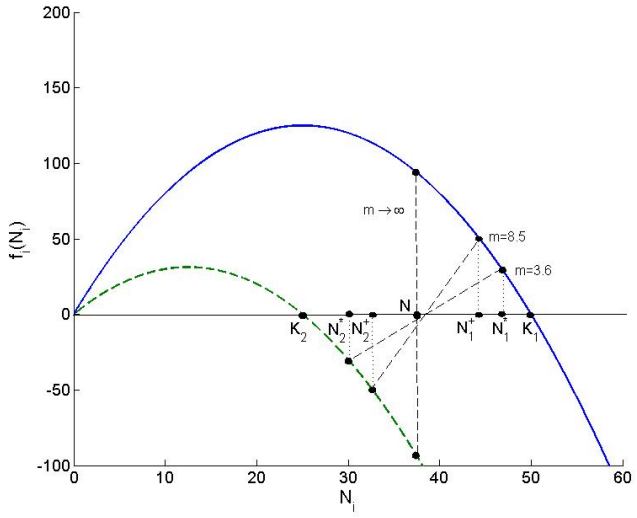

Figure 2.3: Change in growth rate as population size increases. Solid line represents growth of patch 1, dashed line growth of patch 2, with patch 1>patch 2. If $m = 0$ equilibria are at K_1 and K_2. As m increases equilibrium from patch 1 decreases from K_1 to N_1^* as $m = 3.6$ and N_1^+ as $m = 8.5$. The equilibrium in patch 2 increases from K_2 to N_2^* at $m = 3.6$ and N_2^+ at $m = 8.5$. As m increases to infinity the equilibria in both patches tend to a common intermediate value.

ure, each curve shows the growth of a single patch as a function of population size. Condition 2.6 implies that the system is in equilibrium when the y-value of one curve is equal to the negative y-value of the second. When this is the case, the corresponding x-co-ordinates give the equilibrium values. Furthermore, the gradient between these two equilibrium points is proportional to the movement rate between the patches. Therefore, if there is no movement in the system then each patch is at equilibrium at its respective carrying capacity. As movement increases, the larger patch reduces in size and the smaller patch increases until both patches attain a common patch size of

$$\mathbf{N_C} = \frac{a_1 + a_2}{b_1 + b_2}$$

in the constant recruitment model, and

$$\mathbf{N_L} = \frac{r_1 + r_2}{r_1/K_1 + r_2/K_2}$$

in the case of logistic growth. Using these common values, we are able to determine whether coupling the patches causes a change in the total population, at least as $m \to \infty$. In the case

of constant recruitment, in the absence of coupling, the total population is given by

$$T_0 = \frac{a_1}{b_1} + \frac{a_2}{b_2}.$$

In the limit as $m \to \infty$, the total population is $T_\infty = 2\mathbf{N_C}$. The difference between these totals is therefore

$$\begin{aligned} T_{diff} =& T_\infty - T_0 \\ =& \frac{2(a_1 + a_2)}{b_1 + b_2} - \left(\frac{a_1}{b_1} + \frac{a_2}{b_2}\right) \\ =& \frac{(b_1 - b_2)(b_2 a_1 - b_1 a_2)}{b_1 b_2 (b_1 + b_2)}. \end{aligned} \tag{2.8}$$

$T_{diff} = 0$ if either $b_1 = b_2$, hence the death rates of both patches are equal, or $a_1/b_1 = a_2/b_2$ and the equilibria of the patches in the absence of movement are equal, hence the patches will support the same number of individuals. If neither of these conditions are satisfied, then

$$T_{diff} \begin{cases} < 0, \text{ if } b_i > b_j \ \& \ \frac{a_j}{b_j} > \frac{a_i}{b_i} \\ > 0, \text{ if } b_i > b_j \ \& \ \frac{a_i}{b_i} > \frac{a_j}{b_j} \end{cases} \tag{2.9}$$

If $T_{diff} < 0$, then the coupled total is less than the total population of the two isolated patches. If $T_{diff} > 0$, then coupling the patches increase the total population as $m \to \infty$.

Extending the Holt model to include asymmetric movement rates we see that this analysis no longer applies. Asymmetric movement rates are characterised here by their ratio $m_1/m_2 = \phi$, where $m_2 = m$, and $m_1 = \phi m$. A value of $\phi < 1$ therefore implies that $m_1 < m_2$, with this condition reversed if $\phi > 1$. It is possible to show that as the basic rate of movement, m increases, then the ratio of the populations at equilibrium, $N_1/N_2 \to 1/\phi$, and hence

$N_1/N_2 \to m_2/m_1$. This result is shown by simply rearranging equation (2.4) giving

$$0 = f(N_1) - \phi m N_1 + m N_2 \tag{2.10}$$

$$\phi m N_1 = f(N_1) + m N_2 \tag{2.11}$$

$$\frac{N_1}{N_2} = \frac{f(N_1)}{\phi m N_2} + \frac{1}{\phi}, \qquad \to \frac{1}{\phi} \quad \text{as} \quad m \to \infty. \tag{2.12}$$

This has the intuitive consequence that if $\phi < 1$, so movement out of patch 1 is less than movement out of patch 2, then the population size in patch 1 is greater than that of patch 2 and vice versa. The ratio of the two patches at equilibrium as $m \to \infty$ is therefore independent of the growth rates within the patches.

2.3.2 Harvesting in coupled patches

In reality, harvesting within a connected patch system will impact not only the patch being directly harvested, but also the surrounding areas. Removing individuals from an area will reduce the number of migrants to the surrounding regions. Here we discuss harvesting in a coupled system in terms of both the effort required and a given yield and the reduction in harvested population. We look specifically at the two growth functions detailed in the single species case: constant recruitment and logistic growth.

Constant recruitment model over two patches

In the first case, we extend the model with constant recruitment (2.2) to two coupled patches, both of which have growth functions of this form. This full model is given by

$$\frac{dN_1}{dt} = a_1 - b_1 N_1 - m_1 N_1 + m_2 N_2 - c_1 N_1 \tag{2.13}$$

$$\frac{dN_2}{dt} = a_2 - b_2 N_2 - m_2 N_2 + m_1 N_1 - c_2 N_2. \tag{2.14}$$

In the absence of any movement or harvesting between the patches, each patch reaches its equilibrium at $N_i = a_i/b_i$. As movement between the patches increases, the larger patch gets smaller and the smaller patch increases. If both patches are equal, then symmetric movement will not affect the equilibria. The general expression for the equilibrium, in the absence of

any harvesting is given by

$$N_i^* = \frac{a_i(b_j + m_j) + a_j m_j}{(b_1 + m_1)(b_2 + m_2) - m_1 m_2}$$

which, as movement increases, is limited by $N_i = (a_1 + a_2)/(b_1 + b_2)$. The first question to address here is the issue of yield for a given effort. In the single patch model, with constant harvesting effort c, the population reaches equilibrium at $N^* = a/(b + c)$, and the yield is given by

$$Y(c) = \frac{ac}{b + c}$$

hence the yield increases with effort, and saturates at a maximum of $Y(\infty) = a$. This yield equates to removing all individuals as soon as they enter the population. In the coupled system, harvesting of a single patch whilst leaving the second patch untouched ($c_1 > 0, c_2 = 0$), gives a yield of

$$Y_1(c_1, 0) = c_1 N_1^* = \frac{c_1(a_1 b_2 + (a_1 + a_2)m_2)}{c_1(b_2 + m_2) + (b_1 + m_1)(b_2 + m_2) - m_1 m_2}.$$

In this case the yield saturates at

$$Y_1(\infty, 0) = \frac{a_1 b_2 + (a_1 + a_2)m_2}{b_2 + m_2}$$

as $c_1 \to \infty$. Hence coupling of the two patches sees an increase of yield for a given effort in comparison to the yield of a single patch. Rewriting this expression for the limit of the yield gives

$$Y(\infty, 0) = a_1 + a_2 \left(\frac{m_2}{m_2 + b_2} \right)$$

which can be thought of as removal of all those born into patch 1, a_1, plus those born in patch 2 multiplied by the probability of moving from patch 2 to patch 1, $a_2(m_2/(m_2 + b_2))$. In this limit, the population in patch 1 is effectively zero, since all individuals are removed as soon as they enter the patch. The equilibrium population in patch 2 is given by

$$N_2^* = \frac{a_2(b_1 + m_2 + c_1) + a_2 m_1}{c_1(m_2 + b_2) + (m_1 + b_1)(m_2 + b_2) - m_1 m_2}$$

which as $c_1 \to \infty$ reduces to

$$N_2^* = \frac{a_2}{m_2 + b_2}.$$

Hence this population can also be significantly reduced if movement out of patch 2 is large enough. Harvesting of the population within a single patch can hence have a serious effect on the coupled population.

If harvesting occurs in both patches, then the yield in a given patch will be dependent on the harvesting effort in both patches. The yield in patch i is therefore given by

$$Y_i(c_1, c_2) = \frac{c_i(a_j m_j + a_i(b_j + m_j + \mathbf{c_j}))}{(b_2 + m_2 + \mathbf{c_2})(b_1 + m_1 + c_1) - m_1 m_2} \tag{2.15}$$

with the expressions highlighted in bold showing the additional effect of a joint harvesting strategy on the yield in patch i. The total yield if both patches are harvested is then given by

$$Y_T = Y_1 + Y_2 = \frac{(a_1 b_2 + (a_1 + a_2)m_2)c_1 + (a_2 b_1 + (a_1 + a_2)m_1)c_2 + (a_1 + a_2)c_1 c_2}{(b_2 + m_2 + c_2)(b_1 + m_1 + c_1) - m_1 m_2} \tag{2.16}$$

The change in yield as c_1 and c_2 increase is given in figure 2.4(a) in which it is clear that the total yield is bounded above, and $Y_T \to a_1 + a_2$ as $(c_1, c_2) \to (\infty, \infty)$. This upper limit is expected since $a_1 + a_2$ is the total influx of new individuals into the system per unit time. A yield of $a_1 + a_2$ is hence a complete removal of all individuals in this constantly replenishing, or stocked system. The single patch yield, given by (2.15) tends to

$$Y_1(c_1, \infty) = \frac{c_1 a_1}{b_1 + m_1 + c_1}$$

as $c_2 \to \infty$. This is also expected, since this limit equates to the yield in patch 1, with a constant emigration rate, and no immigrants. Figure 2.4 (a) shows this limiting behaviour, but also highlights the decrease in yield as harvesting in patch 2 increases from $c_2 = 0$.

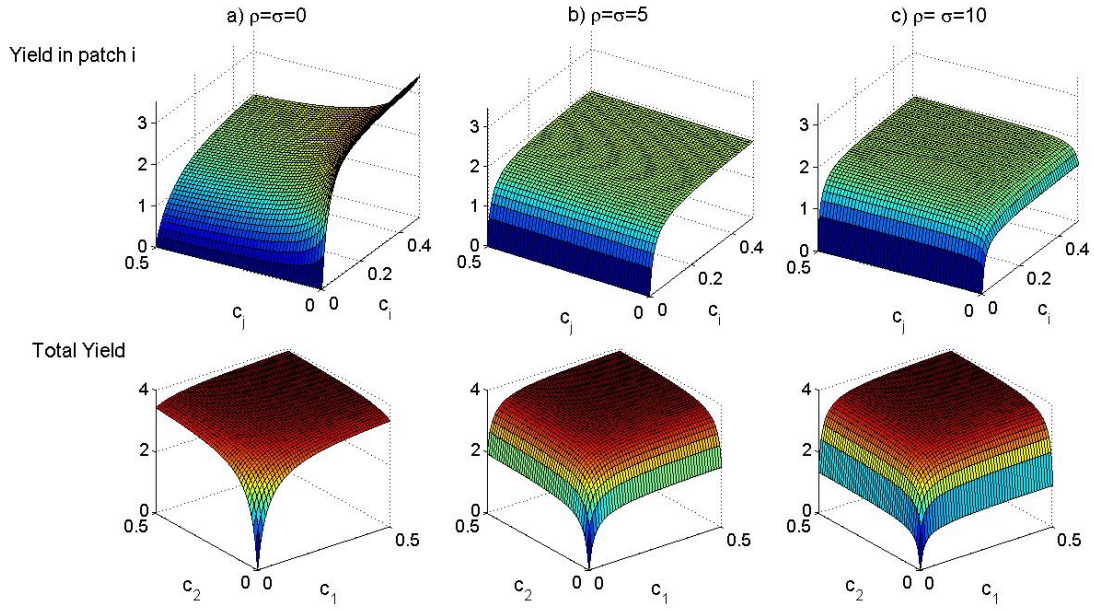

Figure 2.4: Change in yield as harvesting effort in both patches varies and linear disturbance increases. Top row shows the change in yield of a single patch, whilst the bottom row shows the change in total yield. 3 strengths of linear disturbance are shown, a) No disturbance, constant movement model, b) weak disturbance $\phi = m_j/b$, c)strong disturbance $\phi > m_j/b$. Parameters used $a_i = 2, b_i = 0.02, m_i = 0.1$

Constant recruitment model with spatial perturbation

The operation of harvesting or culling a mobile population can cause significant disturbance to the remaining population. In response to harvesting or culling practices, many wildlife species have been found to increase their ranging behaviour [139], [1],[122], and subsequently increase contact with surrounding areas. In the model above, we are able to incorporate this spatial perturbation by replacing the constant rate of outward movement, m_1, m_2 with the increasing functions $M_1(c_1), M_2(c_2)$ which are dependent on the harvesting effort applied within each patch c_1, c_2. We define this function to be such that it satisfies $M_1(0) = m_1$ and $M_1'(c_1) \geq 0$ and similarly for patch 2. Once again we examine the yield produced in this model, firstly if only a single patch is harvested, and secondly if harvesting pressure is applied to both patches.

Whilst the precise nature of this movement function is unknown, and very possibly different for different species, an increase in emigration rates away from areas of culling have been observed in several systems from populations of elephants in South Africa [1], to badgers

in the UK [150]. We propose and compare two simple functions to capture this increase in emigration. Firstly we assume that the rate of emigration increases linearly with the harvesting rate. At very high harvesting rates, this model is unrealistic since the decision to move permanently away from the home patch in response to an external stimulus will take time. The second movement function we propose is therefore a Holling Type II response which saturates as harvesting rates increase.

If patch 1 alone is harvested, then in addition to the removal of individuals due to harvesting, movement out of patch 1 will also increase. Harvesting thus has a two-fold effect in terms of population reduction. The yield achieved in patch 1 is thus reduced by this increase of emigration, and becomes

$$Y_1(c_1, 0) = \frac{c_1(a_1 b_2 + (a_1 + a_2)m_2)}{c_1(b_2 + m_2) + (b_2 + m_2)(b_1 + M_1(c_1)) - m_2 M_1(c_1)},$$

which, as $c_1 \to \infty$, tends to

$$Y_1(\infty, 0) = a_1 \left(\frac{b_2 + m_2}{b_2 + m_2 + b_2 L} \right) + a_2 \left(\frac{m_2}{b_2 + m_2 + b_2 L} \right)$$

where $L = \lim_{c_1 \to \infty} M_1(c_1)/c_1$. This value is less than the constant movement yield given above if $L > 0$. Figure 2.4 illustrates this property, when $c_j = 0$, the yield decreases along the c_i axis as the strength of disturbance increases (from (a) to (b) to (c))

If harvesting pressure is applied to both patches, then the total yield, given by

$$Y_T(c_1, c_2) = \frac{c_1(a_1 b_2 + (a_1 + a_2)M_2(c_2)) + c_2(a_2 b_2 + (a_1 + a_2)M_1(c_1)) + (a_1 + a_2)c_1 c_2}{(b_1 + M_1(c_1) + c_1)(b_2 + M_2(c_2) + c_2) - M_1(c_1)M_2(c_2)} \tag{2.17}$$

once more reaches an upper limit of $a_1 + a_2$ as $(c_1, c_2) \to (\infty, \infty)$. Whilst this limit in the extreme is the same regardless of the effect of disturbance, for moderate, and realistic harvesting strategies, the yields can be different. In order to show this behaviour we investigate two specific examples of movement functions. We compare the behaviour given both a linearly increasing and a saturating disturbance function as harvesting effort is increased. These functions are shown in figure 2.5

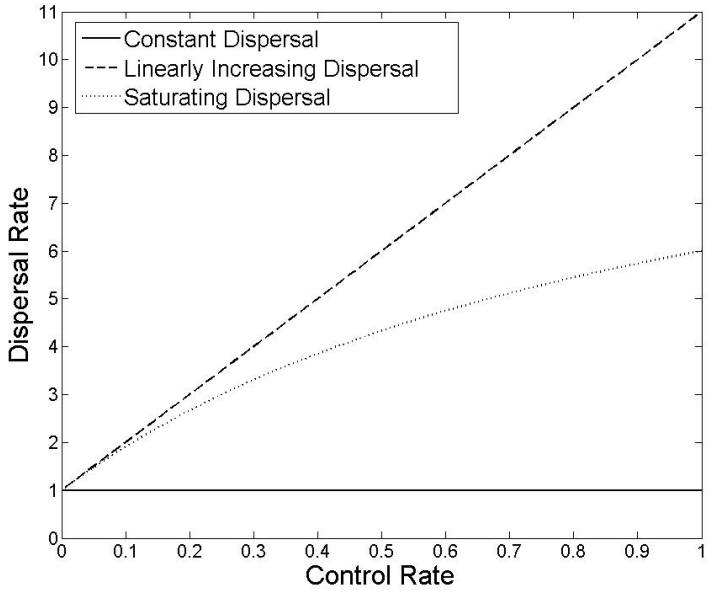

Figure 2.5: Illustration of the different disturbance functions described in the text as harvesting or population control rate increases.

Linear Disturbance

Firstly we assume that movement increases linearly with harvesting effort, with the specific functions in this case given by $M_1(c_1) = m_1 + \sigma c_1$ and $M_2(c_j) = m_2 + \rho c_j$ where σ and ρ measure the strength of disturbance. In the following sections, we assume for simplicity, that $a_1 = a_2 = a$ and $b_1 = b_2 = b$, and hence the patches are equal in demographic properties. In the case of linear perturbation, the individual patch yields and the total yield are given by

$$Y_1(c_1, c_2) = \frac{ac_1(b + 2m_2 + 2\rho c_2 + c_2)}{(b + m_1 + \sigma c_1 + c_1)(b + m_2 + \rho c_2 + c_2) - (m_1 + \sigma c_1)(m_2 + \rho c_2)}, \tag{2.18}$$

$$Y_2(c_1, c_2) = \frac{ac_2(b + 2m_1 + 2\sigma c_1 + c_1)}{(b + m_1 + \sigma c_1 + c_1)(b + m_2 + \rho c_2 + c_2) - (m_1 + \sigma c_1)(m_2 + \rho c_2)}, \tag{2.19}$$

$$Y_T(c_1, c_2) = \frac{ab(c_1 + c_2) + 2a(m_1 + m_2) + 2a[\sigma c_1 c_2 + \rho c_1 c_2 + c_1 c_2]}{b(b + m_1 + m_2 + \sigma c_1 + \rho c_2) + c_1 m_2 + c_2 m_1 + (\sigma c_1 c_2 + \rho c_1 c_2 + c_1 c_2)}. \tag{2.20}$$

Figure 2.4 shows the change in yield in patch 1 alongside the total yield for varying c_1 and c_2, as the strength of disturbance increases. Here we assume that disturbance acts equally within each patch, hence $\sigma = \rho$. It is clear from this figure that for low $\sigma = \rho$, that is a weak level of disturbance (figure 2.4 a), the yield obtained in patch 1 begins high when $c_2 = 0$ and

decreases as harvesting in the second patch increases. This decrease in yield in patch 1 as harvesting in patch 2 increases is due to the reduction in immigration into patch 1 as the coupled population is reduced. As the strength of disturbance increases (figure 2.4 b) and c)), the initial yield, with $c_2 = 0$ is lower and harvesting of the patch 2 actually causes an increase in the patch 1 yield. Differentiating the yield in patch 1, $Y_1(c_1, c_2)$ with respect to c_2, we are able to show that

$$\frac{dY_1}{dc_2} = \frac{ac_1(b + c_1 + 2m_1 + 2\sigma c_1)(b\rho - m_2)}{[(b + m_1 + \sigma c_1 + c_1)(b + m_2 + \rho c_2 + c_2) - (m_1 + \sigma c_1)(m_2 + \rho c_2)]^2} \tag{2.21}$$

which is positive for $\rho > m_2/b$ and negative for $\rho < m_2/b$. Biologically, these parameter groupings suggest that if the rate of linear disturbance out of patch 2 is greater than the ratio of outward movement to natural death of patch 2, then a joint harvesting effort across both patches will cause an increased yield in patch 1. This is a result of the relatively high level of disturbance. If there is no harvesting in patch 2, then individuals are forced out of patch 1 at an increased rate, but only move into patch 1 at the natural baseline rate m_2. The net effect of this movement will lead to a significantly smaller patch size, and hence a reduction in single patch yield (when $c_2 = 0$) as $\rho = \sigma$ increases. When $\rho > m_2/b$, then any level of harvesting in patch 2 will force individuals into patch 1 at a rate high enough to significantly increase the population in patch 1 and hence increase yield.

Saturating Disturbance

If the movement function saturates with increasing harvesting effort, then the situation is analytically more difficult. In this case, we use the example functions $M_1(c_1) = m_1 + \sigma c_1/(1+c_1)$ and $M_2(c_2) = m_2 + \rho c_2/(1+c_2)$. In these cases, as effort increases to infinity, $M_1(c_1) \to m_1 + \sigma$ and $M_2(c_2) \to m_2 + \rho$. The change in yield for this model as the strength of disturbance $\rho = \sigma$ increases is given in figure 2.6. In this case, as the strength of disturbance increases, the initial yield in patch 1 ($c_2 = 0$) decreases. However, whereas in the linear disturbance model, a low initial yield grows/declines monotonically to a maximum/minimum, as harvesting in patch 2 increases, when movement saturates we see for a given c_1, an increase in yield with increasing c_2 up to a maximum, followed by a decrease. The yield in patch 1 for fixed harvesting effort

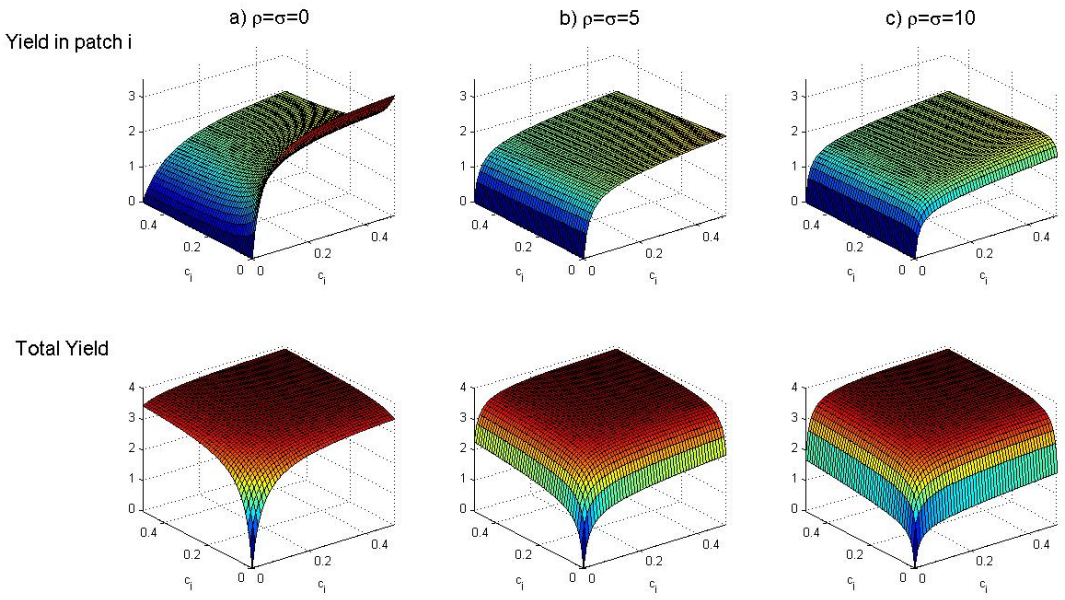

Figure 2.6: Change in yield as harvesting effort in both patches increase for saturating disturbance levels for increasing strength of disturbance. Top row shows the change in yield of a single patch, whilst the bottom row shows the change in total yield. 3 strengths of saturating disturbance are shown, a) No disturbance, constant movement model, b) weak disturbance, c)strong disturbance. Parameters used $a_i = 2, b_i = 0.02, m_i = 0.1$

c_1, as harvesting effort in patch 2 c_2 increases is given in figure 2.7. The behaviour of the yield in this model as c_2 increases is explained as follows. For very low or zero c_2, the increased strength of disturbance forces more individuals out of patch 1 and hence results in a drop in yield in patch 1 at $c_2 = 0$ for increasing $\rho = \sigma$. However, for small levels of harvesting in patch 2, if $c_2 < c_1$, the disturbance in patch 2 causes an increase in immigrants to patch 1 and hence an increase in equilibrium and yield. As c_2 increases further, $c_2 > c_1$, the harvesting effort in patch 2 exceeds that in patch 1 and hence the number of immigrants to patch 1 from patch 2 decreases and so the yield decreases. The models examined above assume that disturbance is caused simply by applying an increased harvesting effort. However, in many cases, particularly structured populations or compartmental models, where a specific age or disease class is targeted for harvesting, it may be reasonable to assume that the level of disturbance increases with total number of individuals removed, rather than just the effort applied. This is the approach taken in chapters 3 and 5, when modelling the impact of spatial disturbance on disease spread. When disturbance is modelled in this way, the yields of both patches show

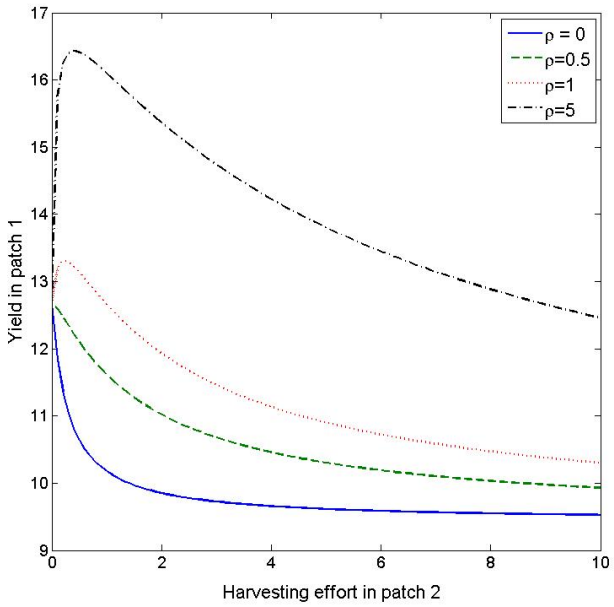

Figure 2.7: Change in yield in patch 1 for $c_1 = 5$ as strength of saturating disturbance increases. For high levels of disturbance the initial increase in yield becomes more exaggerated.

qualitatively similar results to the non-linear movement shown in figure 2.6.

Harvesting in coupled patches with logistic growth

The constant recruitment model of the previous sections gives us analytic tractability and may be relevant for systems where individuals are stocked at a constant rate (for example some farms or fisheries). In this section, we assume that the population is governed by a more natural reproductive process, modelled by logistic growth

$$f_i(N_i) = r_i N_i \left(1 - \frac{N_i}{K_i}\right). \tag{2.22}$$

For simplicity, and to isolate the effects of harvesting, we assume a symmetry between the patches, with the exponential growth rate and the carrying capacity of the two patches being

equal $r_1 = r_2 = r$ and $K_1 = K_2 = K$. The full model detailed in this section is given by

$$\frac{dN_1}{dt} = rN_1\left(1 - \frac{N_1}{K}\right) - m_1N_1 + m_2N_2 - c_1N_1 \tag{2.23}$$

$$\frac{dN_2}{dt} = rN_2\left(1 - \frac{N_2}{K}\right) - m_2N_2 + m_1N_1 - c_2N_2 \tag{2.24}$$

The positive equilibrium of this system is the solution of a cubic, and is hence analytically intractable. In the absence of any harvesting, $(c_1, c_2) = (0, 0)$, it is possible to show that the $(N_1, N_2) = (0, 0)$ equilibrium is always unstable, for $r > 0$. Using phase plane analysis, we are also able to discern that the positive equilibrium (N_1^*, N_2^*) is always stable if it exists, see appendix A for details. Through stability analysis of the zero equilibrium, we are also able to discern the extinction threshold for harvesting. Whereas in the constant recruitment model, there was no extinction equilibrium, and in all cases, cessation of harvesting practice would see a regeneration of the population to it's natural state, the presence of this extinction threshold in the logistic model means that harvesting at a high enough rate can cause unrecoverable extinction to the population. In the single patch model, this critical harvesting effort was reached when $c > r$, that is when harvesting effort exceeded the growth rate. If the patch to be harvested were coupled with a second patch, this threshold condition changes. The effect of harvesting in a single patch $(c_1 > 0, c_2 = 0)$ is analysed through linear stability analysis about the $(0, 0)$ equilibrium. The Jacobian matrix of the harvested system at this point is given by

$$J = \begin{pmatrix} r - m_1 - c_1 & m_2 \\ m_1 & r - m_2 \end{pmatrix}. \tag{2.25}$$

As in appendix A, the stability of this point depends on the values $r - m_1$ and $r - m_2$. The outcomes of the four possible cases are given below, see appendix B for details.

1. $r - m_1 > 0$, $r - m_2 > 0$: If growth rate is faster than movement out of both patches, then harvesting of a single patch will be insufficient to drive the entire population to extinction. In this case, whilst it may be possible to apply sufficient effort that the harvested population is effectively zero, the coupled population will survive. Cessation of harvesting in this case will see an eventual regrowth of the harvested population due

to immigrants from patch 2.

2. $r - m_1 < 0$, $r - m_2 < 0$: Here the movement out of either patch occurs at a higher rate than the growth rate within each patch. In this case, the extinction threshold is given by

$$c_1 > r + \frac{rm_1}{m_2 - r}. \tag{2.26}$$

If the harvesting effort satisfies this inequality, then the removal of individuals within patch 1 causes a sufficient reduction in the populations of both patches that the entire system goes extinct and cannot recover. The threshold given above has a minimum of $c_1 > r$ when there is no movement and the system reduces to the single patch case. As movement increases, this threshold is increased , indicating that a coupled population is more robust to harvesting than a single patch. This is due to the influx of individuals from the patch which is not harvested. Harvesting effort can therefore be increased without causing extinction, however if harvesting is large enough, then extinction will be caused in both the harvested and the non-harvested patch.

3. $r - m_1 > 0$, $r - m_2 < 0$: If movement out of patch 1 is lower than growth, and movement out of patch 2 is higher, then the extinction threshold is given as in (2.26), and increasing movement results in an increase in threshold. In this case, harvesting effort is targeted at an important area which has a high level of inward movement, a pseudo-sink [145]. Targeting this area makes the population as a whole more vulnerable to extinction. This result highlights the importance of avoiding key areas and ecosystems when applying harvesting effort to prevent extinction. Alternatively these pseudo-sinks should be targeted if the goal of harvesting or culling is to eradicate the population.

4. $r - m_1 < 0$, $r - m_2 > 0$: If outcome 3 is reversed, and harvesting is focussed on an area where movement out is greater than movement in, then the population is robust to harvesting in a single area and will not be forced to extinction. Once again, as in case 1, the effect of harvesting patch 1 does not have a sufficient effect on the second patch since in this case individuals are leaving patch 1 faster than they are entering it. Patch 1 in this case is a pseudo source to patch 2 [145].

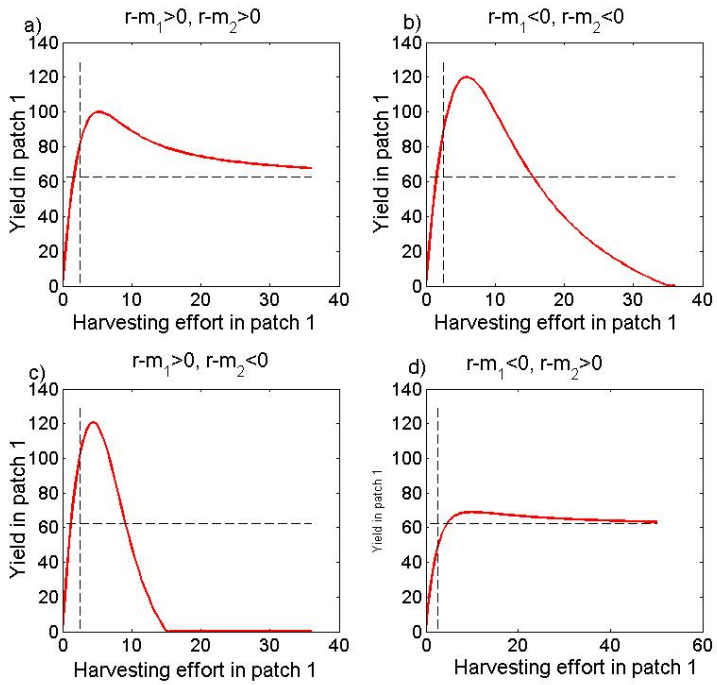

Figure 2.8: Yield in patch 1 as harvesting effort increases in the four cases outlined above. In case a) and d) harvesting in a single patch does not cause complete population extinction, in b) and c) the yield goes to zero when the population is extinct. Dashed lines in the plots show the harvesting effort and maximal sustainable yield for a single patch with logistic growth. Parameters $r_i = 5$, $K_i = 50$, $m_i = 2$ or 6.

The above discussion is concerned with ensuring that the population being harvested is not driven to extinction. However, as in the single patch case. we are also concerned with maximising the yield of a harvested population. Since we are unable to find the equilibrium value of this model analytically, we are unable to find an expression for the yield in all cases. Simulation results, as shown in figure 2.8, suggest that a coupled patch leads to an increase in the yield obtained when compared to an uncoupled patch. To understand how the coupling of populations affects the yield, we will analyse the yield when movement is large. Here, as in section 2.3.1, we allow the ratio between the two movement rates to be given by $m_1/m_2 = \phi$, with $m_1 = \phi m$ and $m_2 = m$. By varying this ratio, we are able to account for the three possible cases, $m_1 < m_2$, $m_1 = m_2$ and $m_1 > m_2$ corresponding to $\phi < 1$, $\phi = 1$ and $\phi > 1$ respectively. By employing the analysis of Holt [79], we have shown that the ratio of N_1/N_2

tends to $1/\phi$ as $m \to \infty$, hence for high levels of movement the equilibrium sizes tend to

$$N_1^* = K\left(1 - \frac{c_1 + \phi c_2}{(1+\phi)r}\right)$$
$$N_2^* = \phi K\left(1 - \frac{c_1 + \phi c_2}{(1+\phi)r}\right) \tag{2.27}$$

Harvesting in a single patch therefore gives a yield of

$$Y = c_1 K\left(1 - \frac{c_1}{(1+\phi)r}\right),$$

which achieves it's maximum value at

$$Y_{max} = \frac{Kr(1+\phi)}{4}. \tag{2.28}$$

This yield is achieved at a harvesting effort of $c_1 = (1+\phi)r/2$. From this formulation the maximal sustainable yield for high movement rates increases linearly with movement ratio. As the ratio increases, the movement into patch 1 becomes much higher than the movement out, causing an increase in the size of patch 1 and hence the yield. When movement occurs at equal rates, this maximal yield is given by $Kr/2$ which is twice the yield of a single isolated patch of size K. Hence, as movement tends to infinity, in regards to the yield, the patch structure dissolves to a single large patch of size $2K$. This formulation of the maximal yield also shows that for any level of coupling, $\phi > 0$, then it will always be possible to achieve a maximal yield greater than that of a single patch.

The above expression for Y_{max} is only applicable for very large m. The change in maximal sustainable yield for low and moderate values of m is shown in figure 2.9. This figure shows that for $\phi < 1$ ($m_1 < m_2$) the maximal sustainable yield attains its maximum for a moderate movement rate. For $\phi > 1$ ($m_1 > m_2$), for similarly moderate levels of movement, the maximal sustainable yield drops before increasing to the maximum as $m \to \infty$. This increase in yield for $\phi < 1$ is a result of a higher rate of movement into patch 1 than out. This imbalance causes the population size in patch 1 to swell and leads to a higher yield for moderate movement rates. As the rate of movement increases, the population in patch 2 decreases due to the knock on

effect of harvesting in patch 1. Hence for high m, the numbers of individuals moving between the patches per unit time balance, and the maximum sustainable yield approaches Y_{max}. The inverse of this phenomenon is observed when $\phi > 1$. In this case, the rate of movement out of patch 1 is greater than movement in, and hence for low m, the population size in patch 1 is significantly decreased by the introduction of coupling. Once again, as $m \to \infty$, the patches balance and the maximum yield tends to Y_{max}

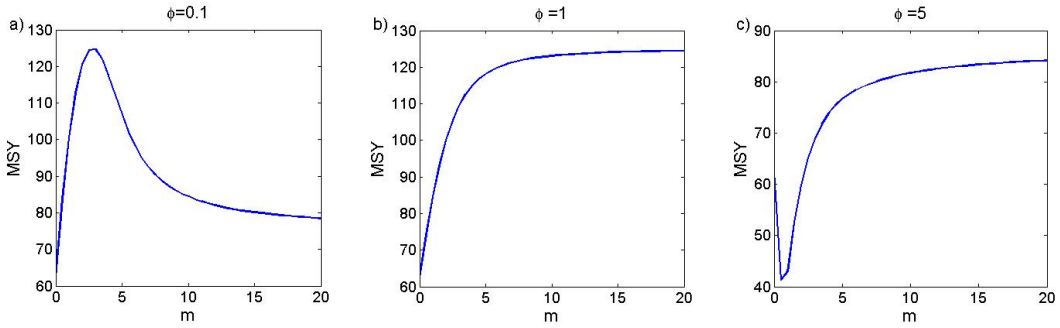

Figure 2.9: Change in maximal sustainable yield, if a single patch is harvested, as movement rate increases for a) $\phi < 1$ where movement into patch 1 is greater than movement out, b)$\phi = 1$ where movement between patches occurs at equal rates, and c)$\phi > 1$ where movement out of patch 1 is greater than movement in.

If harvesting effort is applied to both patches, then a combined harvesting strategy may possibly drive the population to extinction where harvesting of a single patch would not. The general threshold for extinction is given by

$$c_1 = \frac{m_1 m_2}{c_2 + m_2 - r_2} + r_1 - m_1 \tag{2.29}$$

This threshold is shown as a curve in the $c_1 - c_2$ plane (figure 2.10), and any combined harvesting strategy above this threshold will lead to population extinction. Below this threshold, the population in either patch decreases as the harvesting effort increases, but remains stable and will regenerate to natural levels if harvesting effort is stopped. The yield however increases to a maximum before decreasing to zero at the extinction threshold, as shown in figure 2.11.

The extinction threshold, detailed in appendix C, is dependent only on the growth rates and the movement rates, hence the size of the population or the carrying capacities of the patches do not affect the necessary conditions for extinction. The threshold is given by the upper

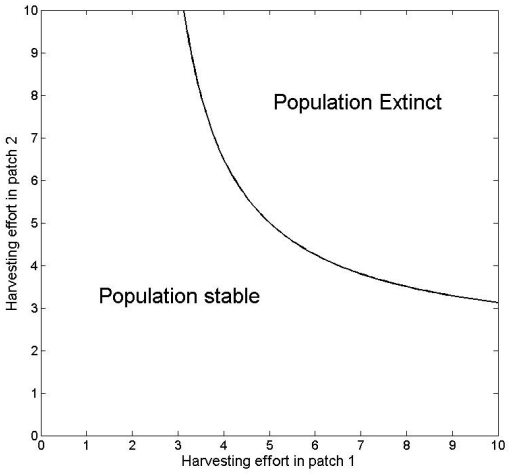

Figure 2.10: Threshold in $c_1 - c_2$ plane outlining regions where the population persists and where harvesting drives the population to extinction, when $m_1 = m_2$

branch of the hyperbolic curve, and regardless of dispersal rate, will always pass through the point $c_1 = r_1, c_2 = r_2$. These control rates are the rates required for extinction in completely isolated patches, hence to eradicate disease from the entire system either $c_2 > r_2$ or $c_1 > r_1$. As movement increases, the curve of this threshold decreases, and the threshold tends to a straight line given by $c_2 = r_1 + r_2 - c_1$, and the sum of the control efforts must be greater than or equal to the sum of the growth rates for extinction.

In this case, as $m \to \infty$, the population equilibria are given in equations (2.27) with the relative yields given by

$$Y_1 = c_1 K \left(1 - \frac{c_1 + \phi c_2}{(1+\phi)r}\right), \qquad Y_2 = c_2 \phi K \left(1 - \frac{c_1 + \phi c_2}{(1+\phi)r}\right) \tag{2.30}$$

and the total yield given by

$$Y_T = K(c_1 + \phi c_2)\left(1 - \frac{c_1 + \phi c_2}{(1+\phi)r}\right) \tag{2.31}$$

Steady state analysis of these surfaces in $c_1 - c_2$ shows that the maximum yield within each patch is located on the axis, meaning that the maximum yield in patch 1, is found when the harvesting effort in patch 2 is zero, and vice versa. If, we consider the total yield, then as

$m \to \infty$, the total yield achieves its maximum along the line

$$y = \frac{(1+\phi)r}{2\phi} + \frac{c_1}{\phi}$$

as shown in figure 2.11

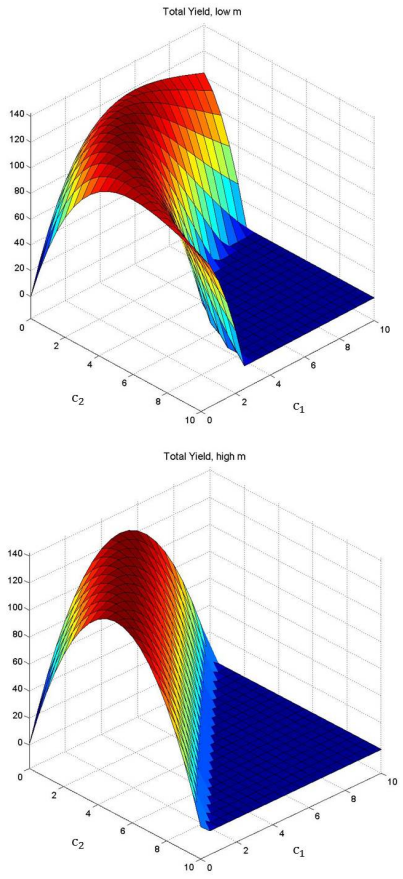

Figure 2.11: Total yield achieved in logistic model as c_1 and c_2 vary. Maximum yield is attained along a threshold curve which tends to a straight line at high movement rates (lower plot).

Spatial perturbation in the logistic model

If the population is spatially perturbed in response to the harvesting effort applied, then the behaviour of both the extinction threshold and the yields within each patch will change. We use the linear and saturating disturbance functions as in the constant recruitment model below to detail this effect. In the first instance, we shall look at the effect of harvesting in a single patch whilst leaving the coupled patch unscathed. Once more, for clarity, we assume

that both patches are equal in size and movement rate, unless otherwise stated.

Linear disturbance $M_1(c_1) = m_1 + \sigma c_1$

The extinction threshold if harvesting is carried out in patch 1 only is given by the upper branch of

$$c_1 = \frac{(r_1 - m_1)(r_2 - m_2) - m_1 m_2}{r_2(1+\sigma) - m_2}$$

which has an asymptote at $r_2(1+\sigma) - m_2 = 0$. If movement out of patch 2 and into patch 1 is such that $m_2 > r_2(1+\sigma)$ then patch 1 is a source of individuals to patch 2, and hence patch 2 is vulnerable to extinction when patch 1 is harvested. This is in contrast to the condition in the previous section whereby patch 2 was vulnerable if $m_2 > r_2$, Hence, for a given movement rate m, the higher the strength of disturbance, the higher the harvesting effort must be to cause extinction, this relationship is shown in figure 2.12. When harvesting occurs in a single

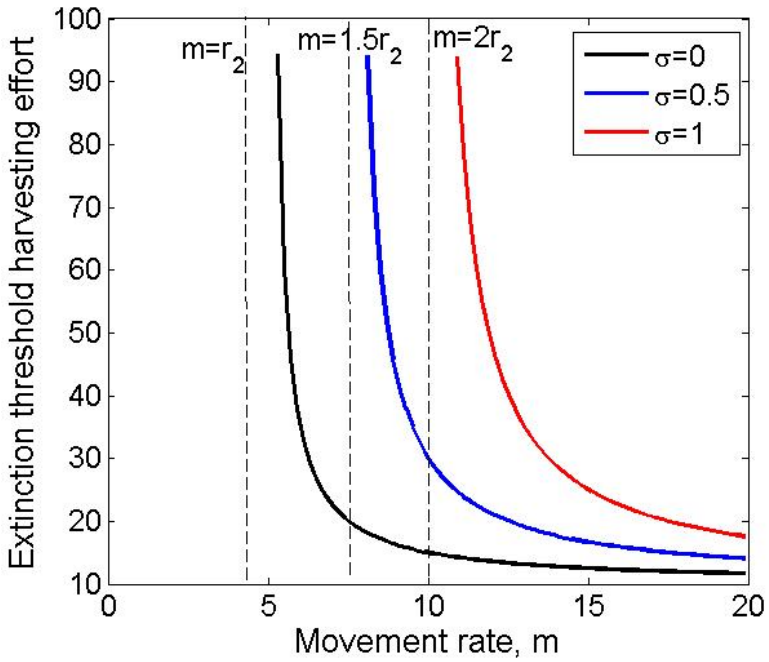

Figure 2.12: Decrease in extinction threshold as movement increases for increasing strength of disturbance. Extinction occurs above the line, hence for a given movement rate m, the higher the disturbance, the more effort is required to drive the system to extinction.

patch, disturbance causes the population to become more robust to extinction. Therefore, movement out of a patch in response to harvesting benefits not only the individuals which

may avoid being caught, but also the entire population is less likely to go extinct due to this movement.

If harvesting occurs across both patches, then the general form of the extinction threshold is given by

$$c_1 = \frac{M_1(c_1)M_2(c_2)}{M_2(c_2) + c_2 - r} + r - M_1(c_1).$$

If disturbance in response to harvesting is linear, then the threshold is given by

$$c_1 = \frac{r_1(m_2 + (1+\rho)c_2 - r_2) + m_1(r_2 - c_2)}{m_2 + (1+\rho+\sigma)c_2 - (1+\sigma)r_2}$$

and has the following properties

1. For symmetric natural movement ($m_1 = m_2$) and equal harvesting efforts ($c_1 = c_2$), the threshold point is also given by $c_1 = c_2 = r$. The extinction thresholds with and without perturbation intersect at this point. This property is true regardless of disturbance function.

2. This threshold has asymptotes at

$$c_2 = \frac{(1+\sigma)r_2 - m_2}{1+\rho+\sigma}, \qquad c_1 = \frac{(1+\rho)r_1 - m_1}{1+\rho+\sigma}$$

The second of these properties enables us to derive conditions whereby extinction is easier or harder to achieve if spatial perturbation occurs. If we assume that the disturbance acts with equal strengths within both patches ($\rho = \sigma = \epsilon$), then, the asymptotes of the extinction threshold can be rewritten as

$$c_1 = A_1(\epsilon) = r_1 - m_1\left(\frac{1+\epsilon(r_1/m_1)}{1+2\epsilon}\right), \qquad c_2 = A_2(\epsilon) = r_2 - \left(\frac{1+\epsilon(r_2/m_2)}{1+2\epsilon}\right)$$

and differentiating these with respect to the strength of disturbance gives

$$A_i'(\epsilon) = -\frac{r_i - 2m_i}{(1+2\epsilon)^2}.$$

Hence the asymptotes of the threshold are equal to $r_i - m_i$ for constant movement, decrease as disturbance increases if $r_i/m_i > 2$ and increases with increasing disturbance if this condition is reversed. If exponential growth is greater than twice the rate of emigration, then an increase in movement in response to harvesting, means that the system is more vulnerable to extinction at lower harvesting rates than if movement were constant.

Saturating disturbance $(M_1(c_1) = m_1 + \sigma c_1/(1 + c_1), M_2(c_2) = m_2 + \rho c_2/(1 + c_2))$
For the saturating disturbance function, the behaviour of the thresholds is not easy to discern analytically. However, since for low effort, $\sigma c_1/(1 + c_1) \approx \sigma c_1$ and $\rho c_2/(1 + c_2) \approx \rho c_2$, it is reasonable to assume that if the extinction threshold occurs at relatively low values of c_1 and c_2, then the two disturbance functions will behave similarly. Since the thresholds intersect at $c_1 = c_2 = r$, if r is low, then the entire threshold will be low, and as r increases, the efforts required for extinction will rise. Simulations show that for low r, the thresholds behave in quantitatively similar ways. As harvesting effort increases, the saturating disturbance function saturates at $M_1(c_1) = m_1 + \sigma$ and $M_2(c_2) = m_2 + \rho$. Hence for high r, the extinction threshold has asymptotes which tend to $c_1 \approx r - m_1 - \sigma$ and $c_2 \approx r - m_2 - \rho$. This means that if growth is sufficiently high, and movement saturates with increasing harvesting effort, then regardless of the within patch parameters, the extinction threshold will always be lower with perturbation than without. Hence, if movement saturates, and growth is high, perturbation will always make it easier to cause extinction.

Maximum sustainable yield with spatial perturbation

In the final section of this chapter we aim to assess the impact of spatial perturbation on the maximum sustainable yield in the logistic model over two patches. To do this we will look at both the effect as strength of disturbance increases, and also the change in yield in patch 1 for a given effort, as the effort in patch 2 increases. In this way we hope to detail the effect of working with, or ignoring the behaviour of surrounding harvested patches. In the first instance, the behaviour of the maximal sustainable yield is qualitatively the same regardless of whether disturbance is linear or saturating, and all simulation results are given using linear

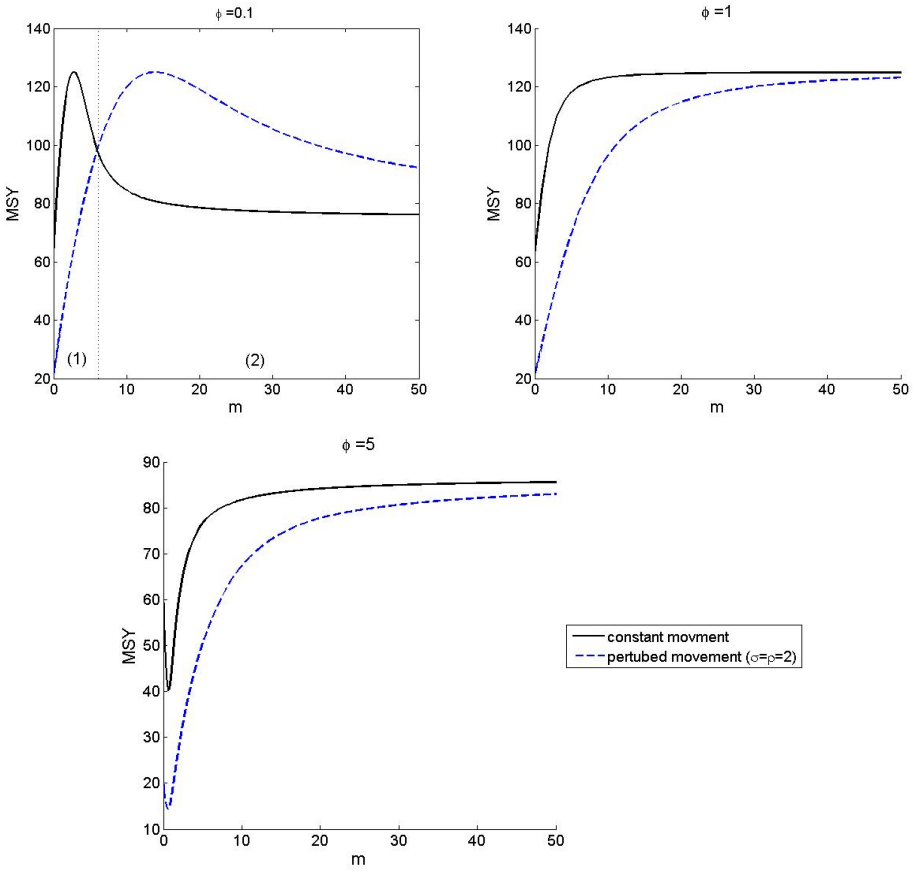

Figure 2.13: Maximal sustainable yield as natural movement rate increases. Comparison of constant movement model (black lines) with linear perturbation (blue dashed lines)

perturbation. If only a single patch is harvested in a coupled system, then constant movement predicts that, for high m, the maximal yield will be given by equation (2.28). This limiting case is the same regardless of movement function and is hence the limit for high levels of natural dispersal even if the system is spatially perturbed. However, for moderate, natural movement rates, the maximal sustainable yield is given in figure 2.13. These plots show that if $m_1 < m_2$ ($\phi < 1$) then there is a range of natural movement rates for which spatial perturbation causes a decrease in the maximal yield obtainable, (region (1)). In this case, for very rapid natural movement, perturbation sees the maximal yield increased (region (2)). If movement is symmetric ($\phi = 1$) or is skewed so that $m_2 > m_1$ ($\phi > 1$), then perturbation in response to harvesting in patch 1 forces the maximal sustainable yield to be always lower than the constant movement model predicts.

Simulation results for the yield of combined harvesting strategies targeting both patches in this system are given in figure 2.14. If harvesting is asymmetric then the yield is lower if the system is perturbed. For example, if c_2 is high, and c_1 is low, then the perturbed system will see individuals from patch 2 forced out, and fewer individuals from patch 1 forced in hence a lower population in patch 2 and a lower total yield since this patch is the focus of the largest effort. The maximum total yield possible is unchanged under spatial perturbation, however, the maximum possible yield in a single patch decreases as strength of disturbance increases (figure 2.15). If movement is constant, then the maximal yield within each patch is obtained when that patch alone is harvesting. However, as the strength of disturbance increases, it is beneficial for patch i if patch j harvests by a small amount. This is because those individuals forced out by disturbance will be compensated for to some extent by those forced in from the second patch. The total maximal yield is always obtained using the same strategy (the black point in figure 2.16). For high levels of disturbance, the maximum strategy within each patch tends to this optimal total strategy.

2.4 Discussion

The work presented in this chapter is an exploration of the impact of movement of individuals between independently controlled patches, and the consequences that these movements have on the yield obtained from harvesting the individuals. By considering both the constant recruitment model and the logistic growth model, we are able to assess the importance of joint harvesting strategies across two patches for the case where the populations are 'stocked' at a constant rate, as well as a naturally reproducing population. By assuming a constant rate of natural movement between the two patches, a constant, per capita, rate of migrants is built into the model. This assumption has the consequence that any positive population in either patch will produce immigrants into the second, coupled patch of the system. It has been shown previously, [79], that a high rate of constant movement between the two patches reduces the heterogeneity in the population sizes, causing the patches to become more similar in size. We have extended the work of Holt [79] in section 2.3.1, to the case when the movement rate between the patches is not equal, and have shown that ratio of the population sizes

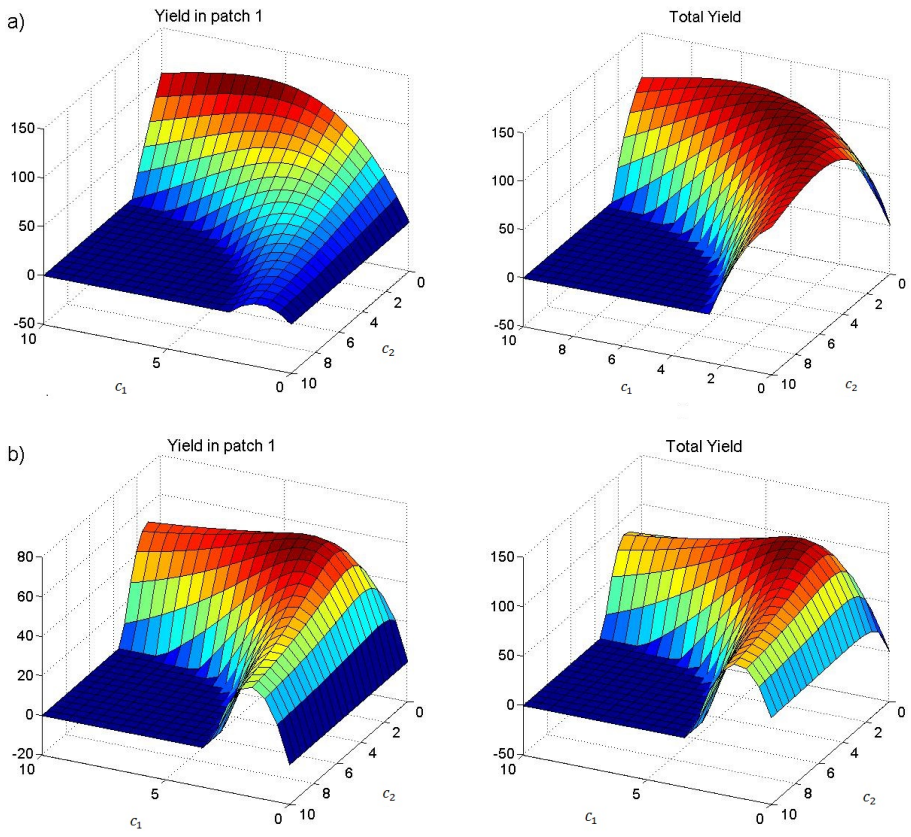
a)
Yield in patch 1
Total Yield
b)
Yield in patch 1
Total Yield
c_1
c_2

Figure 2.14:

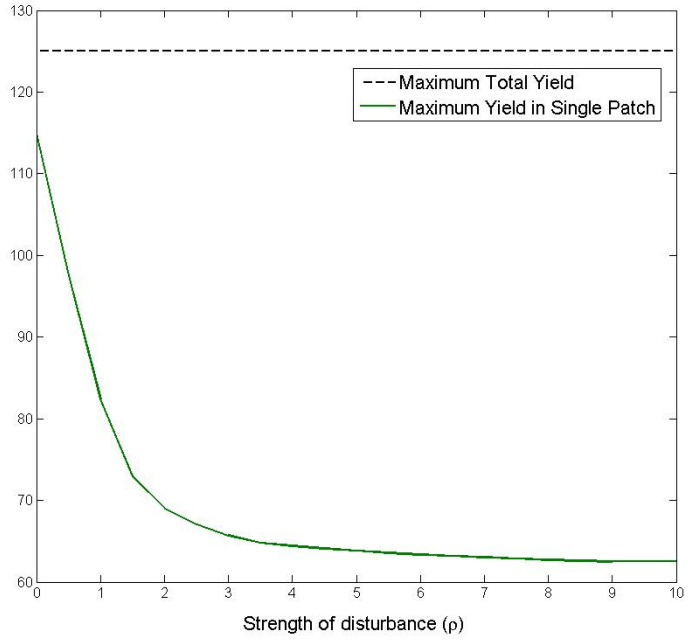

Figure 2.15: Change in maximum yield with increasing strength of disturbance. Total yield (dashed line) is constant, but within patch yield decreases as strength of disturbance increases

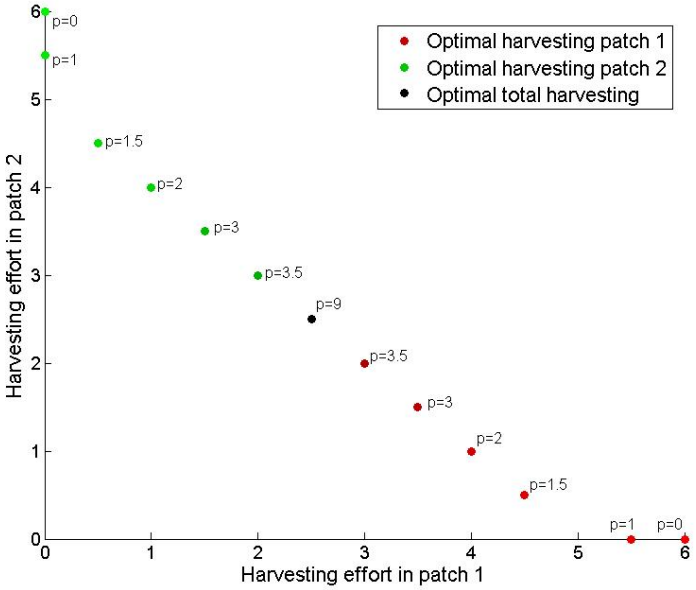

Figure 2.16: Plot of optimal harvesting strategies producing maximum yield in patch 1 (red), patch 2 (green) and the maximum total yield (black). For low ρ, the optimal within patch strategy harvests only that patch. As ρ increases, the optimal strategy moves to a joint harvesting strategy and converges on the strategy for maximising total yield as disturbance increases.

N_1/N_2 as movement tends to infinity, tends to the inverse of the ratio of the emigration rates. Hence, if individuals leave patch 1 at a rate which is twice as fast as those leaving patch 2, then as movement increases, maintaining this ratio, the population in patch 1 will tend to half the size of that found in patch 2.

If a single patch is harvested in a coupled system, then the constant influx of individuals from the neighbourhood may be sufficient to sustain the population. If the populations are constantly stocked, modelled by the constant recruitment growth function, then the yield increases and saturates for increasing effort. We have shown that the coupling of two patches increases this upper limit of the yield. If however, the populations reproduce in a more natural way, as modelled by the logistic growth function, then the yield reaches a maximum before decreasing as the populations are over harvested. The maximal sustainable yield is found to be higher in the coupled patch than in an isolated population, once again due to the constant influx of immigrants. In the case of logistic growth however, it is possible to drive the entirety of the populations over both patches to extinction if the patch being harvested is a pseudo sink. This term is used to describe a patch which has a low rate of emigration to other patches. Immigrants into this patch are more likely to remain there for a sustained period of time, and hence harvesting in this area, whilst likely to produce a high yield, makes the surrounding populations more vulnerable to extinction.

Harvesting across both patches, a constant effort c_i and increasing c_j, leads to a reduction in yield in patch i, due to the decrease in the number of immigrants as the population in patch j is increasingly harvested. If the populations are disturbed by the practice of harvesting, such that their emigration rate out of the harvested patch is increased, then this reduction in yield can be reversed. If disturbance is sufficiently high, then the yield in the neighbouring patch, j, may be increased by harvesting in patch i. This is of course to the detriment of the yield in patch i due to individuals fleeing the harvesting practice. Spatial perturbation or disturbance in a naturally reproducing system may however mean that a higher harvesting effort is required to force a system to extinction. Fleeing the effects of harvesting, not only prolongs the life of those individuals, but may also lead the entire system of patches to be sustained.

This is because the pseudo-sink property previously discussed, is countered by the increase in emigration rate. Thus a patch which was a pseudo-sink will have this property reduced, and hence the whole population over the two patches becomes more robust to harvesting.

In this chapter, we have discussed only the consequences of harvesting, and disturbance on the total population sizes present in each patch. However, an increase in the emigration rate out of a patch, whilst making the population sizes more robust to harvesting, may lead to an unnatural skew in the balance of the ecosystem. This in turn may result in an increase in predation on one of the species, an increase in competition for resources, or an increase in the transmission of disease [75],[56], [136]. It is the last of these possibilities that is addressed in the following chapter.

Chapter 3

The impact of increased dispersal in response to disease control in patchy environments

3.1 Preamble

This chapter has been published in the *Journal of Theoretical Biology*, credited to R. Lintott, R. Norman and A. Hoyle [93]. The form in which this work appears is an exact copy of the published article. As such, this chapter has a slightly different style to the other chapters in this thesis, and the notation in this chapter is not the same as used throughout. For clarity therefore, table 3.1 has been included to highlight the difference in notation between this chapter and the preceding one.

Parameter Name	Rest of thesis	Chapter 3
Birth rate	a	μ or m
Death rate	b	ν or v
Migration rate	m	a

Table 3.1: Difference in notation between the rest of this thesis and the parameters used throughout this chapter

3.2 Introduction

Around 60% of all species of infectious agent are zoonotic, with the vast majority of these having reservoirs within animal populations [130, 153]. With such a large proportion of human infection contracted through this route, it is of little surprise that management of wildlife populations through culling, vaccination, habitat management and others (as reviewed by Wobeser [149]) is becoming a key part of disease control [35]. Human well being is not the only reason for increasing control of wildlife diseases. Wildlife populations which are reservoirs for livestock diseases such as bovine tuberculosis or bluetongue are often targeted for control to prevent costly outbreaks in livestock populations [108, 151, 97, 58]. Game species, managed for hunting are also at an increased risk of disease outbreaks due to unnaturally high population densities during hunting seasons [57]. If wild populations are to be targeted for disease control then models used to predict appropriate, cost effective control strategies must be able to capture all of their key population characteristics in order to produce realistic and useful predictions.

Simple, classical models of epidemic control generally consider a species which is uniformly, randomly distributed over an area of homogeneous landscape [6]. This premise restricts the biological realism of the models leading to oversimplified predictions of required control strategies. The assumption of homogeneity in wildlife populations fails to account for clustering of groups of individuals either within social groups, for example pack animals or social insect populations, or due to habitat fragmentation. This clustering of populations into areas of high population density divided by areas with fewer individuals can be modelled in several ways. Network models are able to detail the spread of disease over a wide area, and have been successfully used to evaluate the effectiveness, and cost of control strategies [47]. This type of modelling is invaluable in efforts to control livestock diseases and has been used extensively since the 2001 foot and mouth epidemic to optimise future control strategies in the face of another outbreak [135, 134]. Network analysis is particularly useful when contact networks can be traced, and are known throughout a population. In the UK, movements of livestock are well documented and hence these contact networks can be accessed. In the case of wildlife populations, this process of contact tracing is almost impossible and other methods must be

developed.

The movements of wildlife populations are determined by the structure of the habitat available and by the specific behaviour of the population. For many species, dispersal is an essential trait. The resources available within an area inhabited by a species will not change with an increasing number of offspring, and it is often necessary for offspring to disperse to find sufficient resources and establish their own territories [148]. As well as these natural motivations for dispersal, individuals may be forced to leave an area in response to human disturbance. Much research has gone into assessing the impact of human disturbance on wildlife species, particularly in terms of conservation strategies [12, 55]. The presence or absence of humans in an area populated by a wild species may have a significant impact on the behaviour of that species [39]. In the context of infectious disease control, human disturbance is necessary in the implementation of any active control strategy. In the case of wild animal populations a natural response to this disturbance is to move away from the controlled area. This natural behaviour is seen in countless species. In Colorado, for example, Rocky mountain elk (*Cervus elaphus nelsoni*) populations have been found to move out of their home range in response to the hunting season [32]. In England, the wide spread of bovine TB is often attributed to the movement of the European Badger (*Meles meles*). Badgers infected with bovine TB have been observed to forage over a larger area than healthy badgers [54]. It has also been observed that in areas where culling takes place, badgers are likely to extend their territory and ranging behaviour and are thus likely to encounter badger setts or areas housing cattle which otherwise would have been uninfected [151]. The theoretical models presented here aim to assess the importance of the effects of this disturbance on disease control thresholds. This perturbation effect is a factor which is largely overlooked, with models assessing the impact of control strategies in isolation whilst neglecting the explicit effects of disturbance. Swinton *et. al.* (1997) investigated this perturbation effect for a badger population by assuming that transmission of bovine tuberculosis increased with removal of individuals [129], however this model did not address the movement of individuals between distinct groups, nor the interaction with a secondary, bovine, host. This scenario will be considered in section 3.4.

Epidemiological models are often created for the purpose of evaluating an optimal control

strategy aimed at eradicating an infection with the minimum cost to the environment and the minimum financial cost [47, 134, 138]. Realistic models are essential in the evaluation of optimal control strategies, since over estimation of control may have negative economic or environmental implications, whilst underestimation may result in persistence of infection and failure of the control strategy. In this paper, we aim to evaluate the effect of disturbance increased dispersal between two populations on the prediction of optimal control strategies in a simple model. Whilst the models investigated are entirely theoretical, we predict that the results obtained and the insight into the behaviour of the control thresholds will be generalisable to realistic situations and thus inform future control regimes. In the first part of the paper, we use a simple two patch model [144] as the basis of our investigations. Control maps, 2-dimensional graphs showing regions of successful and failed control strategies, are used to compare the effect of increased dispersal due to increased control. Since different species will respond in different ways to human disturbance, we consider three functional responses. Firstly we assume that dispersal is unchanged with control, secondly dispersal increases linearly with control, and finally it is assumed that dispersal increases to some maximum then saturates, indicating that, at high levels of control, there is no additional disturbance to the population. This third functional form is similar to the effect used by Swinton *et. al.* [129], and whilst it is more biologically sound, this model is analytically intractable.

The second part of this paper uses this two patch single species model to investigate the importance of between patch movements on disease dynamics in multiple hosts. Around 80% of the worlds pathogens are generalist, making the interactions between hosts paramount in considering disease controls [153]. The interest in population and disease dynamics of multiple hosts have been of increasing interest [107, 16, 23, 62, 63, 60, 61] particularly with regards to wildlife reservoirs which are able to transmit infectious diseases to humans or livestock populations. The interactions between multiple hosts provide ecologists with options for control strategies. Greenman and Hoyle [60] were able to determine the characteristics of disease reservoirs in terms of the infection invasion matrix and to provide criteria for optimal control of a multi-host pathogen in two species. We extend this work by considering a two patch system. It is assumed that each patch is home to two species, one which we term

'livestock' and whose movement is controlled, and one which is termed 'wildlife' which is free to move between the two patches. We investigate the necessary control strategies when the livestock population is the reservoir for infection, when the wildlife population is the reservoir, and when it is the interaction of both species which sustains the pathogen.

3.3 Single Species models of disease control in two patches

The model we consider is a two patch extension of a standard, and well documented SI model [6, 7, 84]. We consider two patches consisting of dynamic populations made up of individuals which may be either susceptible or infected with total population size within each patch given by $N(t) = S(t) + I(t)$. Individuals are introduced to the population at a constant rate ν_i and it is assumed that newly introduced individuals are susceptible. A constant recruitment rate is a simplification of any biological system, however it is appropriate here as a first approximation in order to simplify the dynamic behaviour of the population in the absence of control, and to isolate the impact of different dispersal functions on this simple system. Individuals leave the population through death at a constant per capita rate μ_i with infected individuals dying at an additional per capita rate of γ_i with subscripts denoting patch number. Infection is transmitted within patch only, and the rate of infection is given by β_i, we assume that transmission is through direct contact between infected and susceptible individuals, and follows the assumptions of mass-action [15]. The two patches are coupled by movement of individuals from one patch to the next (from i to j) at a rate $A_i(c_i)$ which may depend on the control parameters c_1 and c_2. In the absence of control it is assumed that individuals disperse at a constant per capita rate $a_i = A_i(0)$. Model 3.1 gives the general form of the two patch

model with disease control.

$$
\begin{aligned}
&\text{Patch 1}\\
&\frac{dS_1}{dt} = \nu_1 - \beta_1 S_1 I_1 - \mu_1 S_1 - c_1 S_1 - A_1(c_1) S_1 + \phi A_2(c_2) S_2\\
&\frac{dI_1}{dt} = \beta_1 S_1 I_1 - (\mu_1 + \gamma_1 + c_1) I_1 - A_1(c_1) I_1 + \phi A_2(c_2) I_2\\
&\text{Patch 2}\\
&\frac{dS_2}{dt} = \nu_2 - \beta_2 S_2 I_2 - \mu_2 S_2 - c_2 S_2 - A_2(c_2) S_2 + \phi A_1(c_1) S_1\\
&\frac{dI_2}{dt} = \beta_2 S_2 I_2 - (\mu_2 + \gamma_2 + c_2) I_2 - A_2(c_2) I_2 + \phi A_1(c_1) I_1.
\end{aligned}
\tag{3.1}
$$

The parameter ϕ is a measure of how hazardous dispersal is and indicates the proportion of dispersing individuals which successfully reach their target patch. It may be assumed that those $(1-\phi)$ individuals which do not reach the target patch either die or become resident in areas outside the scope of the model. It is assumed that dispersal is equally hazardous to individuals from either patch, hence the same proportion is lost moving from patch 1 to patch 2, as is lost moving from patch 2 to patch 1. This assumption could be relaxed by the introduction of a directed risk parameter ϕ_i giving the loss of individuals moving from patch i to j. We control this system by removing individuals from patch i at the constant, per capita, rate c_i. This control could be implemented in various ways. The model is written such that control is given as an additional death rate, which would suggest that the species considered is to be culled, however, in terms of the dynamics of the system, any reduction in the carrying capacity of the environment, eg through habitat management, removal or quarantine of individuals would have the same effect.

Model (3.1) provides the basis for considering and comparing three different functional responses to control. We evaluate the necessary conditions for disease exclusion when (i) dispersal is constant and therefore unchanged by control $A_i(c_i) = a_i$, (ii) dispersal increases linearly with control, $A_i(c_i) = a_i + \kappa_i c_i N_i$ and (iii) dispersal increases but saturates with increasing control, the third case is given by a Holling Type II function with $A_i(c_i) = a_i + \frac{\kappa_i c_i N_i}{1+hc_i}$. The functions defined in (ii) and (iii) are given in terms of the total, within patch population size N_i, this accounts for the fact that direct control applied to any infectious class will

cause disturbance to the population as a whole. This also results in larger populations being affected more severely by disturbance and having subsequently higher dispersal rates than smaller populations. The parameters κ_i determine the increase in movement per individual controlled and in all simulations this parameter is assumed to be 1, although a higher rate would suggest that for each individual removed, more than one individual leaves the patch due to disturbance. The dispersal function in (iii) ranges between a_i and $a_i + \frac{N_i}{h}$ as control is increased, and the three dispersal functions are given in Figure 3.1.

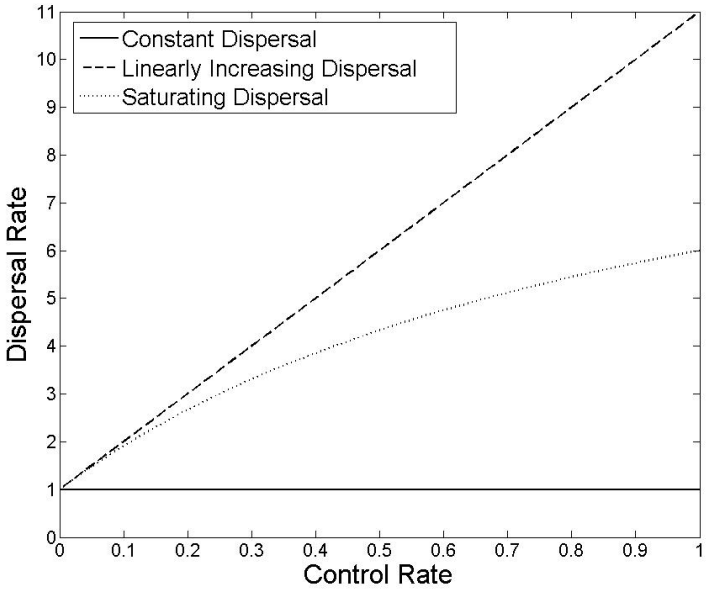

Figure 3.1: Dispersal functions considered in the three different cases

3.3.1 Methods of Analysis

For each of the dispersal functions we are able to find the pathogen exclusion threshold which defines the necessary conditions to eradicate the disease from the entire system. Whilst complete eradication of disease may not always be the goal of the control strategy, the pathogen exclusion threshold provides a useful metric by which to judge the effect of dispersal in response to control. This threshold may be defined as the curve in $c_1 - c_2$ space satisfying $R_0 = 1$ where R_0 is the basic reproductive number as defined in [38, 141]. This threshold is found by taking a rare invader approximation [60].

By taking the rare invader approximation, the 4×4 Jacobian of the full 2 patch disease

model can be decoupled to give the 2×2 infection invasion matrix which allows us to evaluate whether introduction of a small amount of infection will cause growth of the infectious classes, (i.e spread of disease) or an immediate decline in infection, such that the disease is unable to establish itself. This threshold between disease spread and decline is given by the sign of the maximum eigenvalue, λ_{max} of the infection invasion matrix. A positive eigenvalue giving growth of infection and negative giving decline. In the absence of control this matrix and its eigenvalues will be defined by the parameters of the system. The introduction of control in this system will serve to reduce the maximum eigenvalue, with a successful control strategy being one which forces the maximum eigenvalue into the negative half plane. Since we are interested in using control strategies to rid a system of disease, the origin in control space, ($c_1 = c_2 = 0$) will always give a positive λ_{max}, hence the disease is assumed to be naturally endemic in the system. The same parameter values are used throughout all simulations unless otherwise stated, and are based loosely on the population and disease parameters for bovine TB in badgers given in [8], the sensitivity of the models to these parameters is tested in section 3.3.4.

Of course, the rare invader analysis details the spread of infection if control is applied when the infection is in its early stages. Whilst this approach is often used to calculate R_0, and thus determine the potential for a population to sustain a pathogen, in practice control strategies are usually applied when the disease is already endemic in the population. The analysis detailed above ensures the local stability of the disease free equilibrium, but this does not prove that controls introduced at endemic levels will be sufficient for disease eradication. In order to do this, the local behaviour of the endemic equilibrium must be investigated. The endemic equilibrium is the positive solution of the equations given in (3.1) with left hand side equal to zero. Since analysis of this equilibrium is intractable, in order to test the stability of the endemic equilibrium, extensive simulations have been carried out, with a range of parameter values, an example of which is shown in figure 3.4. These simulations confirm that the threshold for stability of the endemic equilibrium coincides with the pathogen exclusion threshold found by the rare invader analysis. These thresholds provide necessary conditions for pathogen exclusion and are applicable even if control is applied to a population in which infection is endemic. Figure 3.2 gives the time series of the total number infected over both

patches, and the effect of applying control at different points after infection. As predicted by the pathogen exclusion threshold in Figure 3.3, the rates of control $(c_1, c_2) = (0.2, 1)$ result in the disease being eradicated and the number of infected individuals becoming zero regardless of level of infection when control is initiated

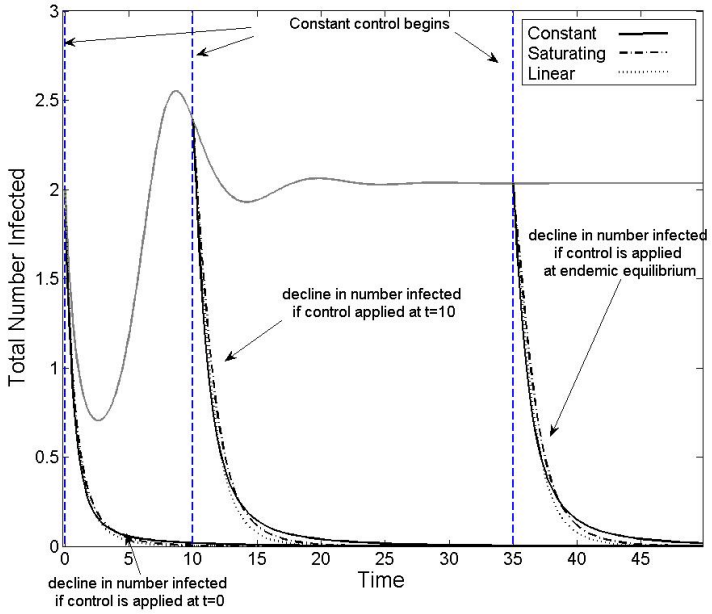

Figure 3.2: Time series showing total number of infected individuals. The solid line is the number in the absence of control, with the number of infected after control shown in black. The control dependent dispersal models both show a faster rate of eradication than constant dispersal for the same control rates. Parameters used $\nu_i = 2, \mu_i = 0.2, \gamma_i = 1, \beta_1 = 0.308, h = 1, \kappa = 1, i = 1, 2$. Control parameters used $c_1 = 0.2, c_2 = 1$

3.3.2 Properties of Pathogen Exclusion Thresholds

One of the key factors in the evaluation of the pathogen exclusion threshold is the equilibrium achieved by the system in the absence of disease. Since we are controlling both susceptible and infected individuals, this disease free equilibrium will depend on the level of control applied. Thus the change in the pathogen exclusion threshold may be explained in part by the behaviour of this equilibrium. In the absence of control ($c_1 = c_2 = 0$, and $A_i(0) = a_i$), the disease free equilibrium is given in all models by

$$S_i^* = \frac{a_j\nu_i + \phi a_j\nu_j + \mu_j\nu_i}{a_2\mu_1 + a_1\mu_2 + \mu_1\mu_2 + (1-\phi^2)a_1a_2}. \tag{3.2}$$

Throughout this paper, unless otherwise specified, we begin simulations with identical patches in order to isolate the effect of control dependent dispersal. In this case, if both patches are equal sizes and dispersal becomes skewed such that individuals leave patch i at a higher per capita rate than patch j, then the patch with highest rate of outward dispersal will lose individuals faster than gaining them and hence the population in patch i will become smaller, whilst the population in patch j will become larger. The addition of control into this model shifts the equilibrium to

$$S_i^* = \frac{A_j(c_j)\nu_i + \phi A_j(c_j)\nu_j + (\mu_j + c_j)\nu_i}{A_1(c_1)(\mu_2 + c_2) + A_2(c_2)(\mu_1 + c_1) + (\mu_1 + c_1)(\mu_2 + c_2) + (1 - \phi^2)A_1(c_1)A_2(c_2)}. \quad (3.3)$$

The behaviour of the equilibria for mixed control strategies is intuitive, with control applied within a patch causing a reduction in the equilibrium size of that patch. Control of a single patch alone will lead to a monotonic reduction in size of the uncontrolled patch only when dispersal is constant. If dispersal is dependent on control, then controlling a single patch will cause an influx of individuals into the uncontrolled patch thus swelling its numbers. If natural dispersal is fast enough, or the control rate is high enough, then control of a single patch will cause a decline in the size of the uncontrolled patch due to constant removal of naturally dispersing individuals. When dispersal is given as a function of the control parameters, the equilibria must be estimated through simulations. It is possible to show (Appendix D) that in the models considered, the unique positive steady state is always locally stable for biologically relevant parameter values. Once this equilibrium has been determined, it is possible to construct the infection invasion matrix given in (3.4)

$$J(c_1, c_2) = \begin{pmatrix} P_1 - c_1 - A_1(c_1) & \phi A_2(c_2) \\ \phi A_1(c_1) & P_2 - c_2 - A_2(c_2) \end{pmatrix} \quad (3.4)$$

where $A_i(c_i)$ is dependent on the model being analysed, and is evaluated at the disease free equilibrium and $P_i = \beta_i S_i^* - \mu_i - \gamma_i$. Once this matrix is constructed, it is possible to find the maximum eigenvalue, and determine how this eigenvalue changes with varying levels of control.

Given that the infection invasion matrix (3.4) has positive off diagonal terms, we are

able to use the Perron-Frobenius Theorem [123] to find the upper and lower bounds on the maximum eigenvalue. This eigenvalue will be bounded above and below by

$$row_{min} \leq \lambda \leq row_{max} \tag{3.5}$$

$$col_{min} \leq \lambda \leq col_{max} \tag{3.6}$$

where $row_{min/max}, col_{min/max}$ are the minimum and maximum row and column sums respectively. For all dispersal functions $A_i(c_i)$, in the case of complete dispersal ($\phi = 1$), one can show (Appendix E) that the maximum eigenvalue of (3.4) is bounded by the column sums

$$\min\{P_1 - c_1, P_2 - c_2\} \leq \lambda \leq \max\{P_1 - c_1, P_2 - c_2\}.$$

If both patches have equal properties (recruitment, death and transmission rates) and are controlled at equal rates, then the equilibria are independent of dispersal function. In this case, $c_1 = c_2$ and $P_1 = P_2$ in the inequality above, it is clear that under these conditions, λ_{max} is constant and equal for all models. We expect, therefore that the pathogen exclusion thresholds for all models will be equal when $c_1 = c_2$. This convergence is shown in Figure 3.3.

In the case of a hazardous barrier ($\phi < 1$), the bounds on the eigenvalue are again given by the column sums of matrix 3.4

$$\min\{P_1 - c_1 - (1-\phi)A_1, P_2 - c_2 - (1-\phi)A_2\} \leq \lambda \leq \max\{P_1 - c_1 - (1-\phi)A_1, P_2 - c_2 - (1-\phi)A_2\}.$$

In this case the bounds on the maximum eigenvalue explicitly depend on the dispersal mechanism being considered, hence we would expect a more significant difference in thresholds in this case. Indeed when the intrinsic, within patch properties are equal such that $P_1 = P_2$ and the control rates applied to each patch are equal such that $c_1 = c_2$, then the higher the dispersal rate $A_i(c_i)$, the lower we expect the threshold to be. This is since a higher dispersal rate reduces the bounds on the maximum eigenvalue. As shown in Figure 3.1, constant dispersal occurs at a lower rate than saturating dispersal, which occurs at a lower rate than linear dispersal, and hence the threshold for the constant dispersal model should be higher than the control dependent dispersal models. The difference in thresholds in this case is shown in

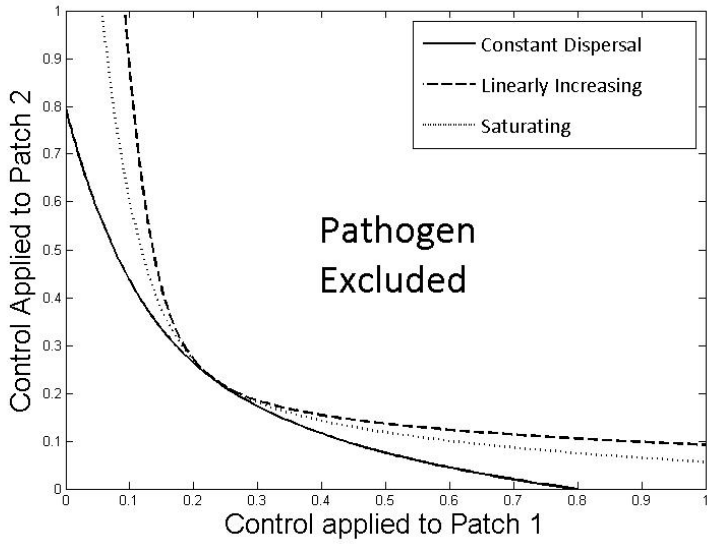

Figure 3.3: Pathogen exclusion thresholds for each of the three models considered when both patches are reservoirs for infection. Both models with increasing dispersal in response to control show similar behaviour. For these parameters, higher levels of control are required if dispersal increases in response to control. Parameters used $\nu_i = 2, \mu_i = 0.2, \gamma_i = 1, \beta = 0.308, a_i = 1, \phi_i = 1, h = 1, \kappa = 1, i = 1, 2$.

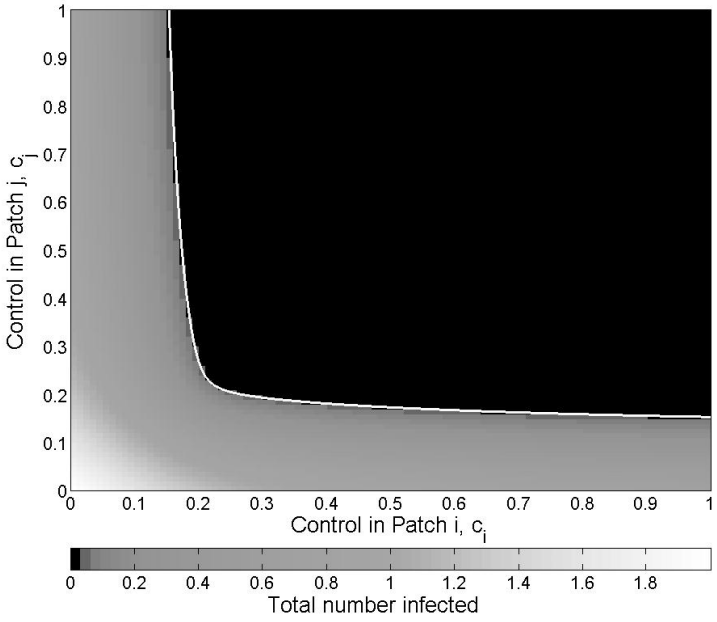

Figure 3.4: The total number of infected individuals at equilibrium as control is varied in the case of constant dispersal. The threshold for the endemic equilibrium is shown to intersect with the pathogen exclusion threshold (white line). This result holds for all dispersal mechanisms. Parameters used $\nu_i = 2, \mu_i = 0.2, \gamma_i = 1, \beta = 0.308, a_i = 1, \phi_i = 1, i = 1, 2$.

Figure 3.5. This reduction in threshold corresponds to a lower requirement for control and is the result of a greater number of individuals failing to reach their target patch during dispersal. This result confirms the intuitive idea that if the boundary between the two patches is hazardous to the species considered, for example a busy road or river, then the control strategies required would be less severe than if all dispersal was successful. If the control strategies cause an increase in dispersal, then an even lower rate of control is required since the disturbance caused will incorporate an additional level of control by forcing individuals to cross a potentially fatal boundary.

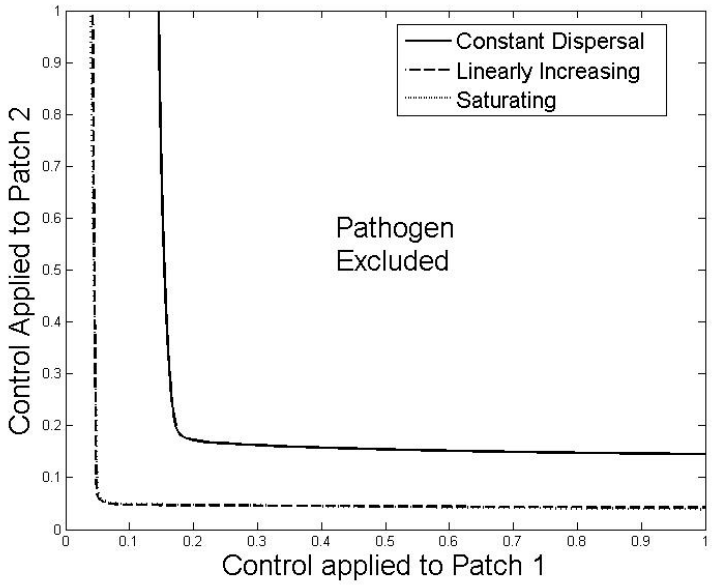

Figure 3.5: Control map showing the thresholds for all models when 50% of the dispersing population fail to reach their target patch. Parameters used $\nu_i = 2, \mu_i = 0.2, \gamma_i = 1, \beta = 0.308, \phi_i = 0.5, h = 1, \kappa = 1 a_i = 0.1, i = 1, 2$.

It is clear that if both $P_1 - c_1$ and $P_2 - c_2$ are negative, then for all $0 \leq \phi \leq 1$, $\lambda_{max} < 0$ and the pathogen will be unable to persist in the environment. The amount of control necessary is thus intrinsically linked to the values of P_i. These values can be thought of as determining the disease thresholds of the patch in isolation, and will thus determine whether or not the patch is a reservoir of infection.

3.3.3 Reservoirs of Infection

An isolated population may be able to support an infection without the need for transmission from an outside source. If this is the case, this population is termed a reservoir of infection [73]. Mathematically, this definition corresponds to the condition that $P_i = \beta S_i - \mu_i - \gamma_i > 0$. When considering the coupling of two patches through dispersal, the dynamics of a population in isolation may influence the control strategies chosen. In the absence of dispersal ($A_1 = A_2 = 0$) and of any control strategy ($c_1 = c_2 = 0$), with the two patches in isolation, the eigenvalues of (3.4) are P_1 and P_2 respectively. There are three different scenarios to consider in a single species system, (i) neither patch is a reservoir ($P_1, P_2 < 0$), (ii) a single patch only is a reservoir ($P_i > 0, P_j < 0$) or (ii) both patches are reservoirs ($P_1, P_2 > 0$).

$P_1, P_2 < 0$

If neither patch is a reservoir, then the disease is not supported by either patch in isolation. If two non-reservoir patches are connected to allow dispersal between populations, then the pathogen exclusion threshold is given when the maximum eigenvalue of (3.4) is zero

$$0 = P_1 + P_2 - A_1 - A_2 + \sqrt{(P_1 + P_2 - A_1 - A_2)^2 - 4((P_1 - A_1)(P_2 - A_2) - \phi^2 A_1 A_2)}. \quad (3.7)$$

If $P_1, P_2 < 0$, the trace of (3.4) is negative, and for this condition 3.7 to be satisfied we require only that

$$((P_1 - A_1)(P_2 - A_2) - \phi^2 A_1 A_2) < 0$$

which cannot be satisfied for any A_i when $P_1, P_2 < 0$. This result suggests that two non-reservoir patches in isolation will not be able to support the pathogen even if connected. This result relies on the assumption that movement between two patches has no effect on the population equilibrium. This assumption is only valid if both patches are identical, and dispersal occurs at equal rates. If this is the case, then increasing the dispersal equally between patches has no impact on the population size within a single patch. However, if dispersal is biased towards one patch to the detriment of the other, then the numbers of individuals in one patch will swell, whilst the other patch will deplete in population size. This may

cause a drastic change in the population size allowing the larger patch to exceed the critical community size [73], become a reservoir for infection, and hence lead to the persistence of disease. If dispersal is incomplete ($\phi < 1$) the same qualitative results apply, however the difference in dispersal rates must be much more severe to force a non-reservoir patch to reach the critical community size.

$P_i > 0, P_j < 0$

If a single patch is a reservoir and is therefore a source of infection for the second population it can be shown that dispersal between patches will be sufficient for disease persistence. This result is analogous to that found in Greenman & Hoyle [60] when considering multiple hosts within a single patch, only a single reservoir is required to sustain disease in a two-host or two-patch system. If a single reservoir patch causes infection to be transmitted into a non-reservoir patch, then a reduction in the dispersal rate between patches through barrier control, through erecting fencing or other physical barriers, would be sufficient for the disease to die out in the non-reservoir patch, allowing control to be focussed on the reservoir patch. This case represents the idea that an infected patch is spreading disease to an otherwise disease free patch through the connectivity and dispersal of the population and supports the idea, posited by Hess [75], that there may be negative consequences to increased connectivity of patchy landscapes. The control map for this situation is given in Figure 3.6. The pathogen exclusion threshold for constant dispersal is as we would expect, it predicts that control of the reservoir patch alone is sufficient to exclude the pathogen. However, the thresholds for both of the control dependent dispersal models tell a different story. In these cases it is necessary to apply control to both patches simultaneously. Control of a single source patch is insufficient to exclude a pathogen if dispersal is influenced by control. This result is again due to the dispersal caused by disturbance of the population and highlights the significance of considering the connectivity between patches in disease control. If control measures cause individuals from an infected patch to move at a higher rate into areas unable to support the pathogen, then both populations must be directly controlled to effectively rid the system of the disease. If the reservoir patch alone is controlled, then the increased movement into the non-reservoir patch causes the numbers in that patch to swell and transmission of infection

to increase within the non-reservoir patch. Taken to the extreme, this situation can be used

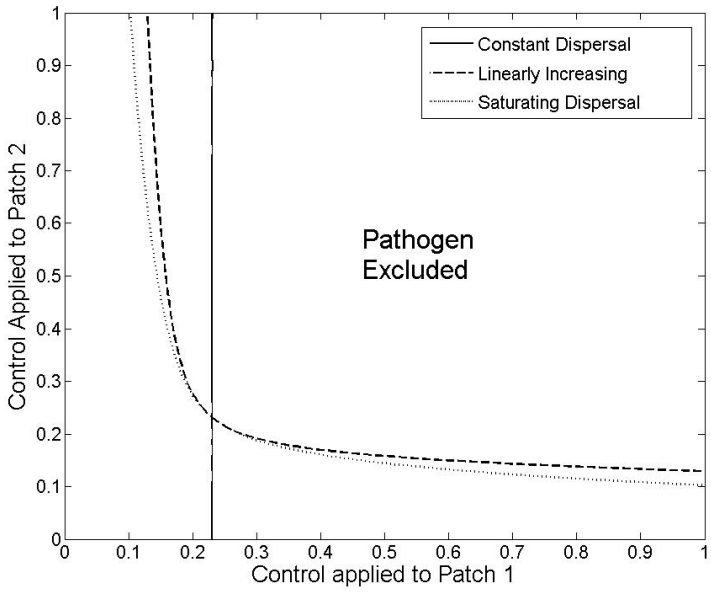

Figure 3.6: Control map for initially distinct patches, when patch 1 is a reservoir of infection and patch 2 is unable to support the infection alone. Control dependent dispersal models show that control strategies must be applied to both patches in order to exclude the pathogen, suggesting that at high levels of disturbance, control strategies cannot simply be focused on areas of infection. Parameters used $\nu_i = 2, \mu_1 = 0.2, \mu_2 = 0.5, \gamma_i = 1, \beta = 0.308, \phi_i = 1, h = 1, \kappa = 1, a_i = 0, i = 1, 2$.

to look at the effect of disturbance due to control on initially distinct patches ($a_i = 0$), there is no natural dispersal between patches, and when one patch is infected and the other is disease free. If we assume that the introduction of control causes sufficient disturbance that individuals from these distinct patches begin to interact, then control of the original source patch is insufficient for disease eradication and could lead to the sustainment of disease into a previously disease free area.

Examining the dynamics in more detail, we are able to determine the difference in number controlled in comparison with the number of individuals which move as a result of disturbance. Figure 3.7 shows the difference in the number of individuals moved between the constant, saturating and linear models. Indeed this case considers two distinct patches such that only the movement in response to control causes them to be connected. The saturating model sees fewer individuals moved than the linear, which is to be expected since the linear increasing

model predicts a greater increase in dispersal rate. Figure 3.7 also shows the drop in the number controlled in patch i, in the saturating and linear models in comparison with the constant dispersal. This is due to the drop in population size due to the outward movement of individuals. Figure 3.7 looks at the case when only one patch is controlled, however, this property is observed for any asymmetric control strategy. The patch with the higher control rate will see a reduction in the number removed by control, and an increase in the number disturbed as we move from constant dispersal, to the saturating and linear models. If we increase the level of control applied to a patch, then we see an increase in the number controlled in each of the models. For the control dependent dispersal models however, we see a reduction in the number moved at higher control levels compared with lower controls. This is due to the reduction in patch size through control, leading to lower levels of disturbance. Thus at higher control rates, the influence of the number controlled directly on the patch size, and the disease dynamics becomes more significant.

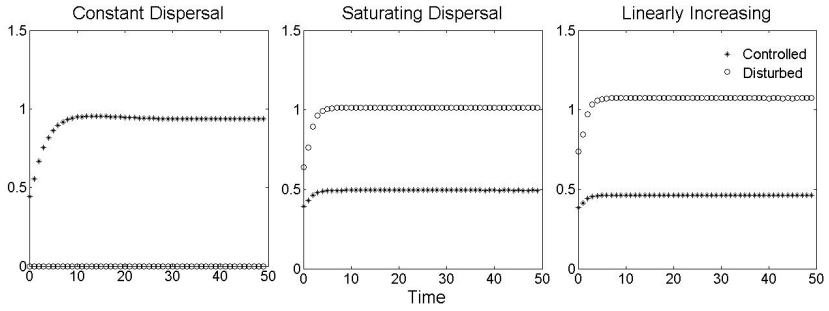

Figure 3.7: Number removed through control compared with number moved out of patch through disturbance in the case of $P_1 > 0, P_2 < 0$. Control is only applied to the reservoir patch (patch 1). Parameter values: $\nu_i = 2, \mu_1 = 0.2, \mu_2 = 0.5, \gamma_i = 1, \beta_i = 0.308, a_i = 0, \phi = 1, h = 1, \kappa = 1, c_1 = 0.5, c_2 = 0, i = 1, 2$

$P_1, P_2 > 0$

If both populations are able to support the pathogen in isolation, then in order to exclude the pathogen any control strategy must be sufficient to remove disease from both patches. If the connectivity between patches, and therefore the dispersal rate is increased, then this causes a decrease of the threshold as given in Figure 3.8. In this case, efforts to increase the connectivity between patches may ease the amount of direct control required for pathogen

exclusion, making it possible to exclude the pathogen from both patches with control of a single patch only. It is shown in Figure 3.8 that increasing natural dispersal has a much less significant effect when dispersal is dependent on control. One possible explanation for this phenomena is that the baseline level of dispersal represents the number of emigrants out of and immigrants into a patch. If dispersal is increased by control within a patch, then the number of emigrants out of a patch will increase, without a subsequent increase in the number of immigrants. Thus for a given control rate c_i in patch i, increased dispersal will result in a further increase in individuals leaving patch i with the chance of introducing, or propagating infection in patch j. Hence control of patch j is still needed to eliminate infection from the whole system.

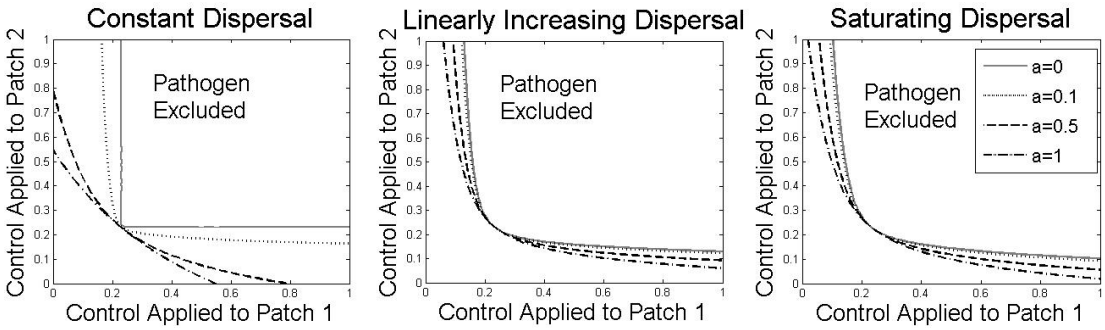

Figure 3.8: Reduction of pathogen exclusion threshold in $c_1 - c_2$ space as natural dispersal increases, shown for all models considered. The model with constant dispersal shows the most striking change in threshold, with the control dependent dispersal models showing a more gradual reduction. Parameters used $\nu_i = 2, \mu_i = 0.2, \gamma_i = 1, \beta = 0.308, \phi_i = 1, h = 1, \kappa = 1, i = 1, 2$.

3.3.4 Parameter dependence of single species model

Since the disease free equilibria of the control dependent dispersal models are analytically intractable, the results of the previous section have been found through simulations using a numerical ODE solver (ode15s) in MATLAB. In order to assess the robustness of these results we must test the behaviour of the system in response to change in the parameters

used. We focus this section on the case when both patches are reservoirs in isolation, and aim to determine how the qualitative properties of these thresholds change with disease dependent parameters. As we would expect, diseases with high transmission rates require higher rates of control in order to completely eradicate infection. Highly lethal diseases, (high γ) require a lower rate of control than less harmful pathogens. Pathogens which cause little or no death are able to survive for long infectious periods and therefore have a higher probability of being transmitted. If γ is high, then the chance of the infected individual dying before they are able to transmit the disease will be greater. Hence the need for higher levels of control at low values of γ.

In the previous simulations the constant dispersal model has generally had a higher threshold than the control dependent dispersal models. When this is the case, the simple 2 patch model with constant dispersal overestimates the amount of control required to exclude the pathogen. However, for certain parameter values, it is found that the order of the thresholds switched, with constant dispersal having a lower threshold than disturbance dependent dispersal. In this case, constant dispersal models will underestimate the amount of control required, leading to ineffective control strategies if movement is increased by control. In these regions of parameter space, the increased movement in response to control is a much more significant problem for disease control.

In order to determine the full effect of varying β and γ on the order of the thresholds, extensive simulations have been run to produce the maps in $\beta - \gamma$ space in figure 3.9. We present two maps comparing a low natural dispersal ($a_i = 0.1$) and a higher natural dispersal ($a_i = 1$). The figures 3.9 split the $\beta - \gamma$ (tranmission-virulence) parameter space into regions determined by the order of the thresholds for the three dispersal functions. These regions are described as (i) disease free (DF), indicating that the pathogen is naturally unable to survive, (ii) Constant dispersal predicts the lowest threshold, with the saturating and linear dispersal models predicting higher control strategies ($C < S < L$). In these cases, when control is uneven between patches, such that $c_i < c_j$, the surge in individuals out of patch j into patch i negates the lower control strategy c_j, leading to an increase in the population in patch j which is able to support the pathogen. (iii) Constant dispersal predicts a higher control strategy than saturating or linearly increasing dispersal functions ($S < L < C$).

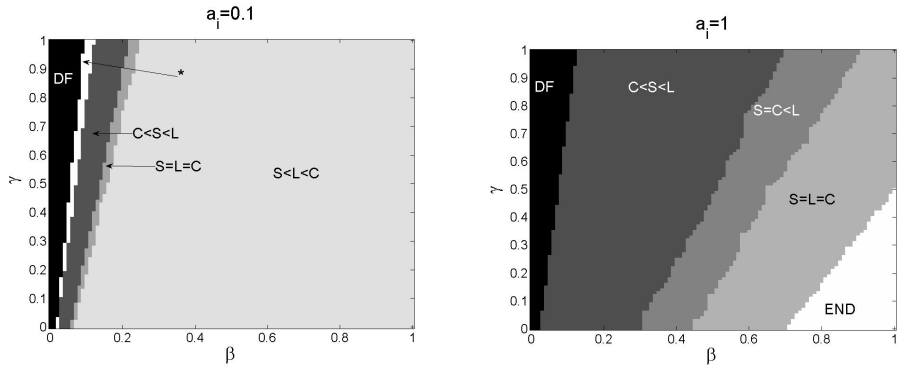

Figure 3.9: Map showing the properties of the control thresholds as β and γ are varied. Parameter space is divided into 4 sections: DF=disease free, *=Disease free at origin, but control leads to infection, $C < S < L$=constant dispersal predicts the lowest threshold, and may underestimate control if disturbance is caused, C=S=L=no discernable difference between the thresholds for these parameter values, and $S < L < C$=control dependent dispersal predicts a lower threshold than constant dispersal models. Parameters used $\nu_i = 2, \mu_i = 0.2, \phi_i = 1, h = 1, \kappa = 1, i = 1, 2$.

In these regions, the constant model may overestimate the amount of control, however this model will still be suitable for the design of control strategies as the predicted controls will be sufficient to eradicate the disease. (iv) The linear model predicts a higher threshold, and there is negligible difference between the constant and the saturating dispersal functions, and (v) There is negligible difference between the thresholds on the control space within the region $[0, 1] \times [0, 1]$ ($C = S = L$). The two regions shown in white in figure 3.9 and not mentioned in this list are an area labelled END within which the pathogen fails to be excluded and hence remains endemic on this range of control parameters; and the area labelled $*$, which exhibits an interesting phenomenon whereby in the absence of control, the population is naturally disease free, however, the increased dispersal due to control forces a change in the population size allowing the pathogen to become established. Thus in this region, it is the control strategies which are creating a suitable environment for disease to take hold. This behaviour highlights the dangers of culling or hunting individuals to the extent that their remaining numbers become so concentrated that the risk of infection is increased (for example in game species [57]).

There are stark differences between the maps shown in figure 3.9. When dispersal is low, the behaviour of the thresholds is determined in a large degree by the change in β, with a large region of this parameter space given the classification ($S < L < C$). If dispersal is low,

then only for very low values of β that constant dispersal is lower than or equal to control dependent dispersal. This is due to the fact that at low levels of β, the threshold occurs at low control levels. At low levels of control, the increase in dispersal in the linear and the saturating models is relatively small. As β increases, the control required increases, and the dispersal due to control has a more significant effect. As figure 3.8 shows, increasing the levels of dispersal causes a flattening, or reduction in the pathogen exclusion threshold. Therefore, at high levels of β, the higher controls required mean that the dispersal due to control increases and the threshold for the linear and saturating models decreases, becoming lower than the constant model. For higher levels of natural dispersal, the constant dispersal threshold is equal to or lower than the control dependent dispersal thresholds for a much wider range of β. This is since the increase in dispersal due to control has a much less significant effect on the population sizes when natural dispersal is high.

3.4 Two host 'Wildlife-Livestock' model

The single species models form a basis for understanding the importance of disturbance and increased dispersal in multi-host models. Multi-host dynamics are particularly relevant when wildlife species act as reservoirs of infection for livestock or domestic animals. The model given in (3.8) represents transmission of infection in a livestock-wildlife system, where the subscripts Li and Wi represent the livestock and the wildlife populations in patch i respectively. The movements of the livestock population are assumed to be restricted such that there is no between patch interaction, and therefore no disease transmission between the two livestock populations. We assume that the livestock populations share a habitat with a wild and free-roaming species which is modelled as in the single species case, and the two species do not

interact in the absence of the pathogen.

$$\text{Livestock}\begin{cases} dS_{Li}/dt &= v_i - \beta_{11}S_{Li}I_{Li} - \beta_{12}S_{Li}I_{Wi} - m_iS_{Li} - c_{Li}S_{Li} \\ dI_{Li}/dt &= \beta_{11}S_{Li}I_{Li} + \beta_{12}S_{Li}I_{Wi} - (m_i+g_i)I_{Li} - c_{Li}I_{Li} \end{cases} \tag{3.8}$$

$$\text{Wildlife}\begin{cases} dS_{Wi}/dt &= \nu_i - \beta_{21}S_{Wi}I_{Li} - \beta_{22}S_{Wi}I_{Wi} - \mu_iS_{Wi} - c_{Wi}S_{Wi} - A_i(c_{Wi})S_{Wi} + \phi A_j(c_{Wj})S_{Wj} \\ dI_{Wi}/dt &= \beta_{21}S_{Wi}I_{Li} + \beta_{22}S_{Wi}I_{Wi} - (\mu_i+\gamma_i)I_{Wi} - c_{Wi}I_{Wi} - A_i(c_{Wi})I_{Wi} + \phi A_j(c_{Wj})I_{Wj}. \end{cases}$$

In the absence of disease and control, the livestock populations achieve equilibrium at $S_{Li} = v_i/m_i$ for $i = 1, 2$, and the wildlife populations achieve equilibria as in the single species case given by (3.3) .

When considering single patch models, the presence of a second host can have drastic consequences on the disease dynamics, the proportion of infected individuals within a population and the controls necessary to rid a population of a pathogen. When considering interacting species, the disease dynamics are determined by the potential for infection of each species. Specifically, whether each species considered is a reservoir for infection or not. Greenman and Hoyle [60, 61] have shown that in multiple host populations, pathogen exclusion may be possible by control of a single species, only if that species is a source of infection to the second, non-reservoir host.

In the two patch case, we must make the distinction between reservoir patches and reservoir hosts. A patch containing two species is a reservoir patch if, in the absence of dispersal, that patch is able to support the pathogen. The patch will support the pathogen if either of the species within that patch is a reservoir host, and would support the pathogen alone in the environment, or if the interaction between the two hosts within a patch is sufficient to support the pathogen. As shown in the single species case, if neither of the patches are reservoir patches, then dispersal between the two will not be sufficient for pathogen persistence, unless dispersal of the wild populations is dramatically skewed one way or the other. However, if

one or both of the patches is a reservoir, then control methods must be employed to free the system of the pathogen. If both patches are reservoirs of infection, then the specifics of control are determined by the within patch disease dynamics. In order to successfully rid the entire two patch system of the pathogen, we must ensure that control is sufficient for infection to be successfully removed from both patches.

There are a number of possible control strategies which may be implemented when dealing with two hosts over multiple patches. It is often the case that disease control will be focussed on the domestic populations in the first instance, with control of wild populations avoided unless absolutely necessary [111], with this in mind, we first consider the necessary conditions for successful disease control whilst controlling only the livestock species of the population. We then go onto investigate a wildlife only control, and finally a joint strategy controlling all wildlife and livestock by independent rates.

It is trivial to show that control of a single species, either wildlife or livestock, will be successful only if the controlled species is responsible for the pathogen persistence. If the host to be controlled is the reservoir of infection, or the infection is sustained only by the interaction of two hosts, then control of a single species will be sufficient for pathogen exclusion. If however, the host which is uncontrolled is a reservoir, then pathogen exclusion is not possible. We therefore only compare the cases when the pathogen is supported by a single species to be controlled, or by the interaction of two non-reservoir hosts.

3.4.1 Control of Livestock Only

If direct control strategies are applied to the livestock population only, then there will be no disturbance of the wildlife population, and all three previously considered models will predict the same threshold. Hence we only consider the constant dispersal model. If the livestock species is the reservoir for infection within each patch, and serves to support the pathogen in the wildlife population, then control of wildlife alone will never result in pathogen exclusion. The livestock population must be controlled to a level which prevents the pathogen being supported by that population.

If the livestock is a reservoir or it is the interaction of the two species which supports the pathogen within each patch, then an increase in the rate of dispersal between wild populations

may help to reduce the amount of livestock control required over the two patches. Figure 3.10 shows that, as in the single species case, a higher rate of dispersal, and therefore increased mixing of two wild populations causes a reduction of the pathogen exclusion threshold with livestock control. A higher level of control in one patch will have a more severe effect on the second if the two patches are coupled at a high rate. This may allow levels of control to be reduced in some areas and increased in others, allowing the pressure of control strategies to be eased for some farms. If all populations of livestock are to be controlled at the same rate, then the impact of the wildlife host does not affect the necessary control.

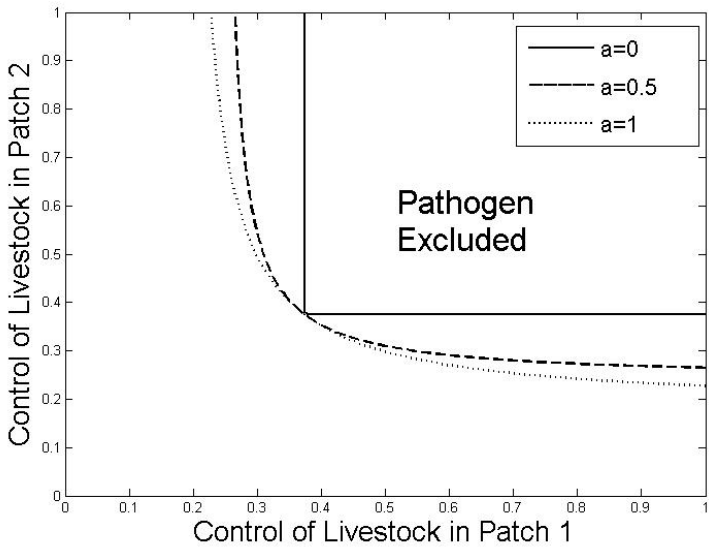

Figure 3.10: Increased coupling, increasing the parameter a, of spatially distinct livestock populations by movement of wildlife may ease the required amount of control. Asymmetric control strategies may prove more cost effective in this situation. Here the pathogen is supported by the interaction of both species. Parameters used $\nu_i = v_i = 2, \mu_i = m_i = 0.5, \gamma_i = g_i = 1, \beta_{ii} = 0.05, \beta_{ij} = 0.5, \phi_i = 1, h = 1, \kappa = 1 i = 1, 2$.

3.4.2 Control of Wildlife Only

If the wildlife population alone is controlled, then we would expect the results to be similar to the single species case. Of course, when the between species transmission, β_{ij} is 0 then the thresholds are identical to the single species case. Increase of between species transmission leads to a significant increase in the necessary control rates for pathogen exclusion, as shown in Figure 3.11. The order of the thresholds, as discussed in section 3.3.4 remains unchanged

by this increase in β_{ij}. If the wildlife species is a reservoir for infection, the necessary control strategy is significantly larger than if the pathogen were supported by the interaction of both species. This result is intuitive since the reservoir species will exert a higher force of infection on the community and therefore require more control [40]. In the case where the pathogen is sustained by the interaction between the two species, reduction in between species transmission will significantly reduce the amount of direct control required. In the extreme, if this contact can be reduced to zero, then the pathogen will be unable to survive. This highlights the importance of reducing contact between multiple hosts in order to lower the burden of control.

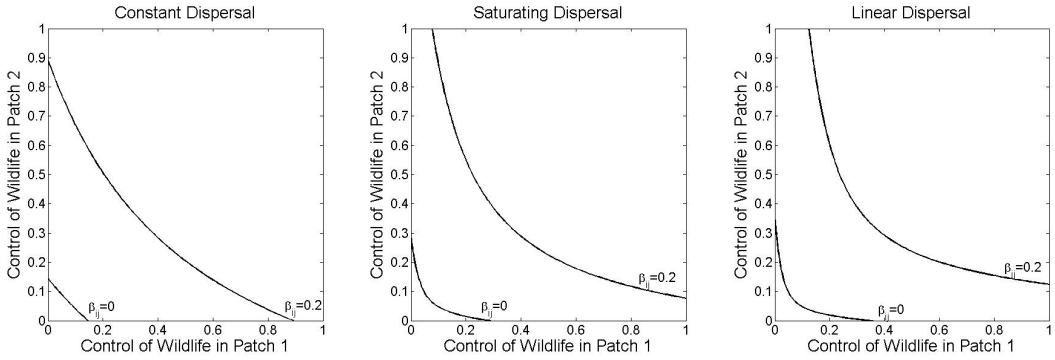

Figure 3.11: Increase in threshold shown for all three dispersal functions when between host contact, β_{ij} is increased. Here the wildlife species is the reservoir of infection and must be controlled to exclude the pathogen. Parameters used $a_i = 1$, $\phi = 1$, $\nu_i = 2$, $\mu_i = 0.2$, $\gamma_i = 0.1$, $\beta_{ii} = 0.05$, h=1,$\kappa = 1$, $v_i = 2$, $m_i = 0.5$, $g = 1$

3.4.3 Mixed Control of Both Wildlife and Livestock

If both species are controlled simultaneously, and controls are equal across both patches, then any increase in dispersal has no effect on the ultimate threshold for pathogen exclusion. The single species model predicts that equal controls applied across both patches will have the same threshold independent of the dispersal rate, so this result is to be expected.

If both species are required for pathogen persistence, then control of both species will have an impact on the pathogen exclusion threshold. Figure 3.12 shows the reduction in threshold in $c_{W1} - c_{W2}$ space as the control applied to the livestock population is increased in the case of constant dispersal. Similar control maps are given when dispersal is increased with control. Control of the livestock species reduces the required control of wildlife species in this

system, highlighting the importance of a joint control strategy. Since livestock populations are managed constantly, reducing the size, and density of the livestock population will have a beneficial effect on the pathogen exclusion threshold, and will be easier to administer than the often high levels of wildlife control required to eradicate the pathogen. This is modelled here by a continuous control applied to the livestock population, however the same outcome would be achieved if the livestock population was reduced in discrete intervals, or by any other feasible, and less intensive method. In Figure 3.12, the three thresholds given are given for $c_L = 0$, which represents no reduction in livestock population abundance, $c_l = 0.1$ which gives approximately a 17% reduction in livestock abundance, and finally $c_L = 0.2$ which represents a 40% reduction in livestock abundance. Livestock farmed at less intensive levels will therefore reduce the risk of infection from wildlife, and in the case of infection, disease will be easier to control through wildlife control if livestock are farmed less intensively.

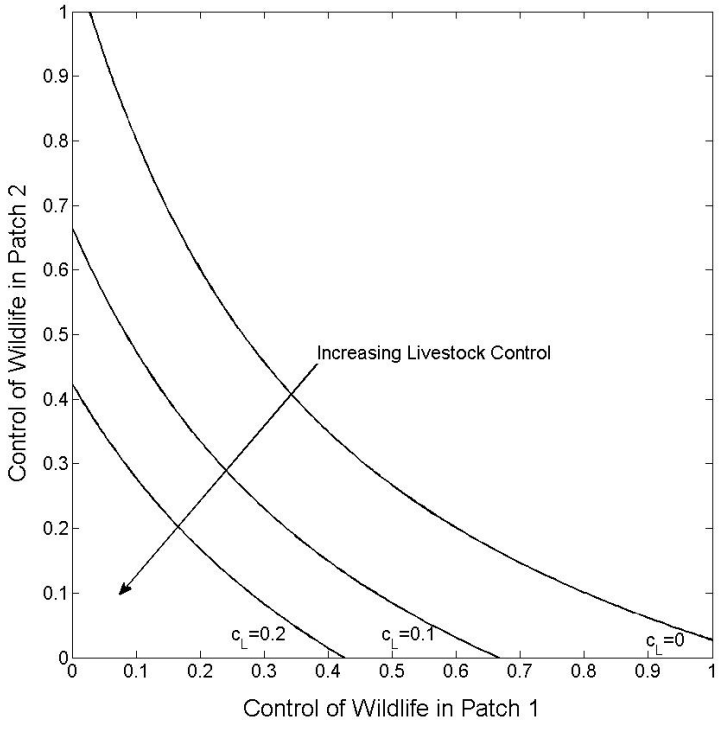

Figure 3.12: Decreasing threshold as control of livestock population increases if both species are needed to support the pathogen. Control map shown for constant dispersal only. Parameters used $\nu_i = v_i = 2, \mu_i = m_i = 0.5, \gamma_i = g_i = 1, \beta_{ii} = 0.05, \beta_{ij} = 0.5, \phi_i = 1, i = 1, 2$.

3.5 Discussion

The models presented here are used to investigate the impact of dispersal of individuals between spatially distinct patches of habitat and the implications of this dispersal for disease control. A single host, two patch, SI model (3.1) is proposed based on the assumption that human disturbance of a population, through the implementation of invasive disease control strategies such as culling, may cause individuals to leave their home patch at an increased rate. The motivation behind this research is a desire to explain the mechanisms underpinning disease transmission between wildlife and livestock hosts. This transmission is particularly important due to the emergence and widespread incidence of diseases such as bovine TB and bluetongue. As such, the parameters chosen throughout this paper have been loosely based on estimates taken from [8] and approximate the spread of bovine TB in a population of badgers.

It was found that the disturbance/control dependent dispersal models predict a different pathogen exclusion threshold when compared to the constant dispersal model. These thresholds converge to the same control strategy if both patches are identical, dispersal is equal between the patches, and control is applied equally to both patches (Figure 3.3), however this situation is realistically unlikely. Figures 3.9 show that, if natural dispersal is high enough, then for a large range of transmission rates, and hence a large range of potential pathogens, constant dispersal gives a lower threshold than control dependent dispersal. Indeed, in this case insufficient control strategies will see a reduction in disease incidence in the patch with higher control, and an increase in the incidence in the other patch. This is due to the movement of both susceptible and infected individuals out of the controlled patch. This response to control was recorded in badgers during the randomised badger culling trial in the UK [102]. This result suggests that insufficient regard for surrounding populations when implementing a control strategy may lead to persistence of disease. Infectious diseases such as bovine tuberculosis in badgers [102], chronic wasting disease in mule deer [51] and hendra and nipah viruses in bat populations [36] have been shown to have important spatial characteristics being transmitted between populations through dispersal or migration. We have shown that any increase in this natural level of dispersal may cause an increase in the level of necessary control. It

is therefore essential to take these dispersal factors into consideration when designing control strategies.

Connectivity is often cited as being a means for disease spread and increased proliferation of a pathogen from a reservoir patch into disease free areas [75]. Reservoir patches may be targeted in isolation as a method of control, however, Figure 3.6 reveals that, whilst this strategy would work for constant dispersal rates, when control methods cause disturbance, then both the reservoir and the non-reservoir patch must be controlled in order to achieve pathogen exclusion. This result is found in both the single species and the two host case and may have significant consequences for disease control between captive and wild populations to prevent disease spread between isolated areas of captivity such as farms.

The results from a basic two patch model reveal a similar pattern when one species is free moving and the other is stationary and unable to roam. In this case however, we were able to see the effect of movement of a wildlife reservoir on disease spread in two distinct areas of livestock. Figure 3.10 shows that increased interaction between the patches of wildlife, through increased connectivity, may ease the level of control required in a single farm. Mixed control strategies targeting both livestock and wildlife populations will be effective when both species support the pathogen, however our models show that targeting livestock alone is insufficient if the wildlife population is a reservoir, and vice versa.

The models considered here are basic models, designed to isolate the effect of increased dispersal. The results presented suggest that controlling disease in patchy habitats may be more complex than constant dispersal models would initially predict. The thresholds produced by these models give the necessary conditions for pathogen exclusion, and hence provide conditions for optimal control schemes. We have shown that for low transmission or high virulence, constant dispersal models can underestimate the required control strategy. As transmission increases, all thresholds increase however the constant dispersal model responds more sensitively, such that at higher transmission rates, the constant dispersal threshold is higher than the control dependent thresholds. Optimisation of disease control strategies aims to minimise the rates of control, and therefore the cost of control. This cost may be given by the financial burden of the control strategy, or in terms of loss of life and animal welfare, or a combination of these factors. The pathogen exclusion thresholds define a key constraint to

optimal control, with overestimation of thresholds causing the predicted control methods to be suboptimal, resulting in a greater financial spend than necessary or in an unnecessary loss of life.

The models considered here are based on basic assumptions of population growth and dispersal throughout a landscape. In particular, reproduction is given in this paper by a constant rate ν_i. Realistically, reproduction will be impacted by density dependent factors which would produce a logistic-type growth curve. Excess culling (or harvesting) a biological population will result in a population decline to extinction as the population is unable to replace itself [81]. This phenomenon does not occur in the model presented here, due to the constant recruitment term and hence the idea of maximum sustainable yield [105] is not coherent for this model. The balance between culling a species to extinction, and culling sufficiently so as to eradicate a disease is an important one, and is the focus of future research. A closer critique of the mechanisms of dispersal, including density dependent migration would also help to increase the realism and thus the applicability of this model. This work may also be extended to form part of a metapopulation analysis to evaluate the disturbance effect of populations over a large number of patches. The interesting results apparent from a simple model such as this form a firm basis for further investigation of the effect of disturbance on disease spread in wild populations and its implications for control.

Chapter 4

Density dependent movement: implications for harvesting practices

4.1 Introduction

In the previous chapters, we have investigated how harvesting practices and disease control strategies are changed when populations are coupled by movement or dispersal between distinct areas. Dispersal can however be governed by several processes. The process of dispersal is often described as the cumulative effect of three separate individual decisions: emigration (the decision to leave a patch), movement (the distance, and direction etc) and immigration (the decision to remain in a patch) [24, 148]. It has been suggested, that reducing these three processes down to a single constant rate is an oversimplification stemming from the lack of consistent empirical descriptions of dispersal [24]. Many studies focus only on a single part of this process [24], hence it is difficult to discern the key factors affecting dispersal for a given species which may then be incorporated into a theoretical model. In this chapter, we aim to target a middle ground between the extremes of complete reduction of the process to a single parameter, and modelling each facet of dispersal distinctly. In particular we focus more specifically on the local, environmental drivers for emigration. In the models considered here, we investigate the impact that local population density has on this process and the implications that density dependent movement has in terms of harvesting practices and population control.

There is a rich experimental literature supporting the hypothesis that local population density affects the process of emigration in a variety of species. For example, many species of aphid (family *Aphididae*) have migratory life stages which will develop only at high density, preventing dispersal at low population densities [37]. Density dependent emigration has also been observed in species of beetle inhabiting cow pats [113], as well as female root voles *Microtus oeconomus* [2]. In these and other examples, individuals may be forced out of a patch by high population densities and limited resources. By using 'population density' in this context we shall refer to the ratio of the population size to the carrying capacity. The carrying capacity of a patch is defined as 'the maximum population size that can be supported indefinitely by a given environment, at which intraspecific competition has reduced the per capita net rate of increase to zero' [17]. If the population density within an environment is greater than 1, then the population size exceeds its carrying capacity and the per capita growth rate of individuals within the patch is negative. This chapter aims to quantify the effect of density dependent movement in terms of the population response to harvesting practices, as well as the change in yield predicted by considering these density dependent effects. These considerations are discussed initially in a simple model with no disturbance before being developed to include a perturbation response to harvesting efforts.

4.2 Density dependent emigration in a 2-patch system

4.2.1 General Dynamics

If individuals are forced to leave their original patch due to high densities, then we assume that the rate of movement out of a patch increases with population density. If we consider a general growth function $f(N_i)$, then the carrying capacity of the patch is given by the equilibrium solution of

$$\frac{dN_i}{dt} = f(N_i),$$

where $f(N_i)$ could, for example, be given by constant recruitment or logistic growth. If we define the carrying capacity of patch i in isolation as K_i, then density dependent emigration

can be modelled in the following way

$$\begin{aligned}\frac{dN_1}{dt} =& f(N_1) - m\left(\frac{N_1}{K_1}\right)^s N_1 + m\left(\frac{N_2}{K_2}\right)^s N_2 \\ \frac{dN_2}{dt} =& f(N_2) - m\left(\frac{N_2}{K_2}\right)^s N_2 + m\left(\frac{N_1}{K_1}\right)^s N_1 \end{aligned} \tag{4.1}$$

where the parameter m represents the species dependent rate of response to crowding. If m is high then the species moves at a faster rate for a given density. For simplicity, in the basic model, we assume that this quantity is the same across both patches. This is not unreasonable, since it represents the particular response of the species to its local environment. Note that this assumption does not necessarily imply that the movement rate between patches are equal, since the rate of movement is dependent on the population density multiplied by this constant. The parameter $s \geq 0$ defines the strength of the density dependent emigration response, with $s = 0$ equating to a density independent response, and hence a constant per capita movement rate. In this case, when $s = 0$, the model is identical to that discussed in chapter 2. This model is based on that given by Amarasekare [5]. The per capita, and total movement rates, for different strengths of density dependence, are shown in figure 4.1 which highlights the distinction between constant and density dependent per capita movement rates. If the per capita movement is constant, then individuals in a very small population will have the same per capita movement rate as those at a very high population density. Even with a very weak level of density dependence, the per capita rate of movement will decrease to zero for very low population densities. In terms of the total movement rate, the number leaving the patch per unit time, decreases to zero as the population density decreases. This is true for both the constant movement model as well as the density dependent model. Density dependence simply reduces the total rate of movement faster than the constant movement model.

Recall from chapter 2 that as the constant movement rate m increases, the equilibrium of the patch sizes tend to the same value ($N_1^* = N_2^*$) as $m \to \infty$ if movement is symmetric (where $m = m_1 = m_2$), and tend to $\phi N_1^* = N_2^*$ as $m \to \infty$ if movement is asymmetric ($m = m_2$ and $\phi = m_1/m_2$). In the density dependent model however, the movement rate is varied with the population size. As the response rate m increases to infinity, we are able to find the equivalent ratio of the population sizes. By taking the first equation in (4.1) at

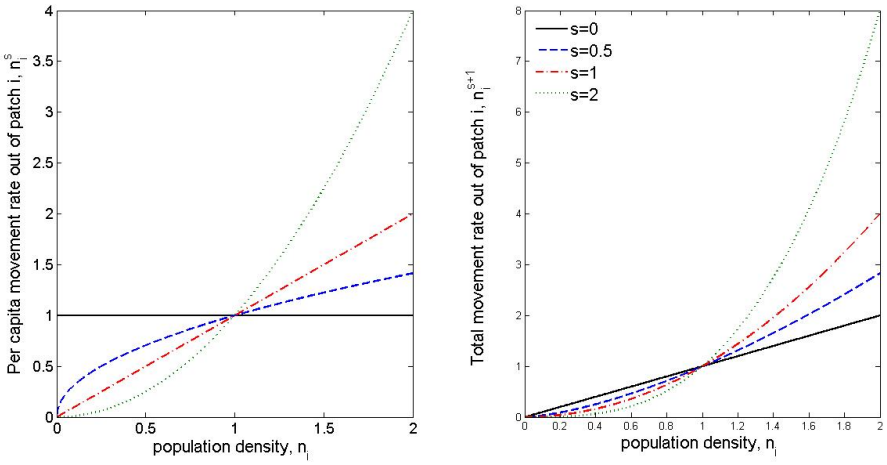

Figure 4.1: Per capita (left), and total (right) movement rates against population density for increasing strength of density dependence s.

equilibrium,

$$0 = f(N_1) - m\left(\frac{N_1}{K_1}\right)^s N_1 + m\left(\frac{N_2}{K_2}\right)^s N_2 \tag{4.2}$$

$$m\left(\frac{N_1}{K_1}\right)^s N_1 = f(N_1) + m\left(\frac{N_2}{K_2}\right)^s N_2 \tag{4.3}$$

$$\frac{N_1^{s+1}}{N_2^{s+1}} = \frac{K_1^s f(N_1)}{N_2^{s+1} m} + \frac{K_1^s}{K_2^s} \tag{4.4}$$

which, as $m \to \infty$ reduces to

$$\frac{N_1^{s+1}}{N_2^{s+1}} = \frac{K_1^s}{K_2^s} \tag{4.5}$$

$$\frac{N_1}{N_2} = \left(\frac{K_1}{K_2}\right)^{s/(s+1)}. \tag{4.6}$$

This implies that if the carrying capacity of patch 1 is larger than the carrying capacity of patch 2, then the population size in patch 1 will remain larger than that of patch 2 even if movement between the patches is very frequent. Density dependent dispersal therefore limits the synchrony between distinct patches, meaning that a patchy landscape will remain patchy even if there is high potential for dispersal. If both patches in a two patch system are of equal carrying capacities, then the system will attain a stable equilibrium at $(N_1^*, N_2^*) = (K, K)$.

For a full comparison with the constant movement model detailed in chapter 2, we explore the behaviour of this model, and therefore evaluate the impact of density dependent emigration for two potential growth functions. Constant recruitment models the dynamic response of a constantly stocked system, whilst logistic growth models a naturally reproducing population.

4.2.2 Constant recruitment model

In the case of constant recruitment, $f(N) = (a - bN)$, an increase in population density has the dual effect of increasing the death rate of the population as well as increasing the outward movement. The rate of recruitment into the population is however unchanged by population density or harvesting. The carrying capacity of each patch in this case is given by $K_i = a_i/b_i$. The two patch model is therefore given by

$$\frac{dN_1}{dt} = a_1 - b_1 N_1 - m\left(\frac{b_1 N_1}{a_1}\right)^s N_1 + m\left(\frac{b_2 N_2}{a_2}\right)^s N_2 - c_1 N_1 \tag{4.7}$$

$$\frac{dN_2}{dt} = a_2 - b_2 N_2 - m\left(\frac{b_2 N_2}{a_2}\right)^s N_2 + m\left(\frac{b_1 N_1}{a_1}\right)^s N_1 - c_2 N_2, \tag{4.8}$$

where c_i is the constant harvesting rate in patch i. In the absence of any harvesting, a symmetric system ($a_1 = a_2 = a, b_1 = b_2 = b$) will always reach equilibrium at $N_i = a/b$ within both patches. This can easily be shown by substituting this value into the equations (4.8) and confirming that the system is indeed at equilibrium and $dN_i/dt = 0$.

$$\frac{dN_i}{dt} = a - b\frac{a}{b} - m\left(\frac{ba}{ab}\right)^s \frac{a}{b} + m\left(\frac{ba}{ab}\right)^s \frac{a}{b} \tag{4.9}$$

$$= a - a - m\frac{a}{b} + m\frac{a}{b} \tag{4.10}$$

$$= 0. \tag{4.11}$$

Any asymmetry in the system is in part compensated for by the coupling of the two patches which acts to reduce the difference in population size. If we consider two isolated patches with populations at their carrying capacities such that $a_1/b_1 > a_2/b_2$, and open a corridor between these patches such that dispersal is able to occur (this is done mathematically by

increasing m, such that $m > 0$), then initially, the dynamics of the larger patch are given by

$$\frac{dN_1}{dt} = a_1 - b_1\frac{a_1}{b_1} - m\left(\frac{a_1 b_1}{b_1 a_1}\right)^s \frac{a_1}{b_2} + m\left(\frac{a_2 b_2}{b_2 a_2}\right)^s \tag{4.12}$$

$$= m\left(\frac{a_2}{b_2} - \frac{a_1}{b_1}\right) < 0. \tag{4.13}$$

The larger patch thus decreases in density since individuals leave this patch at a faster rate than those entering it from patch 2. It can similarly be shown that patch 2 increases in population density due to this imbalance of movement. The decrease in population density slows down the rate of movement out of patch 1, and the increase in density increases the rate of movement out of patch 2. The extent to which the population density affects the movement rate is governed by the magnitude of the parameter s. As s increases, any change in density will have an increasingly more significant impact on the movement rate. Hence the reduction in density of the larger population, will lead to a severe drop in movement rate if s is high. This will curb the number of migrants leaving the patch, and maintain a higher population density. The population size within each patch is shown in figure 4.2 for a range of s. Since the larger patch will always be the reduced in density as a result of coupling, and this patch makes the most significant contribution to the population as a whole, this severe reduction in dispersal out of the larger patch has a strong effect on the distribution of the population across the patches. Therefore increasing s maintains the asymmetry in the patches closer to their isolated carrying capacity for a given value of m.

Harvesting in the constant recruitment model

In the following simulations, we have assumed that both patches have equal carrying capacities (a/b) in the absence of any harvesting. It is therefore the practice of harvesting the populations that introduces asymmetry in the populations. In the first instance we assume that a single patch alone is harvested.

Harvesting a single patch

Recall from Chapter 2, that if the harvesting effort is applied to a single, isolated population,

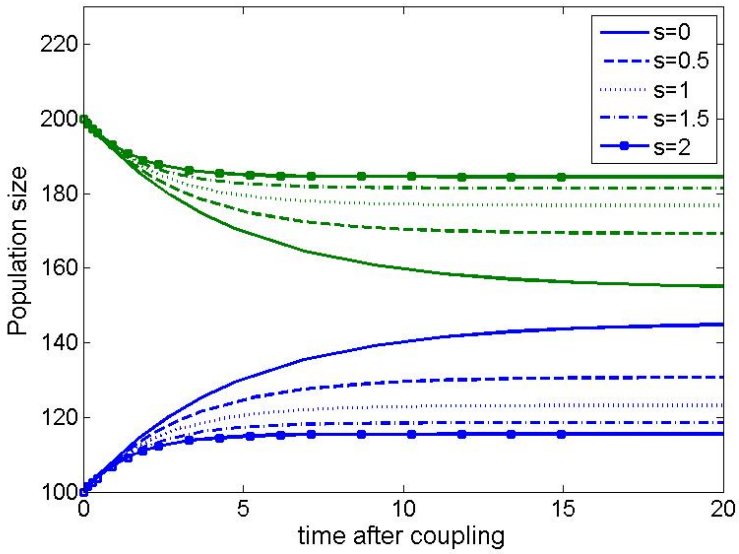

Figure 4.2: Population size after coupling of two, asymmetric patches. Patch 1, green lines, has a higher carrying capacity than patch 2, blue.

then the equilibrium will decrease to

$$N_C = \frac{a}{b+c}.$$

If a corridor of dispersal is now opened up between this patch and another, unharvested patch of similar size (denoted N_2, with equilibrium a/b), then the harvested population size will change dependent on the equation

$$\frac{dN_C}{dt} = a - bN_C - m\left(\frac{b}{a}N_C\right)^s N_C + mN_2 - cN_C \tag{4.14}$$

$$\frac{dN_C}{dt} = a - \frac{ba}{b+c} - m\left(\frac{b}{b+c}\right)^s \frac{a}{b+c} + m\frac{a}{b} - \frac{ca}{b+c} \tag{4.15}$$

$$\frac{dN_C}{dt} = ma\left(\frac{c+b(1-\Omega)}{b(b+c)}\right) > 0, \qquad \Omega = \left(\frac{b}{b+c}\right)^s \leq 1. \tag{4.16}$$

Since this rate of change is positive, the harvested population will increase in response to coupling with a separate patch. As the strength of density dependence s increases, Ω decreases, and dN_C/dt becomes more positive. This suggests that strong density dependent dispersal can lead to a faster repopulation, and compensatory response to harvesting if a wildlife corridor between similar sized patches is opened. This of course does not tell us any-

thing about the ultimate patch size reached, rather the rate of movement into the patch. The precise population size reached cannot be found analytically in the general density dependent movement case, however, we are able to show the effect of increasing the strength of density dependence through simulation results. Figure 4.3 shows the response of the harvested population after it is coupled with an identical, but unharvested patch for a range of density dependent movement strengths. The three graphs show the change in harvested population for different harvesting efforts. A low harvesting effort, $c = 0.002 = 0.1b$, shows an increase in harvested population as density dependent movement, s increases. This result is also seen as the harvesting effort is increased to be equal to the death rate $c = 0.02$. The increase in harvested equilibrium as density dependent movement increases is due to the reduction in emigrants out of the harvested population. If s is high, then a very small reduction in population density will cause a more significant reduction in emigrants. The net flow of individuals in the harvested patch will therefore be dominated by immigrants from patch 2. This leads to an increase in the equilibrium population in the harvested patch. For very high harvesting efforts, $c = 0.2$, relative to the natural death rate, density dependent movement can have a detrimental response to the equilibrium population size. At high harvesting rates, individuals are removed from the patch soon after they arrive. In this case, the reduction in emigrants is sufficient to reduce the patch 2 population. This leads to a reduction in the number of immigrants into the harvested patch, and a reduction in equilibrium size as the strength of density dependence increases.

The results shown in figure 4.3 for the behaviour of the harvested patch after coupling are reversed for the coupled patch. At low harvesting efforts, density dependent movement predicts a lower coupled population size than constant movement. This relationship switches as harvesting effort increases, and is a direct response to the dynamic behaviour described in the case of the harvested patch.

It is unclear from figure 4.3 whether the harvested population at equilibrium changes monotonically with strength of density dependence for a given harvesting effort. Simulation results (figure 4.4) show that as the strength of density dependence increases, approaching a step function, as assumed by Prentice [114], the equilibrium population of the harvested patch (i) increases monotonically for low harvesting rates, (ii) increases to a maximum before

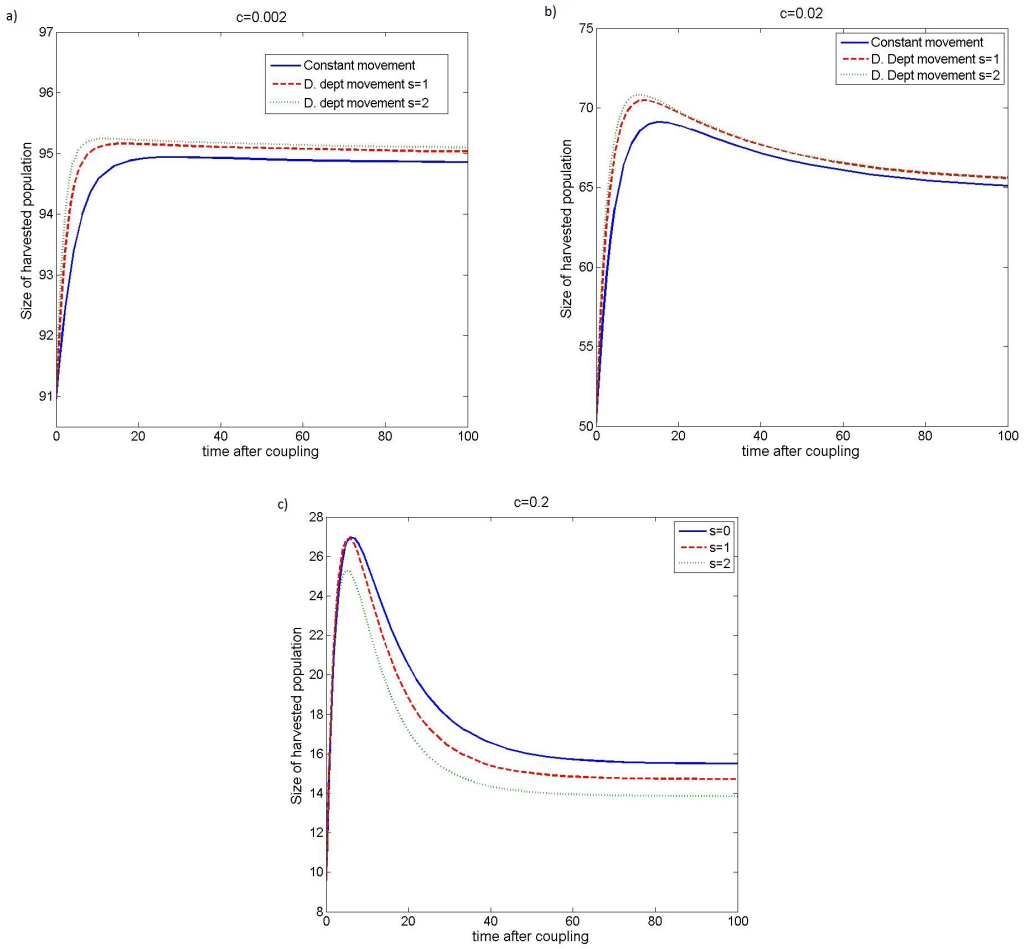

Figure 4.3: Population size in harvested patch after coupling with a similar, unharvested patch. The density dependent movement model shows higher population size than the constant movement model. Initial values are isolated patch equilibria. Parameters used $a = 2, b = 0.02, m = 0.1$.

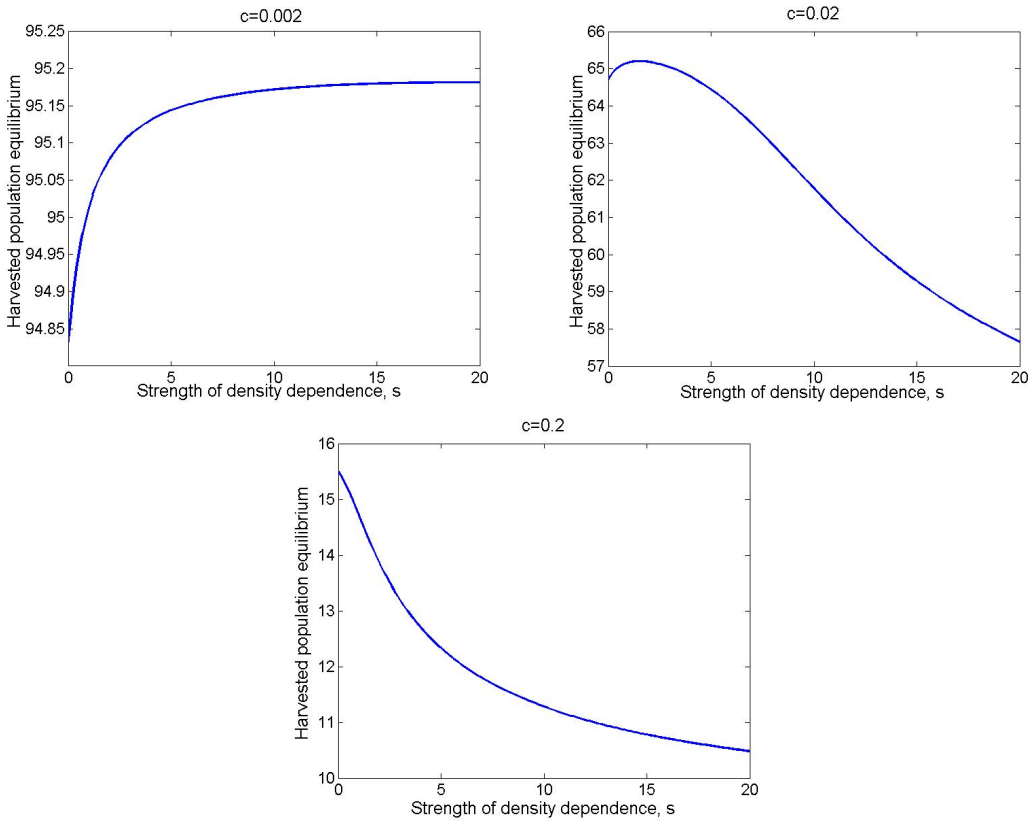

Figure 4.4: Population size at equilibrium of harvested population for increasing strength of density dependence. Parameters used $a = 2, b = 0.02, m = 0.1$

decreasing below the population given by constant movement for harvesting rates similar to natural death, (iii) decreases monotonically for very high harvesting rates. Quantifying the strength of the density dependence in the movement rate can therefore have important consequences in terms of the population sizes predicted by the model.

Figure 4.4 highlights the proportional difference in population equilibrium size. The y-axis scale of figure 4.4 a) is very small, indicating that at very low harvesting effort, even a very strong density dependent effect has a negligible effect on the population. For higher harvesting effort the difference in strength of density dependence becomes more pronounced, as can be seen with respect to the yield shown in figure 4.5.

Given that for very low harvesting efforts, the population size predicted by the density dependent model is higher than that predicted by the constant movement model, and for high harvesting levels this relationship is switched, we may expect the behaviour of the yield predicted by the corresponding models to mimic this relationship. In chapter 2, we found

the expression for the yield in the constant movement model, when only a single patch was harvested, was given by

$$Y = c_1 N_1^* = \frac{c_1(a_1 b_2 + (a_1 + a_2)m_2)}{c_1(b_2 + m_2) + (b_1 + m_1)(b_2 + m_2) - m_1 m_2}. \tag{4.17}$$

Adapting this expression for the density dependent model, the yield can be expressed as

$$Y = c_1 N_1^* = \frac{c_1(a_1 b_2 + (a_1 + a_2)m\theta_2)}{c_1(b_2 + m\theta_2) + (b_1 + m\theta_1)(b_2 + m\theta_2) - m^2\theta_1\theta_2}. \tag{4.18}$$

where $\theta_i = (N_i^*/K_i)^s$, and $K_i = a_i/b_i$. This yield is monotonically increasing as c_1 increases, with the limit as $c_1 \to \infty$ given by

$$Y \to a_1 + \frac{a_2 m(N_2/K_2)^s}{m(N_2/K_2)^s + b_2}. \tag{4.19}$$

This expression, as with constant movement, is made up of the birth rate in patch 1 plus the birth rate in patch 2 multiplied by the probability of moving from patch 2 to patch 1. If both patches are equal in the absence of harvesting, then harvesting in patch 1 alone will lead to a reduction in both populations such that $N_i^*/K_i < 1$ in both patches. In a symmetric system, an increase in the strength of density dependent emigration will therefore lead to a reduction in yield, since $(N_2/K_2)^s$ decreases for increasing s. This result is shown in figure 4.5. This figure confirms that at high harvesting efforts, the yield is lower for density dependent movement than the constant movement model. This is the expected result given the equilibrium behaviour shown in figure 4.3. At low harvesting efforts, we would expect the density dependent model to predict a higher yield than constant movement, however, figure 4.5 shows that at such low harvesting efforts the difference in yields is negligible.

If however, harvesting takes place in an asymmetric system, such that the natural carrying capacity of patch 1 is greater than that of patch 2 ($K_1 > K_2$), this result does not always apply. In this case, coupling of the two patches causes a decrease in size of the larger patch, such that $N_1^*/K_1 < 1$, but an increase in size of the smaller patch in the absence of harvesting. This leads the population density in patch 2 to be $N_2^*/K_2 = \theta_2 > 1$. Harvesting the larger patch will therefore have the effect that the population density in patch 1 is reduced further,

and the population density in patch 2 is reduced such that $N_2^C/K_2 < \theta_2$ (where N_2^C is the population equilibrium in patch 2 during harvesting). For intermediate harvesting efforts, however, this second condition does not necessitate that $N_2^C/K_2 < 1$, and hence it is possible that an increase in the strength of density dependent emigration may result in an increase in yield. In any case, as the harvesting effort increases, the patch 2 population is decreased enough to reduce the rate of immigration into the harvested patch, and eventually the yield predicted by this model will be less than that predicted by the constant model. This is shown in figure 4.6.

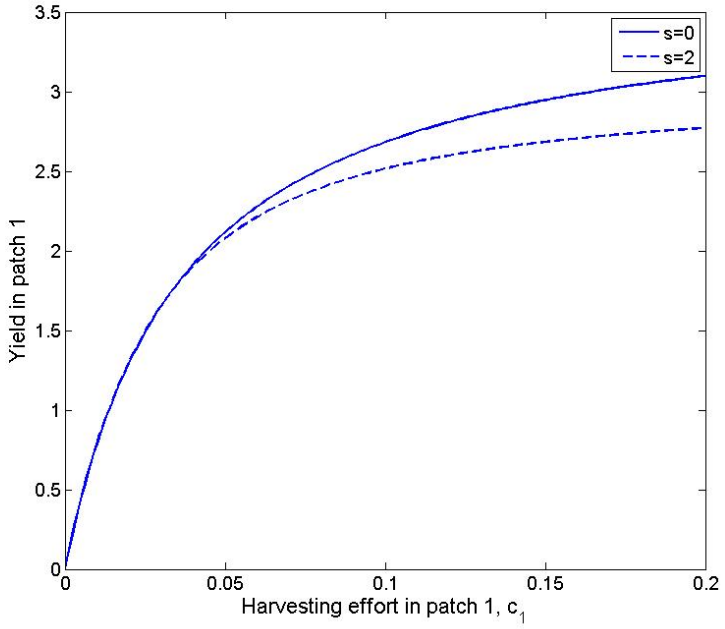

Figure 4.5: Yield obtained from a single patch in a symmetric two patch system. Solid line shows the constant movement model, dashed line shows density dependent movement. Parameters used: $a = 2, b = 0.02, m = 0.1$.

Yield if both patches are harvested

The discussion above has concerned the population and yield of the single harvested patch within a two patch system. However, the harvesting effort applied in a single patch has a knock on effect on the population dynamics of the coupled patch. Specifically, harvesting will cause a reduction in the size of the coupled population due to removal of potential immigrants. In the density dependent model, there are a number of other factors that affect the popula-

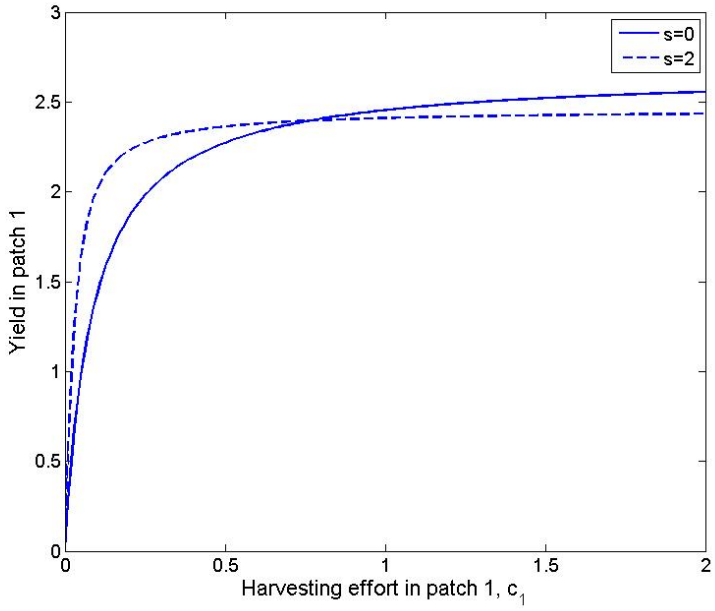

Figure 4.6: Yield obtained from a single patch in an asymmetric system. Here the larger of the two patches is harvested. In this case, density dependent emigration leads to an increase in yield. Parameters used: $a = 2, b_1 = 0.02, b_2 = 0.2, m = 0.1$.

tion sizes. Harvesting reduces the rate at which migrants leave the harvested patch and enter the coupled patch. We would expect therefore that an increase in the strength of density dependence leads to a decrease in the population size of the coupled patch. Harvesting will also however reduce the population size of the coupled patch which will trigger the density dependent movement response, and prevent individuals leaving, hence buffering the coupled patch against the effects of harvesting.

If both patches are harvested, then the yield is given by

$$Y_i(c_1, c_2) = \frac{c_i(a_j m\theta_j + a_i(b_j + m\theta_j + c_j))}{(b_1 + m\theta_2 + c_2)(b_1 + m\theta_1 + c_1) - m^2\theta_1\theta_2}. \tag{4.20}$$

In a fully symmetric system, with equal demographic parameters, and equal harvesting efforts, then the populations in both patches equal

$$N_i^* = \frac{a}{b + c}$$

and the yields are hence given by

$$Y_i(c, c) = \frac{ca}{b + c}.$$

We are therefore interested in the predicted yield when harvesting occurs asymmetrically. Figure 4.7 shows the difference between the constant movement model, and the density dependent movement model with $s = 1$ in terms of both the population equilibrium in patch i, and the yield in patch i. Cooler regions, dark blue, represent regions where the constant movement model predicts a higher population size or yield than the density dependent model. These regions fall predominantly below the $c_i = c_j$ line, and hence occur when $c_i > c_j$. If this is the case, then harvesting in patch 1 is more intense than the effort in patch 2. In these regions, the behaviour of the system is essentially the same as that described in the single patch case. If however, $c_j > c_i$, then the population size, and hence the yield predicted in patch i is lower in the constant movement model than the density dependent model. This is because the difference in patch sizes is maintained more in the density dependent model than the constant. In the constant movement model, the disparity in harvesting effort is compensated for by the movement of individuals. Since a lower harvesting rate in patch 1, would lead to a larger population there than in patch 2, density dependent movement will maintain this higher population, whereas constant movement forces the patches to become more synchronised. It is clear from this difference in predicted yields that neglecting the effects of density dependent movement in coupled systems could lead to predictions that are too high, if neighbouring patches are harvesting at lower rates, or too low if neighbouring patches are harvesting at higher rates.

4.2.3 Logistic growth model

Harvesting and Extinction Conditions

As discussed in chapter 2, the constant recruitment model provides us with a simple model of limited population growth, and is an appropriate approximation for stocked and managed systems. The constant recruitment model also enables more analysis due to its simple form. However, as in chapter 2, we wish to also consider a more realistic growth function which allows reproduction to be regulated by intraspecific competition, modelling this by logistic

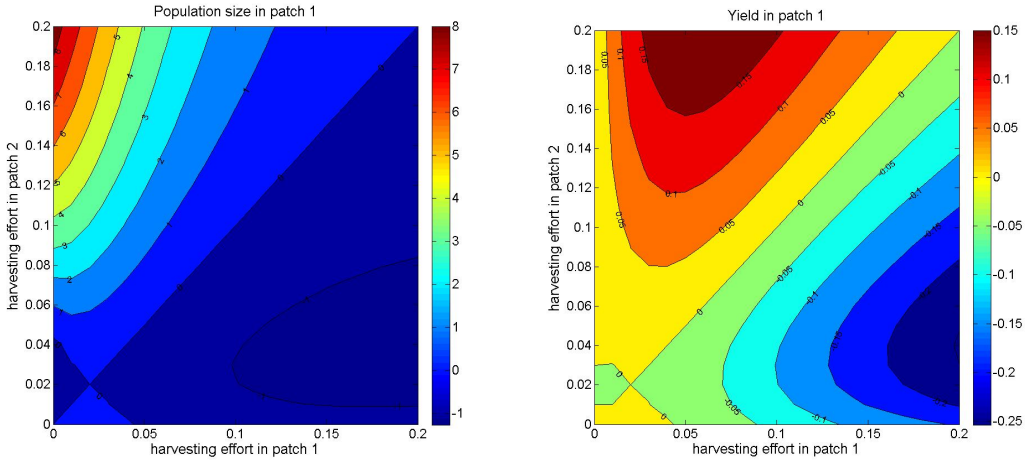

Figure 4.7: Left: Difference in patch 1 population size predicted by density dependent model with $s = 1$ and constant model. Negative areas show regions where density dependent model predicts lower population size than constant. Right: Difference in yields predicted in patch 1, as harvesting efforts across both patches vary. Negative regions indicate where density dependent movement predicts a lower yield than constant movement. Parameters used $a = 2, b = 0.02, m = 0.1$.

growth. The full two patch model is therefore given by

$$\frac{dN_1}{dt} = r_1 N_1 \left(1 - \frac{N_1}{K_1}\right) - m\left(\frac{N_1}{K_1}\right)^s N_1 + m\left(\frac{N_2}{K_2}\right)^s N_2 - c_1 N_1 \tag{4.21}$$

$$\frac{dN_2}{dt} = r_2 N_2 \left(1 - \frac{N_2}{K_2}\right) - m\left(\frac{N_2}{K_2}\right)^s N_2 + m\left(\frac{N_1}{K_1}\right)^s N_1 - c_2 N_2. \tag{4.22}$$

The logistic model differs from the constant recruitment model in that, if harvesting is carried out at a fast enough rate, then it is possible to drive the system to extinction. The extinction equilibrium $(N_1, N_2) = (0, 0)$, is stable in the density dependent model if the eigenvalues of

$$J = \begin{pmatrix} r_1 - c_1 & 0 \\ 0 & r_2 - c_1 \end{pmatrix} \tag{4.23}$$

are both negative. The eigenvalues of matrix J are given by $\lambda_1 = r_1 - c_1$, and $\lambda_2 = r_2 - c_2$. For positive growth rates $(r_1, r_2 > 0)$ density dependent movement therefore implies that harvesting in a single patch will never be sufficient to drive the population to extinction. In fact the extinction threshold in the density dependent model is identical to that in a system of two uncoupled, isolated populations. Both patches must be harvested at rates exceeding their

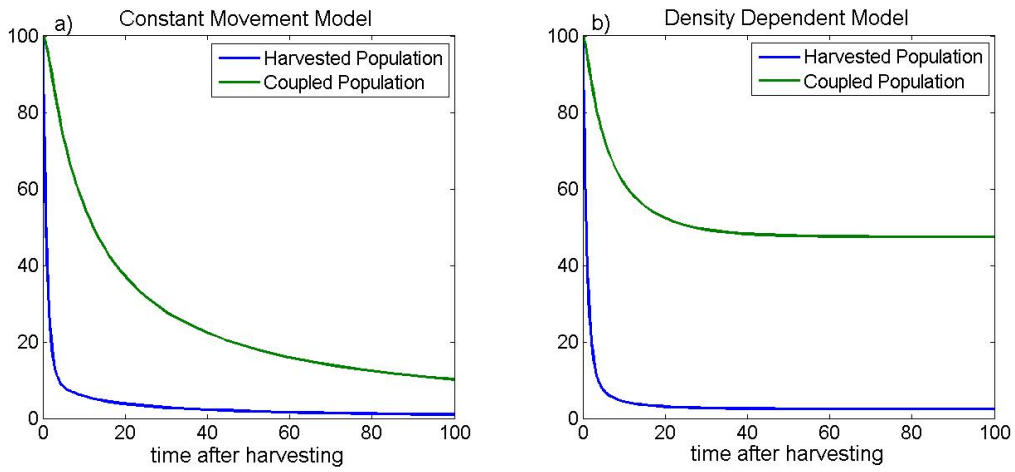

Figure 4.8: Comparison between constant movement model a), and density dependent model b) when a single patch is harvested. Density dependent movement allows the coupled patch to maintain a much higher equilibrium. Parameters used $r_1 = r_2 = 0.09, K_1 = K_2 = 100, m = 0.1, c_1 = 1$.

growth rates in order to drive the system to extinction. This is because harvesting reduces the population size, therefore reducing the movement rate between the patches.

Harvesting in a single patch

If a single patch is harvested, the rate at which individuals leave the harvested patch and enter the coupled patch is reduced. This in turn causes a reduction in the size of the coupled patch. Since reproduction is density dependent, as well as movement, in the logistic model, this reduction in population size causes the number of emigrants from the coupled patch to reduce, and the growth rate to increase. This allows the coupled population to recover from the effects of harvesting in it's neighbour, and to maintain a positive equilibrium. The effect of harvesting in a single patch can clearly be seen in figure 4.8. Here the harvested population is not significantly different between the constant and the density dependent model, however, the coupled population is much more severely affected by harvesting in the constant movement model than in the density dependent case.

Whilst it appears in figure 4.8 that the harvested population does not differ by a significant amount between models, the equilibrium value in the density dependent model is in fact higher than that predicted by the constant model, albeit by a small amount. The equilibrium size of the harvested patch is shown in figure 4.9 as the strength of density dependence in-

creases. In the logistic growth model, as in the constant recruitment, we observe an increase in harvested equilibrium for low harvesting effort, $c < r_1$, however, as harvesting increases $c = r_1$, the harvested population shows an increase if density dependence is small, however, for very strong density dependence, the population begins to drop.

Harvesting in both patches

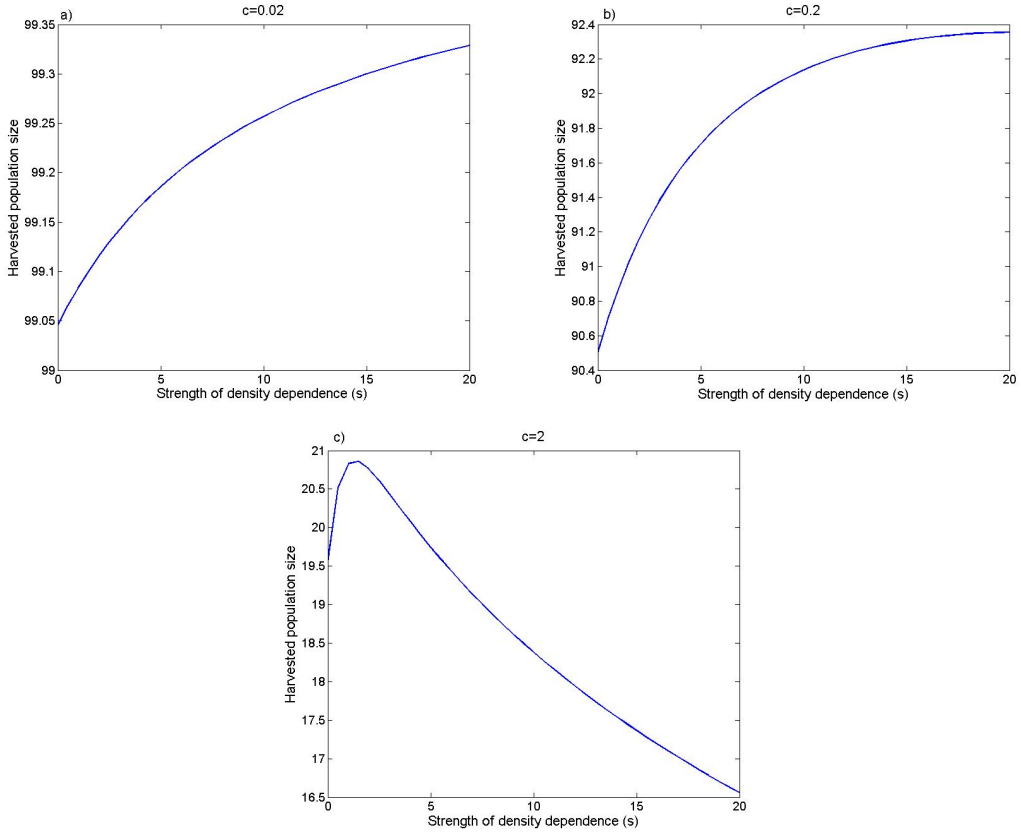

Figure 4.9: Harvested population size as strength of density dependence increases in the logistic growth model. Parameters used $r = 2, K = 100, m = 0.1$

As seen in the constant recruitment model, equal harvesting rates, across equal patches maintain the symmetry in both models, and hence the effect does not differ between constant or density dependent movement. If however, the harvesting rates do not balance, $c_2 = \alpha c_1$, then for $\alpha \neq 1$ the equilibrium values are shown in figure 4.10. In this figure, the x-axis shows the harvesting effort applied in patch 1, with $c_2 = 0.5c_1$ in plot a), and $c_2 = 1.5c_1$ in plot b). The blue lines show the change in patch 1 equilibrium, and the green show the patch 2

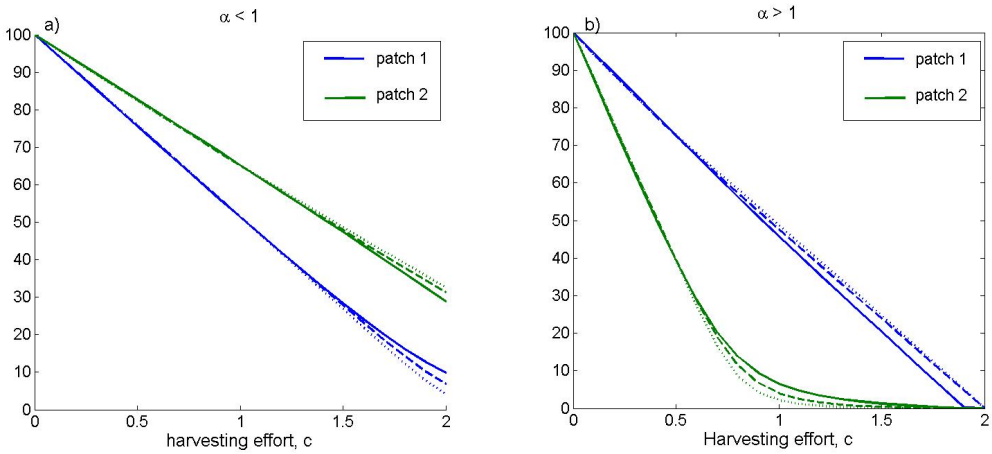

Figure 4.10: Equilibrium sizes as effort increases for asymmetric harvesting efforts. Plot a) is for $c_2 = 0.5c_1$ and plot b) is when $c_2 = 1.5c_1$. Solid lines give equilibrium values for constant movement, dashed show the results when $s = 1$, and dotted show $s = 2$.

equilibrium. It is clear from these plots that for very small harvesting effort, the addition of density dependence into the model makes very little difference, the lines for the three cases considered ($s = 0, 1, 2$) are on top of each other. However, as the harvesting effort in patch 1 approaches the growth rate in patch 1, $c_1 \to r_1$, the differences between the models become more apparent. In plot a), $\alpha < 1$ and patch 2 is harvested at a lower rate than patch 1. In this case, density dependent movement causes a decreases the population size in patch 1 and an increase in the population size in patch 2. The converse is seen in figure b). However in both cases, the patch with the lower harvesting effort sees an increase in population size if movement is density dependent, and the patch with the higher effort sees a decrease in size. This reflects the results when a single patch alone is harvested, and the reasoning behind these dynamics is the same. These properties are shown in contour plots in figure 4.11. The vivid regions of these plots, deep blue and yellow-red show the divergence of the two models close to the extinction threshold.

Yield if a single patch is harvested

As the strength of density dependence increases, the yield follows the equilibrium behaviour shown in figure 4.9. In all of theses cases, for weakly density dependent movement, $s \approx 1$, the equilibrium is higher than that predicted by the constant model. We would therefore

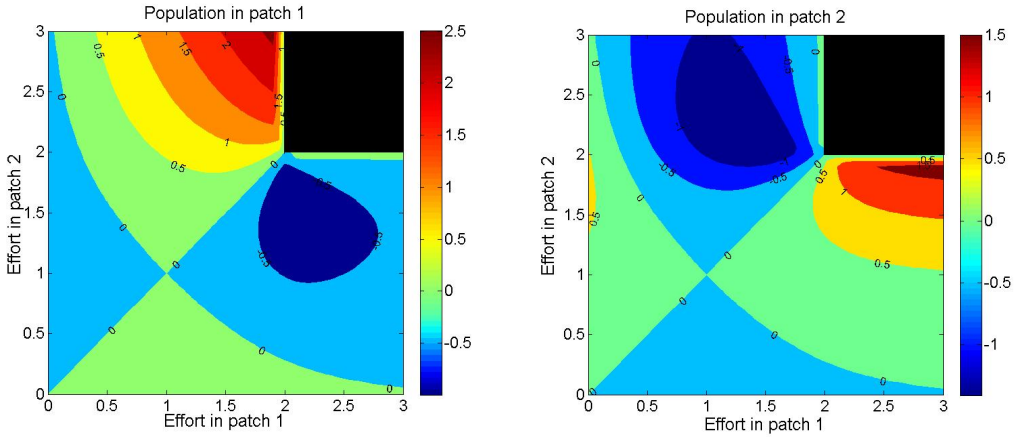

Figure 4.11: Contour plots showing regions where density dependent model predicts higher yield than constant (warm regions), and vice versa (cool regions). Black square represents extinction.

expect that the yield predicted by the density dependent model for $s = 1$ is higher than that predicted by the constant movement model. This is shown in figure 4.12. Figure a) of 4.12 shows the yield if both patches have positive growth rates, and are therefore sources of individuals to other patches. In this case, it is impossible to eradicate the population entirely through harvesting in a single patch alone. In the second plot of figure 4.12, the growth rate in patch 2 is negative, and the harvested patch is a source, in a source-sink system. In this case, harvesting at a high enough rate drives the population to extinction. In both these cases, density dependent dispersal predicts a higher yield.

Yield if both patches are harvested

Once again, we expect the yield if both patches are harvested to follow the equilibrium populations shown in figures 4.10 and 4.11. This is indeed the case and the yield produces a similar contour map to that shown in figure 4.11.

4.3 Density dependent emigration in perturbed systems

In the following sections, we address the impact that spatial perturbation, in response to harvesting practices, has on this system. In the previous models discussed throughout this chapter, harvesting practices have been viewed as equivalent to a natural reduction in pop-

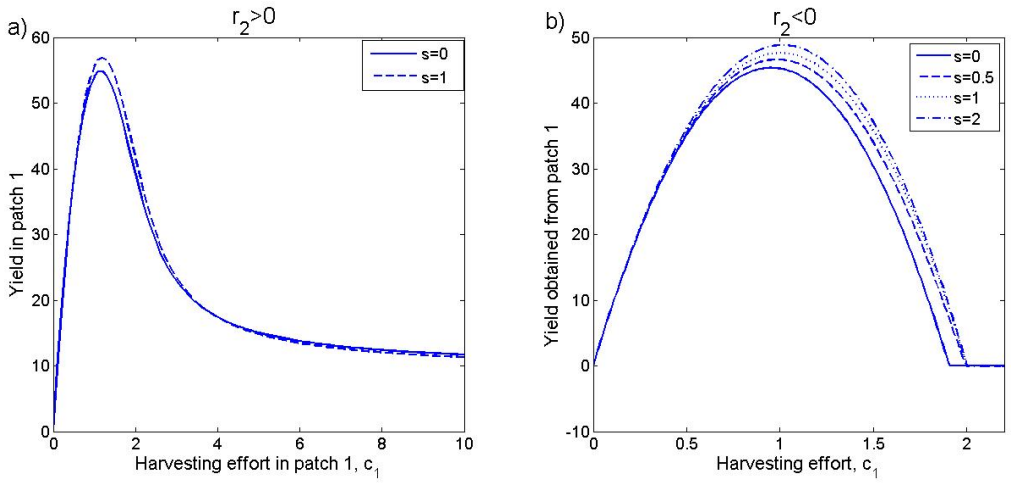

Figure 4.12: Yield obtained from patch 1 for different strengths of density dependence. Increasing density dependence leads to an increase in the yield. Parameters used: a) $r_1 = r_2 = 2, K_1 = K_2 = 100, m = 0.1$, b) $r_2 = -2$.

ulation density. Accordingly, movement away from the harvested patch has reduced as the population density is reduced. However, the behaviour of individuals in the presence of disturbances such as hunting can be vastly different to their response to natural population reduction. For example, a significant increase in the number of 'take-offs' in a population of snow geese (a good measure of disturbance response) was observed in response to hunting activities [13]. This increased avoidance behaviour differs from the response to natural levels in population reduction due to the effect of human interference in the natural environment. Evolved traits for optimising movement activities to take advantage of lower population numbers may be overcome by these external factors which may be perceived as an imminent threat to life and therefore cause a more extreme avoidance behaviour.

In chapter 2, we have shown that both a linearly increasing movement rate, and a saturating movement rate cause qualitatively similar behaviour. In this section we therefore consider only the linear function. The addition of density dependent movement into the model provides the mechanism whereby removal of individuals, through harvesting, acts in two opposing ways. Firstly, harvesting is assumed to cause disturbance to the resident population and increase emigration from the patch. This outward flux is counteracted by the second consequence of harvesting which is to reduce the size of the resident population. The reduced population density causes a reduction in the emigration rate, and a subsequent reduction in

the number of individuals which would naturally leave the patch. Density dependent dispersal therefore provides a buffer to the effects of disturbance in terms of population numbers. We would therefore expect that the yield predicted under the assumption of density dependent movement would be higher than that predicted by constant movement in spite of spatial perturbation.

In chapter 2, we assumed that any disturbance was modelled by an increase in the rate of movement in addition to the natural rate. For a direct comparison with those results, we use the same assumptions here. The perturbation effect is therefore modelled by the following general model

$$\frac{dN_1}{dt} = f(N_1) - mN_1\left(\frac{N_1}{K_1}\right)^s - \sigma c_1 N_1 + mN_2\left(\frac{N_2}{K_2}\right)^s + \rho c_2 N_2 - c_1 N_1 \tag{4.24}$$

$$\frac{dN_2}{dt} = f(N_2) - mN_2\left(\frac{N_2}{K_2}\right)^s - \rho c_2 N_2 + mN_1\left(\frac{N_1}{K_1}\right)^s + \sigma c_1 N_1 - c_2 N_2, \tag{4.25}$$

with the perturbed rate of movement out of a patch of the form $M_1(c_1) = m_1\left(\frac{N_1}{K_1}\right)^s + \sigma c_1$. In this section we detail the effect of this form of spatial disturbance on the yield obtained in both the constant recruitment model, and the logistic growth model, when either one or both patches are harvested. We then investigate the impact that density dependent movement has on the population dynamics once harvesting is stopped.

4.3.1 Perturbation effect with constant recruitment

Harvesting in a single patch

In the first instance, we assume that patch 1 alone is harvested, whilst patch 2 is left untouched. In the constant recruitment model we have shown (figure 4.5) that if both patches are of equivalent carrying capacity, then the yield obtained in a single patch in the density dependent emigration model is less than that given by the constant movement model. It has also been shown in Chapter 2 that as the strength of disturbance (perturbation effect) increases, the yield obtained in decreases for any given harvesting rate. This result holds regardless of the form of movement, either constant or density dependent. Figure 4.13 shows the change in yield obtained when only patch 1 is harvested ($c_2 = 0$), as the strength of

disturbance increases. In all cases, it is clear that increasing disturbance causes a decrease in yield as is to be expected due to the reduction in population. At very low rates of harvesting, ($c_1 = 0.002$) the relative effect of disturbance is low, even if the response per unit effort is high. In this case the actual reduction in yield is low, and the difference between the models could be considered to be negligible. From figure 4.13, it is clear that the relationship between the thresholds in the absence of disturbance is maintained as the strength of disturbance increases. For example, if in the absence of disturbance the density dependent model predicts a higher yield than the constant, then even for high levels of disturbance this relationship is maintained.

Figure 4.13 shows only this relationship for three harvesting rates. It is clear from these plots that for low harvesting rates, the density dependent model predicts a higher yield than the constant movement model, with this relationship switching as harvesting effort increases. In order to gain an understanding of the importance of perturbation as the harvesting rate increases, the figures shown in 4.14 show the difference in the yields predicted by the two models. The contours shown in these plots show where the yield predicted by the density dependent model is equal to that predicted by the constant movement model ($Y_{DD} - Y_C = 0$). The plots in figure 4.14 show this contour for two cases, weak and strong coupling between the populations. It is clear that for a system of weakly coupled patches, with a low rate of movement between them, then the difference in the models is dependent on both the harvesting effort applied and the strength of disturbance. For low ρ, i.e weak disturbance, and low c_1, the density dependent model predicts a higher yield than the constant movement model. This is due to the density dependent reduction in emigration rate out of patch 1 in response to the population reduction. As harvesting effort increases, the population in patch 2 becomes more significantly reduced. The density dependent response in this case causes a reduction in the number of immigrants into patch 1, and hence the constant movement model predicts a higher yield. Increasing the strength of disturbance in this case offsets the reduction in the patch 2 population, due to the influx of individuals out of patch 1. This maintenance in size of patch 2 population maintains the immigrants into patch 1, and hence the density dependent movement model predicts a higher yield than the constant for a larger range of harvesting rates. If the natural rate of movement is high, then figure 4.14 shows that the strength of

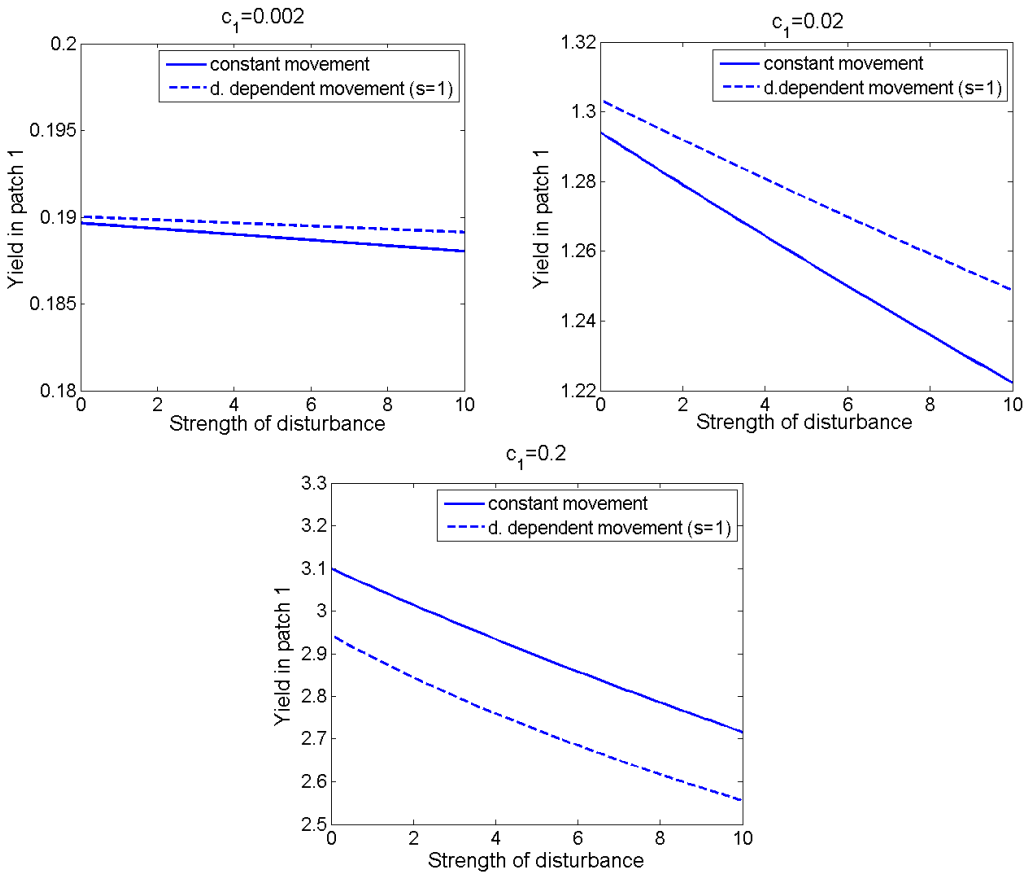

Figure 4.13: Change in yield in patch 1 as strength of disturbance varies. In all cases, increasing disturbance causes a decrease in yield obtained due to an increase in emigrants in response to harvesting. Parameters used $a_i = 2, b_i = 0.02, m = 0.1, c_2 = 0$

disturbance becomes much less significant and the difference between the predicted yields is strongly dependent on the harvesting effort applied. For a low harvesting rate of around $c_1 = 0.045$, $\rho = 0$ would predict that the constant movement model has a higher yield than the density dependent model. As disturbance increases, then this relationship switches. This harvesting rate is however so close to the threshold, that the difference between the predicted yields is slight, with the largest difference between the yields, for the strongest level of disturbance evaluated, $\rho = 10$, being around 0.4%.

Harvesting across both patches

The results described above apply only to harvesting a single patch in a coupled system. We now consider the effect of harvesting both patches simultaneously. Previously, we have shown

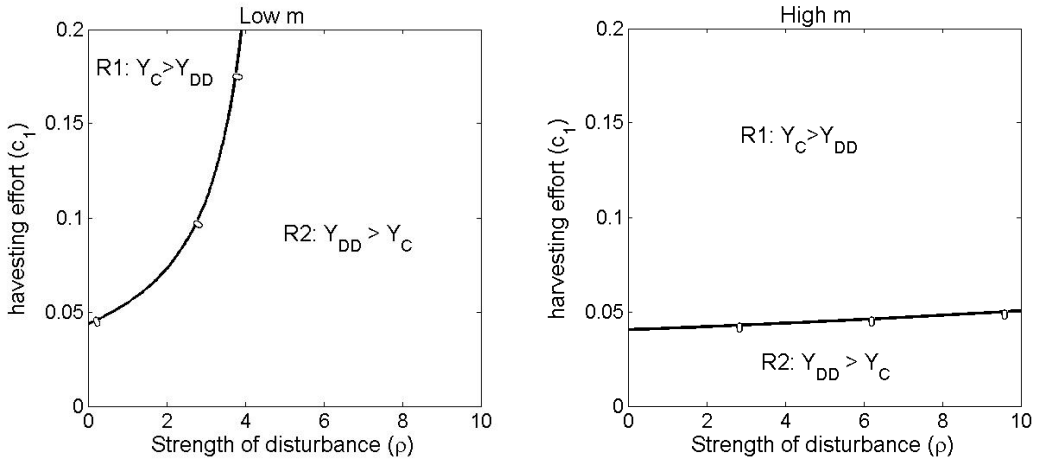

Figure 4.14: Parameter space showing difference in yields predicted by the constant and the density dependent models as c_1 and ρ are varied. R1 shows the region where the constant movement model predicts a higher yield in patch 1 than the density dependent movement model. R2 shows the reversal of this condition. Parameters used $a_1 = 2, b_1 = 0.02$, low $m = 0.1$, high $m = 1$.

that symmetric patches, harvested at equal rates will reach the same yield given by

$$Y = \frac{ac}{b+c}.$$

This yield is independent of both the strength of density dependence in movement, and also the strength of disturbance observed in response to harvesting. If however harvesting between the two patches is unequal, with $c_2 = \alpha c_1$, then the asymmetry in harvesting practices triggers a density dependent response in movement. In this case, the yield predicted by the constant movement model and the density dependent model will be different. In Chapter 2, we were able to show that, with linear disturbance, the yield in patch i, as c_j increases, either increases if $\rho > m_2/b$, or decreases if $\rho < m_2/b$, as shown in figure 4.15 (a). In the density dependent case, we are unable to find the exact threshold, however, simulation results detailing the yield in patch 1 for a given effort, as the effort in patch 2 changes are shown in figure 4.15(b). These show that for high enough levels of disturbance $\rho = 2$ in this example, the predicted yields are qualitatively similar, with the patch 1 yield increasing monotonically. However, for intermediate levels of disturbance, ($\rho = 0.5, 1$) the yield obtained in patch 1 sees an initial drop as harvesting in patch 2 increases before a 'recovery' of the yield to higher levels as the neighbouring harvesting rate increases further.

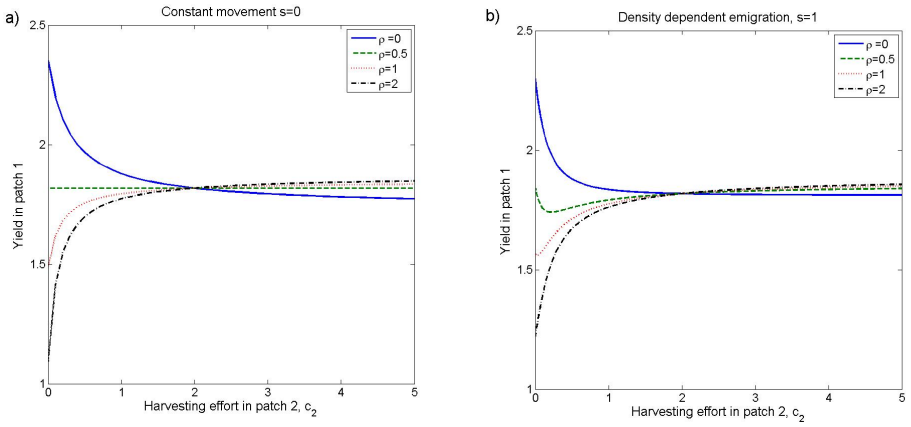

Figure 4.15: Yield achieved in patch 1 as harvesting effort in patch 2 varies, for a constant harvesting effort in patch 1.

This dip in yield is due to the density dependent response of the patch 2 population for low levels of harvesting. The reduction in population density reduces the movement out of patch 2 and into patch 1. As the harvesting rate intensifies in patch 2, the density dependence is overcome by the strength of the perturbation effect, and individuals leave the patch due to disturbance. This leads to an increase in immigrants into patch 1, and therefore an increase in the yield obtained there. Figure 4.15 shows the yield in patch 1 for a single harvesting effort. In order to capture the effect of density dependent movement more generally, we compared the yield predicted in patch i by the constant model and the density dependent model for a range of both c_1 and c_2. The difference in predicted yields is demonstrated in the contour plots in figure 4.16. These plots confirm that when $c_1 = c_2$, the effect of density dependent movement is cancelled out by the symmetry of the system. If $c_j > c_i$, then the density dependent model predicts a higher yield in patch i than the constant model. If $c_i > c_j$, then the density dependent model predicts a lower yield in patch i than the constant movement model. Figure 4.16 also shows the effect of increasing the strength of disturbance ρ when harvesting across both patches. We see that for high ρ, the difference between the models becomes less pronounced. This is to be expected since density dependence offsets the effects of perturbation, so will have a stronger effect for weak perturbation. As ρ increases, the strength of disturbance dominates the dynamics, and the difference induced by the movement rates is reduced.

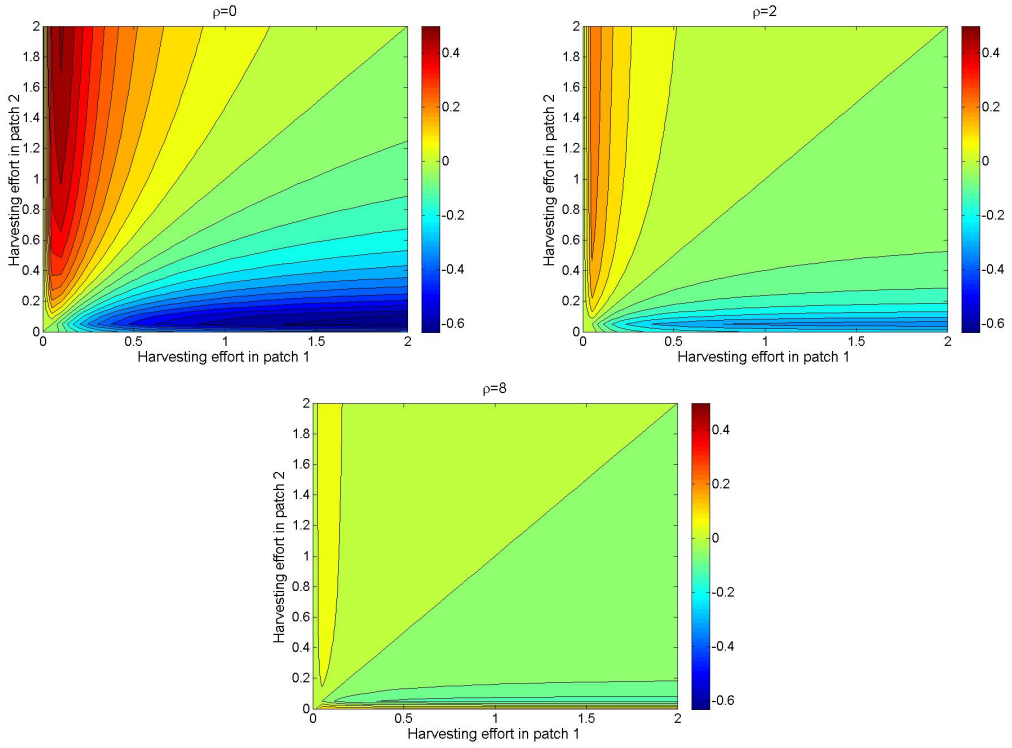

Figure 4.16: Contour plots showing differences in patch 1 yield between density dependent model ($s = 1$) and constant movement model. Positive regions show where density dependent model predicts a higher yield.

4.3.2 Perturbation effect in the logistic growth model

In the case of the logistic growth model, we once again assume that disturbance leads to an increase in movement in addition to the natural rate. This leads to

$$\frac{dN_1}{dt} = r_1 N_1 \left(1 - \frac{N_1}{K_1}\right) - mN_1 \left(\frac{N_1}{K_1}\right)^s - \rho c_1 N_1 + mN_2 \left(\frac{N_2}{K_2}\right)^s + \rho c_2 N_2 - c_1 N_1 \quad (4.26)$$

$$\frac{dN_1}{dt} = r_2 N_2 \left(1 - \frac{N_2}{K_2}\right) - mN_2 \left(\frac{N_2}{K_2}\right)^s - \rho c_2 N_2 + mN_1 \left(\frac{N_1}{K_1}\right)^s + \rho c_1 N_1 - c_2 N_2. \quad (4.27)$$

Harvesting in a single patch

In this case, if a single patch alone is harvested, Jacobian matrix evaluated at the $(0, 0)$ equilibrium is given by

$$J(0,0) = \begin{pmatrix} r_1 - \rho c_1 - c_1 & 0 \\ \rho c_1 & r_2 \end{pmatrix}. \quad (4.28)$$

The eigenvalues of which are given by

$$\lambda_1 = r_1 - \rho c_1 - c_1 \quad (4.29)$$

$$\lambda_2 = r_2. \quad (4.30)$$

As shown in the unperturbed model, extinction is only possible in this system if the unharvested patch is a population sink, with intrinsic growth rate $r_2 < 0$. If $r_2 > 0$, then the unharvested population will always produce immigrants into the harvested patch, allowing this patch to be repopulated once harvesting is ceased. If patch 2 is a sink, then total population extinction will occur if

$$c_1 > \frac{r_1}{1 + \rho}$$

hence an increase in the perturbation effect (ρ) will lead to a reduction in the harvesting effort needed to cause extinction. In contrast to the constant movement model, the necessary condition for population extinction relies only on the population growth rate and the strength of the perturbation effect. As the strength of perturbation increases this threshold decreases to zero, and is not affected by the strength of the natural movement rate, since this tends to zero at low densities.

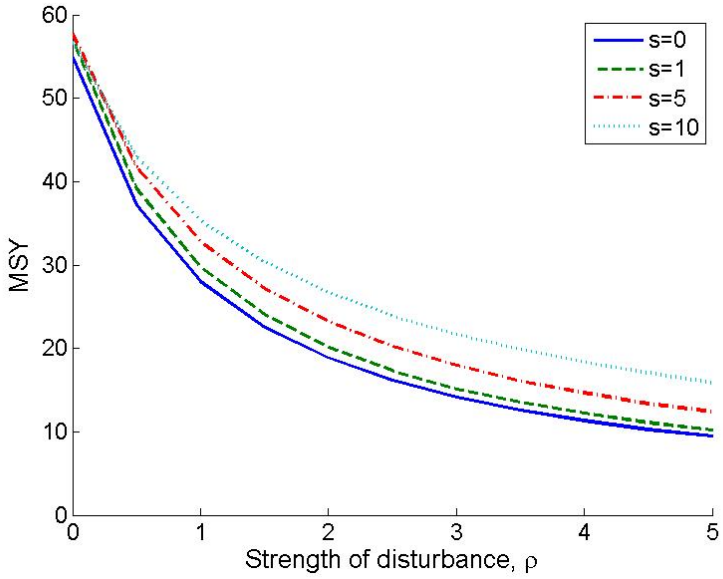

Figure 4.17: Maximal sustainable yield obtained from harvesting in patch 1 as strength of disturbance increases. Different lines represent different strengths of density dependent emigration. Fixed parameters: $r_1 = r_2 = 2, K_1 = K_2 = 100, m = 0.1$.

The unperturbed system, exemplified in figure 4.12 has shown that density dependent movement causes an increase in the maximal sustainable yield obtained from harvesting a single patch. In the perturbed system, we observe a similar increase in the MSY as the strength of density dependence increases. Figure 4.17 shows the change in MSY as the strength of disturbance increases. As observed in the constant recruitment model, an increase in disturbance causes a reduction in the yield obtained. Also noticeable from figure 4.17 is the fact that increasing the strength of the density dependent movement response, in strongly perturbed systems, causes a more significant increase in the MSY obtained. For low rates of disturbance ρ, the effect of density dependence in terms of the yield is very small. This result is clarified in figure 4.18 which shows the change in maximal sustainable yield as the strength of density dependent emigration increases. The four plots represent increasing strengths of disturbance. Whilst high levels of disturbance will cause a reduced yield compared to low disturbance, if a system is disturbed, then density dependent movement predicts a higher yield than a constant rate of movement.

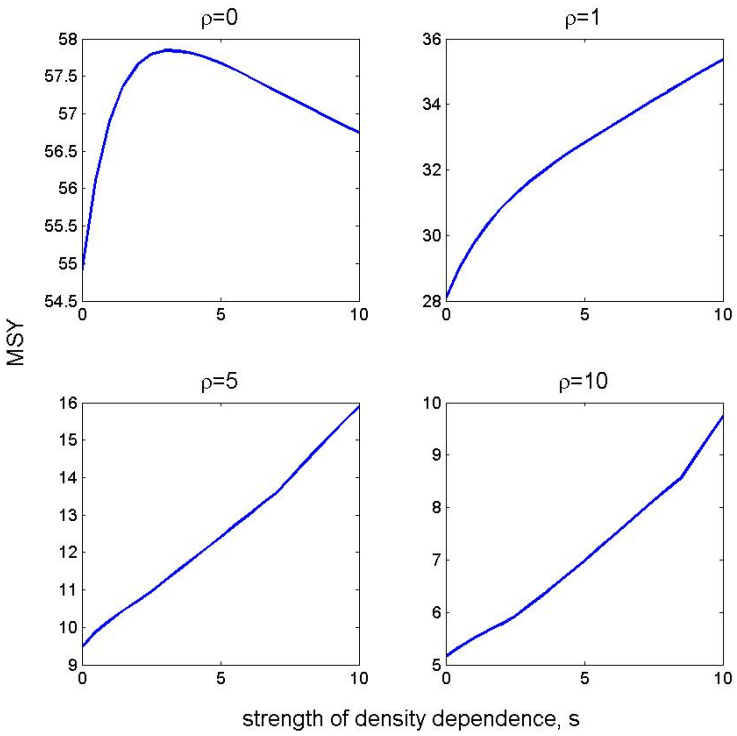

Figure 4.18: Maximal sustainable yield as the strength of density dependent emigration increases. Different graphs represent increasing strengths of disturbance.

Harvesting across both patches

If harvesting is carried out across both patches, then the equivalent of the Jacobian matrix in (4.28) is given by

$$J(0,0) = \begin{pmatrix} r_1 - \sigma c_1 - c_1 & \rho c_2 \\ \sigma c_1 & r_2 - \rho c_2 - c_2 \end{pmatrix}. \tag{4.31}$$

The $(0,0)$ equilibrium is therefore stable when

$$c_1 > \frac{r_1((1+\rho)c_2 - r_2)}{(1+\rho+\sigma)c_2 - (1+\sigma)r_2}. \tag{4.32}$$

As in the case of the constant movement model, for a symmetric system of patches, with $r_1 = r_2 = r, \rho = \sigma$ and $c_1 = c_2$, then the extinction threshold is given by the point $c_1 = c_2 = r$. As such, this point is independent of both the strength of disturbance and the strength of density dependent emigration. Away from this point, the strength of perturbation begins to take effect. The extinction threshold in this model has asymptotes at

$$c_1 = \frac{(1+\sigma)r_1}{1+\sigma+\rho}, \qquad c_2 = \frac{(1+\rho)r_2}{1+\sigma+\rho}, \tag{4.33}$$

which are at higher values of c_1, c_2 than the equivalent asymptotes in the constant movement model. This indicates that a higher level of harvesting effort is required to cause population extinction if movement rates are density dependent. This broad qualitative result is true for any strength of disturbance.

4.4 Discussion

In this chapter, we have expanded the work presented in Chapter 2, to consider the effect that density dependent movement of individuals between patches has on the population sizes found within those patches, and also the yield. This study is predominantly a comparison between the constant movement model in chapter 2, and the analogous model with density

dependent movement. We have shown that density dependent movement between patches limits the synchrony of the population sizes in a patchy environment. Synchrony between patches is often observed in metapopulation or patch models where the rate of movement between patches is high. This leaves the populations vulnerable to the dynamics of surrounding patches. Catastrophic events such as local patch extinctions have a much wider ranging and serious impact if the coupled populations have a high degree of synchrony. We have shown that density dependent movement buffers individual patches against the dynamics of other patches, thus providing a mechanism for a population within a patch to survive surrounding catastrophes. This buffering effect is also seen in regards to the effects of harvesting. We have shown that, whilst harvesting causes a more severe reduction in the target patch if movement is density dependent, the unharvested patch, or area of lower harvesting rate, has an increased population size if movement is assumed to be density dependent. The addition of density dependent movement in the model suggests that harvesting efforts may be more targeted than the constant movement model would suggest. Spatial disturbance or perturbation in this model offsets the effects of density dependence, with the difference between the density dependent, and the constant models becoming less significant for high levels of disturbance.

In terms of the yield attained, if a single patch in this system is harvested, we have shown that the density dependent movement model predicts a higher yield only if the harvesting rate is low. This is due to the reduction in emigration as a density dependent response to population reduction. An increase in movement due to spatial disturbance suggests that the density dependent movement response gives a higher yield than constant movement for a higher range of harvesting efforts. We have shown that the density dependent movement model changes the dynamics and the effect of harvesting a population, we now wish to investigate the combination of density dependent movement and the control of disease in this patchy environment, and this is the focus of the following chapter.

Chapter 5

Density dependent movement: implications for disease control

5.1 Introduction

The following chapter builds on the work presented in the previous two chapters by combining the density dependent movement function with a directly transmitted disease. As in chapter 3 we are concerned here with culling the populations across both patches for the purpose of disease control. We consider the asymptotic conditions of long term constant control strategies and compare the pathogen exclusion thresholds calculated with those in chapter 3. In addition to the long term control conditions, this chapter also investigates the transient effects of culling in this system, along with the population and disease dynamic consequences of ceasing a culling strategy prior to disease eradication.

We begin by focusing on the difference in disease control conditions due to density dependent emigration only. The second section of this chapter then considers the effect that spatial perturbation has on this system.

5.2 SI model with density dependent emigration

5.2.1 General dynamics

We begin this section with a description of the full, two patch, SI model with density dependent movement. As we have done in chapter 3, for increased analytic tractability, we consider only the constant recruitment growth function. The full model is therefore given by

$$\begin{aligned}
\frac{dS_1}{dt} &= a_1 - b_1 S_1 - \beta_1 S_1 I_1 - m\left(\frac{N_1}{K_1}\right)^s S_1 + m\left(\frac{N_2}{K_2}\right)^s S_2 - c_1 S_1 \\
\frac{dI_1}{dt} &= \beta_1 S_1 I_1 - (b_1 + \gamma_1) I_1 - m\left(\frac{N_1}{K_1}\right)^s I_1 + m\left(\frac{N_2}{K_2}\right)^s I_2 - c_1 I_1 \\
\frac{dS_2}{dt} &= a_2 - b_2 S_2 - \beta_2 S_2 I_2 - m\left(\frac{N_2}{K_2}\right)^s S_2 + m\left(\frac{N_1}{K_1}\right)^s S_1 - c_2 S_2 \\
\frac{dI_2}{dt} &= \beta_2 S_2 I_2 - (b_2 + \gamma_2) I_2 - m\left(\frac{N_2}{K_2}\right)^s I_2 + m\left(\frac{N_1}{K_1}\right)^s I_1 - c_2 I_2,
\end{aligned} \tag{5.1}$$

where $N_i = S_i + I_i$ and $K_i = a_i/b_i$. As in the previous chapter, the assumption of density dependence means that the movement rates between the patches are determined by the relative population densities, the parameter m is therefore a measure of the access between the patches. If m is high, and the system is at equilibrium, then the rate of movement between the patches is fast. In the absence of infection, this model reduces to that detailed in chapter 4, and in the case that $s = 0$, the model reduces to the two patch, SI model with constant movement, as detailed in chapter 3. The aim of this chapter is to quantify the epidemic effects of increasing parameter s, and moving from a constant movement rate between patches, to a density dependent one. This is done by evaluating the pathogen exclusion threshold, following the analysis detailed in [93]. The pathogen exclusion threshold is the bifurcation curve in $c_1 - c_2$ space where the disease free equilibrium $(S_1^*, 0, S_2^*, 0)$ changes from instability to stability. This curve is found by evaluating the Jacobian matrix at this point. In the case of strictly density dependent movement, $s > 0$, this Jacobian is given by

$$J = \begin{pmatrix} A & B \\ 0 & C \end{pmatrix} \tag{5.2}$$

where

$$A = \begin{pmatrix} -b_1 - m(s+1)\left(\frac{b_1 S_1}{a_1}\right)^s - c_1 & m(s+1)\left(\frac{b_2 S_2}{a_2}\right)^s \\ m(s+1)\left(\frac{b_1 S_1}{a_1}\right)^s & -b_2 - m(s+1)\left(\frac{b_2 S_2}{a_2}\right)^s - c_2 \end{pmatrix}, \tag{5.3}$$

$$B = \begin{pmatrix} -(s+1)m\left(\frac{b_1 S_1}{a_2}\right)^s & (s+1)m\left(\frac{b_2 S_2}{a_2}\right)^s \\ (s+1)m\left(\frac{b_1 S_1}{a_1}\right)^s & -(s+1)m\left(\frac{b_2 S_2}{a_2}\right)^s \end{pmatrix} \tag{5.4}$$

$$C = \begin{pmatrix} \beta_1 S_1 - (b_1+\gamma_1) - m(s+1)\left(\frac{b_1 S_1}{a_1}\right)^s - c_1 & m(s+1)\left(\frac{b_2 S_2}{a_2}\right)^s \\ m(s+1)\left(\frac{b_1 S_1}{a_1}\right)^s & \beta_2 S_2 - (b_2+\gamma_2) - m(s+1)\left(\frac{b_2 S_2}{a_2}\right)^s - c_2 \end{pmatrix}. \tag{5.5}$$

Since this matrix is block upper triangular, the eigenvalues of J are equal to the eigenvalues of A and C. It is possible to show that the eigenvalues of A always have negative real part, since the maximum eigenvalue is bounded by $\{-b_1 - c_1, -b_2 - c_2\}$ and stability of the disease free equilibrium is therefore determined entirely by the eigenvalues of the infection invasion matrix C. As in the case of constant movement, we are able to determine the pathogen exclusion threshold which is given by the upper branch of the hyperbola defined by $det(C) = 0$. The pathogen exclusion threshold is therefore given by

$$c_2 = \beta_2 S_2^* - (b_2+\gamma_2) - m(s+1)\left(\frac{b_2 S_2^*}{a_2}\right)^s - \frac{m^2(s+1)^2(b_1 S_1^*)^s(b_2 S_2^*)^s)}{a_1^s a_2^s\left(\beta_1 S_1^* - (b_1+\gamma_1) - m(s+1)\left(\frac{b_1 S_1^*}{a_1}\right)^s - c_1\right)}, \tag{5.6}$$

which has asymptotes at

$$\begin{aligned} c_1 =& \beta_1 S_1^* - (b_1+\gamma_1) - m(s+1)\left(\frac{b_1 S_1^*}{a_1}\right)^s \\ c_2 =& \beta_2 S_2^* - (b_2+\gamma_2) - m(s+1)\left(\frac{b_2 S_2^*}{a_2}\right)^s. \end{aligned} \tag{5.7}$$

Comparing this threshold to the constant movement case, when $s = 0$, we see that the pathogen exclusion threshold for constant movement has asymptotes at

$$\begin{aligned} c_1 =& \beta_1 S_1^* - (b_1+\gamma_1) - m \\ c_2 =& \beta_2 S_2^* - (b_2+\gamma_2) - m. \end{aligned} \tag{5.8}$$

It must be noted that the difference between these thresholds is not simply defined by the density dependent term $(s+1)\left(\frac{b_1 S_1^*}{a_1}\right)^s$. The equilibrium populations S_i^* are dependent on the control strategy applied, and will differ depending on the form of movement. In particular, we have shown in the previous chapter that density dependent movement can lead to a reduced culling effect for a given effort in the culled population, and an increased effect in the coupled population when compared to the constant movement model if culling rates are low, and a reversal in this relationship if culling is more intensive, with $c_i >> b_i$. Since we are unable to find an explicit expression for the population size in the density dependent model, we must rely on simulation results to elucidate these differences. We address the differences in these thresholds by considering three cases: (i) both patches are symmetric, and neither is a reservoir of infection, (ii) both patches are symmetric and both are reservoirs of infection, (iii) one patch is a reservoir for infection, coupled to a second non-reservoir patch.

5.2.2 Reservoirs of infection

Recall from chapter 3 that a reservoir of infection is defined as a population which could sustain an infectious agent in the absence of any coupling with surrounding populations. Mathematically, a patch is a reservoir of infection if $P_i = \beta_i S_i^* - b_i - \gamma_i > 0$, where S_i^* is the disease free equilibrium of patch i. We have previously shown that, if movement between two patches occurs at a constant rate, then the pathogen can be excluded from the system simply by culling the reservoir patch. Here we compare the properties of the pathogen exclusion thresholds between the constant model and the density dependent movement model with $s = 1$ in the three cases outlined above.

$\mathbf{P_1 < 0, P_2 < 0}$

We have shown in chapter 3 that constant rate of movement between non-reservoir patches is insufficient to sustain an infection. The same holds true in the case of density dependent dispersal. The coupling of patches in both the constant movement case, and the density dependent movement case causes a level of homogenisation of the population sizes. That is, any difference in population size between the two patches will be reduced by coupling. Thus, even if the two patches have very different population sizes, if neither patch in isolation could

support infection, coupling will only serve to reduce the size of the larger population, and will therefore be insufficient to maintain the infection.

$\mathbf{P_1 > 0, P_2 > 0}$

If both patches are reservoirs of infection in isolation and movement is constant, then an increase in the movement rate between patches will cause a significant reduction in the necessary control efforts [93]. Since any positive culling strategy (c_1, c_2) will reduce the populations in both patches, assuming both patches are symmetric with equal demographic and disease parameters, then both $b_1 S_1/a_1$ and $b_2 S_2/a_2$ will be less than 1. If this is the case, then the asymptotes of the pathogen exclusion threshold will increase for increasing s and density dependent emigration will lead to an increase in the control strategy necessary for disease eradication. This is shown in figure 5.1.

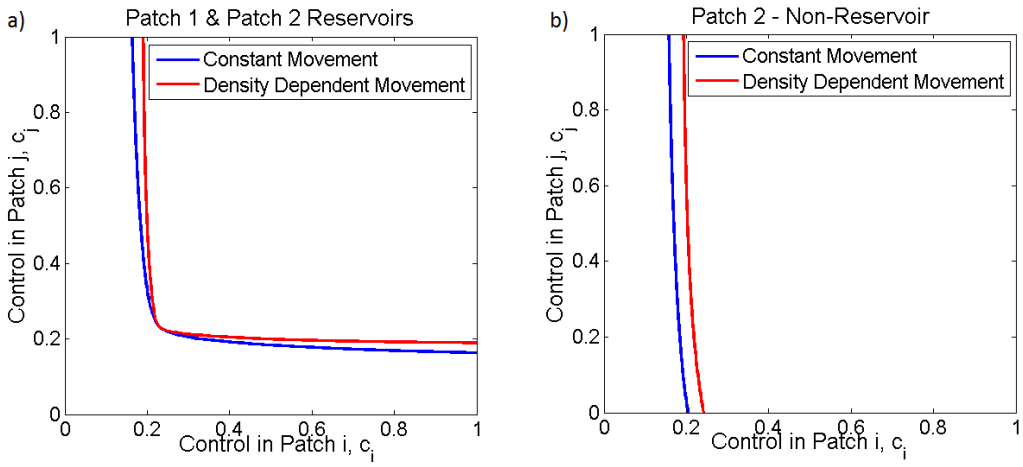

Figure 5.1: Pathogen exclusion thresholds for constant movement model (blue) and density dependent movement model (red). Density dependent movement requires a more intensive level of control to eradicate disease due to the decline in movement rates. Parameters used: a) $a_1 = a_2 = 2, b_1 = b_2 = 0.2, m = 1, \beta_1 = \beta_2 = 0.308, \gamma_1 = \gamma_2 = 1$. b) $a_1 = a_2 = 2, b_1 = 0.2, b_2 = 0.5, m = 1, \beta_1 = \beta_2 = 0.308, \gamma_1 = \gamma_2 = 1. s = 1$

This increase in the pathogen exclusion threshold for density dependent movement is a product of the reduction in movement rate as the population is reduced by culling. As the populations are decreased through culling, the movement between the patches is reduced. A reduction in the movement rate leads to a higher pathogen exclusion threshold which is closer to that

predicted if the two patches were in isolation. The culling effort applied in one patch has a reduced effect on the coupled patch if the coupling strength is weak, meaning that for a given effort in patch 1, a higher effort is required in patch 2 in order to achieve disease eradication.

$\mathbf{P_1 > 0, P_2 < 0}$

If there is a difference in the size of the two patches such that in isolation, one would be a reservoir, and the second would not support the infection, then the extent of coupling may have one of two outcomes. Either, coupling may cause the infection to die out, as the larger patch is reduced in size, or it may facilitate the disease to spread, as infected individuals are able to migrate into areas where infection would naturally die out. If either patch is large enough to maintain the disease, then the whole system will become infected.

The two models considered respond differently to the coupling strength. The parameter m in the constant movement model is the rate at which individuals move from one patch to the other. In the density dependent model, individuals move at this rate if both patches are at their carrying capacity, and so the parameter m takes on a different role. It is perhaps more correctly thought of as the potential for the patches to be coupled. In the constant movement model, the populations always use this potential to full effect, whereas in the density dependent model, a reduced population, below its carrying capacity, will migrate at a lower rate than m, and the movement of an inflated population will be mediated by the size of this parameter. Varying this parameter will therefore affect the equilibrium size of the population resident in each patch. Figure 5.2 considers only the effect in this change of population size on the reservoir potential for infection, showing $P_i = \beta_i S_i^* - b_i - \gamma_i$ for both patches as they are increasingly coupled. This figure is divided into two regions. In region (1), infection is able to spread in both models as patch 1 is a reservoir and hence a source of infection to patch 2. In region (2) in figure 5.2, the constant model predicts that $P_1 < 0$. In the constant model in this case, infection would naturally die out as the asymmetry in the populations is smoothed out by coupling. However, as discussed in chapter 4, if movement is density dependent, then the patches maintain more of their isolated heterogeneity in spite of coupling. In the density dependent model therefore, increasing the potential for coupling, by opening up a corridor

between patches of habitat, is not sufficient to cause higher rates of movement, and does not affect the population sizes as much. Patch 1 therefore remains a reservoir of infection and a source to patch 2 because the patch 1 population is maintained at a high enough level.

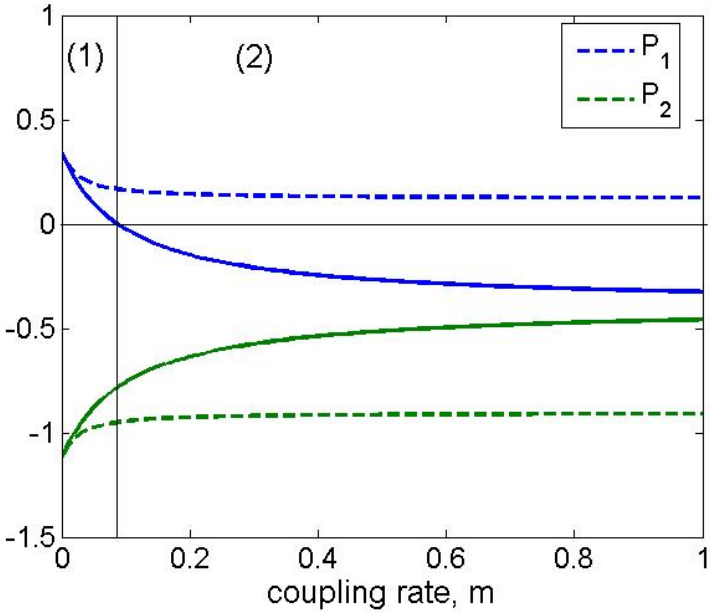

Figure 5.2: Reservoir property P_i of patch i as the coupling between the patches, m, is increased. In isolation, $m = 0$, patch 1 is a reservoir of infection, $P_1 > 0$, and patch 2 is a non-reservoir. Solid line represents constant movement model, dashed line is density dependent movement.

An example pathogen exclusion threshold for asymmetric patches is shown in figure 5.1 (b), showing clearly that it is much easier to eradicate disease if movement is constant rather than density dependent.

These results show that it can be significantly harder to eradicate disease in a patchy system if movement between patches is density dependent. Pathogen exclusion thresholds give a good indication of the necessary conditions for disease eradication, however, tell us nothing about the difference between the models in terms of transient dynamics. We address this problem directly by comparing the transient dynamics of both the constant and the density dependent models.

5.2.3 How does density dependent movement affect transient dynamics?

The aim of this section is to evaluate whether density dependent movement affects the length of time to eradication if sufficient control is applied. Throughout this section, we use parameters which require an approximately 70% removal of individuals within each patch for complete disease eradication. This figure has been chosen as an example to be in line with the UK government's targets for the badger cull carried out in October 2013 [110]. We shall compare the time to disease eradication if this culling intensity is achieved, as well as investigating the transient dynamics if this target is not met.

A note on parameter choices

The overall aim of this thesis is to determine the general qualitative impact of movement between patches on the necessary conditions for population and disease control. As such, the parameters throughout are chosen to show the particular behaviour being discussed. In this section we wish to demonstrate the thought process used when determining a simple culling strategy, and how movement between patches affects this assumption. To do this, we fix the carrying capacity within each patch to be 100. This can be done somewhat arbitrarily, and here we use a constant birth rate $a = 2$ and a per capita death rate of $b = 0.02$. The unit in which time is measured is also somewhat arbitrary, however if we assume that time is measured in months, then these demographic parameters tell us that, on average, 2 new individuals are welcomed into the population each month, and the average lifespan of a healthy individual is $1/0.02 \approx 50$ months, which is just over 4 years. In the following section we wish to create a system whereby a cull of 70% of the population is necessary for disease eradication. We make the assumption that this figure is based on a single patch model. In a single patch, the disease free equilibrium in the absence of a cull is $a/b = 100$, and the equilibrium of the culled population is $a/(b + c)$. The percentage reduction in population caused by the cull, is therefore given by

$$100 \times \frac{(a/b - a/(b + c))}{a/b} = 100 \times \frac{c}{b + c} \tag{5.9}$$

and hence, a 70% reduction in population is achieved by a culling rate of 0.0467 per month, throughout this section we approximate this by a culling rate of $c = 0.05$. The remaining

parameters in the model are the transmission rate β and the virulence of the infection, γ. We assume that the infection is only slightly virulent and therefore set $\gamma = 0.002$ to be a factor of 10 smaller than the natural death rate. This leaves us with only one parameter which must be fixed. We have assumed that this reduction in population is sufficient for disease eradication, hence we must have

$$\frac{\beta a}{b+c} - (b+\gamma+c) < 0.$$

This requires that the transmission rate is set at approximately 0.00243. In the following simulations we use the transmission rate $\beta = 0.0024$.

Transient effects with density dependent emigration

If the single patch defined by the parameters above is coupled by movement to a second identical patch, then the pathogen exclusion threshold of the two patch system is given in figure 5.3. The blue line here represents the constant movement model with $m = 0.1$, and the red line in this figure shows the threshold if emigration is density dependent (with $s = 1$). It is clear, that as in the earlier discussion, the two thresholds intersect when $c_1 = c_2 \approx 0.05$. If the patches are not culled evenly, however density dependent movement requires a higher combined culling strategy.

If we cull both patches evenly at just above the necessary rate $c_1 = c_2 = 0.06$, (strategy C1 in Figure 5.3) then the symmetry between the patches negates any effect of density dependent movement, and both models predict identical transient effects. These are shown in figures 5.4 (a-d). In both cases, the infection rapidly takes off in the population, reaching its peak prevalence in approximately 45 months (5.4 (a)). The disease is endemic, affecting approximately 90% of the population within each patch (5.4 (b)). Once culling begins, the infected population decreases rapidly, whilst the susceptible population decreases for a short time, before increasing due to the removal of infected individuals. It should be reiterated here that both susceptible and infected individuals are culled at the same rates, and hence any increase in susceptibles is due to the drop in transmission rate as the population size is depleted. With a culling rate in both patches of 0.06, the infected population takes approximately 175 months

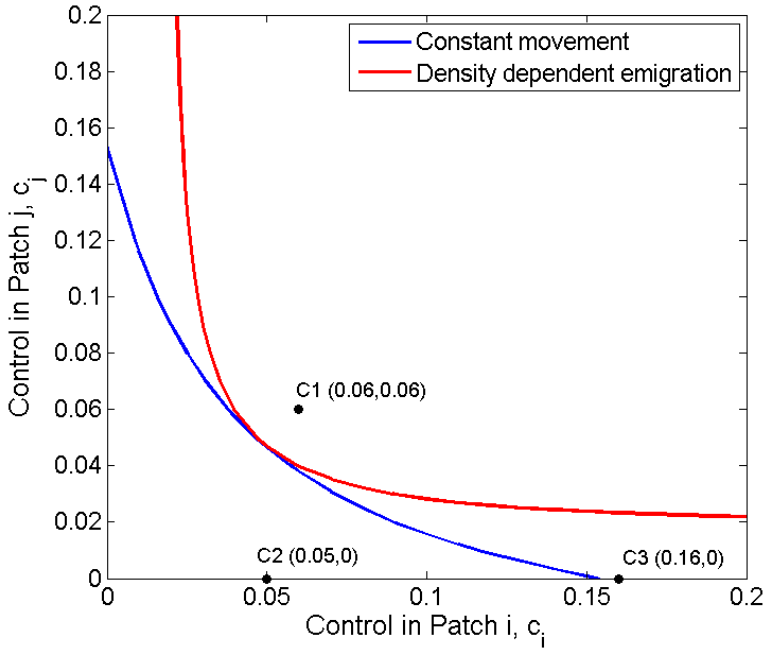

Figure 5.3: Pathogen exclusion thresholds for parameters estimated in section 4.1. Blue threshold represents constant movement ($s = 0$) and red threshold shows the density dependent emigration model ($s = 1$). Parameters used: $a_i = 2, b_i = 0.02, \gamma_i = 0.002, \beta_i = 0.0024, m = 0.1$ for $i = 1, 2$.

to drop below 1%. This long time to pathogen exclusion highlights the limitations of using only the pathogen exclusion threshold as a condition for disease control, and the importance of considering transient dynamics. In these simulations, we ran the model with this culling rate for 1000 months, and took the population sizes after this as our initial conditions for figure 5.4d. This final figure shows the regrowth of the population, achieving 99% of its carrying capacity in approximately 250 months.

If only a single patch in this system can be culled, then the pathogen exclusion threshold is clearly (from figure 5.3) going to be different depending on the type of movement exhibited by the species. If a single patch model is used to estimate the required rate of culling, the predicted rate would be $c = 0.05$ (strategy C2 in figure 5.3) in this example, which is below the pathogen exclusion threshold regardless of the movement rate. Culling at this rate would allow the infection to persist in the population in both the constant movement, and the density dependent emigration model, as shown in figure 5.5. In both models, as expected, culling

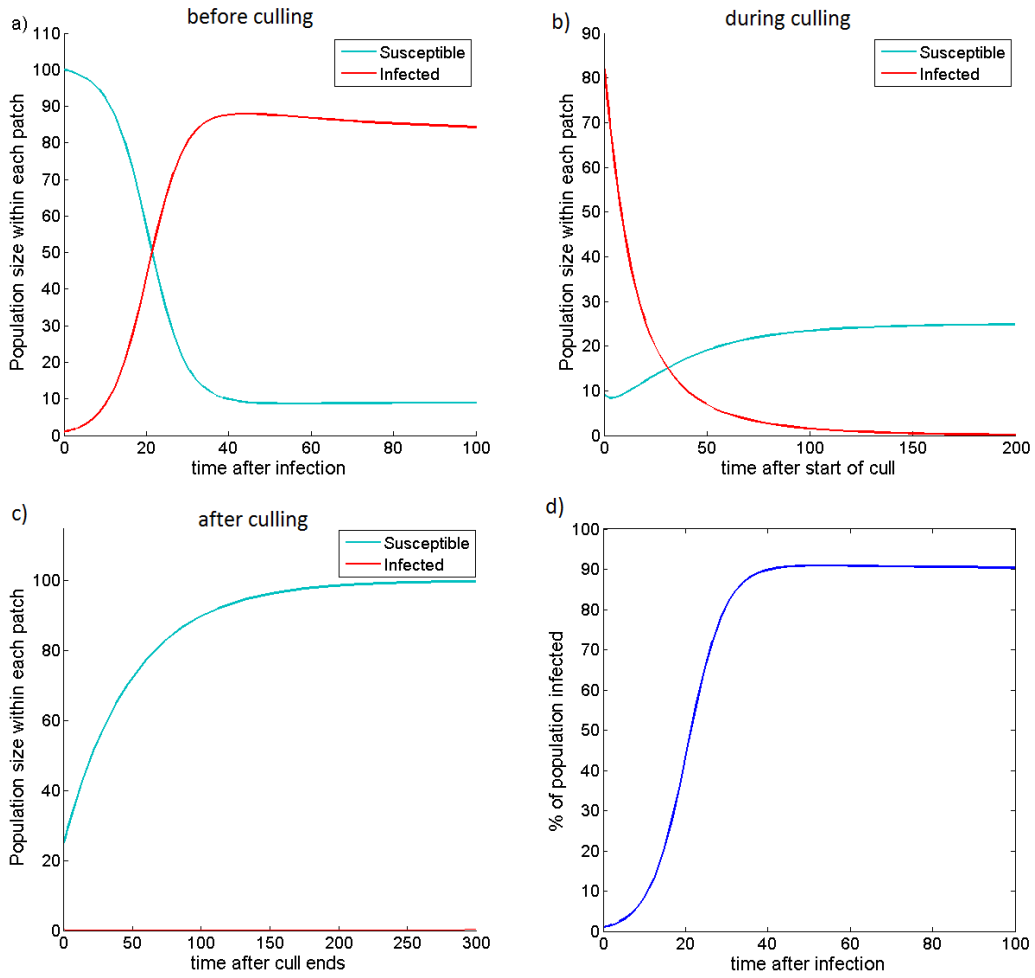

Figure 5.4: Identical transient dynamics of both constant movement and density dependent movement models if both patches are culled equally. Plots a)-c) show the dynamics before, during and after cull, showing regrowth of population after disease has been eradicated. Both models predict identical behaviour. Parameters used $a_i = 2, b_i = 0.02, \beta_i = 0.0024, \gamma_i = 0.002, m_i = 0.1, c_i = 0.05$.

leads to a more significant drop in the population of patch 1 that patch 2. The number of infected individuals in both patches decreases significantly, however the susceptible population in patch 2 (not culled) sees a more significant increase during the culling period than the culled patch. This is because the susceptible population in patch 1 is suppressed by the cull. Once the cull is ended, the susceptible population in patch 1 sees an initial increase due to the reduced infected population. However, as the number of infected individuals in patch 1 increases, the number of susceptibles decreases. The number of infected individuals in patch 2 increases more slowly than patch 1 after the cessation of culling, but the number

of susceptible individuals in patch 2 does not see a significant increase after culling, only a drop in number due to infection.

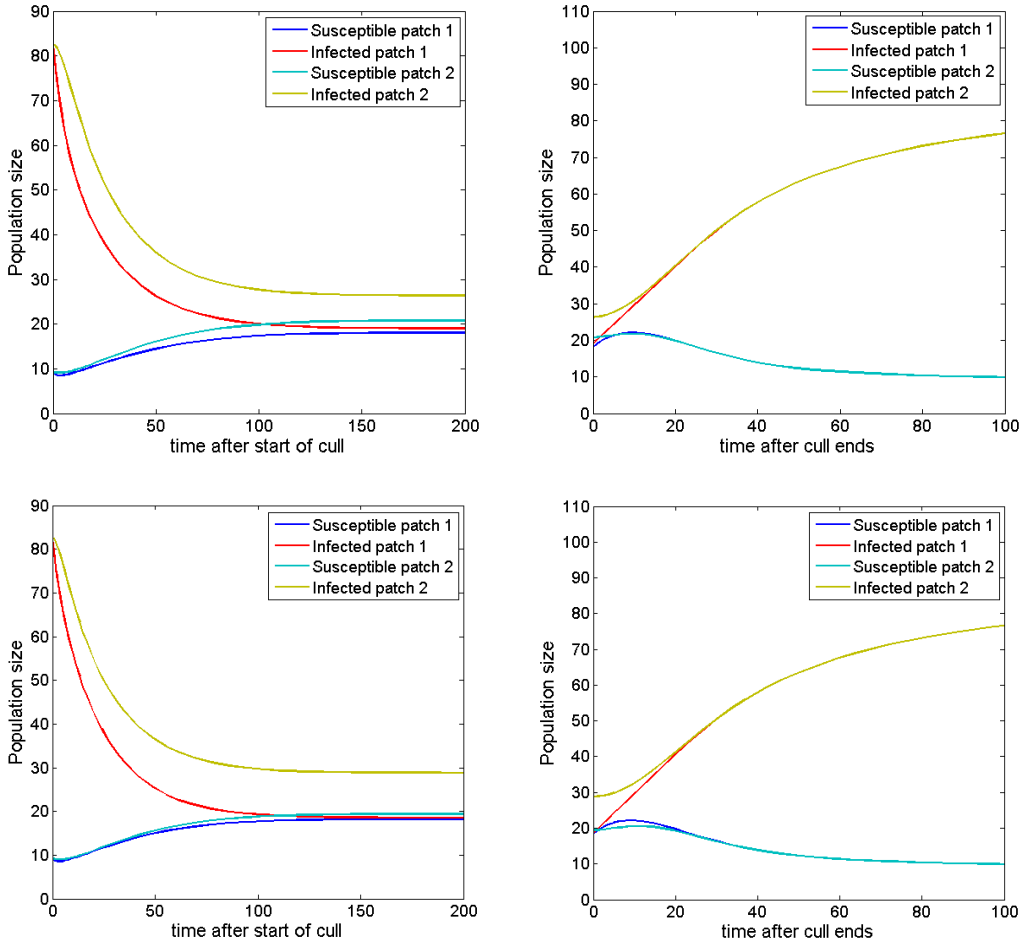

Figure 5.5: Transient dynamics of constant movement model (top row), and density dependent model with $s = 1$ (lower row) if patch 1 alone is culled at a rate of 0.06. Culling rate is insufficient to rid the population of infection. Parameters used $a_i = 2, b_i = 0.02, \beta_i = 0.0024, \gamma_i = 0.002, m_i = 0.1, c_1 = 0.06, c_2 = 0$.

The density dependent emigration model, figure 5.5 lower row, shows the same qualitative behaviour as described above, however the reduction in the infected population in patch 2 (not culled) is less significant. This leads to a smaller susceptible population in patch 2 due to the larger number of infected individuals. This reduced effect on patch 2 is due to the reduction in movement induced by culling patch 1. The increase in the susceptible population in patch 1 is slightly more significant after the cessation of culling. This is due to the fact

that patch 2 has a larger population, and therefore a faster movement rate into patch 1. The smaller population in patch 1 means that the movement rate out of this patch is much slower, and hence this imbalance means that the net movement of individuals causes patch 1 to swell in size more significantly than the constant movement model.

If the constant movement model is used to calculate the required level of control in patch 1, then a rate of around 0.15 would be predicted. In figure 5.6 we have used a culling rate in patch 1 of 0.16 (strategy C3 in figure 5.3). It is clear from these plots that eradication is achieved in the constant movement model, whereas the disease persists in the density dependent model. This persistence occurs because culling in patch 1 reduces the population, and hence the rate of emigration. This leads to an imbalance in movement rates, since emigration out of patch 2 is higher due to the larger patch size. This imbalance in movement means that individuals arrive into the culled patch faster than they leave, and the culling rate predicted by the constant movement model is insufficient.

The density dependent pathogen exclusion threshold for these parameter values does not, in fact, cross the axes. This indicates that control of a single patch will always be insufficient to cause complete eradication of disease since the second patch will always support the pathogen.

For the final part of this section, we will look at the effect of a successful, but skewed control strategy in both models. To do this, we fix the culling rate in patch 2 at $c_2 = 0.05$ and allow that of patch 1 to vary from 0 to 1. From the thresholds in figure 5.3, we expect all values of $c_1 > 0.05$ to cause total eradication of infection in both models. We are interested in the effect of density dependent movement on the time to pathogen exclusion. Since we cannot find this time analytically, we must define complete extinction for the purpose of simulations. In the simulations used to produce figure 5.7 we have assumed an infection free system corresponds to one where the number of infected individuals within each patch is below 0.001. More severe tolerances have been tested and the same qualitative behaviour is observed. The roughness of the curves shown in this figure are due to this cut off in the numerical simulation, however lower tolerances do not serve to significantly smooth the curves out. Figure 5.7 shows that,

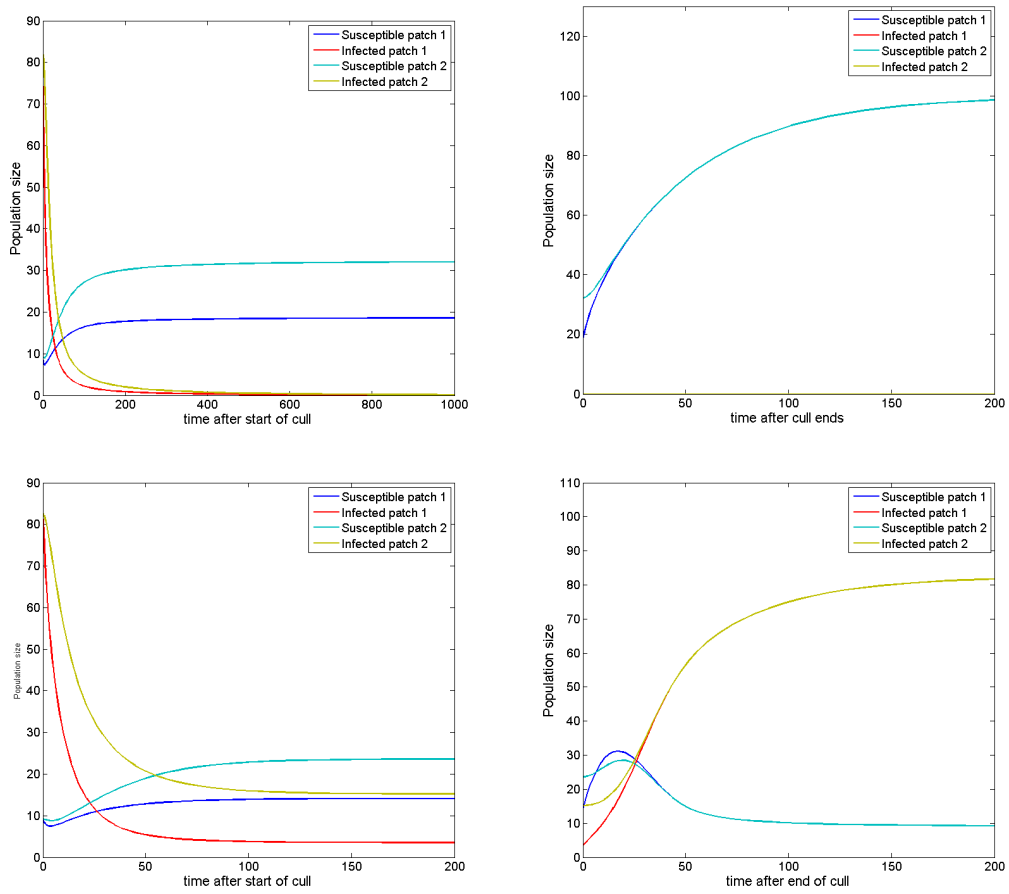

Figure 5.6: Transient dynamics of constant movement model (top row), and density dependent emigration model (lower row). Left column shows dynamics during cull, right column shows population regrowth after cull ends. Parameters used $a_i = 2, b_i = 0.02, \beta_i = 0.0024, \gamma_i = 0.002, m_i = 0.1, c_1 = 0.16, c_2 = 0$.

whilst both models do indeed predict pathogen exclusion for $c_1 > 0.05$, the constant movement model predicts a faster rate of removal than the density dependent emigration model. If movement is influenced by the population density in this way, then the constant movement model will therefore predict both a rate of control which may be insufficient, as well as predicting that control may be ceased earlier than necessary. Neglecting density dependent emigration may therefore lead to persistence of the pathogen even in the face of seemingly suitable control strategies.

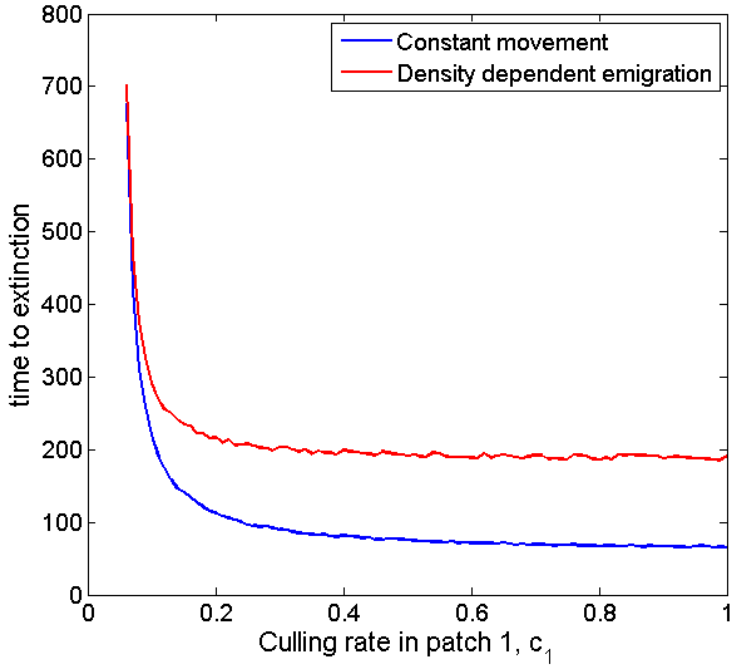

Figure 5.7: Time to extinction as control in patch 1 varies for both the constant movement model and density dependent emigration. Parameters used $a_i = 2, b_i = 0.02, \beta_i = 0.0024, \gamma_i = 0.002, m_i = 0.1, c_2 = 0.05$.

5.3 What difference does spatial perturbation make if movement is density dependent?

Chapter 3 has detailed the effect of spatial perturbation on the pathogen exclusion threshold if the movement rate in the absence of culling is constant. Here we aim to evaluate the effect of spatial perturbation on the density dependent model. In order to do this, we assume that the perturbation effect is modelled by an increasing movement rate, which increases linearly with the total number of individuals removed. Hence the full model in the perturbed case is

given by

$$\begin{aligned}
\frac{dS_1}{dt} &= a_1 - b_1 S_1 - \beta_1 S_1 I_1 - m\left(\frac{N_1}{K_1}\right)^s S_1 - m\rho c_1 N_1 S_1 + m\left(\frac{N_2}{K_2}\right)^s S_2 + m\rho c_2 N_2 S_2 - c_1 S_1 \\
\frac{dI_1}{dt} &= \beta_1 S_1 I_1 - (b_1 + \gamma_1) I_1 - m\left(\frac{N_1}{K_1}\right)^s I_1 - m\rho c_1 N_1 I_1 + m\left(\frac{N_2}{K_2}\right)^s I_2 + m\rho c_2 N_2 I_2 - c_1 I_1 \\
\frac{dS_2}{dt} &= a_2 - b_2 S_2 - \beta_2 S_2 I_2 - m\left(\frac{N_2}{K_2}\right)^s S_2 - m\rho c_2 N_2 S_2 + m\left(\frac{N_1}{K_1}\right)^s S_1 + m\rho c_1 N_1 S_1 - c_2 S_2 \\
\frac{dI_2}{dt} &= \beta_2 S_2 I_2 - (b_2 + \gamma_2) I_2 - m\left(\frac{N_2}{K_2}\right)^s I_2 - m\rho c_2 N_2 I_2 + m\left(\frac{N_1}{K_1}\right)^s I_1 + m\rho c_1 N_1 I_1 - c_2 I_2,
\end{aligned} \tag{5.10}$$

showing the additional per capita migration rate as $m\rho c_i(S_i + I_i)$.

5.3.1 Threshold behaviour

Since the effect of spatial perturbation is additive, and equivalent in both the constant movement and the density dependent movement models, we may expect that the difference in thresholds is maintained, with the density dependent model predicting a higher pathogen exclusion threshold than the constant movement. Simulation results dispute this fact, as exemplified in figure 5.8, which shows that the difference between the thresholds is greatly reduced in the perturbed system, and density dependent movement predicts a lower threshold than constant movement in this case. The threshold shown in figure 5.8 is equivalent to that shown in figure 5.1 with both models perturbed. Spatial disturbance in this case causes an increase in the pathogen exclusion threshold in both the constant and density dependent models, but the increase is less severe in the density dependent model. This result is analogous to the results of chapter 4 which have shown that density dependent movement offsets the effects of disturbance to a certain extent, particularly for low levels of disturbance.

We have shown, in chapter 3, that the effect of perturbation is dependent on the disease specific parameters, with an increase in transmission rate β being particularly important in determining whether disturbance will cause disease eradication to be easier or harder.

In order to investigate this property further, a series of simulations were run to find the

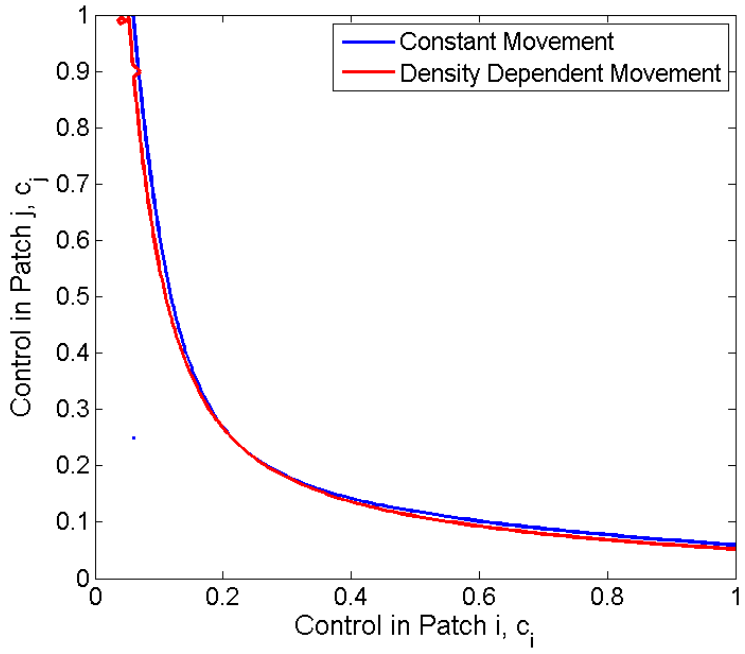

Figure 5.8: Pathogen exclusion thresholds of the perturbed constant movement model (solid line) and density dependent model (dotted). Parameters used $a = 2, b = 0.2, \beta = 0.308, \gamma = 1, m = 1, \rho = 1, \kappa = 1$.

pathogen exclusion thresholds for a range of these disease parameters. The $\beta - \gamma$ (transmission rate-virulence) space was then divided into those areas where i) the system was naturally disease free, ii) the perturbed pathogen exclusion threshold was higher than the unperturbed system, iii) the two thresholds were approximately identical, iv) the pathogen exclusion threshold in the perturbed system was lower than the unperturbed and (v) regions where the disease remained endemic for the range of control parameters considered. In all of the simulations, for comparison with chapter 3, figure 3.9, the range of control rates considered ranged from 0 to 1, leading to a maximum population reduction of around 85% in both patches. In figures 5.9 a) and c), there is a small additional region (*) whereby spatial perturbation induces disease, where otherwise the system would be disease free. The results of these simulations, shown in figure 5.9 suggest that at low connectivity, small m, the effect of spatial disturbance is qualitatively the same regardless of whether movement is constant or density dependent. In this case, plots a) and c) of figure 5.9, the majority of parameter space is occupied by region (iv), suggesting that spatial disturbance makes pathogen exclusion easier. The notable difference between these plots is the presence of region (v) in plot a). As

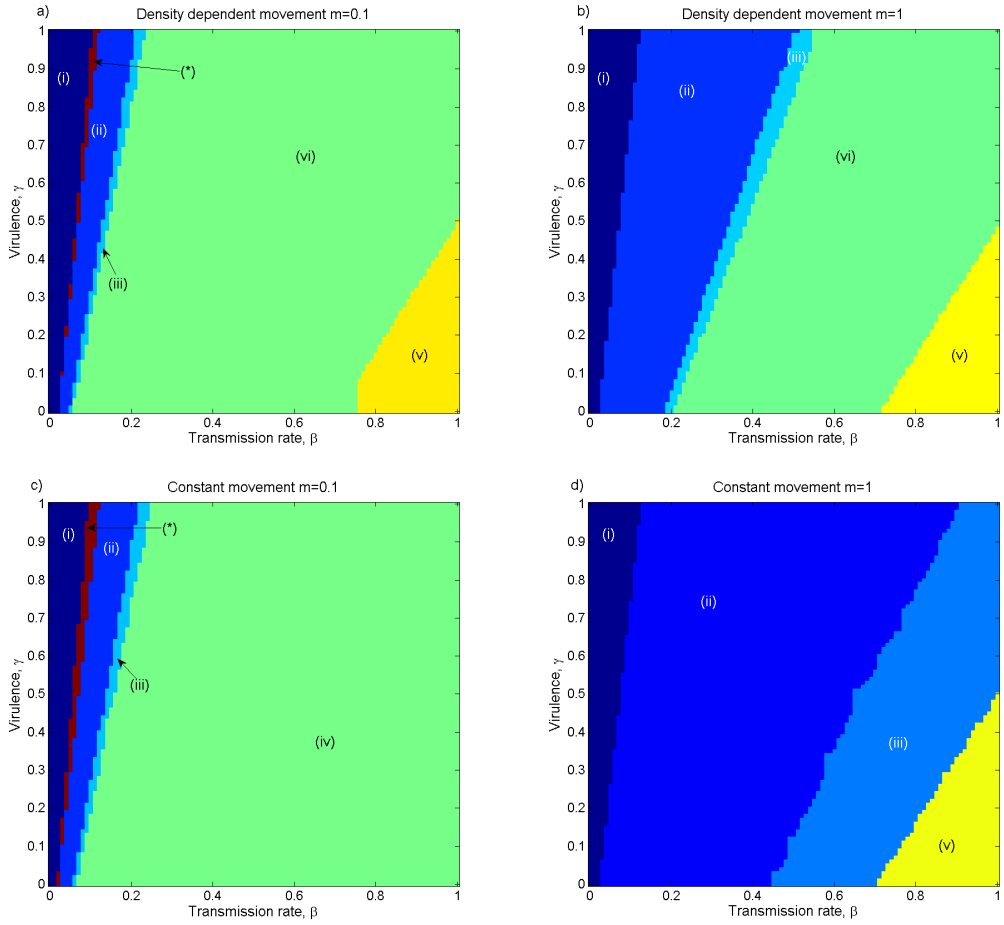

Figure 5.9: Order of pathogen exclusion thresholds as β and γ vary. Left hand plot shows low natural movement rate, right hand shows higher movement rate. The parameter space is divided into 5 main regions. (i) Disease free, (ii) perturbation threshold higher than unperturbed, (iii) perturbed and unperturbed thresholds indistinguishable, (iv) perturbed threshold lower than unperturbed, (v) endemic disease. Region (*) is described in text.

discussed previously in this chapter, density dependent movement raises the threshold when compared to constant movement. This has the effect that at very high transmission rates, the range of control efforts considered is unable to exclude the pathogen if movement is density dependent. The region (*) in plot c) is notably smaller in the density dependent model. This is to be expected, as perturbation has a less significant effect on population sizes if movement is density dependent, leading to a reduced effect which fails to distort the populations enough to become susceptible to pathogen invasion.

The second set of plots, b) and d) in figure 5.9 do show a significant difference. In this case, the patches are assumed to be well connected, with high m, such that movement is

allowed to happen at a faster rate. In this case, the constant movement model predicts that the majority of parameter space is occupied by region (ii), with disturbance making disease eradication more difficult. In the case of constant movement, there is no region where disturbance leads to a reduced threshold. The density dependent model, however, predicts that the majority of parameter space is dominated by this region (iv), where disturbance lowers the pathogen exclusion threshold, making disease easier to control. Figure 5.10 shows the pathogen exclusion thresholds corresponding to the high movement rate cases, $m = 1$, with fixed $\gamma = 0.5$. Here β is either $\beta = 0.2$ or $\beta = 0.5$. It is clear that the higher transmission

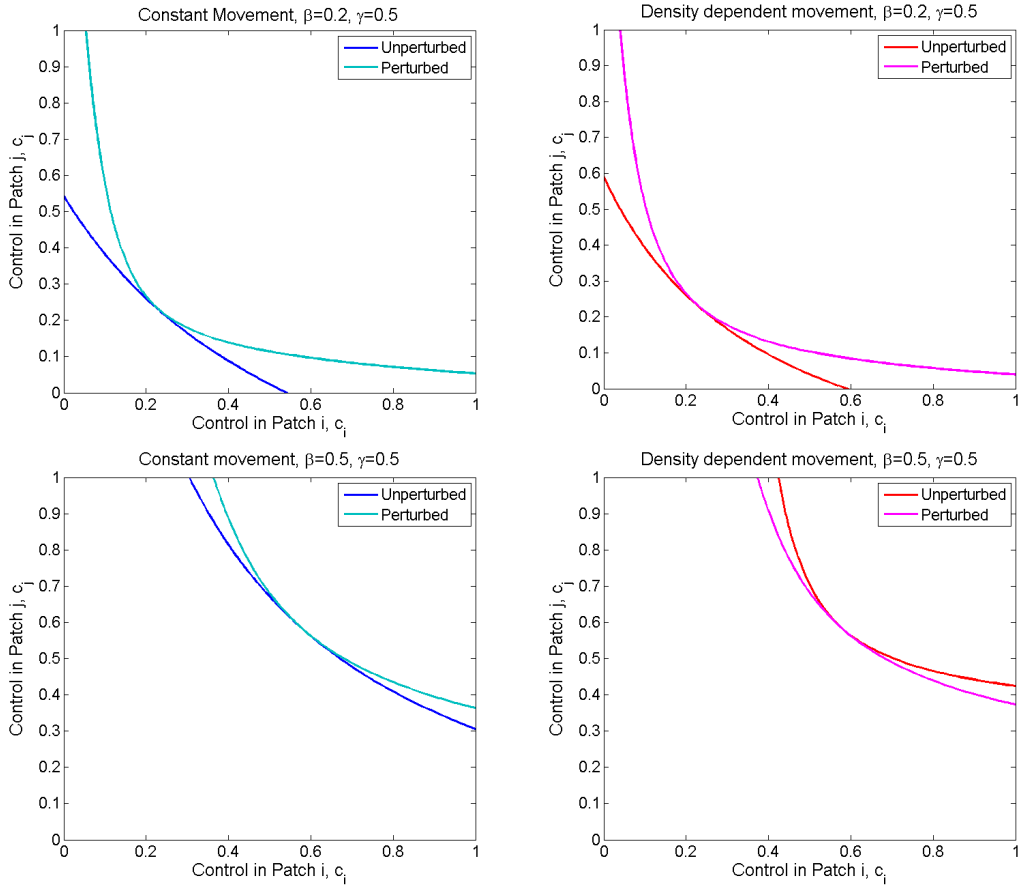

Figure 5.10: Comparison between pathogen exclusion thresholds for low and high transmission rates. Left hand plots show constant movement, right hand plots show density dependent movement. All plots compare perturbed and unperturbed systems. Parameters used $a = 2, b = 0.2, m = 1$.

rate moves the pathogen exclusion threshold higher in both the c_1 and c_2 directions, since a very transmissible disease is harder to control through culling. Therefore, if transmission

is high, then culling efforts must be high in order to eradicate infection. However, if culling rates are high, then the coupling strength, or movement between the patches in the density dependent model is significantly reduced. This leads the pathogen exclusion threshold to be more curved in the density dependent model than the constant movement model. This is seen by comparing the dark blue and red thresholds in the lower row of figure 5.10. At high culling rates, between patch movement in the density dependent model is so severely restricted that any disturbance caused in response to culling is significant enough to overcome this reduction, and hence reduce the pathogen exclusion threshold. At low transmission rates, a relatively weak control effort is required for pathogen exclusion. In this case, perturbation leads to a significant increase in the coupled patch and a higher rate across both patches is necessary to eliminate disease.

In order to investigate this behaviour further, we choose a point in this region, with $\beta = \gamma = 0.5$, and consider in detail the behaviour of the pathogen exclusion threshold, and the transient dynamics of the models in this case.

5.3.2 Transient effect of spatial perturbation

In order to explore the transient effects of spatial perturbation, we shall address the constant movement and the density dependent models individually. For simplicity, we assume that the demographic and disease parameters are equal across both patches, with both populations reaching equilibrium at 100 individuals. Once again, due to the symmetry of the system, if the same effort is applied across both patches, then this symmetry is maintained, and there is no difference in the transient dynamics, regardless of type of movement or spatial perturbation. For comparison with section 2.3, the same parameters are used, hence $a_1 = a_2 = 2$, $b_1 = b_2 = 0.02$, $\gamma = 0.002$ and $\beta = 0.00243$. The pathogen exclusion thresholds for the perturbed systems are shown in figure 5.11, along with the unperturbed thresholds for comparison (dashed lines). This figure shows that perturbation raises the threshold in the constant movement model, and lowers it in the density dependent case. In fact, figure 5.11 shows that the perturbed thresholds for both models are very similar for these parameter values. In the following sections, we consider culling strategies which lie between the unperturbed and perturbed thresholds, these are shown on figure 5.11 and are given by C1 $(0.16, 0)$ for the

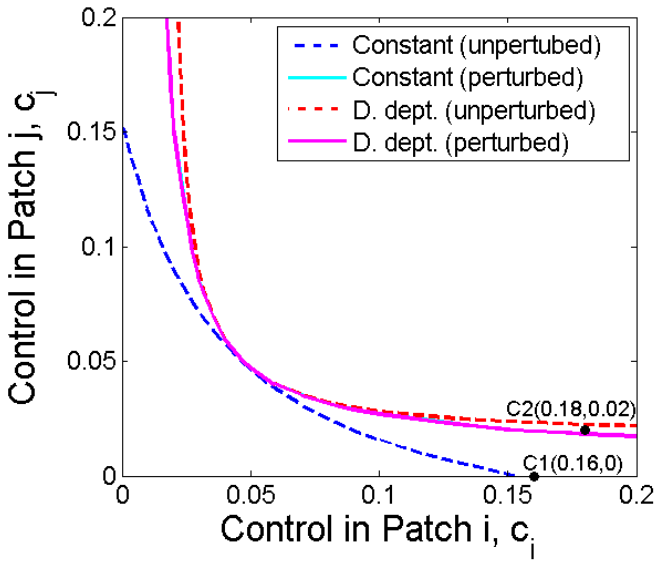

Figure 5.11: Pathogen exclusion threshold for constant and density dependent movement model both with and without perturbation. Parameters used $a = 2, b = 0.02, \gamma = 0.002, \beta = 0.0024, m = 0.1$. (note: the thresholds for both the constant and d.dependent models when perturbed are almost identical, and so not easily discernible.)

constant model and C2 $(0.18, 0.02)$ for the density dependent.

Transient effect of perturbation on constant movement

As mentioned above, in the absence of culling, the perturbed and the unperturbed models are identical. In the constant movement model, with culling strategy C1, the disease progression prior to culling are given in figure 5.4 (a). Once culling commences, the unperturbed model predicts that the infected populations of both patches decrease monotonically to zero, with the infection in patch 1 being reduced faster than patch 2. If the system is perturbed however, figure 5.12 shows a marked increase in the number of susceptible individuals in patch 2, and a significant peak in the initial dynamics of infected individuals due to the influx of individuals from the more intensive culling of patch 1. This disturbance of individuals in patch 1 is reflected in the sharp drop after culling commences in both susceptible and infected in patch 1. In the unperturbed system, the number of infected in patch 1 drop more gradually at first, but continues to drop to a lower level than the perturbed system. In the perturbed system, after the severe initial drop in infection, the number of infected individuals levels out. Correspondingly, the number of susceptible individuals in the constant model drops initially

due to the onset of culling before recovering to a higher level due to the removal of infected individuals. In the perturbed system, because the number of infected individuals stabilises at a higher level, the susceptible population does not recover as much or as quickly if the population is disturbed by the culling strategy.

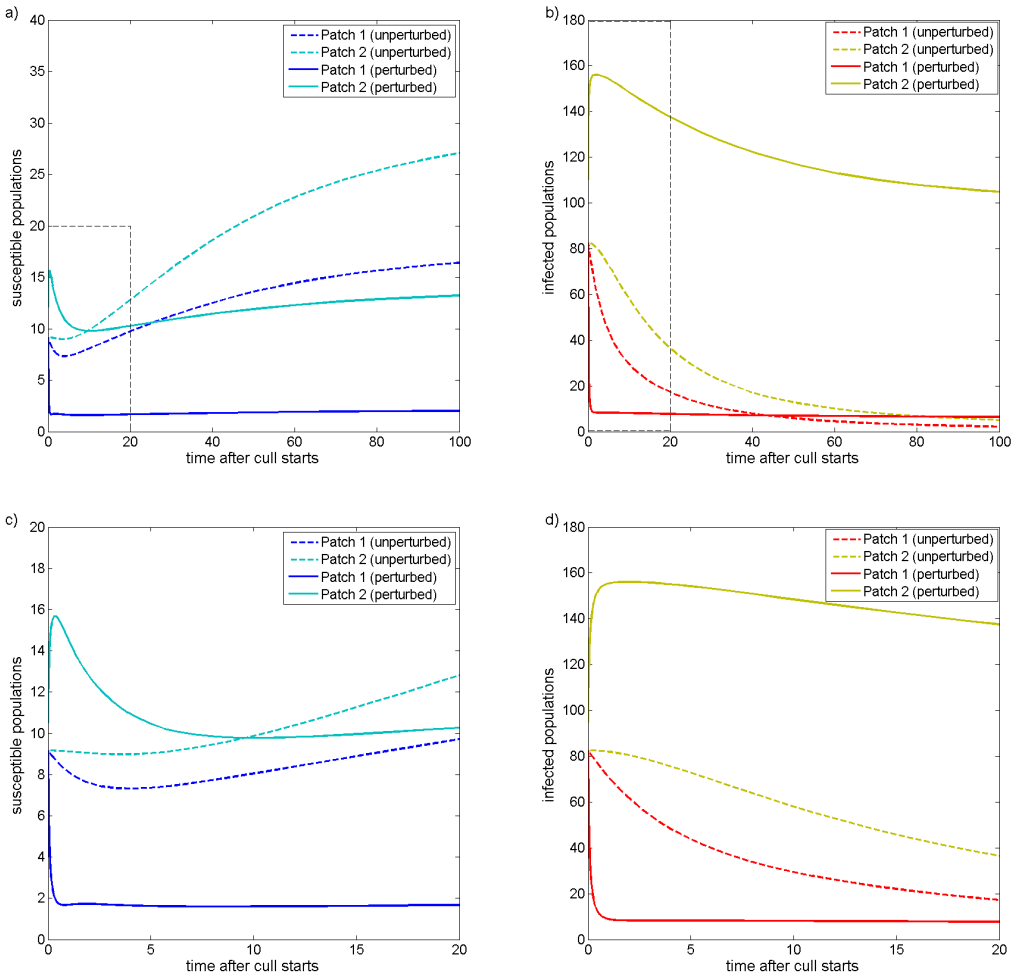

Figure 5.12: Transient dynamics of susceptible ((a) and (c)) and infected ((b) and (d)) classes in the constant movement model under culling strategy C1. Enclosed region in (a) and (b) is shown in (c) and (d) for clarity. Parameters used $a = 2, b = 0.02, \beta = 0.0024, \gamma = 0.002, m = 0.1, c_1 = 0.16, c_2 = 0$.

Transient effect of perturbation on density dependent model

In the case of density dependent movement, in the absence of disturbance, culling strategy C2 leads to a reduction in movement and effectively drives the populations towards isolation. The lower culling rate in patch 2 is insufficient to control infection in an isolated patch, and hence infection is allowed to persist in the density dependent system. If the populations are disturbed by culling, then the combination of outward movement, and direct removal of individuals reduces the population below the critical threshold for disease persistence and disease dies out. In this case, once culling is ceased, it is the unperturbed model that sees the system return to the endemic equilibrium, after a peak in the prevalence as the disease spreads through the increasing population. In the perturbed system, the behaviours of the populations soon after the onset of culling are qualitatively the same as those seen in the constant model and described above. The population in patch 2 sees a severe increase due to the influx of individuals from patch 1 which have been displaced by the culling regime. The population in patch 1 sees an initial rapid drop in population size, however, in the density dependent model, this drop is followed by a gradual recovery of the susceptible population and a continued drop in the infected population. Unlike the constant movement model, where the number of infected individuals stabilised under perturbation at a higher level, perturbation in the density dependent model drives the infected population to zero as shown in figure 5.13.

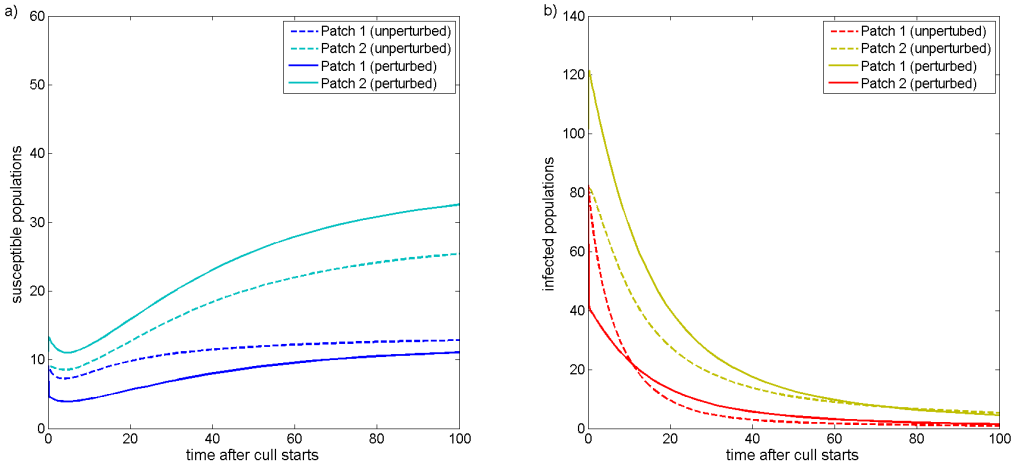

Figure 5.13: Transient dynamics of susceptible (left) and infected (right) populations in the density dependent model with and without spatial perturbation. Parameters used $a = 2, b = 0.02, \beta = 0.0024, \gamma = 0.002, m = 0.1, c_1 = 0.18, c_2 = 0.02$.

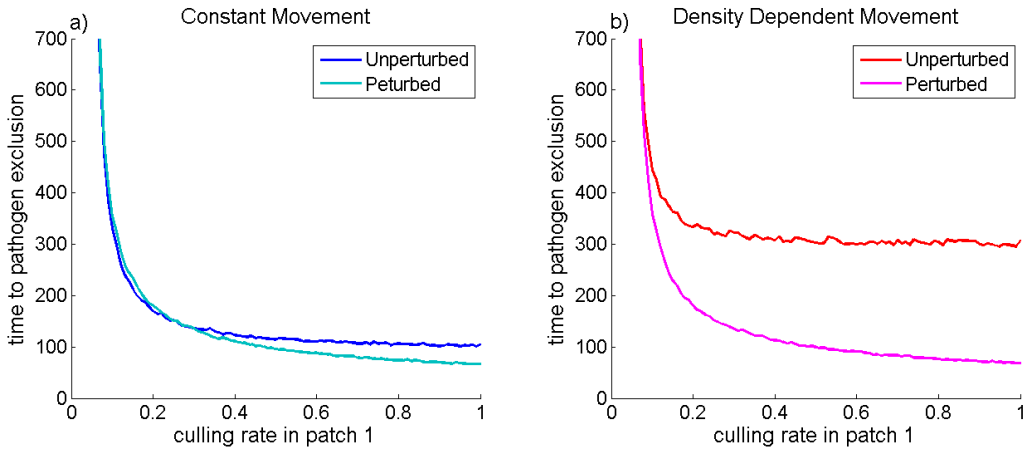

Figure 5.14: Time to pathogen exclusion for the perturbed and unperturbed models, plot a) shows the constant movement model, plot b) shows the density dependent model. Parameters used $a = 2, b = 0.02, \beta = 0.0024, \gamma = 0.002, m = 0.1, c_2 = 0.05$.

Time to pathogen exclusion

In the final section of this chapter we investigate the effect that perturbation has on the time to pathogen exclusion. We have shown in figure 5.7, that density dependent movement increases the time to pathogen exclusion if the system is unperturbed. Here we take the parameter values used in figures 5.12 and 5.13, and fix the control rate applied to patch 2 at $c_2 = 0.05$. Figure 5.14(a) shows the time to pathogen exclusion for the constant model, indicating that perturbation may increase the time to pathogen exclusion for control strategies close to the threshold, however, for less optimal strategies, the time to pathogen exclusion is shorter if the system is perturbed. In the density dependent model (figure 5.14(b)) however, disturbance has the effect of lowering the time to pathogen exclusion for equivalent strategies. This property is due to the fast reduction in the infected population shown in figure 5.13 which happens at a faster rate, and hence shorter time, than in the unperturbed model.

5.4 Discussion

The work presented in this chapter evaluates the impact of density dependent dispersal or movement between discrete habitats on the necessary conditions for disease control. In order to model this density dependence it is assumed that the rate of movement out of each patch increases with population density. Population density is the number of individuals in the patch

divided by the carrying capacity of the patch. For ease of explanation, all results shown assume that the rate of emigration increases linearly with the population density, and all results are shown when $s = 1$. We have shown (figure 5.1) that, when compared to a similar, two patch model with constant movement, the inclusion of density dependent dispersal raises the pathogen exclusion threshold making disease eradication significantly more difficult, and only possible for higher culling rates. Movement has been shown to be strongly density dependent in several systems [2], [98], some of which may be susceptible to invading pathogens. We have shown that controlling these populations via culling, leading to low local densities, will cause the number of emigrants leaving the population to be reduced. This creates an asymmetry in the movement rates between patches. A single control effort targeted at a single patch in a patchy system, will only effect the movement out of the targeted patch. The number of immigrants into the target patch will not be significantly changed, and hence the removal of individuals due to culling will be mediated by the continued influx of neighbouring individuals. Density dependent movement has been shown to increase both the necessary effort for disease exclusion, and also the length of the culling period required in order to reduce the infected population to zero. As discussed in chapter 4, density dependent movement may act as a buffer in a patchy system, guarding populations against the fluctuations in surrounding patches. Whilst this prevents species from going extinct in the case of harvesting in the surrounding areas, this also makes control of disease persistence much more difficult. Disturbance of a population in response to culling mediates the effects of density dependence, maintaining an outward movement during culling. We have shown that this may be beneficial to the cause of pathogen exclusion, leading to a reduced effort required (figure 5.8), as well as a shorter required culling period 5.14. Whilst this result may be harnessed to eliminate infection over a shorter time period, the transient dynamics shown in figure 5.13 shows a marked increase in the number of infected individuals in the uncontrolled patch in the time immediately following the onset of culling. Whilst disturbance may lead to a reduction in pathogen exclusion threshold, and drive the population to extinction in a shorter time, this may be at the risk of inducing a high prevalence for a short period of time.

This analysis of the impact of disturbance behaviour on disease spread in controlled populations is particularly relevant to the spread of bovine TB in the UK badger population. There

is strong evidence to suggest that culled badgers change their ranging behaviour in response to the culling activities [150]. Results from the randomised badger culling trial, a large scale experiment to evaluate the effects of different badger culling strategies on the prevalence of bovine TB, showed that localised culling efforts can help to reduce the incidence of disease within the culled area, whilst increasing the prevalence in surrounding areas [42]. This increase in prevalence in surrounding areas was most striking after the initial cull, with the effect reducing after subsequent culls, indicating a possible density dependent response. Badgers from surrounding areas are allowed to re-enter the culled area once culling has finished. The possibility of this response in the wild badger population means that different efficiencies in culling strategies across the spatial range of the population will lead to local increases in disease prevalence as seen in Figure 5.13. If the controlled population is a reservoir of infection to other populations, as in the case of the culling of badgers to prevent bovine TB in cattle, then this high prevalence could lead to further infections in livestock populations. If culling could be carried out consistently across all areas, then the increased movement caused by culling could potentially lead to a reduction in the time to disease eradication (Figure 5.14), however the potential cost of this strategy makes it unlikely to be achieved in this system.

The pathogen exclusion thresholds in all the models previously discussed have maintained a similar shape, with symmetric patch systems yielding thresholds that pass through a common point, regardless of perturbation, or form that movement takes. In these cases, the symmetry of the system is maintained, and the opposing forces of population movement, culling and growth are in equilibrium. In order to counteract the effects of density dependence, or perturbation, one may assume that this point is the optimal culling strategy. This concept is discussed in detail in the following chapter.

Chapter 6

Optimal control of disease in 2 and 3 patches

6.1 Introduction

The final study in this thesis involves the formulation of the optimal strategies for control of disease in the patchy systems that we have so far considered. Optimal control theory is concerned with finding the 'best' combination of parameters to solve a problem. In the context of control of infectious disease, this 'best' combination will be that which minimises the cost of control [90]. Due to the importance of designing reasonable control policies given the economic constraints, optimal control applied to mathematical models has been used in a range of studies. Historically, models were used to optimise culling practices in livestock systems [77]. With the increasing popularity and realism of mathematical modelling of biological systems, increasingly complex problems. These include control of disease by vaccination or culling on vast national networks as in the case of foot and mouth disease [135], [133], as well as studies of optimal control in metapopulations [121], or multi-species systems [61].

In this chapter, we use Lagrangian optimisation to discuss the optimal control strategy in the models previously defined. Using standard techniques, we are able to draw conclusions about the impact of disturbance on the optimal control strategies in these systems.

Throughout this thesis thus far, we have considered only systems which are divided into two distinct patches. Whilst this may be an appropriate approximation for considering move-

ment at a local scale, for example from inside to outside of a protected area, or area designated for culling, this approach is limited when considering the wider landscape. In this chapter we aim to quantify disease control amongst a wider metapopulation. To do this, we introduce the concept of an optimal control strategy in the two patch system. This optimal control is then scaled up to a system of three patches, enabling us to explore the consequences of different local, spatial configurations of patches on the necessary conditions for disease control.

6.2 Optimal disease control in two patches

6.2.1 Introduction to Lagrangian optimisation

In its simplest terms, optimal control theory is concerned with finding a set of control parameters c_i which optimise a problem subject to a set of constraints. In the case of optimising control of disease in patchy environments, the important constraint is the condition that disease is successfully eradicated. This constraint is non-linear, and hence the problem is a non-linear programming problem (NLPP). The classical constrained non-linear optimisation problem was first explored by Lagrange, and we begin this chapter by providing a general overview of this method. The classical NLPP is defined as follows

$$\text{Minimise} \qquad f(\mathbf{x}) \qquad \text{subject to} \qquad g(\mathbf{x}) = 0, \tag{6.1}$$

where $f(\mathbf{x})$ is the objective function to be minimised, and $g(\mathbf{x}) = 0$ is the constraint. The Lagrangian optimisation method then states that every optimal solution of (6.1) must be a solution of the system

$$\nabla f(\mathbf{x}) - \lambda \nabla g(\mathbf{x}) = 0, \qquad g(\mathbf{x}) = 0 \tag{6.2}$$

the constant λ is the Lagrangian multiplier corresponding to the constraint $g(\mathbf{x})$. This formulation states that the optimal solution of (6.1) is found when the gradients of the objective function $f(\mathbf{x})$ and the constraint $g(\mathbf{x})$ are parallel.

6.2.2 The optimisation problem in 2 patches

The first task in setting up the non-linear programming problem is to define the relevant objective function to be minimised. The aim here is to find the control strategy, defined by the pair of points (c_1, c_2), which minimises the cost of the total effort exerted, whilst also successfully eradicating the pathogen from the system. The cost of a control strategy will, in reality, depend on many factors involved in the logistics of carrying out such a strategy. Of course, there are many economic considerations to take into account when designing a culling strategy. These factors can range above and beyond the simple logistics of carrying out the cull, for example the knock on effect of the local economy if a farmers herd is culled. We cannot hope to capture all the intricacies of this situation in this problem, and so the objective functions are chosen for tractability. We consider two possible objective cost functions:

$$f_1(c_1, c_2) = h_1 c_1 + h_2 c_2 \tag{6.3}$$

$$f_2(c_1, c_2) = \sqrt{(h_1 c_1)^2 + (h_2 c_2)^2}. \tag{6.4}$$

The first of these costs, f_1, is simply the weighted sum of the culling efforts applied to each patch. The coefficients h_i define the cost per unit effort to cull in patch i. For example, if a population to be culled inhabits a particularly difficult or dangerous terrain, then the costs of culling that population may be much higher than the costs of culling a common species in easily accessible landscape. Similarly, the costs of hunting and culling a wild species, may be much higher than culling livestock. The cost defined by f_1 assumes that there is complete independence between the culling efforts of the two patches. The total cost is simply the sum of the costs, and culling in one patch does not change the cost of the second strategy in any way. The second cost function f_2, inherently assumes that the total cost of the joint culling strategy is lower than the sum of the independent strategies. We analyse the consequences of this cost function as an alternative to f_1 in order to represent a culling strategy which is centrally organised across the whole scale of the patch system. If this is the case, then it is feasible that the infrastructure which must be in place in order to cull in a single patch will not be repeated for each subsequent patch, and hence the cost is less than the independent strategies. In the following analysis, we assume that the cost of culling in either patch is

equivalent, and hence we set $h_1 = h_2 = 1$.

A graphical representation of these costs is shown in figure 6.1. Culling strategies which lie on the same straight line contour have the same cost as defined by f_1, whilst culling strategies lying on the same arc have the same cost $f_2(c_1, c_2)$. This figure highlights the difference in the cost functions. For example, take the control strategy defined by the point C in figure 6.1. Under f_1, this strategy would have a cost of 0.8, whilst under f_2 the cost would be 0.6.

The optimisation problem in two patches is constrained by two requirements. The first of

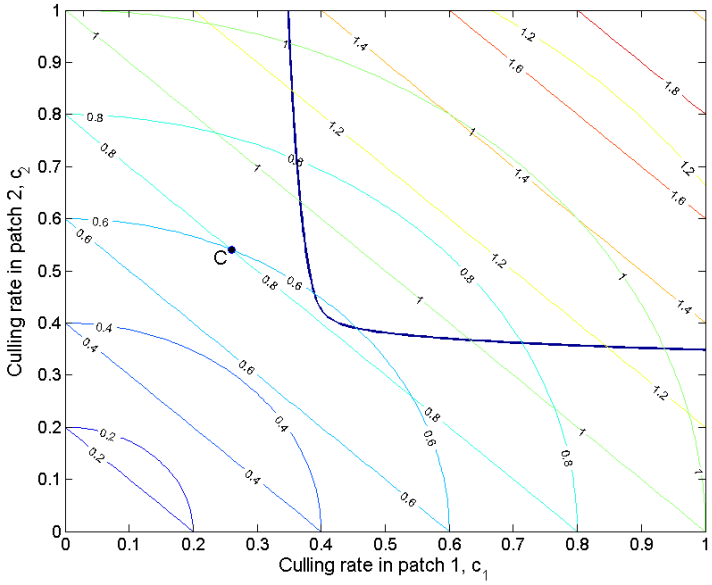

Figure 6.1: Contours showing different costs associated with different culling strategies. Straight line contours represent culling strategies with equivalent costs under $f_1(c_1, c_2)$, whilst concentric circle contours show strategies with equivalent costs under $f_2(c_1, c_2)$. Thick contour gives pathogen exclusion threshold, $g(c_1, c_2) = 0$ and hence represents the constraint for the NLPP.

these is that the culling efforts c_1, c_2 must be non-negative and the second is that the optimal strategy must successfully remove infection from the system. Throughout this thesis, when considering disease control, the pathogen exclusion thresholds have been calculated, providing a boundary in control space, beyond which the disease cannot invade and an endemic disease will no longer be able to persist. This threshold therefore defines the lower bound of the second constraint. If control strategies lie on or above this boundary, then disease will die out. Since both formulations of the cost functions are increasing in both c_1 and c_2, this non-

linear programming problem (NLPP) reduces to finding the (c_1, c_2) which minimise $f_i(c_1, c_2)$ along this threshold.

The optimisation problem can therefore be fully defined as follows:

$$\begin{aligned} \text{Minimise:} \quad & f_i(c_1, c_2) \\ \text{subject to:} \quad & g(c_1, c_2) = 0, \qquad c_1 \geq 0, \qquad c_2 \geq 0 \\ \text{where} \quad & g(c_1, c_2) = (\beta_1 H_1(c_1, c_2) - G_1 - m_1 - c_1)(\beta_2 H_2(c_1, c_2) - G_2 - m_2 - c_2) - m_1 m_2. \end{aligned} \tag{6.5}$$

In this NLPP, the constraint $g(c_1, c_2)$ is the determinant of the Jacobian of the system, discussed in chapter 3. In this formulation, the notation has been slightly condensed, with

$$\begin{aligned} G_i &= \gamma_i + b_i \\ H_i(c_1, c_2) &= \frac{a_i m_j + a_j m_j + a_i(b_j + c_j)}{m_1(b_2 + c_2) + m_2(b_1 + c_1) + (b_1 + c_1)(b_2 + c_2)}. \end{aligned}$$

From condition (6.2) defined above, the minimal control strategy must therefore satsfy

$$\frac{\partial f_i}{\partial c_1} = \lambda \frac{\partial g}{\partial c_1}, \quad \frac{\partial f_i}{\partial c_2} = \lambda \frac{\partial g}{\partial c_2}, \quad g(c_1, c_2) = 0 \tag{6.6}$$

for cost i. It is clear that the gradient of the two cost functions are given by

$$\frac{\partial f_1}{\partial c_1} = 1, \qquad \frac{\partial f_1}{\partial c_2} = 1$$

$$\frac{\partial f_2}{\partial c_1} = \frac{c_1}{\sqrt{c_1^2 + c_2^2}}, \qquad \frac{\partial f_2}{\partial c_2} = \frac{c_2}{\sqrt{c_1^2 + c_2^2}}$$

Differentiating the pathogen exclusion threshold $g(c_1, c_2)$ with respect to the control parameters we have

$$\begin{aligned} \frac{\partial g}{\partial c_1} =& \beta_1\beta_2 \left(\frac{\partial H_1}{\partial c_1} H_2 + H_1 \frac{\partial H_2}{\partial c_1} \right) - \beta_1(G_2 + m_2) \frac{\partial H_1}{\partial c_1} - c_2\beta_1 \frac{\partial H_1}{\partial c_1} - \beta_2(G_1 + m_1) \frac{\partial H_2}{\partial c_1} \\ & - \beta_2(c_1 \frac{\partial H_2}{\partial c_1} + H_2) + (G_2 + m_2 + c_2) \end{aligned} \tag{6.7}$$

and

$$\frac{\partial g}{\partial c_2} = \beta_1\beta_2\left(\frac{\partial H_1}{\partial c_2}H_2 + H_1\frac{\partial H_2}{\partial c_2}\right) - \beta_1(G_2+m_2)\frac{\partial H_1}{\partial c_2} - c_1\beta_2\frac{\partial H_2}{\partial c_2} - \beta_2(G_1+m_1)\frac{\partial H_2}{\partial c_2} - \beta_1(c_2\frac{\partial H_1}{\partial c_2} + H_1) + (G_1+m_1+c_1) \tag{6.8}$$

Where

$$\frac{\partial H_i}{\partial c_i} = -\frac{(a_j m_i + a_i(m_j+b_j+c_j))(m_j+b_j+c_j)}{((m_j(b_i+c_i)+m_i(b_j+c_j)+(b_i+c_i)(b_j+c_j))^2}$$

and

$$\frac{\partial H_i}{\partial c_j} = -\frac{m_i(a_i m_j + a_j(m_i+b_i+c_i))}{(m_i(b_j+c_j)+m_j(b_i+c_i)+(b_i+c_i)(b_j+c_j))^2}$$

Even in the case of fully symmetric patches, with all demographic and disease parameters equal, this problem becomes analytically impossible due to the implicit nature of the function $g(c_1, c_2)$. We must therefore employ a different technique in order to address this optimisation problem. Although we cannot derive the optimal point, we are able to test if a proposed point minimises $f_i(c_1, c_2)$ along the threshold $g(c_1, c_2) = 0$. To do this we must show that the proposed point satisfies the equations given in (6.6).

6.2.3 Symmetric Patches

If both patches are equal in all demographic and disease parameters, we know from the symmetry of the system that the pathogen exclusion threshold is symmetric about $c_1 = c_2$. The shape of the contour shown in figure 6.1, suggests that the control strategy which minimises both f_1 and f_2 occurs when $c_1 = c_2$. If $c_1 = c_2 = c$, and the patches are symmetric, then both populations will achieve their disease free equilibrium at

$$H_i = \frac{a}{b+c}.$$

The pathogen exclusion threshold at this point is therefore given by

$$\left(\beta\frac{a}{b+c} - G - m - c\right)\left(\beta\frac{a}{b+c} - G - m - c\right) - m^2 = 0.$$

Since the disease free equilibria in this case are independent of movement rate m, the threshold at this point is the same regardless of the magnitude of m. It is for this reason that all thresholds converge at this point if the patches are symmetric. Setting $m = 0$, we effectively decouple the system, and find that the pathogen exclusion threshold at this point is equivalent to culling both independent patches sufficiently to drive the pathogen to extinction. If the patches are decoupled, then the pathogen exclusion threshold in a single patch must satisfy

$$\beta \frac{a}{b+c} - \gamma - b - c = 0,$$

and hence

$$c = -2b - \gamma + \sqrt{\gamma^2 + 4\beta a}/2.$$

In order to prove that this point minimises $f_i(c_1, c_2)$, we must show that this point satisfies 6.6. To do this, it is first noted that

$$\nabla f_1(c,c) = \begin{pmatrix} \partial f_1/\partial c_1 \\ \partial f_1/\partial c_2 \end{pmatrix} = \begin{pmatrix} 1 \\ 1 \end{pmatrix} \qquad \text{and} \qquad \nabla f_2(c,c) = \begin{pmatrix} \partial f_2/\partial c_1 \\ \partial f_2/\partial c_2 \end{pmatrix} = \frac{1}{\sqrt{2}} \begin{pmatrix} 1 \\ 1 \end{pmatrix}. \tag{6.9}$$

This implies that the gradient vectors of both the objective cost functions are in the same direction, at this point, and hence if culling strategy (c, c) minimises f_1, then it also minimises f_2. Using the Lagrangian conditions given in 6.6, the gradient vector of the constraint, that is the pathogen exclusion threshold, must be parallel to the gradient of the objective function, and so

$$\nabla g = \begin{pmatrix} \partial g/\partial c_1 \\ \partial g/\partial c_2 \end{pmatrix} = \frac{1}{\lambda} \begin{pmatrix} 1 \\ 1 \end{pmatrix}. \tag{6.10}$$

Hence in order to show that this point (c, c) is the minimum control strategy, it suffices to show that

$$\frac{\partial g}{\partial c_1} = \frac{\partial g}{\partial c_2}. \tag{6.11}$$

By evaluating equations 6.7 and 6.8 along the line $c_1 = c_2$, we can simplify these equations to

$$\frac{\partial g}{\partial c_1} = -\beta m \left(\frac{\partial H_1}{\partial c_1} + \frac{\partial H_2}{\partial c_1} \right) + m \tag{6.12}$$

$$\frac{\partial g}{\partial c_2} = -\beta m \left(\frac{\partial H_1}{\partial c_2} + \frac{\partial H_2}{\partial c_2} \right) + m, \tag{6.13}$$

and from the symmetry of the system $\partial H_1/\partial c_1 = \partial H_2/\partial c_2$ and $\partial H_1/\partial c_2 = \partial H_2/\partial c_1$. Hence equation 6.11 is satisfied and the point (c, c) gives the minimum combined control effort required to exclude infection from a symmetric two patch system, if cost is defined by either f_1 or f_2.

Minimum control, maximum population?

The point which corresponds to the minimum control effort, may be assumed to correspond to the maximum population sizes within each patch, and hence this strategy maintains the largest total population whilst eradicating the disease. This result is intuitive in this case, since control has no other effect than reducing the population. Hence we expect a monotonically decreasing total population as c_1 or c_2 are increased. The total population is given by

$$T(c_1, c_2) = \frac{a(4m + 2b + c_1 + c_2)}{m(2b + c_1 + c_2) + (b + c_1)(b + c_2)} \tag{6.14}$$

which has negative derivatives in both control directions

$$\frac{\partial T}{\partial c_1} < 0, \qquad \frac{\partial T}{\partial c_2} < 0.$$

Increasing either the total sum of the control strategy, or the euclidean distance hence has the effect of decreasing the total population size, and the maximum population along the pathogen exclusion threshold is found when $f_i(c_1, c_2)$ is at its minimum, hence the point (c, c). This result is confirmed by numerical simulations of $f_1(c_1, c_2)$, $f_2(c_1, c_2)$ and $T(c_1, c_2)$ along the pathogen exclusion threshold as shown in figure 6.2. This result shows that if two patches are equal in size, and the movement between them is constant and at equal rates,

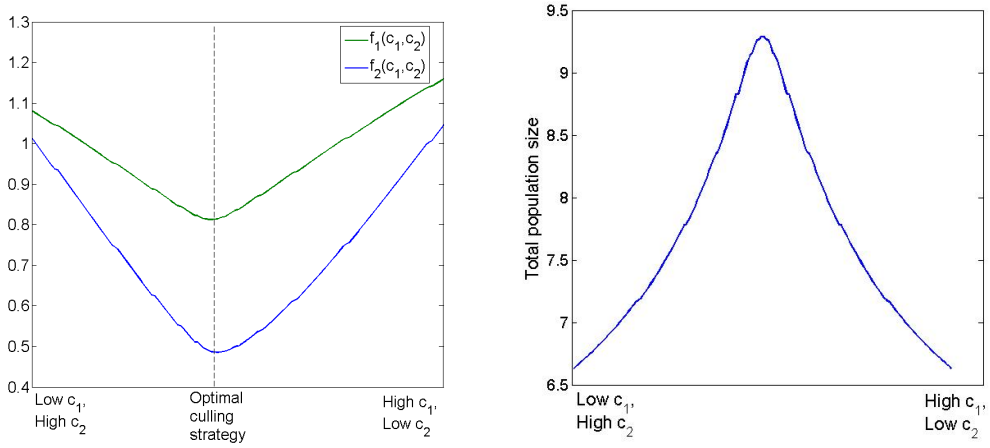

Figure 6.2: Left: Total cost combined control strategy along pathogen exclusion threshold as evaluated by f_1 and f_2. Minimum shown appears approximately when $c_1 = c_2$. Right: Total disease free population size achieved along pathogen exclusion threshold. Maximum shown at approximately $c_1 = c_2$.

then the spatial distinction between the two patches does not affect the necessary conditions for disease control. The necessary control strategy applied to each patch to ensure disease eradication whilst maximising the total population is equal to that derived from modelling the two patches independently. This result is to be expected since the net movement in this case is zero, and each patch is effectively independent.

6.2.4 Asymmetric Patches

Asymmetry in the patches can be introduced in many ways, either demographically or epidemiologically. For example, two patches may be asymmetric in their carrying capacities, hence the size of one patch is different to the size of the other, and the amount of resources each patch contains differs. In this model this can be thought of as either a change in the constant recruitment term $a_1 \neq a_2$ or in the per capita death term $b_1 \neq b_2$. Since the constant recruitment term is not dependent on the population within the patch, and can be thought of as a predominantly external driver for population growth, we shall assume that this is constant between both patches. The asymmetry in patch size must therefore be modelled by varying the per capita death term. A high b_i means that individuals have, on average a short life span of $1/b_i$, and we think of patch i as being a 'small' patch, with a low carrying capacity. To be explicit in our evaluation of asymmetry, we will assume that the death rates

are related by the ratio $b_1 = \phi b_2$ with $\phi < 1$. Hence patch 2 has a lower death rate than patch 1, implying a higher carrying capacity and is the larger patch. Figure 6.3 represents the

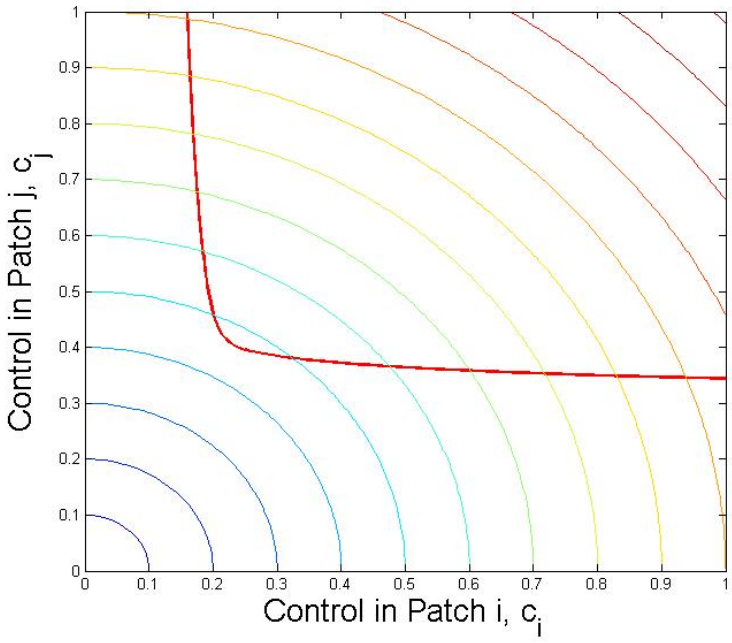

Figure 6.3: Asymmetric patches with $b_1 > b_2$. Here $\phi = 1/20$.

NLPP for this asymmetric case. It is clear from this plot that the optimal point no longer lies on the line $c_1 = c_2$. From the structure of the infection invasion matrix, described in detail in chapter 3 and Appendix E, we know that the maximum eigenvalue is bounded by the column sums, and hence in the two patch case

$$\min\{\beta H_1 - \gamma - b - c_1, \beta H_2 - \gamma - \phi b - c_2\} \leq \lambda \leq \max\{\beta H_1 - \gamma - b - c_1, \beta H_2 - \gamma - \phi b - c_2\}$$

In the symmetric system, the minimum control strategy was found when these bounds were equal. We expect, when considering patches of different sizes, that applying control to the larger patch will be more effective. Based on the result in the symmetric case, we propose that the minimum control strategy is found when the forces of infection balance between patches, hence

$$\beta_1 H_1 - \gamma_1 - b_1 - c_1 = \beta_2 H_2 - \gamma_2 - b_2 - c_2.$$

In the case of asymmetry in carrying capacity, this condition is achieved when

$$\beta H_1 - \gamma - b - c_1 = \beta H_2 - \gamma - \phi b - c_2 \tag{6.15}$$

$$c_2 = \beta(H_2 - H_1) + b(1 - \phi) + c_1. \tag{6.16}$$

This equation is dependent on the difference in size of the two populations, given by

$$H_1 - H_2 = \frac{a(b(1-\phi) + c_1 - c_2)}{m(b(1+\phi) + c_1 + c_2) + (b + c_1)(\phi b + c_2)} \tag{6.17}$$

which is zero when

$$b(1 - \phi) + c_1 - c_2 = 0$$

$$c_2 = b(1 - \phi) + c_1. \tag{6.18}$$

The proposed minimum point is therefore the point along the pathogen exclusion threshold which satisfies the ratio (6.18). This is the point at which the culling strategies balance the asymmetry of the system. If the two patches are culled in this ratio, then both populations will be reduced to be equal in size. In order to show that this point minimises the cost of culling, we must once again show that the conditions 6.6 are satisfied. In order to achieve pathogen exclusion along this line in control space, we require that the maximum eigenvalue of the Jacobian matrix, J, is negative, where

$$J = \begin{pmatrix} \beta H_1 - \gamma - b - m - c_1 & m \\ m & \beta H_2 - \gamma - b - m - c_2 \end{pmatrix}. \tag{6.19}$$

Along the line defined by equation (6.18), this condition is given by

$$\frac{\beta a}{b + c_1} - \gamma - b - c_1 = 0 \tag{6.20}$$

and hence the minimum control strategy is given by the point (C_1, C_2) where

$$C_1 = \left[-2b - \gamma + \sqrt{\gamma^2 + 4\beta a}\right]/2 \tag{6.21}$$

$$C_2 = [-2\phi b - \gamma + \sqrt{\gamma^2 + 4\beta a}]/2. \tag{6.22}$$

Firstly we must find the gradient of the functions $f_i(c_1, c_2)$ at this point. These are given by

$$\nabla f_1(C_1, C_2) = \begin{pmatrix} 1 \\ 1 \end{pmatrix}, \qquad \text{and} \qquad \nabla f_2(C_1, C_2) = \frac{1}{\sqrt{C_1^2 + ((1-\phi)b + C_1)^2}} \begin{pmatrix} C_1 \\ b(1-\phi) + C_1 \end{pmatrix}. \tag{6.23}$$

Since the gradient of the cost defined by f_1 is constant, this expression is not dependent on the culling strategy considered and is the same as in the symmetric case. The gradient of f_2 is however different at this point. Once more, evaluating ∇g at this point gives

$$\nabla g = m\left(1 + \frac{\beta}{(b + c_1)^2}\right)\begin{pmatrix} 1 \\ 1 \end{pmatrix} \tag{6.24}$$

which is parallel to the gradient of f_1. This point therefore minimises the cost as defined by f_1. Defining the cost in this linear manner means that the optimum control strategy in the asymmetric system is independent of the movement function, since this control strategy balances the asymmetry in the populations.

If the cost of culling is defined by $f_2(c_1, c_2)$, then the strategy (C_1, C_2) does not lead to the optimal point. This point was chosen since it is independent of movement between patches, and all models, regardless of the movement rate, will converge at this point for pathogen exclusion. If this point is suboptimal, then the minimum control strategy will depend on the movement rate between patches. To investigate how this optimal point changes with increasing movement, we assume that movement between the patches is equal, hence $m_1 = m_2$. The results presented below are for the two cases where a) both patches are reservoirs of infection, and b) the larger patch is a source of infection to the second, non-reservoir.

Both patches are reservoirs of infection.

Recalling the definition of a reservoir of infection, if both patches are reservoirs then, in the absence of any coupling via dispersal, both patches will support the pathogen and will require independent culling strategies for pathogen eradication. As movement increases, it may be feasible to achieve pathogen eradication through control of a single patch alone. We have shown that a culling rate defined by (C_1, C_2) given above is optimal if the cost of culling is defined as the sum of the culling strategies. This optimum cost is invariant as the rate of movement changes. However, if the cost of culling is given by f_2, the question remains as to how the minimum combined culling strategy changes as movement increases, along with how the burden of control is distributed between the patches. This question must be answered numerically, and the code for the algorithm described below is given in Appendix G.

For each movement rate, m:

1. Evaluate pathogen exclusion threshold in $c_1 - c_2$ space.
2. Store co-ordinates (c_1^i, c_2^i) for all points sampled along this threshold.
3. For each point i along the pathogen exclusion threshold, evaluate the cost of culling $f_2^i = \sqrt{(c_1^i)^2 + (c_2^i)^2}$.
4. Find minimum f_2 along this threshold and store this cost along with corresponding co-ordinates.

Figure 6.4 shows that the minimum total culling effort, defined by $\sqrt{c_1^2 + c_2^2}$ in fact decreases as movement increases. Hence an increase in connectivity between distinct areas reduces the effort required to eradicate the disease. The right hand graph of figure 6.4 shows that this reduction involves a shift in the burden of control, with the rate of control being reduced in the larger patch, whilst the smaller patch is controlled more at higher movement rates. This is due to the synchrony achieved between the two patches at high movement rates, encompassing the fact that the difference in size between the two populations is reduced as coupling via movement increases.

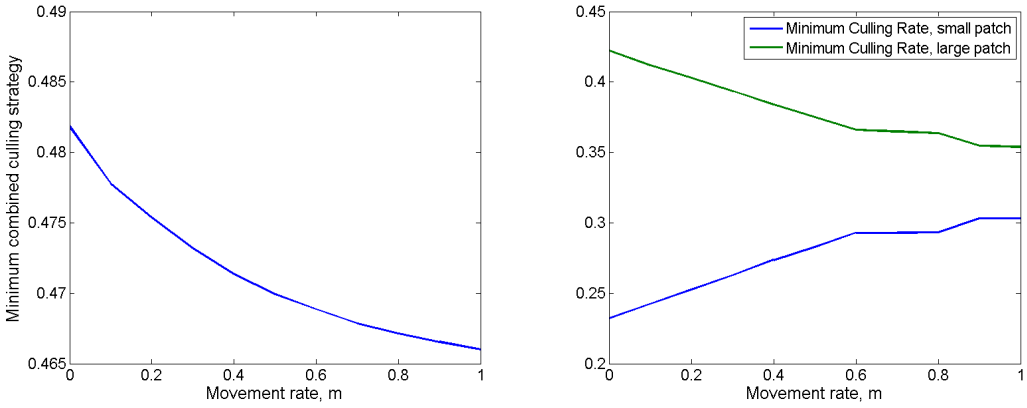

Figure 6.4: Minimum culling rates for pathogen exclusion, as the rate of coupling via dispersal increases. Combined culling effort decreases as movement increases. Culling in patch 2 (larger patch) decreases as movement increases, and more of the burden of control is pushed onto the smaller patch. Parameters used $a = 2, b = 0.2, \phi = 0.05, \beta = 0.308, \gamma = 1$.

One patch is a reservoir of infection, one is a non-reservoir.

If one patch (in the following analysis patch 2) is a reservoir for infection, and is coupled to a second non-reservoir, then from chapter 2 we saw that it is possible to eradicate infection by only controlling the reservoir population if movement is constant. If we wish to minimise the total effort expended, we wish to know if this culling strategy $(c_1, c_2) = (0, C_2)$ is optimal. Once again, we assume the carrying capacity of patch 2 is larger with the death rates in each patch given by $b_1 = b$ and $b_2 = \phi b$ where $\phi < 1$. The rate of culling required in patch 2 is found to be

$$(\beta H_1(c_2) - \gamma - b - m)(\beta H_2(c_2) - \gamma - \phi b - m - c_2) - m^2 = 0 \tag{6.25}$$

$$C_2 = \beta H_2(c_2) - \gamma - \phi b - m - \frac{m^2}{\beta H_1(c_2) - \gamma - b - m}. \tag{6.26}$$

Once again, if this point is optimal it must satisfy equations 6.6, where

$$\frac{\partial f_1}{\partial c_1} = 1, \qquad \frac{\partial f_1}{\partial c_2} = 1, \qquad \text{or} \qquad \frac{\partial f_2}{\partial c_1} = 0, \qquad \frac{\partial f_2}{\partial c_2} = 1 \tag{6.27}$$

depending on the cost function defined. Hence we must show that both

$$\frac{\partial g}{\partial c_1} = \frac{1}{\lambda}, \qquad \frac{\partial g}{\partial c_2} = \frac{1}{\lambda} \tag{6.28}$$

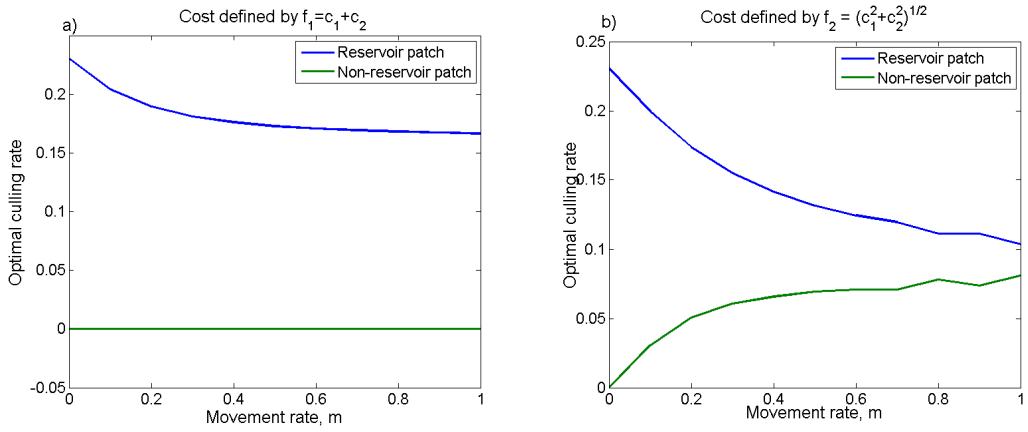

Figure 6.5: Optimal culling strategies as movement rate increases for costs defined by f_1 (a), and f_2 (b). Cost f_1 is minimised by culling the reservoir patch only, whilst f_2 is reduced by employing a mixed strategy.

if $(0, C_2)$ minimises f_1, or

$$\frac{\partial g}{\partial c_1} = 0, \qquad \frac{\partial g}{\partial c_2} = \frac{1}{\lambda} \tag{6.29}$$

for $(0, C_2)$ to minimise f_2. Evaluating $\partial g/\partial c_1$ we have

$$\frac{\partial g}{\partial c_1} = \beta(\beta H_2 - \gamma - \phi b - m - c_2)\frac{\partial H_1}{\partial c_1} + \beta(\beta H_1 - \gamma - b - m)\frac{\partial H_2}{\partial c_1} - (\beta H_2 - \gamma - \phi b - m - c_2). \tag{6.30}$$

Substituting the expression for C_2 into this, $\partial g/\partial c_1$ simplifies to

$$\frac{\partial g}{\partial c_1} = \frac{\beta m^2}{\beta H_1 - \gamma - b - m}\frac{\partial H_1}{\partial c_1} + \beta(\beta H_1 - \gamma - b - m)\frac{\partial H_2}{\partial c_1} - \frac{m^2}{\beta H_1 - \gamma - b - m}. \tag{6.31}$$

If this expression is equal to 1, then the strategy $(0, C_2)$ minimises the cost defined by f_1, whilst it must be zero if $(0, C_2)$ is optimal for f_2. Figure 6.5 shows the optimal culling rates in both patches, as the rate of movement between patches changes. Whilst we are unable to show this analytically, plot a) confirms that the optimal strategy for f_1 is found when the culling rate in patch 1, the non-reservoir patch, is set to zero. If the cost of culling is defined by f_2 however, plot b) shows that the optimal strategy is to cull across both patches. This second result is confirmed mathematically by showing that $\partial g/\partial c_1$ cannot equal zero.

Assuming this condition can be satisfied, equation 6.31 becomes

$$0 = \beta m^2 \frac{\partial H_1}{\partial c_1} + \beta(\beta H_1 - \gamma - b - m)^2 \frac{\partial H_2}{\partial c_1} - m^2.$$

We are then able to insert the expressions for $\partial H_1/\partial c_1$ and $\partial H_2/\partial c_1$, leaving the requirement that

$$0 = -\beta a m^2 \mathbf{A} - m^2 \mathbf{B} - \beta a m \mathbf{C} \tag{6.32}$$

where

$$\mathbf{A} = (2m + \phi b + c_2)(m + \phi b + c_2) > 0 \tag{6.33}$$

$$\mathbf{B} = (m(b(1+\phi) + c_2) + b(\phi b + c_2))^2 > 0 \tag{6.34}$$

$$\mathbf{C} = (\beta H_1 - \gamma - b - m)^2 (2m + \phi b + c_2) > 0 \tag{6.35}$$

and hence equation 6.32 cannot be satisfied and $(0, C_2)$ is not the minimum possible culling strategy. To put this in the context of controlling infectious disease in biological populations, if infectious disease is spread between an area which is a reservoir of infection, and an area which is not a reservoir, then a combined culling effort which targets both patches will minimise the overall amount of effort applied if the combined costs is lower than the sum of the independent control strategies.

6.3 Optimal disease control in 3-patch systems

In order to expand this work to more complex spatial systems we begin by making the addition of a third patch. This expansion of the model allows us to consider the impact of the spatial arrangement of distinct areas, whether individuals enter a patch from two neighbouring sites, or just one. The two potential network structures of a three patch system are shown in figure 6.6. In the first instance, we consider the fully connected model, which in the absence of

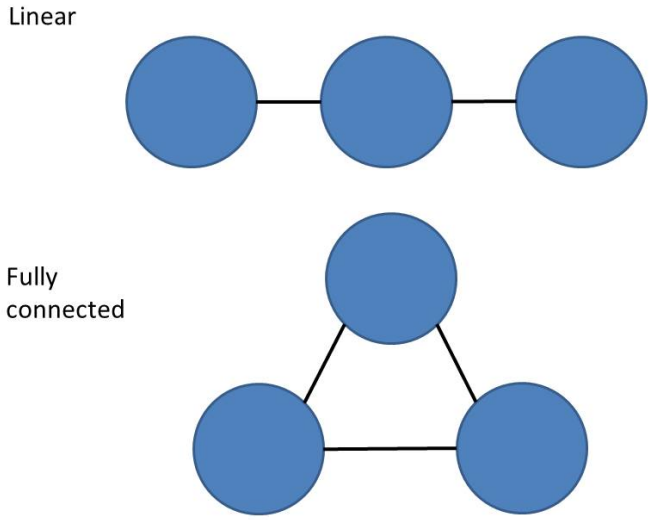

Figure 6.6: Possible structural configurations of a system of three patches

infection is given by

$$\frac{d}{dt}\begin{pmatrix} H_1 \\ H_2 \\ H_3 \end{pmatrix} = \begin{pmatrix} a_1 \\ a_2 \\ a_3 \end{pmatrix} - \begin{pmatrix} b_1 + m_{12} + m_{13} + c_1 & -m_{21} & -m_{31} \\ -m_{12} & b_2 + m_{21} + m_{23} + c_2 & -m_{32} \\ -m_{13} & -m_{23} & b_3 + m_{31} + m_{32} + c_3 \end{pmatrix} \begin{pmatrix} H_1 \\ H_2 \\ H_3 \end{pmatrix}. \tag{6.36}$$

Introducing infection into this model in the same way as in the two patch case will lead to a pathogen exclusion threshold given by a surface $g(c_1, c_2, c_3) = 0$. Once again, if the system is entirely symmetric, and all patches have equal demographic and disease parameters and movement between all patches is equal, then the minimum combined control strategy will be independent of movement rate and will be given by

$$c_1 = c_2 = c_3 = \beta H - \gamma - b.$$

We are however interested in the conditions for disease control in asymmetric systems. In order to investigate the effect of asymmetry on each patch configuration, we assume that the system is comprised of one dominant patch, with significantly larger carrying capacity than the other two smaller patches. For simplicity, we assume that the two smaller patches are

equal in size.

6.3.1 Fully Connected (1 reservoir 2 non-reservoirs): is it optimal to cull just reservoir patch?

In the two patch model, we have shown that even if one patch is a reservoir and a source of infection to the second, it is optimal under f_2, to apply a combined control effort to both patches, whilst the f_1 cost function predicts that it is optimal to cull the reservoir patch alone. Here we consider the case that a single patch, patch 3, in a fully connected system is a source to two non-reservoir patches. It is necessary in the three patch system to develop a numerical algorithm for finding the minimum control strategy. To to do this, we find the pathogen exclusion threshold in $c_1 - c_2$ space, for a number of levels of c_3, as shown in figure 6.7. Along each level of c_3, we find the minimum combined control strategy defined as either f_1 or f_2 and shown by the open circles in figure 6.7. The minimum strategy over all levels of c_3 is given by the closed circle in figure 6.7. Figure 6.7 is a sample output for a limited range of c_3, for a single movement rate. To produce the plots shown in figure 6.8, control parameters were varied such that $(c_1, c_2, c_3) \in [0, 1] \times [0, 1] \times [0, 1]$, with step size given by 0.01. The minimum cost was found within this parameter space for a range of movement rates between 0 and 1. The optimal strategy producing this minimum cost is shown in figure 6.8. The line T in this figure represents the computational tolerance, any points below this line are due to the discretisation of control space, and the step size used. We therefore do not consider control rates below this tolerance to be significantly different to zero. Figure 6.8 shows similar results to the two patch case, if cost is defined as a simple sum, then it is optimal to cull the reservoir patch alone, whilst a combination strategy is preferred if cost is lower than the sum.

6.3.2 Linearly connected: Symmetric patches

It remains to investigate the effect of the linear configuration of patches in this extended system. Here we wish to control disease in three distinct areas which are not fully connected. Individuals in this system must pass through patch 2 in order to move from patch 1 to patch 3, or vice versa. In the first instance, we assume that all patches are equal in terms of

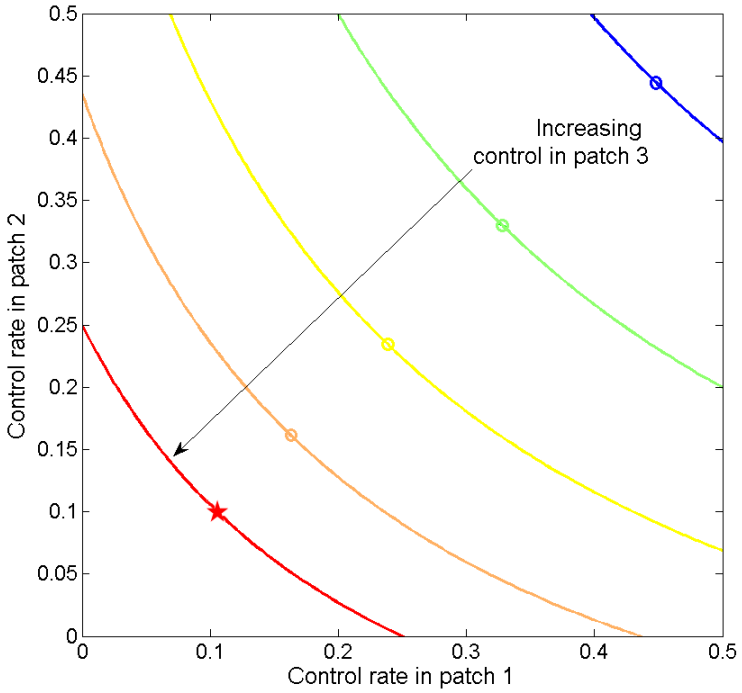

Figure 6.7: Pathogen exclusion threshold in three patches with patch 3 a reservoir of infection to the other patches. Contours show thresholds at increasing levels of control in patch 3, c_3. Minimum control strategy is shown on each level (open circles) and minimum control over all the levels in the simulation is shown by the star. Parameters used $a = 2, b_1 = b_2 = 0.5, b_3 = 0.2, m = 0.1, \beta = 0.308, \gamma = 1$

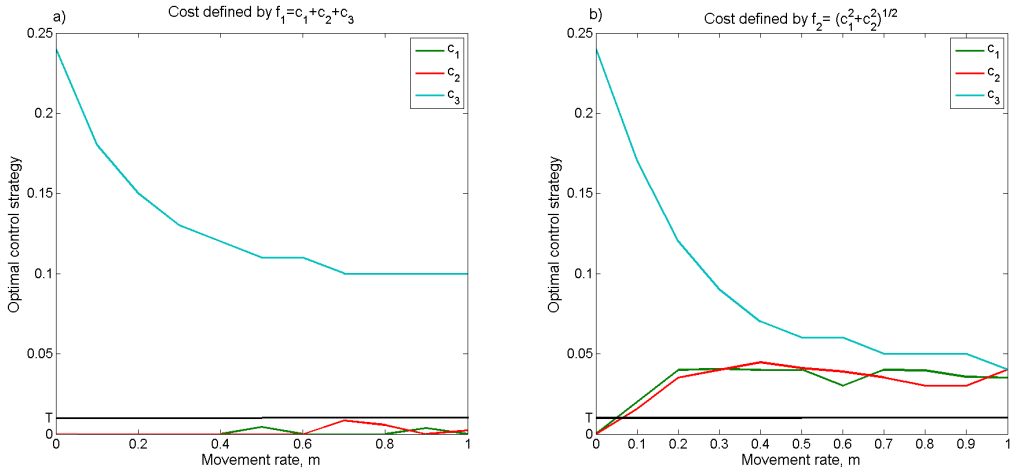

Figure 6.8: Optimal control strategies for a fully connected 3 patch system with patch 3 reservoir. Plot a shows strategies that minimise cost defined by f_1, and b for cost defined by f_2. Parameters used $a = 2, b_1 = b_2 = 0.5, b_3 = 0.2, \beta = 0.308, \gamma = 1$.

demographic parameters, and that movement from one patch to another occurs at the same rate in either direction. In the linear model, the movement matrix M is given by

$$M = \begin{pmatrix} -m_{21} & m_{12} & 0 \\ m_{21} & -m_{12} - m_{32} & m_{23} \\ 0 & m_{32} & -m_{23} \end{pmatrix} \tag{6.37}$$

indicating that individuals in patches 1 and 3 can only move into patch 2, but those from patch 2 may move into either patch 1 or 3. Symmetric patches all achieve the same disease free equilibrium, regardless of network structure, and simulations show that the optimal control strategy is to apply equal control to each patch. This can once more be deduced from the structure of the infection invasion matrix given by

$$IIM = \begin{pmatrix} \beta H_1 - b - \gamma - m & m & 0 \\ m & \beta H_2 - b - \gamma - 2m & m \\ 0 & m & \beta H_3 - b - \gamma - m \end{pmatrix}. \tag{6.38}$$

Since movement between any two patches is symmetric, even if the network is not fully connected, in a symmetric system, the maximum eigenvalue will be given by $\lambda = \beta H - b - \gamma$, and hence control of all patches by this amount will result in pathogen exclusion and is the minimum possible combination of control. The pathogen exclusion thresholds for both the fully connected and the linear configurations are shown in figure 6.9. Whilst the optimal control strategy may be the same regardless of patch configuration, figure 6.9 shows that at suboptimal points, the configuration may skew the required controls. For example, if we cull patch 2 at a rate of 0.33 individuals per unit time, then for pathogen exclusion in the fully connected system, patch 1 must be culled at a rate of at least 0.31 individuals per unit time. If the system is connected linearly, then the required control rate in patch 1 is increased to at least 0.32 individuals per unit time. This implies that in a linear structure, the amount of control applied throughout the system has a reduced effect on the extremities. This is due to the effect of culling on the population size. In the fully connected patch, culling any single patch will cause an equal effect on the rest of the network. In the linear model, culling the

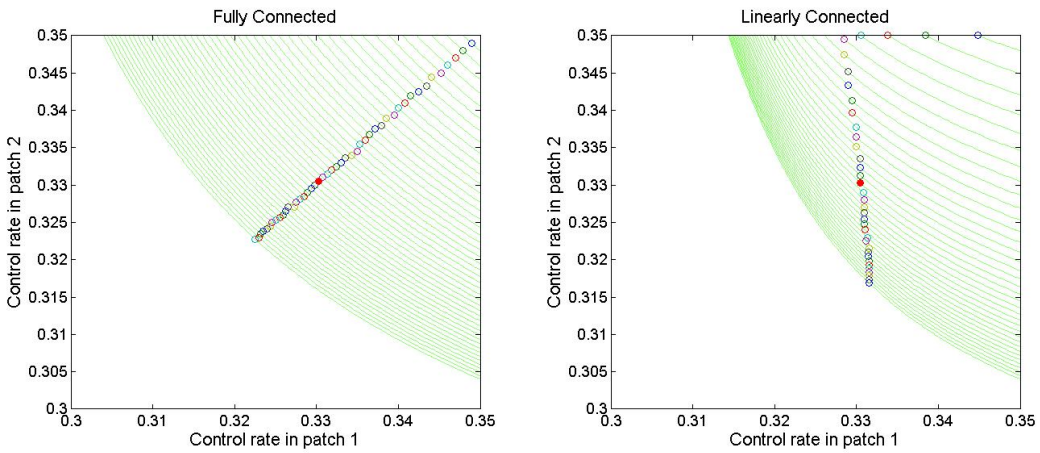

Figure 6.9: Pathogen exclusion thresholds in 3 dimensions, contours show the thresholds at given levels of c_3. Left hand plot shows the contours for the symmetric system, right hand plot shows the linear system. The optimal point in both cases is the same (closed circles).

central patch will have an equal effect on the end patches, however, culling an end patch, patch 1 for example, will lead to a greater reduction in the population size of patch 2 than that in patch 3. The effect of control reduces the further from the control the patch is. These results hold regardless of whether the cost of the culling strategy is given by f_1 or f_2.

6.3.3 Linearly connected: reservoir in central position

If the patch network is made up of a single reservoir of infection located at the central node in a linearly connected system, and the cost of culling is defined by the sum of the culling rates, then, as in the two patch case, the simulation results show that it is optimal to control only the central patch, as shown in figure 6.10 a). If however the cost of culling is defined by $f_2(c_1, c_2, c_3)$, (figure 6.10 b)) then the majority of the culling effort should be targeted on the reservoir of infection, however, as the rate of movement between patches increases, the optimal culling strategy increases in the non-reservoir patches, and decreases in the reservoir. It appears from these simulation results, that if $m > b_{res}$, where b_{res} is the death rate in the reservoir patch, then the optimal culling strategy does not change as m increases. If this is the case, then $1/m < 1/b_{res}$ and the average length of time spent in a patch before moving is shorter than the average lifespan of the individuals, and hence each individual is expected to move patches at least once in their lifetime. If this is the case, then the optimal culling

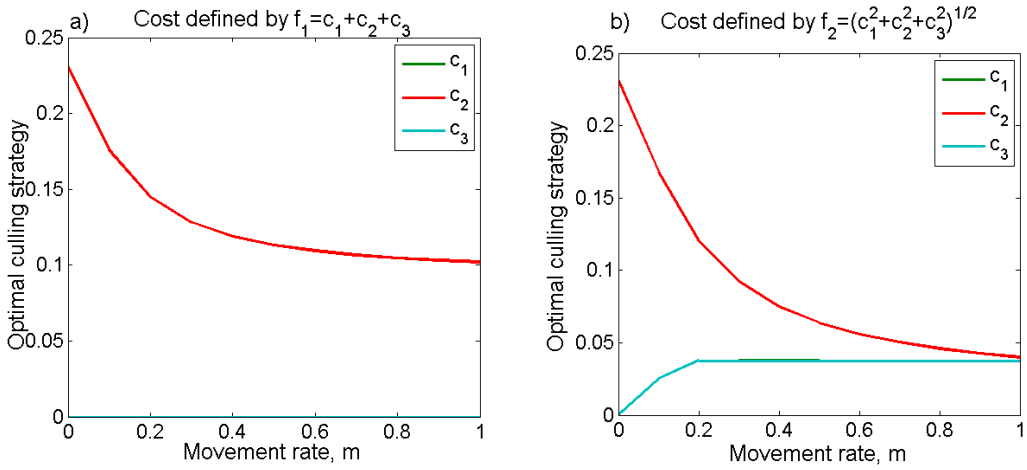

Figure 6.10: Optimal culling strategies for a linearly connected system, with a reservoir of infection at the central patch, patch 2. Plot a) shows optimal strategy for cost defined by f_1 and b) shows strategy for f_2. Parameters used: $a_i = 2, b_1 = b_3 = 0.5, b_2 = 0.2, \beta = 0.308, \gamma = 1$

strategy does not depend on the specific movement rate.

6.3.4 Linearly connected: reservoir at end position

If the reservoir of infection is situated at the end of the three patch linear configuration, then once again, the $f_1(c_1, c_2, c_3)$ cost function predicts that the optimal strategy is simply to control the reservoir alone. As in the previous cases, if the cost is defined by $f_2(c_1, c_2, c_3)$, then a mixed strategy is optimal. The reservoir patch should take the main burden of culling with the optimal culling rate decreasing with increasing distance. As the movement rate between the patches increase, then the optimal strategy is to decrease the culling rate in the reservoir, and increase it in the other patches. As the movement rate increases, the optimal culling effort in the central patch increases to a maximum before decreasing and saturating at the same level as the culling effort in patch 3, the furthest from the reservoir.

6.4 Conclusions/discussion

The work presented in this chapter has been an investigation in the optimal control of infectious disease in patchy systems. The two potential cost functions predict the same minimal control strategy if the system is symmetric, that is, if all patches are of equal size, with equal

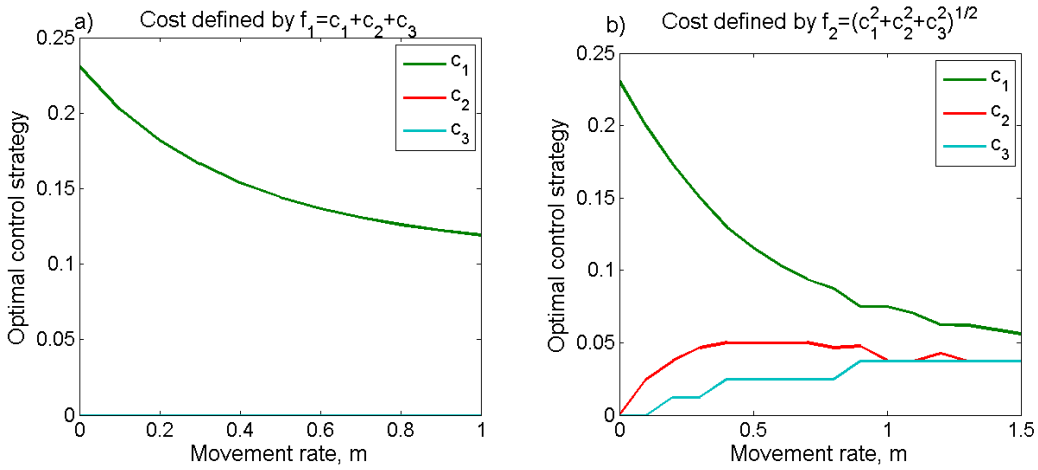

Figure 6.11: Optimal control strategy for a linearly connected system of three patches, with reservoir of infection in patch 1, as the movement rate between the patches increases. Plot a) shows the optimal strategies for f_1 and plot b) shows the strategies for f_2.

response to disease. This optimal strategy is to cull all patches equally. This strategy is identical to that predicted by considering each patch in isolation, and using a simple model, such as those discussed in many textbooks [105], [7], [84]. Simple models are therefore a good approximation to necessary conditions for culling if patches of habitat, and the populations to be culled are similar, however, this approximation fails when distinct, and asymmetric populations interact through dispersal. In this case, the act of movement between the patches causes a synchrony between the patches. Our results in two patches suggest that, if the difference in populations is a result of different death rates, due to the patch specific conditions, then the asymmetry can be counteracted by adjusting the culling strategy. The adjusted culling strategy shown in equation (6.18) compensates for the asymmetry, and suppresses the populations to the same size. If the cost of culling is measured as a sum of independent strategies, then it is optimal to adopt this method, and to force the total population to be evenly distributed between the patches. If however the culling strategies are assumed to be jointly managed, and cost is measured, or example, by the function f_2, then the burden of culling should be focussed on the larger patch. In both cases, an increase in movement between the patches reduces the required strategy. This is in good agreement with our previous results discussed in chapters 3 and 5, which show that increasing the rate of movement between patches lowers the pathogen exclusion threshold.

Scaling the two patch system up to three patches, we have considered firstly the case where all patches are demographically equivalent, and have equal rates of movement between populations. In this system, simulation results show that all patches should be culled equally, and this strategy is optimal regardless of the cost function, or the configuration of the patches. If there is an asymmetry between the patches in the three patch case, with one patch being a reservoir of infection to the others, then the optimal culling strategy, if cost is calculated by the sum of the individual culling rates, is to target the reservoir patch alone. If however, the cost is calculated by $f_2(c_1, c_2, c_3)$, then it is optimal to control all patches. As has been found in the two patch case, increasing the movement between the two patches leads to a reduction in the total cost of culling. In the case of the f_2 cost function, the burden of culling is redistributed as movement increases, with an increasing culling rate applied to the non-reservoir patches. These results suggest that the movement between patches can heavily influence the necessary culling regime to eradicate infection. Simple models, assuming each patch is a closed, uncoupled population, are appropriate for equivalent sized populations, but will predict suboptimal strategies for systems consisting of reservoir and non-reservoir patches. In these cases, the effect of movement on the population size and the spread of disease should be taken into account.

Chapter 7

Discussion

7.1 Thesis aims and key findings

The overall aim of this thesis has been to evaluate the effect of spatial coupling, and disturbance, on the effects of harvesting or culling a free moving population. In order to do this we have used the framework of a two patch, ordinary differential equation model of two populations coupled via dispersal of individuals between the patches. This within-patch, metapopulation type model has been used in the research of many ecological systems in particular dynamics of butterfly metapopulations [21],[67],[70], plant ecology [3], or lion conservation in Africa [41] however, the effects of population control on this type of system are not well known. In this final discussion of the work presented here, we shall outline the key results of this work, before discussing the ecological consequences of these results. We then go on to outline the direction of future research and extensions to this work.

7.1.1 Population dynamic consequences of harvesting (Chapters 2 and 4)

It has long been known that coupling of patches of individuals leads to a level of synchrony, or homogeneity between the populations in patch models [48],[20]. By modelling the dispersal of individuals by a constant per capita rate, any difference in the population sizes is reduced. Through the work presented in chapters 2 and 4 of this thesis, we have shown that the coupling of two patches in this way causes an increase in yield if only one of the patches is harvested. This result holds regardless of whether movement is constant or density dependent

and is independent of the growth rate of the populations. By allowing, or facilitating a porous boundary of a patch, the harvested population is constantly replenished by both the reproduction of the resident population, and also by the influx of immigrants into the harvesting zone from neighbouring sites.

The work presented in chapter 4 compares the predicted yield if movement is constant with that predicted if movement is density dependent. We have shown that density dependent movement reduces the synchrony between the patches, and this form of dispersal maintains the heterogeneity in patch size. In constantly stocked systems, with growth defined by the constant recruitment function, harvesting efforts produce a reduced yield if movement is density dependent, when compared to the constant movement model. Neglecting the impact of density dependence in this system can therefore lead to overestimation of the achievable yields. If population growth is logistic, then density dependent movement predicts a higher yield than the constant model, and hence constant movement underestimates the potential yield. This difference in model behaviour is due to the feedback produced by harvesting in the logistic model. In this case, the population is able to bounce back from the removal of individuals by increasing the growth rate. In the constant recruitment model there is no feedback to the growth rate of the population, and hence the population size, and therefore the yields achieved are detrimentally affected by harvesting.

Combined harvesting strategies, where c_1 is fixed and c_2 increases, leads to a reduction in the patch 1 yield due to an increase in removal of individuals from the population as a whole. If however, surviving individuals in the population react to harvesting by dispersing or emigrating from the patch at an increased rate, then a combined strategy may be optimal. If this is the case, then a single harvesting strategy will force individuals out of the harvested patch, decreasing the yield. If the second patch is harvested in combination, then the second patch is no longer a refuge, and those forced out of patch 1 are more likely to be replaced by those forced out of patch 2. Hence a combination strategy can lead to a higher yield if harvesting causes disturbance. It is therefore essential, when devising harvesting strategies to understand the effects of the migration of individuals from and to the area to be harvested, whilst also understanding the impacts of surrounding harvesting efforts.

7.1.2 Consequences of disease control (Chapters 3 and 5)

The work presented in chapters 3 and 5 detail the impact of spatial coupling on the necessary control strategies which will ensure disease eradication. In these sections, we have focussed on a constant recruitment growth rate and have shown that the coupling of two patches can reduce the burden of control. For a given control rate in patch 1, increasing the rate of coupling between patches causes a decrease in the required control rate in patch 2. We have shown that density dependent movement will cause an increase in the pathogen exclusion threshold when compared with the constant movement model, and this is due to the reduction in efficacy of the control on the surrounding areas if movement is density dependent.

Density dependent movement hence provides a buffer against the removal of individuals. Whilst this is detrimental in terms of disease eradication, it may highlight an evolutionary advantage, offering protection against predation or other risks to the population. Density dependent movement allows a patch to become a refuge for the individuals residing there, and prevents small populations being exposed to the risks involved in dispersal.

If individuals are disturbed by the onset of culling strategies, then this effect may either increase, or decrease the pathogen exclusion threshold depending on the infectious parameters of transmission and virulence. In general, for very low transmission rates, perturbation will lead to an increase in the necessary culling strategies. If this is the case, neglecting the perturbation effect will predict pathogen exclusion thresholds which are insufficient to exclude the disease. This underestimation may lead to a long term disease control strategy which will never be sufficient to eradicate the disease due leading to a large waste of money and effort. As transmission increases, there is a switch in thresholds, and perturbation may predict that pathogen exclusion requires less control effort than a similar model without perturbation. In this case however, transient dynamics show that culling causes a period of unnaturally high prevalence in the surrounding patches. Whilst pathogen exclusion may be achieved more easily in a perturbed system, culling strategies which cause this prevalence may need to be avoided.

Analysis of the threshold behaviour for a range of transmission and virulence parameters has also shown that there is a region whereby, in the absence of any culling, the system is

naturally disease free, yet the disturbance caused by the culling strategy forces the populations to become squeezed and hence to become susceptible to disease spread. This phenomenon has not previously been discussed in the modelling literature, and may be a crucial consequence of human intervention in natural populations. This 'squeezing' of populations into concentrated groups raises not only the chance of infection becoming endemic in the population in question, but also increases the risk of infection to alternative hosts or to humans.

7.1.3 Optimal disease control strategies (Chapter 6)

The work presented in chapter 6 confirms that if control strategies are independent, and the total cost of culling is the sum of the costs of each strategy, then the minimal strategy is to account for the difference in size of the populations, forcing the populations to be equal in size. If the populations in the patch system are similar in size, and the movement between patches is symmetric, then the minimal control strategy is independent of the rate of movement. In this case, the minimal culling strategy is exactly that predicted by the uncoupled system of differential equations. Patch dynamics must be taken into account when this property is not met. In the case of asymmetric patches, the movement rate will determine the population densities at equilibrium and will be key to minimising the control strategy.

7.2 Ecological relevance of this work

7.2.1 Harvesting and population control

The patch dynamics explored throughout this thesis are applicable to a range of ecological systems . Patches may be formed due to the social structure and behaviour of a species. Herding or other social segregation behaviours, as exhibited by deer and other ungulates, are an example of this [4]. In these populations, large social groups are formed and offer individuals protection from predation. In order to maintain the population density, and to reduce genetic inbreeding, offspring, particularly males, are likely to disperse [116],[147][128]. Patch structure may also be due to a lack of homogeneous resource, for example roosting populations of bats inhabit large maternity colonies which are coupled by the movement of individuals, such as solitary males, between roosts. Alternatively, patchy dynamics may be

the result of anthropomorphic factors such as habitat fragmentation i.e agricultural expansion or urbanisation. Discretisation of a habitat into patches may also be imposed on a habitat due to ownership of land. If this is the case, one could argue that movement of individuals between these 'patches' will be more frequent, since the patch structure is not a natural part of the population structure. This arbitrary human division of habitat is particularly relevant in the case of fishing territories in regions such as the North sea. Many of these populations are, or could potentially be targets for active control strategies. Harvesting of wild populations may occur for several reasons. These include to reduce the population density within a given area, or alternatively to obtain a sustainable yield from the population. Proper management of harvesting strategies is key to maintaining a healthy, and functioning natural environment, and many systems have been destroyed by poorly planned harvesting strategies [106], [29]. Mathematical modelling is an important tool in predicting the potential impact of a proposed harvesting strategy, and it is therefore important to understand the theoretical consequences of a model. Until recently [129], [114],[115] the issue of spatial perturbation has been unaddressed in the literature, and to our knowledge, has never been addressed in the context of harvesting and yield dynamics.

We have shown that if the purpose of a harvesting strategy is to obtain a yield in an area, then it is important to understand, and co-operate with the management of surrounding patches. If there is a level of disturbance, then from the management perspective of an individual patch, it may be optimal to develop a combined harvesting strategy with the surrounding patches, and hence to be able to catch those individuals forced out of other areas. If the aim of a harvesting strategy is to rid an area of a population, then we have shown that if similar sized patches are coupled, then the minimum harvesting strategy is to cull both patches equally. However, if an area is difficult to control, then it may be possible to indirectly curtail the population growth by increasing the harvesting effort in surrounding patches, and allowing dispersal between habitats.

7.2.2 Disease control

Culling of individuals in order to reduce the population density, and hence the rate of disease transmission, occurs in a wide variety of ecological contexts, many of which fall into the patchy

framework discussed here [66]. The recent drive to counteract the negative effects of habitat loss and fragmentation through opening up wildlife corridors brings with it the potential for an increase in disease spread through a network of patches [56].

The primary motivation for this work was the relevance of the perturbation effect to the control of bovine tuberculosis in badgers, and the transmission of this bacterium from the wildlife reservoir to the domestic cattle population. During the randomised badger culling trial, it was found that a higher incidence of infection was found in areas surrounding culling sites. The transient results shown in chapter 5 agree with this finding, showing that an increase in movement can lead to a very high number of infected individuals in the immediate aftermath of the onset of the cull. Over time, this prevalence will drop, however, the high numbers reached are significantly higher than they would have reached naturally, and may take several years to return to even natural levels of infection.

As discussed above, our results have shown that the effect of spatial disturbance may be either beneficial or detrimental in terms of the necessary control strategy, depending on the particular characteristics of the disease involved. It is theoretically possible therefore, that the perturbation effect may be used to reduce the control strategy required. Once more, the transient dynamics in chapter 5 show that, even when this is possible, this threshold condition shows only the asymptotic behaviour of the infectious population. In the immediate aftermath of the cull, even when the disease can be theoretically wiped out, we have shown that very a high prevalence is achieved. This may have dire consequences, particularly if the system is a reservoir of infection to other species of wildlife or livestock as in the case of bovine TB.

7.3 Future research

The work presented here is just the beginning of a potentially rich and productive investigation into the dynamic consequences of spatial perturbation. We have only considered the impact of human interference in natural populations through direct removal of individuals. However, species may be perturbed by many different factors, both anthropomorphic and natural. It would be of great interest to extend this work to model the perturbation induced by the introduction of a predator, or natural competitor into the environment. This would force the

resident population in a similar way to culling, by reducing the number of individuals able to survive within an area, and potentially encouraging the movement of individuals out of the patch. However, a predator-prey system with this framework would have a natural feedback to the predator population, and therefore may have interesting dynamic consequences to be explored.

In many of the examples discussed here, only a specific subset of the population is likely to disperse. In many systems, the mechanisms of dispersal are sex specific, with different sexes of the same species often requiring different resources. The impact of spatial perturbation on the sex bias in a population, and the wider ecological or evolutionary consequences of this would therefore be a rich field of research.

Spatial perturbation is may also be induced in species without direct removal. The framework presented here could also be used to investigate the behavioural changes observed in species when encountering communal feeding sites such as shared flowers in insect systems [46], or the impact of diversionary feeding schemes. An increase in contact rates between species has already been noted in red and grey squirrels populations who come into contact more often in urban areas due to aggregated food resources; with subsequent increases in disease transfer. Similarly, supplementary feeding of bird populations has led to territorial breakdowns of social structures which in turn lead to greater contact either between species or between distinct social groups of the same species.

The work presented in this thesis has scratched the surface of the potential implications of coupled patches, and the impact of spatial disturbance in these systems, in this thesis, we have opened the door to investigate this impact further, and to make a significant contribution to the understanding of population and disease control.

Appendix A

Instability of Zero Equilibrium in Logistic Model over 2 patches

The stability of the zero equilibrium is determined by the Jacobian matrix evaluated at $(0, 0)$. This matrix is given by

$$J = \begin{pmatrix} r_1 - m_1 & m_2 \\ m_1 & r_2 - m_2) \end{pmatrix}. \tag{A.1}$$

For stability, we require that both the trace of the Jacobian is negative, and the determinant is positive, i.e

$$Tr(J) = r_1 - m_1 + r_2 - m_2 < 0$$
$$Det(J) = (r_1 - m_1)(r_2 - m_2) - m_1 m_2 > 0$$

If either of these conditions are not satisfied, then the zero equilibrium is unstable. There are four conditions to consider

1. $r_1 - m_1 > 0$ and $r_2 - m_2 > 0$. If this is the case then the $Tr(J) > 0$ and $(0, 0)$ is unstable.

2. $r_i - m_i > 0$ and $r_j - m_j < 0$. Here the product of $(r_1 - m_1)(r_2 - m_2) < 0$ and hence $det(J) < 0$ and $(0, 0)$ is unstable.

3. $r_1 - m_1 < 0$ and $r_2 - m_2 < 0$. In this case, $Tr(J) < 0$. At first glance it is not clear

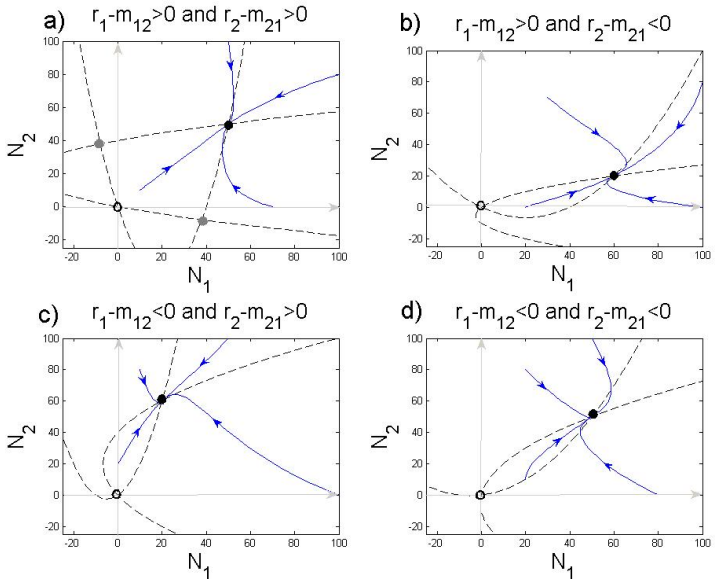

Figure A.1: Phase plane analysis of the equilibria of the logistic model with dispersal between two patches. Stable, positive equilibrium is shown as the closed black circle, with the open circle showing the $(0, 0)$ equilibrium. Grey circles signify non-viable (not biologically possible) equilibria. All positive trajectories approach the stable positive equilibrium.

that $det(J) < 0$ also, however, rearranging we see that

$$\begin{aligned} det(J) &= r_1 r_2 - r_1 m_2 - r_2 m_1 \\ &= r_1(r_2 - m_2) - r_2 m_1 < 0 \end{aligned}$$

since $r_2 - m_2 < 0$.

Hence for all cases, if $r_i > 0$ and $m_i > 0$ as required, then the zero equilibrium is unstable. Instability of the zero equilibrium alone does not guarantee stability of the positive equilibrium, however, by phase plane analysis of this system we are able to determine representative phase planes for each stability determining case. Figure A.1 shows the phase planes for each of the four cases. In all cases there are two viable equilibria, one at $(0, 0)$ and a coexistance, positive equilibrium. In all cases, this positive equilibrium is stable, with all trajectories originating in the positive quadrant approaching this equilibrium.

Appendix B

Extinction thresholds for logistic model, harvesting in one patch

If harvesting effort is applied to patch 1 at a constant per capita rate, x, then the population is forced to extinction when the $(0,0)$ equilibrium is stable. This stability occurs when the eigenvalues of

$$J = \begin{pmatrix} r_1 - m_1 - x & m_2 \\ m_1 & r_2 - m_2) \end{pmatrix}. \tag{B.1}$$

are both negative. As in appendix A, we use conditions on the trace and determinant of this matrix to determine stability in 4 cases.

1. $r_1 - m_1 > 0$, $r_2 - m_2 > 0$: Here, for simplicity, we label $r_1 - m_1 = P$, and $r_2 - m_2 = Q$, where P, Q are both positive.

$$\text{Trace:} \quad P + Q - x < 0 \tag{B.2}$$

$$x > P + Q \tag{B.3}$$

$$\text{Determinant:} \quad PQ - xQ - m_1 m_2 > 0 \tag{B.4}$$

$$PQ - m_1 m_2 > Qx \tag{B.5}$$

$$x < P - \frac{m_1 m_2}{Q}. \tag{B.6}$$

In order to satisfy both these conditions we require that x lies between $P + Q$ and

$P - m_1 m_2/Q$. This requires that

$$P + Q < P - \frac{m_1 m_2}{Q} \tag{B.7}$$

$$Q^2 < -m_1 m_2. \tag{B.8}$$

This resulting contradiction shows that if $r_1 - m_1 > 0$ and $r_2 - m_2 > 0$, then harvesting of patch 1 alone is always insufficient to cause extinction.

2. $r_1 - m_1 < 0$, $r_2 - m_2 < 0$: Here let $r_1 - m_1 = -P$ and $r_2 - m_2 = -Q$.

$$\text{Trace:} \qquad x > -P - Q \tag{B.9}$$

$$\text{Determinant:} \qquad PQ + xQ - m_1 m_2 > 0 \tag{B.10}$$

$$x > \frac{m_1 m_2}{Q} - P \tag{B.11}$$

The trace condition is always true for $x \geq 0$ hence the extinction threshold is equivalent to the determinant condition.

3. $r_1 - m_1 > 0$, $r_2 - m_2 < 0$: Here let $r_1 - m_1 = P$, $r_2 - m_2 = -Q$.

$$\text{Trace:} \qquad x > P - Q \tag{B.12}$$

$$\text{Determinant:} \qquad x > \frac{m_1 m_2}{Q} + P \tag{B.13}$$

Here $x > max(P - Q, P + m_1 m_2/Q)$ hence $x > P + m_1 m_2/Q$.

4. $r_1 - m_2 < 0$, $r_2 - m_2 > 0$. Let $r_1 - m_1 = -P$ and $r_2 - m_2 = Q$ then.

$$\text{Trace:} \qquad x > Q - P \tag{B.14}$$

$$\text{Determinant:} \qquad x < -\frac{m_1 m_2}{Q} - P \tag{B.15}$$

which cannot be satisfied for $x \geq 0$ hence extinction is impossible in this case.

Appendix C

Harvesting in a 2 patch logistic growth model

As detailed above, the zero equilibrium is always unstable if $r_i > 0$. Harvesting of this population will change this condition. If harvesting occurs in both patches, then the Jacobian of the system becomes

$$J(c) = \begin{pmatrix} r_1 - m_{12} - c_1 & m_{21} \\ m_{12} & r_2 - m_{21} - c_2 \end{pmatrix}. \tag{C.1}$$

By inspection of the trace and determinant of this matrix we can determine the conditions of the harvesting parameter to ensure stability. In all cases we can see that the trace and determinant of J are given by

$$Tr(J(h)) = r_1 - m_{12} + r_2 - m_{21} - (c_1 + c_2) \tag{C.2}$$

$$Det(J(h)) = (r_1 - m_{12})(r_2 - m_{21}) - m_{12}m_{21} - c_1(r_2 - m_{21}) - c_2(r_1 - m_{12}) + c_1c_2 \tag{C.3}$$

$$\tag{C.4}$$

Hence for stability of the $(0,0)$ equilibrium and therefore extinction of the population the harvesting rate must satisfy both

$$c_1 + c_2 > Tr(J(0))$$
$$c_i > \frac{m_{12}m_{21}}{c_j + m_{ji} - r_j} + (r_i - m_{ij})$$

From the second of the above conditions we are able to show that the intersection of the extinction threshold with the axes in control space is given by

$$\hat{c_i} = \frac{det(J(0))}{r_j - m_j}$$

The extinction threshold is given by the upper branch of the hyperbolic curve $det(J(c)) = 0$. This curve asymptotes at $c_1 = r_1 - m_{12}$ and $c_2 = r_2 - m_{21}$. Hence the four cases given below.

1. $r_1 - m_{12} > 0, r_2 - m_{21} > 0$. Here both asymptotes are positive, and the extinction threshold does not cross the axes in $c_1 - c_2$ space. In this case, harvesting a single species will never result in total population extinction because the unharvested patch will be a source of individuals for the harvested patch.

2. $r_i - m_{ij} > 0, r_j - m_{ji} < 0$. Here the c_i asymptote is positive, and the c_j asymptote is negative, in this case, the extinction threshold crosses the c_i axis but not the c_j axis. This indicates that when one patch is a source to the second, then control of the source patch alone, beyond the threshold $\hat{c_i}$, will lead to population extinction. Control of the sink patch will not cause population extinction.

3. $r_1 - m_{12} < 0, r_2 - m_{21} < 0$. In this case, both asymptotes are negative indicating that excessive harvesting of either patch will cause the entire population over both patches to crash to extinction.

These results are given in Figure C.1

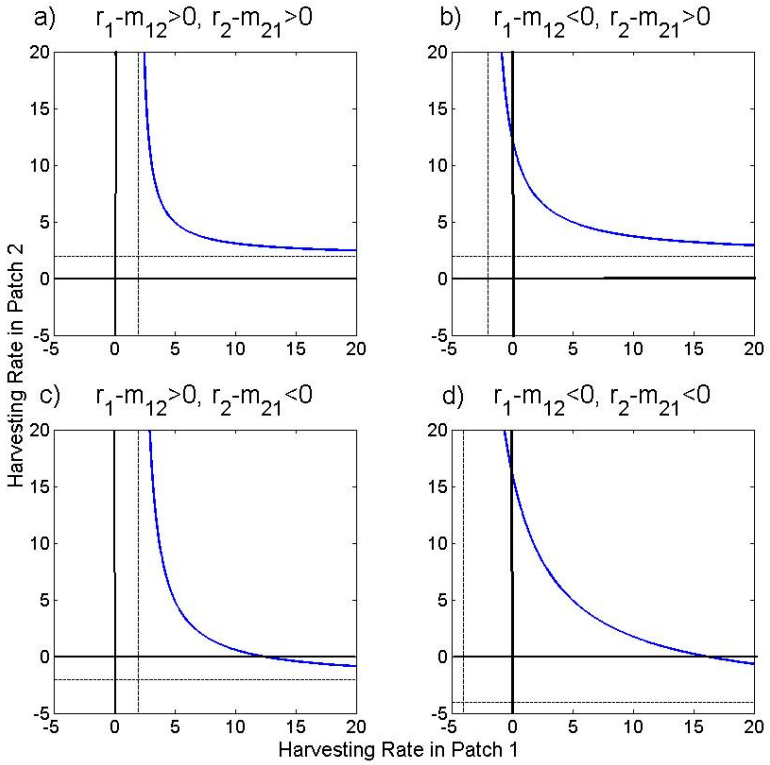

Figure C.1: Extinction thresholds for the four possible cases. Dashed lines indicate asymptotes of the threshold.

Appendix D

Stability of Positive Equilibria

The disease free equilibrium is given by the solution of

$$\nu_1 - (\mu_1 + c_1)S_1 - A_1(c_1)S_1 + A_2(c_2)S_2 = 0 \tag{D.1}$$

$$\nu_2 - (\mu_2 + c_2)S_2 - A_2(c_2)S_2 + A_1(c_1)S_1 = 0. \tag{D.2}$$

The nullclines of this system are given by hyperbolic curves, the positive arms of which intersect in the positive quadrant. This intersection is the unique positive equilibrium for the system. The nullcline of (D.1) is a hyperbola with transverse axis parallel to the S_2-axis while the nullcline of (D.2) is also a hyperbola, perpendicular to the first. If we define $\hat{S_1}$ and $\hat{S_2}$ as the unique positive steady states we can show that this point is locally stable by considering the Jacobian of the disease free system evaluated at this equilibrium.

$$\begin{pmatrix} -\mu_1 - c_1 - A_1'\hat{S_1} - A_1(c_1) & A_2'\hat{S_2} + A_2 \\ A_1'\hat{S_1} + A_1 & -\mu_2 - c_2 - A_2'\hat{S_2} - A_2 \end{pmatrix}. \tag{D.3}$$

where $A_i' = \frac{dA_i}{dS_i}|_{S_i=\hat{S_i}}$.

By evaluating the trace and determinant of this matrix and using the Routh-Hurwitz conditions [105] we can see that this equilibrium is always stable for positive parameters.

$$\text{Trace} = -\mu_1 - c_1 - A_1'\hat{S_1} - A_1(c_1) - \mu_2 - c_2 - A_2'\hat{S_2} - A_2 < 0$$

$$\text{Determinant} = (\mu_1 + c_1 + A_1'\hat{S}_1 + A_1(c_1))(\mu_2 + c_2 + A_2'\hat{S}_2 + A_2) - (A_2'\hat{S}_2 + A_2)(A_1'\hat{S}_1 + A_1) > 0$$

$$= (\mu_1 + c_1)(\mu_2 + c_2) + (A_1'\hat{S}_1 + A_1)(\mu_2 + c_2) + (A_2'\hat{S}_2 + A_2)(\mu_1 + c_2) > 0$$

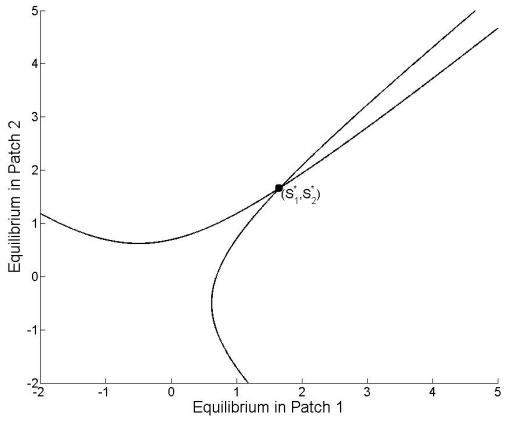

Figure D.1: Nullclines

Appendix E

Bounds on Maximum Eigenvalue of Matrix 3.4

The Perron-Frobenius theorem [123] shows that the maximum eigenvalue λ of a real positive matrix A is real and positive, and is bounded by the maximum and minimum row sum and also by the maximum and minimum column sum, hence the maximum eigenvalue must be bounded by

$$\max\{row_{min}, col_{min}\} \leq \lambda \leq \min\{row_{max}, col_{max}\}.$$

This result can be applied to the maximum eigenvalue of a matrix which is positive but with possibly negative diagonal entries, and hence to the matrix 3.4. We must consider two cases, firstly the case of complete dispersal, when $\phi = 1$ and secondly when $\phi \neq 1$.

1. $\phi = 1$: In this case, the row sums of 3.4 are $P_1 - c_1 - A_1 + A_2, P_2 - c_2 - A_2 + A_1$, the minimum of which is $\leq \min\{P_1 - c_1, P_2 - c_2\}$ and the maximum of which is $\geq \max\{P_1 - c_1, P_2 - c_2\}$. The column sums of 3.4 when $\phi = 1$ are simply $P_1 - c_1, P_2 - c_2$ and hence

$$\min\{P_1 - c_1, P_2 - c_2\} \leq \lambda \leq \max\{P_1 - c_1, P_2 - c_2\}.$$

2. $\phi < 1$: In the case of incomplete dispersal, $\phi < 1$, then the row sums are given by $P_1 - c_1 - A_1 + \phi A_2, P_2 - c_2 - A_2 + \phi A_1$. The column sums are $P_i - c_i - (1-\phi)A_i$. Now if $A_1 \leq A_2$ say, then $P_1 - c_1 - A_1 + \phi A_2 > P_1 - c_1 - (1-\phi)A_2$ and $P_2 - c_2 - A_2 + \phi A_1 <$

$P_2 - c_2 - (1-\phi)A_1$ and hence

$$\min\{P_1-c_1-(1-\phi)A_1, P_2-c_2-(1-\phi)A_2\} \leq \lambda \leq \max\{P_1-c_1-(1-\phi)A_1, P_2-c_2-(1-\phi)A_2\}.$$

Appendix F

MATLAB code for pathogen exclusion threshold

We present below the annotated sample Matlab code for both the constant movement model without perturbation, and the corresponding model with linear perturbation. All pathogen exclusion thresholds follow this format.

```
function threshCRcon(P,x,y)
%pathogen exclusion threshold for constant recruitment, constant dispersal
%model.
%input given by P=vector of parameters, x=range of x values, y=range of y
%values.

nu1=P(1); nu2=P(2);              % birth rates
mu1=P(3); mu2=P(4);              % death rates
beta1=P(5); beta2=P(6);          % transmission rates
gamma1=P(7); gamma2=P(8);        % rate of death due to infection
a1=P(9); a2=P(10);               % movement rates
phi=P(11); rho=P(12);            % hazardous boundary

for k=1:length(y);       % for each (x,y) in range
for h=1:length(x);
   [t,S]=ode15s(@CRconstant,[0 1000],[1 0 1 0],[],P,x(h),y(k)); %run model
S1=S(length(t),1);                                  %to disease free equilibrium
S2=S(length(t),3);

DO=[ beta1*S1-mu1-gamma1-x(h)-a1 rho*a2;          %Jacobian matrix at disease
       phi*a1 beta2*S2-mu2-gamma2-y(k)-a2];       %free equilibrium

    Lambda(k,h)=max(eig(DO));                     %maximum eigenvalue

end
end

contour(x,y,Lambda,[0,0],'r','linewidth',2); %plot contour where Lambda=0
xlabel('Control in Patch i, c_i','fontsize',20)
ylabel('Control in Patch j, c_j','fontsize',20)
legend('Constant')
hold on
end
```

Figure F.1: MATLAB code for pathogen exclusion threshold with constant movement and no spatial perturbation.

```
function threshCRlin(P,d,x,y)
%pathogen exclusion threshold for constant recruitment, linear dispersal
%model.
%input given by P=vector of parameters, x=range of x values, y=range of y
%values.


nu1=P(1); nu2=P(2);              % birth rates
mu1=P(3); mu2=P(4);              % death rates
beta1=P(5); beta2=P(6);          % transmission rates
gamma1=P(7); gamma2=P(8);        % rate of death due to infection
a1=P(9); a2=P(10);               % movement rates
phi=P(11); rho=P(12);            % hazardous boundary

for k=1:length(y); % for each (x,y) in range
for h=1:length(x);
   [t,S]=ode15s(@CRlinear,[0 1000],[1 0 1 0],[],P,d,x(h),y(k)); %run model
                                                %to disease free equilibrium
S1=S(length(t),1);
S2=S(length(t),3);
 %Jacobian matrix at disease free equilibrium
 D1=[beta1*S1-mu1-gamma1-x(h)-a1-x(h)*S1 rho*(a2+y(k)*S2);
       phi*(a1+x(h)*S1) beta2*S2-mu2-gamma2-y(k)-a2-y(k)*S2];

    Lambda(k,h)=max(eig(D1));        % maximum eigenvalue
end
end


contour(x,y,Lambda,[0,0],'g.-','linewidth',2); %plot contour where Lambda=0
legend('Linear')
xlabel('Control applied to Patch 1','fontsize',20)
ylabel('Control Applied to Patch 2','fontsize',20)
hold on
end
```

Figure F.2: MATLAB code for pathogen exclusion threshold for constant movement model with linear perturbation

Appendix G

MATLAB code for calculating minimum control effort along pathogen exclusion threshold

```
%% Track minimum control strategy with increasing movement rate
% Taking Pathogen Exclusion Threshold, isolate the control rates along the
%threshold and use those to compute the population equilibria at this point.

clear  % clear the workspace
nu=2; nu2=2; %constant recruitment rate
mu=0.2; mu2=0.5;
gamma=1; gamma2=1; %infected death
beta=0.308; beta2=0.308; %transmission
phi=1; rho=1; %hazardous boundary
d=1;
a=0:0.1:1;
for m=1:length(a);
x0=0; y0=0; %minimum control rate
xm=1; ym=1; % maximum control rate
P=100; K=100; %control increment
x=linspace(x0,xm,P);
y=linspace(y0,ym,K);
Diff=nan(length(y),length(x)); % create matrix for eigenvalues
    for k=1:length(y);
        for h=1:length(x);
            [t,S]=ode15s(@twopatch,[0 1000],[10 10],[],nu,nu2,mu,mu2,
            phi,rho,a(m),a(m),x(h),y(k));
            S1=S(length(t),1);
            S2=S(length(t),2); %DFE
            DO=[ beta*S1-mu-gamma-x(h)-a(m) rho*a(m);
                phi*a(m) beta2*S2-mu2-gamma2-y(k)-a(m)]; %Jacobian

            Diff(k,h)=max(eig(DO));  %eignvalues throughout parameter space
        end
    end
%plot contour when max eigenvalue =0,
 %store co-ords along this threshold in Cmatrix
Cmatrix=contour(x,y,Diff,[0,0],'r','Linewidth',2)
 hold on
contour(x,y,M1,[0,0],'b-');
contour(x,y,M2,[0,0],'b-');

for g=2:length(Cmatrix);
    Cull1(g-1)=Cmatrix(1,g);
    Cull2(g-1)=Cmatrix(2,g);
    [t,H]=ode15s(@twopatch,[0 1000],[10 10],[],nu,nu2,mu,mu2,phi,rho,a(m),
    a(m),Cull1(g-1),Cull2(g-1)); % Solve ODE for disease free equilibrium
end
C=sqrt(Cull1.^2+Cull2.^2);
[M,I]=min(C);
mindist(m)=M;
minx(m)=Cull1(I);
miny(m)=Cull2(I);
end
figure
plot(a,minx,a,miny)
figure(4)
scatter(minx,miny)
figure
plot(a,mindist)
```

Figure G.1: Matlab code used in Chapter 6 to calculate minimum cost along the pathogen exclusion threshold

Bibliography

[1] R. Aarde, I. Whyte, and S. Pimm. Culling and the dynamics of the kruger national park african elephant population. *Animal Conservation*, 2(4):287–294, 1999.

[2] J. Aars and R. A. Ims. Population dynamic and genetic consequences of spatial density-dependent dispersal in patchy populations. *The American Naturalist*, 155(2):252–265, 2000.

[3] H. M. Alexander, B. L. Foster, F. Ballantyne, C. D. Collins, J. Antonovics, and R. D. Holt. Metapopulations and metacommunities: combining spatial and temporal perspectives in plant ecology. *Journal of Ecology*, 100(1):88–103, 2012.

[4] J. Alves, A. Alves da Silva, A.M.V.M. Soares, and C. Fonseca. Sexual segregation in red deer: is social behaviour more important than habitat preferences? *Animal Behaviour*, 85(2):501–509, 2013.

[5] P. Amarasekare. The role of density-dependent dispersal in source-sink dynamics. *Journal of Theoretical Biology*, 226(2):159–168, 2004.

[6] R.M. Anderson and R.M. May. Population biology of infectious diseases: Part i. *Nature*, 280(5721):361–367, 1979.

[7] R.M. Anderson and R.M. May. *Infectious diseases of humans*, volume 1. Oxford university press Oxford, 1991.

[8] R.M. Anderson and W. Trewhella. Population dynamics of the badger (*Meles meles*) and the epidemiology of bovine tuberculosis (*Mycobacterium bovis*). *Philosophical Transac-*

tions of the Royal Society of London. Series B, Biological Sciences, 310(1145):327–381, 1985.

[9] J. Arino, R. Jordan, and P. Van den Driessche. Quarantine in a multi-species epidemic model with spatial dynamics. *Mathematical Biosciences*, 206(1):46–60, 2007.

[10] J. Arino and P. Van den Driessche. A multi-city epidemic model. *Mathematical Population Studies*, 10(3):175–193, 2003.

[11] M. Artois. Wildlife infectious disease control in europe. *Journal of Mountain Ecology*, 7:89–97, 2003.

[12] C.M. Beale and P. Monaghan. Human disturbance: people as predation-free predators? *Journal of Applied Ecology*, 41(2):335–343, 2004.

[13] A. Bechet, J.-F. Giroux, and G. Gauthier. The effects of disturbance on behaviour, habitat use and energy of spring staging snow geese. *Journal of Applied Ecology*, 41(4):689–700, 2004.

[14] J.R. Beddington and R.M. May. Harvesting natural populations in a randomly fluctuating environment. *Science*, 197(4302):463–465, 1977.

[15] M. Begon, M. Bennett, R.G. Bowers, N.P. French, S.M. Hazel, and J. Turner. A clarification of transmission terms in host-microparasite models: numbers, densities and areas. *Epidemiology and Infection*, 129(1):147–153, 2002.

[16] M. Begon and R.G. Bowers. Host-host-pathogen models and microbial pest control: the effect of host self regulation. *Journal of Theoretical Biology*, 169(3):275–287, 1994.

[17] M. Begon, C.R. Townsend, and J.L. Harper. *Ecology: from Individuals to Ecosystems.* Blackwell Pub., 2009.

[18] D. Bernoulli. Essai dune nouvelle analyse de la mortalité causée par la petite vérole et des avantages de linoculation pour la prévenir. *Histoire de lAcad. Roy. Sci.(Paris) avec Mém. des Math. et Phys. and Mém*, pages 1–45, 1760.

[19] R.J.H. Beverton and S.J. Holt. On the dynamics of exploited fish populations. *Fishery Investigations Series 2: Sea Fisheries*, 19, 1957.

[20] O.N. Bjørnstad, R.A. Ims, and X. Lambin. Spatial population dynamics: analyzing patterns and processes of population synchrony. *Trends in Ecology & Evolution*, 14(11):427–432, 1999.

[21] D.A. Boughton. Empirical evidence for complex source-sink dynamics with alternative states in a butterfly metapopulation. *Ecology*, 80(8):2727–2739, 1999.

[22] W.D. Bowen and D. Lidgard. Marine mammal culling programs: review of effects on predator and prey populations. *Mammal Review*, 43(3):207–220, 2013.

[23] R.G. Bowers and M. Begon. A host-host-pathogen model with free-living infective stages, applicable to microbial pest control. *Journal of Theoretical Biology*, 148(3):305–329, 1991.

[24] D.E. Bowler and T.G. Benton. Causes and consequences of animal dispersal strategies: relating individual behaviour to spatial dynamics. *Biological Reviews*, 80(2):205–225, 2005.

[25] F. Brauer and C. Castillo-Châavez. *Mathematical Models in Population Biology and Epidemiology*. Springer, 2012.

[26] F. Brauer and D.A. Sanchez. Constant rate population harvesting: equilibrium and stability. *Theoretical Population Biology*, 8(1):12–30, 1975.

[27] N.F. Britton. *Essential Mathematical Biology*. Springer Verlag, 2003.

[28] J.D. Broadfoot, R.C. Rosatte, and D.T. O'Leary. Raccoon and skunk population models for urban disease control planning in Ontario, Canada. *Ecological Applications*, 11(1):295–303, 2001.

[29] M.G. Burgess, S. Polasky, and D. Tilman. Predicting overfishing and extinction threats in multispecies fisheries. *Proceedings of the National Academy of Sciences*, 110(40):15943–15948, 2013.

[30] M.J. Caley, M.H. Carr, M.A. Hixon, T.P. Hughes, G.P. Jones, and B.A. Menge. Recruitment and the local dynamics of open marine populations. *Annual Review of Ecology and Systematics*, 27:477–500, 1996.

[31] S.P. Carter, R.J. Delahay, G.C. Smith, D.W. Macdonald, P. Riordan, T.R. Etherington, E.R. Pimley, N.J. Walker, and C.L. Cheeseman. Culling-induced social perturbation in eurasian badgers *Meles meles* and the management of tb in cattle: an analysis of a critical problem in applied ecology. *Proceedings of the Royal Society B: Biological Sciences*, 274(1626):2769–2777, 2007.

[32] M.M. Conner, G.C. White, and D.J. Freddy. Elk movement in response to early-season hunting in Northwest Colorado. *The Journal of Wildlife Management*, 65(4):926–940, 2001.

[33] F. Courchamp, T. Clutton-Brock, and B. Grenfell. Inverse density dependence and the allee effect. *Trends in Ecology & Evolution*, 14(10):405–410, 1999.

[34] L. Danon, A.P. Ford, T. House, C.P. Jewell, M.J. Keeling, G.O. Roberts, J.V. Ross, and M.C. Vernon. Networks and the epidemiology of infectious disease. *Interdisciplinary Perspectives on Infectious Diseases*, 2011, 2011.

[35] P. Daszak, A.A. Cunningham, and A.D. Hyatt. Emerging infectious diseases of wildlife–threats to biodiversity and human health. *Science*, 287(5452):443, 2000.

[36] P. Daszak, R. Plowright, J.H. Epstein, J. Pulliam, S. Abdul Rahman, H.E. Field, C.S. Smith, K.J. Olival, S. Luby, and K. Halpin. *The emergence of Nipah and Hendra virus: pathogen dynamics across a wildlife-livestock-human continuum* in *Disease ecology: community structure and pathogen dynamics.* Oxford University Press, USA, 2006.

[37] R.F. Denno and M.A. Peterson. Density-dependent dispersal and its consequences for population dynamics. *Population Dynamics: New Approaches and Synthesis.*, pages 113–130, 1995.

[38] O. Diekmann, J.A.P. Heesterbeek, and J.A.J. Metz. On the definition and the computation of the basic reproduction ratio R_0 in models for infectious diseases in heterogeneous populations. *Journal of Mathematical Biology*, 28(4):365–382, 1990.

[39] S.S. Ditchkoff, S.T. Saalfeld, and C.J. Gibson. Animal behavior in urban ecosystems: modifications due to human-induced stress. *Urban Ecosystems*, 9(1):5–12, 2006.

[40] A. Dobson. Population dynamics of pathogens with multiple host species. *American Naturalist*, 164(5):64, 2004.

[41] S. Dolrenry, J. Stenglein, L. Hazzah, R.S. Lutz, and L. Frank. A metapopulation approach to african lion (*Panthera leo*) conservation. *PloS one*, 9(2):e88081, 2014.

[42] C.A. Donnelly, R. Woodroffe, D.R. Cox, F.J. Bourne, C.L. Cheeseman, R.S. Clifton-Hadley, G. Wei, G. Gettinby, P. Gilks, H. Jenkins, W.T. Johnston, A.M. Le Fevre, J.P. McInerney, and W.I. Morrison. Positive and negative effects of widespread badger culling on tuberculosis in cattle. *Nature*, 439(7078):843–846, 2006.

[43] C.A. Donnelly, R. Woodroffe, D.R. Cox, F.J. Bourne, G. Gettinby, J.P. Le Fevre, A.M.and McInerney, and W.I. Morrison. Impact of localized badger culling on tuberculosis incidence in british cattle. *Nature*, 426(6968):834–837, 2003.

[44] W. G. Doubleday. Harvesting in matrix population models. *Biometrics*, 31(1):189–200, 1975.

[45] J.C. Dunn, H.E. McClymont, M. Christmas, and A.M. Dunn. Competition and parasitism in the native white clawed crayfish *Austropotamobius pallipes* and the invasive signal crayfish *Pacifastacus leniusculus* in the uk. *Biological Invasions*, 11(2):315–324, 2009.

[46] S. Durrer and P. Schmid-Hempel. Shared use of flowers leads to horizontal pathogen transmission. *Proceedings of the Royal Society of London. Series B: Biological Sciences*, 258(1353):299–302, 1994.

[47] B. Dybiec, A. Kleczkowski, and C.A. Gilligan. Optimising control of disease spread on networks. *Acta Physica Polonica B*, 36(5):1509–1526, 2005.

[48] D.J.D. Earn, P. Rohani, and B.T. Grenfell. Persistence, chaos and synchrony in ecology and epidemiology. *Proceedings of the Royal Society of London. Series B: Biological Sciences*, 265(1390):7–10, 1998.

[49] C.W. Epps, P.J. Palsbøll, J.D. Wehausen, G.K. Roderick, R.R. Ramey, and D.R. McCullough. Highways block gene flow and cause a rapid decline in genetic diversity of desert bighorn sheep. *Ecology Letters*, 8(10):1029–1038, 2005.

[50] L. Fahrig. Effects of habitat fragmentation on biodiversity. *Annual Review of Ecology, Evolution, and Systematics*, 34:487–515, 2003.

[51] M.L. Farnsworth, L.L. Wolfe, N.T. Hobbs, K.P. Burnham, E.S. Williams, D.M. Theobald, M.M. Conner, and M.W. Miller. Human land use influences chronic wasting disease prevalence in mule deer. *Ecological Applications*, 15(1):119–126, 2005.

[52] N.M. Ferguson, C.A. Donnelly, and R.M. Anderson. Transmission intensity and impact of control policies on the foot and mouth epidemic in great britain. *Nature*, 413(6855):542–548, 2001.

[53] J.M. Fryxell, C. Packer, K. McCann, E.J. Solberg, and B.-E. Sæther. Resource management cycles and the sustainability of harvested wildlife populations. *Science*, 328(5980):903–906, 2010.

[54] B.T. Garnett, R.J. Delahay, and T.J. Roper. Ranging behaviour of european badgers (*Meles meles*) in relation to bovine tuberculosis (*Mycobacterium bovis*) infection. *Applied Animal Behaviour Science*, 94(3-4):331–340, 2005.

[55] J.A. Gill, K. Norris, and W.J. Sutherland. Why behavioural responses may not reflect the population consequences of human disturbance. *Biological Conservation*, 97(2):265–268, 2001.

[56] J. Gog, R. Woodroffe, and J. Swinton. Disease in endangered metapopulations: the importance of alternative hosts. *Proceedings of the Royal Society of London. Series B: Biological Sciences*, 269(1492):671, 2002.

[57] C. Gortázar, P. Acevedo, F. Ruiz-Fons, and J. Vicente. Disease risks and overabundance of game species. *European Journal of Wildlife Research*, 52(2):81–87, 2006.

[58] C. Gortázar, E. Ferroglio, U. Höfle, K. Frölich, and J. Vicente. Diseases shared between wildlife and livestock: a european perspective. *European Journal of Wildlife Research*, 53(4):241–256, 2007.

[59] D. Goulson. *Bumblebees: their behaviour and ecology*. Oxford University Press, USA, 2003.

[60] J.V. Greenman and A.S. Hoyle. Exclusion of generalist pathogens in multihost communities. *The American Naturalist*, 172(4):576–584, 2008.

[61] J.V. Greenman and A.S. Hoyle. Pathogen Exclusion from Eco-Epidemiological Systems. *The American Naturalist*, 176(2):149–158, 2010.

[62] J.V. Greenman and P.J. Hudson. Host exclusion and coexistence in apparent and direct competition: an application of bifurcation theory. *Theoretical Population Biology*, 56(1):48–64, 1999.

[63] J.V. Greenman and P.J. Hudson. Multihost, multiparasite systems: an application of bifurcation theory. *Mathematical Medicine and Biology*, 16(4):333, 1999.

[64] J.V. Greenman and R.A. Norman. Environmental forcing, invasion and control of ecological and epidemiological systems. *Journal of Theoretical Biology*, 247(3):492–506, 2007.

[65] P.J. Greenwood. Mating systems, philopatry and dispersal in birds and mammals. *Animal Behaviour*, 28(4):1140–1162, 1980.

[66] I. Gudelj, K.A.J. White, and N.F. Britton. The effects of spatial movement and group interactions on disease dynamics of social animals. *Bulletin of Mathematical Biology*, 66(1):91–108, 2004.

[67] M.S. Guiney, D.A. Andow, and T.T. Wilder. Metapopulation structure and dynamics of an endangered butterfly. *Basic and Applied Ecology*, 11(4):354–362, 2010.

[68] M. Gyllenberg and I. Hanski. Single-species metapopulation dynamics: a structured model. *Theoretical Population Biology*, 42(1):35–61, 1992.

[69] I. Hanski, M. Kuussaari, and M. Nieminen. Metapopulation structure and migration in the butterfly *Melitaea cinxia*. *Ecology*, 75(3):747–762, 1994.

[70] I. Hanski and C.D. Thomas. Metapopulation dynamics and conservation: a spatially explicit model applied to butterflies. *Biological Conservation*, 68(2):167–180, 1994.

[71] L. Hansson. Dispersal and connectivity in metapopulations. *Biological Journal of the Linnean Society*, 42(1-2):89–103, 1991.

[72] A. Harrison, S. Newey, L. Gilbert, D.T. Haydon, and S. Thirgood. Culling wildlife hosts to control disease: mountain hares, red grouse and louping ill virus. *Journal of Applied Ecology*, 47(4):926–930, 2010.

[73] D.T. Haydon, S. Cleaveland, L.H. Taylor, M.K. Laurenson, et al. Identifying reservoirs of infection: a conceptual and practical challenge. *Emerging Infectious Diseases*, 8(12):1468–1473, 2002.

[74] J.A.P. Heesterbeek. A brief history of R_0 and a recipe for its calculation. *Acta Biotheoretica*, 50(3):189–204, 2002.

[75] G. Hess. Disease in metapopulation models: implications for conservation. *Ecology*, 77(5):1617–1632, 1996.

[76] H.W. Hethcote. The mathematics of infectious diseases. *SIAM review*, 42(4):599–653, 2000.

[77] W.G. Hill. Theoretical aspects of culling and selection in dairy cattle. *Livestock Production Science*, 7(3):213–224, 1980.

[78] E.E. Holmes, M.A. Lewis, J.E. Banks, and R.R. Veit. Partial differential equations in ecology: spatial interactions and population dynamics. *Ecology*, 75(1):17–29, 1994.

[79] R.D. Holt. Population dynamics in two-patch environments: some anomalous consequences of an optimal habitat distribution. *Theoretical Population Biology*, 28(2):181–208, 1985.

[80] J. Hone and C.A. Donnelly. Evaluating evidence of association of bovine tuberculosis in cattle and badgers. *Journal of Applied Ecology*, 45(6):1660–1666, 2008.

[81] J.B.C. Jackson, M.X. Kirby, W.H. Berger, K.A. Bjorndal, L.W. Botsford, B.J. Bourque, R.H. Bradbury, R. Cooke, J. Erlandson, J.A. Estes, et al. Historical overfishing and the recent collapse of coastal ecosystems. *Science*, 293(5530):629–637, 2001.

[82] H.E. Jenkins, R. Woodroffe, and C.A. Donnelly. The duration of the effects of repeated widespread badger culling on cattle tuberculosis following the cessation of culling. *PLoS One*, 5(2):e9090, 2010.

[83] P. Kareiva, A. Mullen, and R. Southwood. Population dynamics in spatially complex environments: Theory and data [and discussion]. *Philosophical Transactions of the Royal Society of London. Series B: Biological Sciences*, 330(1257):175–190, 1990.

[84] Matt J Keeling and Pejman Rohani. *Modeling infectious diseases in humans and animals*. Princeton University Press, 2008.

[85] M.J. Keeling. Models of foot-and-mouth disease. *Proceedings of the Royal Society B: Biological Sciences*, 272(1569):1195–1202, 2005.

[86] W.O. Kermack and A.G. McKendrick. Contributions to the mathematical theory of epidemics. ii. the problem of endemicity. *Proceedings of the Royal society of London. Series A*, 138(834):55–83, 1932.

[87] M. Kimura and G.H. Weiss. The stepping stone model of population structure and the decrease of genetic correlation with distance. *Genetics*, 49(4):561, 1964.

[88] H. Kokko and P. Lundberg. Dispersal, migration, and offspring retention in saturated habitats. *The American Naturalist*, 157(2):188–202, 2001.

[89] J.P. Kritzer and P.F. Sale. Metapopulation ecology in the sea: from Levins' model to marine ecology and fisheries science. *Fish and Fisheries*, 5(2):131–140, 2004.

[90] S. Lenhart and J.T. Workman. *Optimal control applied to biological models*. CRC Press, 2007.

[91] R. Levins. Some demographic and genetic consequences of environmental heterogeneity for biological control. *Bulletin of the ESA*, 15(3):237–240, 1969.

[92] R. Levins. Extinction. Some mathematical problems in biology. *American Mathematical Society, Providence, RI*, 75:107, 1970.

[93] R.A. Lintott, R.A. Norman, and A.S. Hoyle. The impact of increased dispersal in response to disease control in patchy environments. *Journal of Theoretical Biology*, 323:57–68, 2013.

[94] J.O. Lloyd-Smith, P.C. Cross, C.J. Briggs, M. Daugherty, W.M. Getz, J. Latto, M.S. Sanchez, A.B. Smith, and A. Swei. Should we expect population thresholds for wildlife disease? *Trends in Ecology & Evolution*, 20(9):511–519, 2005.

[95] D. MacMillan. Tradeable hunting obligationsa new approach to regulating red deer numbers in the scottish highlands? *Journal of Environmental Management*, 71(3):261–270, 2004.

[96] T.R. Malthus. *An essay on the principle of population*. 1798.

[97] F. Mathews, D.W. Macdonald, G.M. Taylor, M. Gelling, R.A. Norman, P.E. Honess, R. Foster, C.M. Gower, S. Varley, A. Harris, et al. Bovine tuberculosis (*Mycobacterium bovis*) in british farmland wildlife: the importance to agriculture. *Proceedings of the Royal Society B: Biological Sciences*, 273(1584):357, 2006.

[98] E. Matthysen. Density-dependent dispersal in birds and mammals. *Ecography*, 28(3):403–416, 2005.

[99] R.M. May, J.R. Beddington, J.W. Horwood, and J.G. Shepherd. Exploiting natural populations in an uncertain world. *Mathematical Biosciences*, 42(3):219–252, 1978.

[100] B.A. Mayle and A.C. Broome. Changes in the impact and control of an invasive alien: the grey squirrel (*Sciurus carolinensis*) in Great Britain, as determined from regional surveys. *Pest Management Science*, 69(3):323–333, 2013.

[101] H. McCallum, N. Barlow, and J. Hone. How should pathogen transmission be modelled? *Trends in Ecology & Evolution*, 16(6):295–300, 2001.

[102] R.A. McDonald, R.J. Delahay, S.P. Carter, G.C. Smith, and C.L. Cheeseman. Perturbing implications of wildlife ecology for disease control. *Trends in Ecology & Evolution*, 23(2):53–56, 2008.

[103] N.J. McPherson, R.A. Norman, N.G.H. Taylor, A.S. Hoyle, and J.E. Bron. Stocking methods and parasite-induced reductions in capture: modelling *Argulus foliaceus* in trout fisheries. *Journal of Theoretical Biology*, 2012.

[104] E.J. Milner-Gulland and E.L. Bennett. Wild meat: the bigger picture. *Trends in Ecology & Evolution*, 18(7):351–357, 2003.

[105] J.D. Murray. *Mathematical biology: an introduction*. Springer, 2002.

[106] A. Mysterud. Trophy hunting with uncertain role for population dynamics and extinction of ungulates. *Animal Conservation*, 15(1):14–15, 2012.

[107] R. Norman and R.G. Bowers. A host-host-pathogen model with vaccination and its application to target and reservoir hosts. *Mathematical Population Studies*, 14(1):31–56, 2007.

[108] D.J. O'Brien, S.M. Schmitt, S.D. Fitzgerald, D.E. Berry, and G.J. Hickling. Managing the wildlife reservoir of mycobacterium bovis: the michigan, usa, experience. *Veterinary Microbiology*, 112(2-4):313–323, 2006.

[109] Department of Food and Rural Affairs. Badger cull - piloting controls on bovine tb. www.gov.uk/government/news/badger-cull-piloting-controls-on-bovine-tb, accessed November 2013.

[110] Department of Food and Rural Affairs. Controlled shooting of badgers in the field under licence to prevent the spread of bovine tb in cattle: Best practice guidance. https://www.gov.uk/government/publications/controlled-shooting-of-badgers-in-the-field-under-licence-to-prevent-the-spread-of-bovine-tb-in-cattle, accessed September 2013.

[111] Department of Food and Rural Affairs. Notifiable avian disease control strategy for great britain. https://www.gov.uk/government/publications/notifiable-avian-disease-control-strategy-for-great-britain, January 2012 (accessed April 2014).

[112] A. Okubo. *Diffusion and ecological problems: mathematical models*. Springer-Verlag (Berlin and New York), 1980.

[113] M. Otronen and I. Hanski. Movement patterns in *Sphaeridium*: differences between species, sexes, and feeding and breeding individuals. *The Journal of Animal Ecology*, 52(3):663–680, 1983.

[114] J.C. Prentice. The perturbation effect in wildlife systems: an emergent property of simple models. *PhD Thesis, University of York*, 2012.

[115] J.C. Prentice, G. Marion, P.C.L. White, R.S. Davidson, and M.R. Hutchings. Demographic processes drive increases in wildlife disease following population reduction. *PloS one*, 9(5):e86563, 2014.

[116] A.E. Pusey. Sex-biased dispersal and inbreeding avoidance in birds and mammals. *Trends in Ecology & Evolution*, 2(10):295–299, 1987.

[117] W.J. Reed. Optimum age-specific harvesting in a nonlinear population model. *Biometrics*, 36(4):579–593, 1980.

[118] W.E. Ricker. Production and utilization of fish populations. *Ecological Monographs*, 16(4):373–391, 1946.

[119] J. Rist, E.J. Milner-Gulland, G. Cowlishaw, and M. Rowcliffe. Hunter reporting of catch per unit effort as a monitoring tool in a bushmeat-harvesting system. *Conservation Biology*, 24(2):489–499, 2010.

[120] R. Ross and H.P. Hudson. An application of the theory of probabilities to the study of a priori pathometry. part ii. *Proceedings of the Royal Society of London. Series A*, 93(650):212, 1917.

[121] R.E. Rowthorn, R. Laxminarayan, and C.A. Gilligan. Optimal control of epidemics in metapopulations. *Journal of the Royal Society Interface*, 6(41):1135–1144, 2009.

[122] L. Scillitani, A. Monaco, and S. Toso. Do intensive drive hunts affect wild boar (*Sus scrofa*) spatial behaviour in Italy? some evidences and management implications. *European Journal of Wildlife Research*, 56(3):307–318, 2010.

[123] E. Seneta. *Non-negative matrices and Markov chains*. Springer Verlag, 2006.

[124] K. Shea. Management of populations in conservation, harvesting and control. *Trends in Ecology & Evolution*, 13(9):371–375, 1998.

[125] J.A. Sherratt, M.A. Lewis, and A.C. Fowler. Ecological chaos in the wake of invasion. *Proceedings of the National Academy of Sciences*, 92(7):2524–2528, 1995.

[126] M.A. Simard, C. Dussault, J. Huot, and S.D. Côté. Is hunting an effective tool to control overabundant deer? a test using an experimental approach. *The Journal of Wildlife Management*, 77(2):254–269, 2013.

[127] G.C. Smith and D. Wilkinson. Modeling control of rabies outbreaks in red fox populations to evaluate culling, vaccination, and vaccination combined with fertility control. *Journal of Wildlife Diseases*, 39(2):278–286, 2003.

[128] A.M. Sparkman, J.R. Adams, T.D. Steury, L.P. Waits, and D.L. Murray. Pack social dynamics and inbreeding avoidance in the cooperatively breeding red wolf. *Behavioral Ecology*, 23(6):1186–1194, 2012.

[129] J. Swinton, F. Tuyttens, D. Macdonald, D.J. Nokes, C.L. Cheeseman, and R. Clifton-Hadley. A comparison of fertility control and lethal control of bovine tuberculosis in badgers: the impact of perturbation induced transmission. *Philosophical Transactions of the Royal Society of London. Series B: Biological Sciences*, 352(1353):619–631, 1997.

[130] L.H. Taylor, S.M. Latham, and E.J. Mark. Risk factors for human disease emergence. *Philosophical Transactions of the Royal Society of London. Series B: Biological Sciences*, 356(1411):983–989, 2001.

[131] A.J. Terry. Impulsive culling of a structured population on two patches. *Journal of Mathematical Biology*, 61(6):843–875, 2010.

[132] D.W. Thomas. Hibernating bats are sensitive to nontactile human disturbance. *Journal of Mammalogy*, 76(3):940–946, 1995.

[133] M.J. Tildesley, P.R. Bessell, M.J. Keeling, and M.E.J. Woolhouse. The role of pre-emptive culling in the control of foot-and-mouth disease. *Proceedings of the Royal Society B: Biological Sciences*, page rspb20090427, 2009.

[134] M.J. Tildesley, T.A. House, M.C. Bruhn, R.J. Curry, M. ONeil, J.L.E. Allpress, G. Smith, and M.J. Keeling. Impact of spatial clustering on disease transmission and optimal control. *Proceedings of the National Academy of Sciences*, 107(3):1041, 2010.

[135] M.J. Tildesley, N.J. Savill, D.J. Shaw, R. Deardon, S.P. Brooks, M.E.J. Woolhouse, B.T. Grenfell, and M.J. Keeling. Optimal reactive vaccination strategies for a foot-and-mouth outbreak in the uk. *Nature*, 440(7080):83–86, 2006.

[136] D.M. Tompkins, A.R. White, and M. Boots. Ecological replacement of native red squirrels by invasive greys driven by disease. *Ecology Letters*, 6(3):189–196, 2003.

[137] J.M.J. Travis and K.J. Park. Spatial structure and the control of invasive alien species. *Animal Conservation*, 7(3):321–330, 2004.

[138] A.R. Tuite, J. Tien, M. Eisenberg, D.J.D. Earn, J. Ma, and D.N. Fisman. Cholera epidemic in Haiti, 2010: Using a transmission model to explain spatial spread of disease and identify optimal control interventions. *Annals of Internal Medicine*, 154(9):593, 2011.

[139] F.A.M. Tuyttens, R.J. Delahay, D.W. Macdonald, C.L. Cheeseman, B. Long, and C.A. Donnelly. Spatial perturbation caused by a badger (*Meles meles*) culling operation:

implications for the function of territoriality and the control of bovine tuberculosis (*Mycobacterium bovis*). *Journal of Animal Ecology*, 69(5):815–828, 2000.

[140] R.E. Urbanek, K.R. Allen, and C.K. Nielsen. Urban and suburban deer management by state wildlife-conservation agencies. *Wildlife Society Bulletin*, 35(3):310–315, 2011.

[141] P. Van den Driessche and J. Watmough. Reproduction numbers and sub-threshold endemic equilibria for compartmental models of disease transmission. *Mathematical Biosciences*, 180(1):29–48, 2002.

[142] J. Verboom, A. Schotman, P. Opdam, and J.A.J. Metz. European nuthatch metapopulations in a fragmented agricultural landscape. *Oikos*, 61(2):149–156, 1991.

[143] P.F. Verhulst. Notice sur la loi que la population suit dans son accroissement. *Corr. Math. et Phys*, 10:113–121, 1838.

[144] W. Wang and X.Q. Zhao. An epidemic model in a patchy environment. *Mathematical Biosciences*, 190(1):97–112, 2004.

[145] A.R. Watkinson and W.J. Sutherland. Sources, sinks and pseudo-sinks. *Journal of Animal Ecology*, pages 126–130, 1995.

[146] A. White, A.D. Watt, R.S. Hails, and S.E. Hartley. Patterns of spread in insect-pathogen systems: the importance of pathogen dispersal. *Oikos*, 89(1):137–145, 2000.

[147] H.M. Whiteside, D.A. Dawson, C.D. Soulsbury, and S. Harris. Mother knows best: dominant females determine offspring dispersal in red foxes (*Vulpes vulpes*). *PloS one*, 6(7):e22145, 2011.

[148] J.A. Wiens. The landscape context of dispersal. *Dispersal*, pages 96–109, 2001.

[149] G. Wobeser. Disease management strategies for wildlife. *Revue Scientifique et Technique (International Office of Epizootics)*, 21(1):159, 2002.

[150] R. Woodroffe, C.A. Donnelly, D.R. Cox, F.J Bourne, C.L. Cheeseman, R.J. Delahay, G. Gettinby, J.P. Mcinerney, and W. Morrison. Effects of culling on badger *Meles meles*

spatial organization: implications for the control of bovine tuberculosis. *Journal of Applied Ecology*, 43(1):1–10, 2006.

[151] R. Woodroffe, C.A. Donnelly, D.R. Cox, P. Gilks, H.E. Jenkins, W.T. Johnston, A.M. Le Fevre, F.J. Bourne, C.L. Cheeseman, R.S. Clifton-Hadley, G. Gettinby, R.G. Hewinson, J.P. McInerney, A.P. Mitchell, W.I. Morrison, and G.H. Watkins. Bovine tuberculosis in cattle and badgers in localized culling areas. *Journal of Wildlife Diseases*, 45(1):128, 2009.

[152] R. Woodroffe, P. Gilks, W.T. Johnston, A.M. Le Fevre, D.R. Cox, C.A. Donnelly, F.J. Bourne, C.L. Cheeseman, G. Gettinby, J.P. McInerney, and W.I. Morrison. Effects of culling on badger abundance: implications for tuberculosis control. *Journal of Zoology*, 274(1):28–37, 2008.

[153] M.E.J. Woolhouse, L.H. Taylor, and D.T. Haydon. Population biology of multihost pathogens. *Science*, 292(5519):1109, 2001.